R/V Mirai MR21-05C Cruise Report

Arctic Challenge for Sustainability II (ArCS II)

Arctic Ocean, Bering Sea, and North Pacific
31 August – 22 October 2021

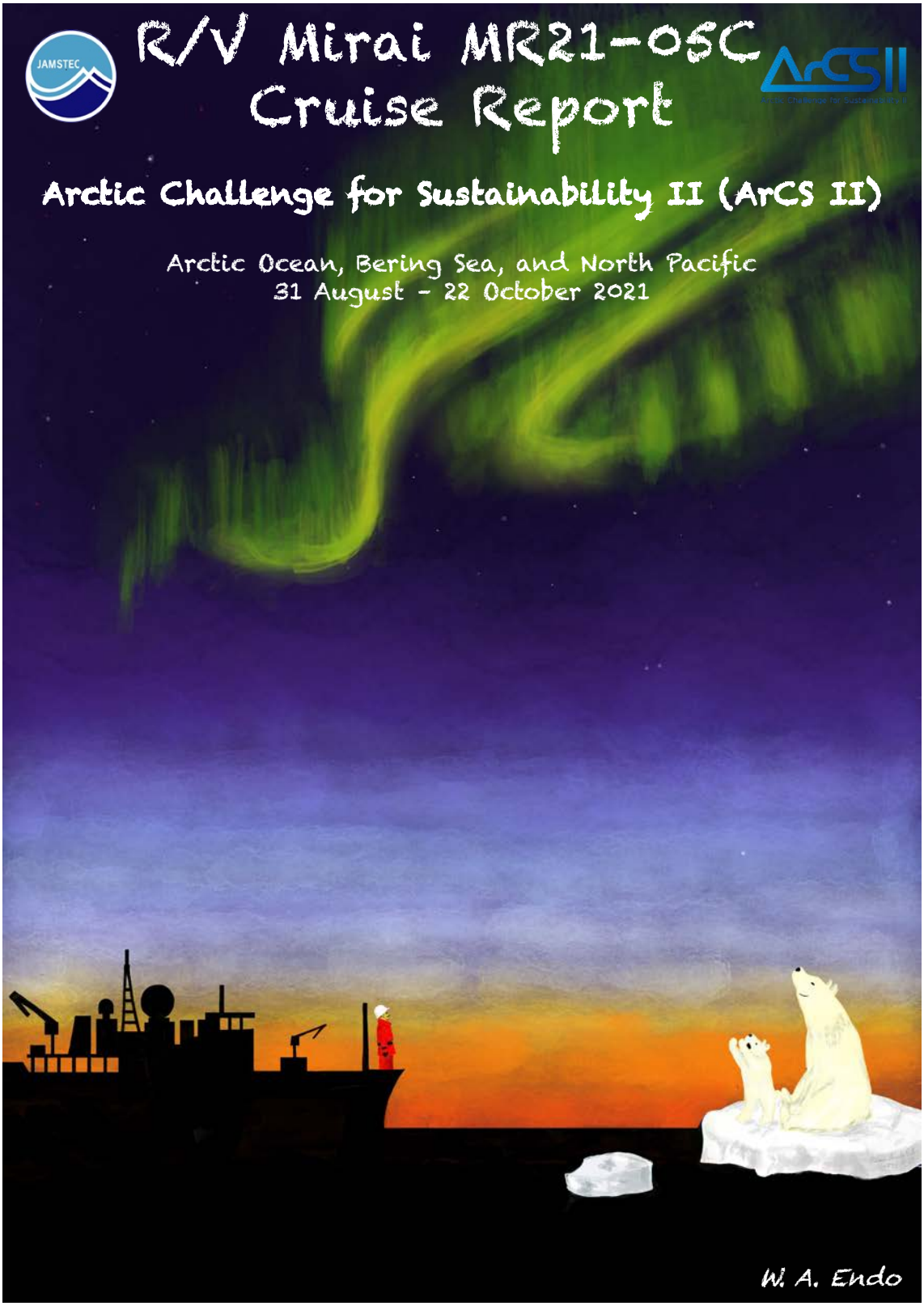

Japan Agency for Marine-Earth Science and Technology
(JAMSTEC)

Contents

1. Cruise Summary

1.1. Objectives

On the basis of our previous observations and theoretical considerations, we have come to realize that the Arctic Ocean plays an important role in global climate changes. The objectives of this cruise are as follows:

a. To quantify on-going changes in ocean, atmosphere, and ecosystem, which are related to the recent Arctic warming and sea ice reduction.
b. To clarify important processes and interactions among atmosphere, ocean, and ecosystem behind Arctic changes, and their effects on human society.
c. To collect data to provide accurate projections and environmental assessments for stakeholders so that they can make appropriate decisions on the sustainable development of the Arctic region.

1.2. Overview

We conducted meteorological and hydrographic surveys including marine biogeochemical samplings in the Pacific sector of the Arctic Ocean, the northern Bering Sea and the North Pacific Ocean on board the R/V Mirai from 31 August to 21 October 2021 under the framework of the Arctic Challenge for Sustainability II (ArCS II) Project (Figure 1.2-1). The research areas included the EEZ and the territorial sea of the USA. The observational activities consisted of CTD/LADCP/water samplings, XCTD, ocean microstructure measurements, wave and surface drifting buoy deployments, bio-optical measurements, zooplankton net samplings, sediment samplings, incubation experiments, ship-board ocean current and surface water monitoring, meteorological measurements and samplings, aerosol observations, trials of an in-water drone, satellite observations, doppler radar, sea ice radar, sea bottom topography, gravity, and magnetic field measurements, and mooring and sediment trap recoveries and deployments (Figure 1.2-1).

According to the report from National Snow and Ice Data Center (NSIDC), the Arctic sea ice appears to have reached its seasonal minimum extent of 4.72 million square kilometer on 16 September 2021, the twelfth lowest in the 38-year satellite record (one of the highest of the past decade). Our research areas in the Pacific sector of the Arctic Ocean sea ice has been remained with low concentration throughout the summer (Figure 1.2-2). Our survey captured anomalously icy condition and related unique oceanographic/atmospheric properties for the last decade in the Chukchi Sea.

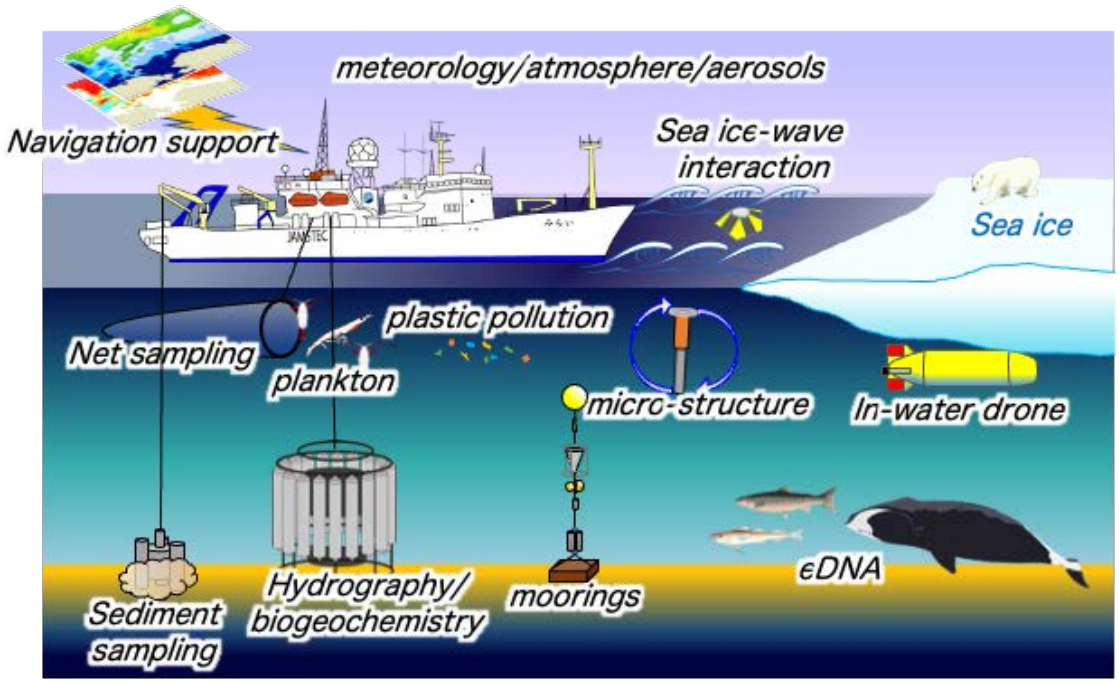

Figure 1.2-1: A schematic of the observational activities during MR21-05C cruise.

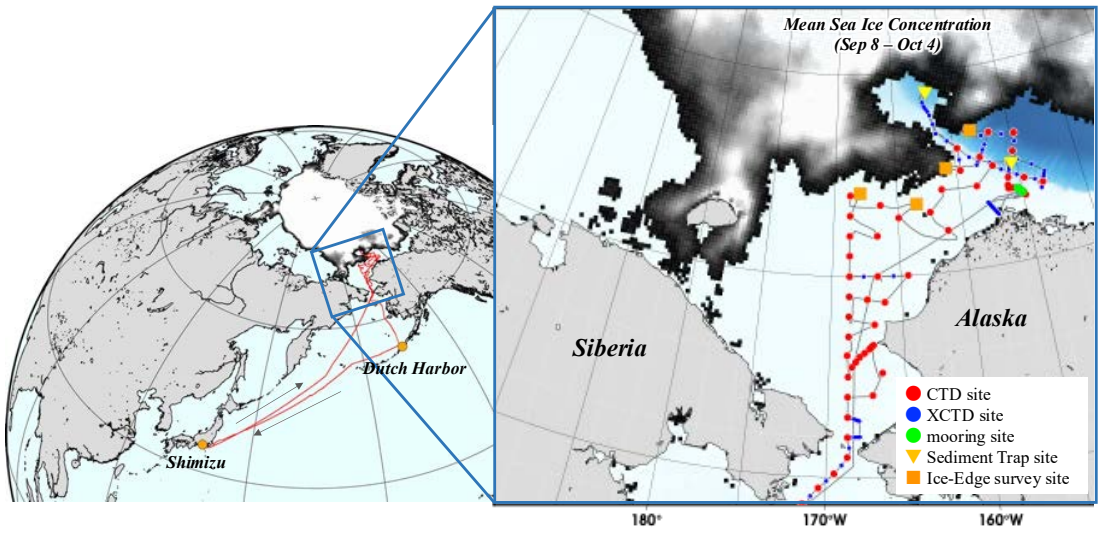

Figure 1.2-2: Map of the entire cruise area (left) and enlarged research areas in the Arctic Ocean (right). The cruise track and average sea ice concentration (provided by JAXA/EORC and the Arctic Data archive System (ADS)) during the observation term are overlayed. Large red dots indicate stations where we conducted oceanographic observations using Conductivity-Temperature-Depth (CTD) sensors and other activities (see 3.1 for the details). Small blue dots indicate where eXpendable Conductivity-Temperature-Depth (XCTD) sensors were deployed (see 3.3 for the details). Green and yellow dots reveal hydrographic and sediment trap mooring sites, respectively (see 3.12 for details). Orange squares are survey sites near the ice-edge (see 4.19 for the details). We also carried out intensive oceanographic surveys under an international

collaboration (Distributed Biological Observatory) off Pt. Hope and Pt. Barrow.

In this cruise, we had 127 oceanographic stations (63 CTD and 64 XCTD stations) including 48 water sampling sites, 44 TurboMAP sites, 17 bio-optics sites, 46 zooplankton net sites, 12 sediment sampling sites, 3 sites for drifting buoy launches, 5 sites for recoveries and deployments of hydrographic and sediment trap moorings. Continuous meteorological and oceanographic observations/samplings were carried out on the cruise track. We also conducted the first trial of an in-water drone, which is designed for oceanographic observation including under the sea ice (see section 5). These missions were successfully completed thanks to great efforts made by the captain, ice pilot, officers, crews, and all the participants in this cruise (Photo 1.2-1). Based on the data obtained in this cruise, we will be able to shed light on the Arctic change and its controlling factors and will contribute to the global climate change studies.

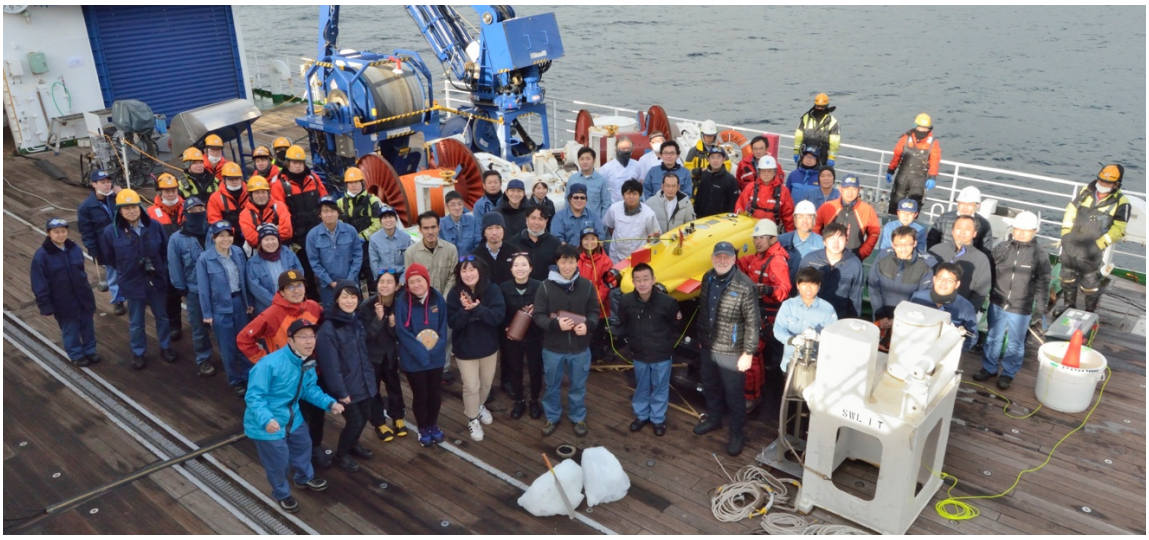

Photo 1.2-1: Commemorative photograph for the participants of R/V Mirai Arctic Ocean cruise in 2021 (taken by T. Kinase).

This cruise included the following 13 studies:

- On board research themes

● Representative of the Science Party [Affiliation]: Amane Fujiwara [JAMSTEC]

○ Title of proposal: Observational study of the Arctic environmental changes: Pacific-Arctic interaction, biogeochemical transport, mixing and marine ecosystem

● Representative of the Science Party [Affiliation]: Fumikazu Taketani [JAMSTEC]

○ Title of proposal: Ship-borne observations of trace gases/aerosols over the Arctic

● Representative of the Science Party [Affiliation]: Hiroshi Yoshida[JAMSTEC]

○ Title of proposal: Research on sea ice observation technology for the purpose of understanding environmental changes in the Arctic ocean

● Representative of the Science Party [Affiliation]: Takuji Waseda [The University of Tokyo]
○ Title of proposal: Observation of air-sea-wave-ice interaction in the Marginal Ice Zone
● Representative of the Science Party [Affiliation]: Takuhei Shiozaki [The University of Tokyo]
○ Title of proposal: Study on export production in the Arctic Ocean
● Representative of the Science Party [Affiliation]: Yusuke Kawaguchi [The University of Tokyo]
○ Title of proposal: Upper Ocean turbulent heat variability in the western Arctic
● Representative of the Science Party [Affiliation]: Daiki Nomura [Hokkaido University]
○ Title of proposal: CO_2, CH_4, and DMS dynamics in the Arctic Ocean
● Representative of the Science Party [Affiliation]: Kohei Matsuno [Hokkaido University]
○ Title of proposal: Spatial distribution of plankton community associated with sea-ice reduction in the Pacific sector of the Arctic Ocean
● Representative of the Science Party [Affiliation]: Tatsuya Kawakami [Hokkaido University]
○ Title of proposal: Analysis of Arctic fish communities using environmental DNA

- Studies not on board
● Representative of the Science Party [Affiliation]: Hotaek Park [JAMSTEC]
○ Title of proposal: Observation of water vapor isotope in the Arctic
● Representative of the Science Party [Affiliation]: Michiyo Kawai [Tokyo University of Marine Science and Technology]
○ Title of proposal: Study on nutrient transport by Summer Pacific Water
● Representative of the Science Party [Affiliation]: Yasunori Tohjima [Hokkaido University]
○ Title of proposal: Ship-board observations of atmospheric greenhouse gases and related species in the Arctic ocean and the western North Pacific
● Representative of the Science Party [Affiliation]: Kei-Ichiro Oshima [Hokkaido University]
○ Title of proposal: Ocean and sea ice dynamics along the Alaskan coast

1.3. Basic information

Name of vessel	R/V Mirai
L x B x D	128.58m x 19.0m x 13.2m
Gross Tonnage:	8,706 tons
Call Sign J	NSR
Cruise code	MR21-05C
Undertaking institute	Japan Agency for Marine-Earth Science and Technology (JAMSTEC)
Chief scientist	Amane Fujiwara Japan Agency for Marine-Earth Science and Technology (JAMSTEC)
Cruise periods	31 August 2021 – 22 October 2021
Port call	5 October 2021, Dutch Harbor (Arrival and leave after an ice pilot disembarkation) 21 October 2021, Shimizu (arrival in port)
Research areas	The Arctic Ocean, Bering Sea and North Pacific Ocean

1.4. Cruise Track

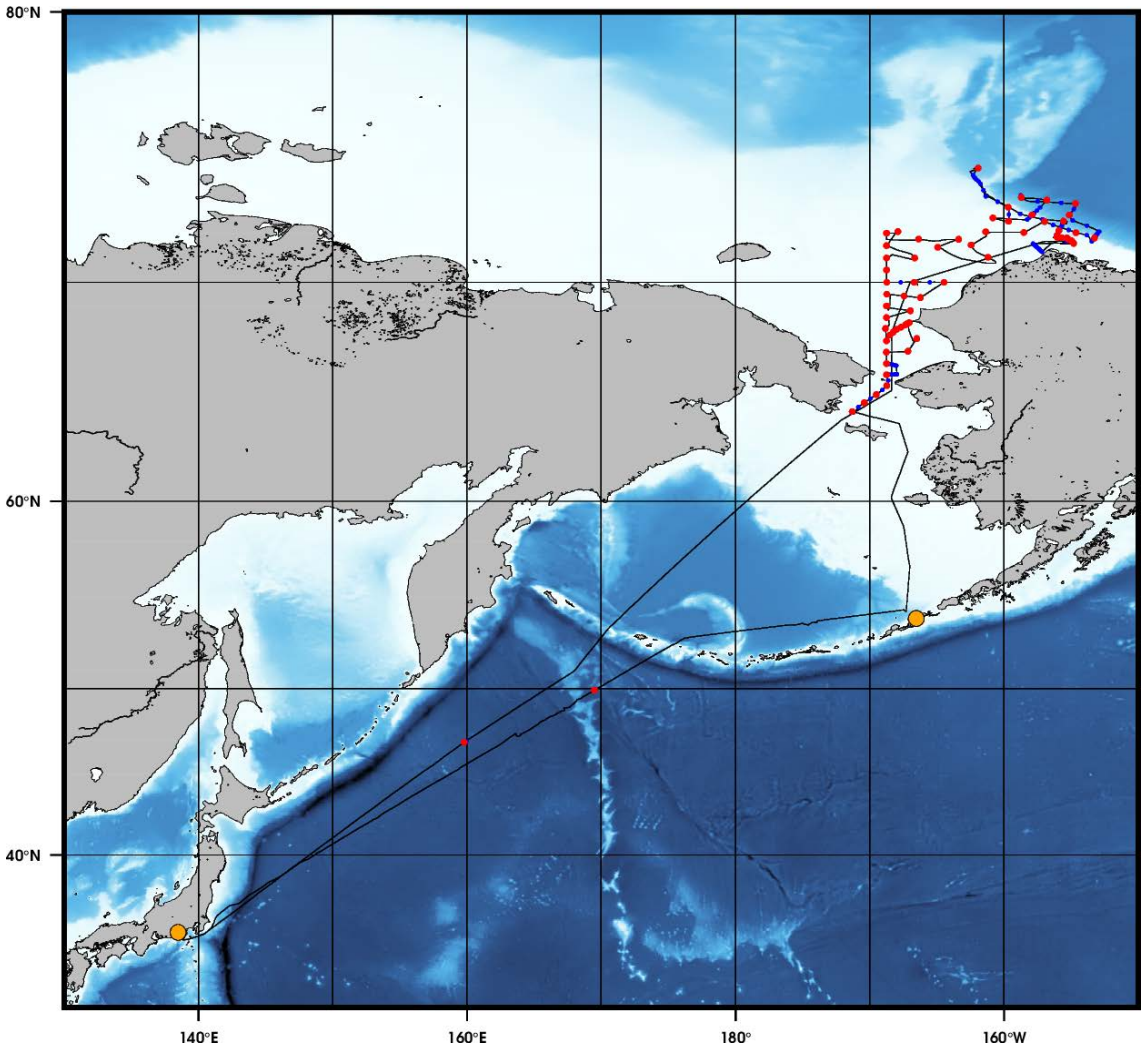

Figure 1.4-1: Cruise track (solid line), CTD (red dots) and XCTD (blue dots) stations of MR21-05C.

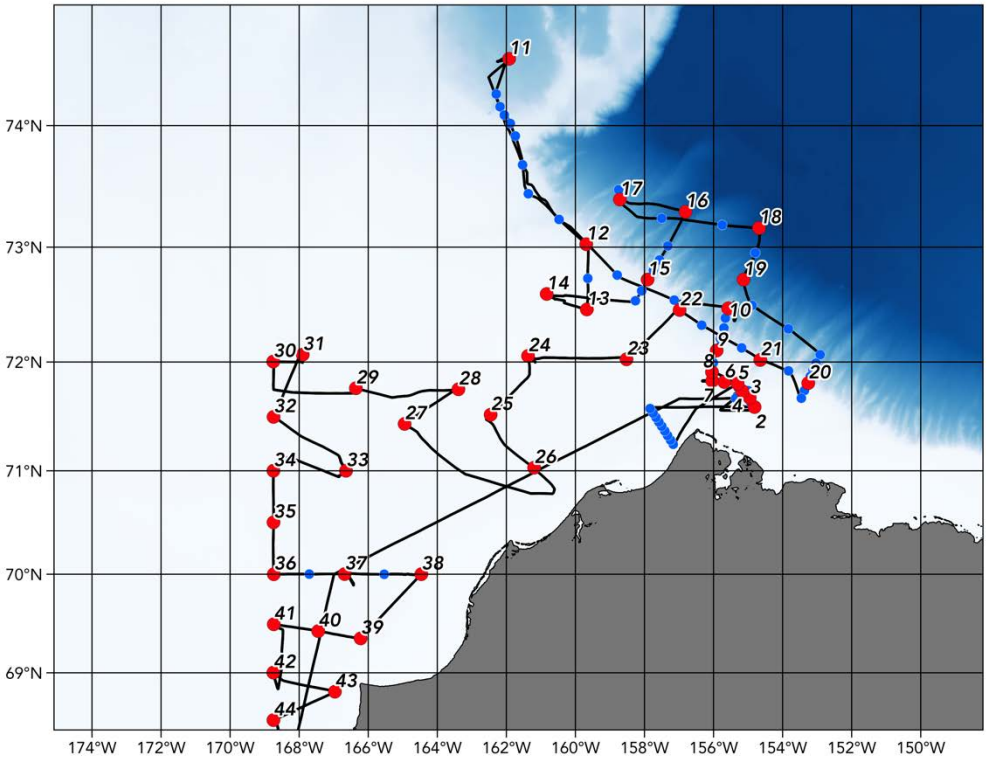

Figure 1.4-2: Detailed cruise track and CTD/XCTD stations for the Chukchi and Beaufort Seas. Station IDs are also shown.

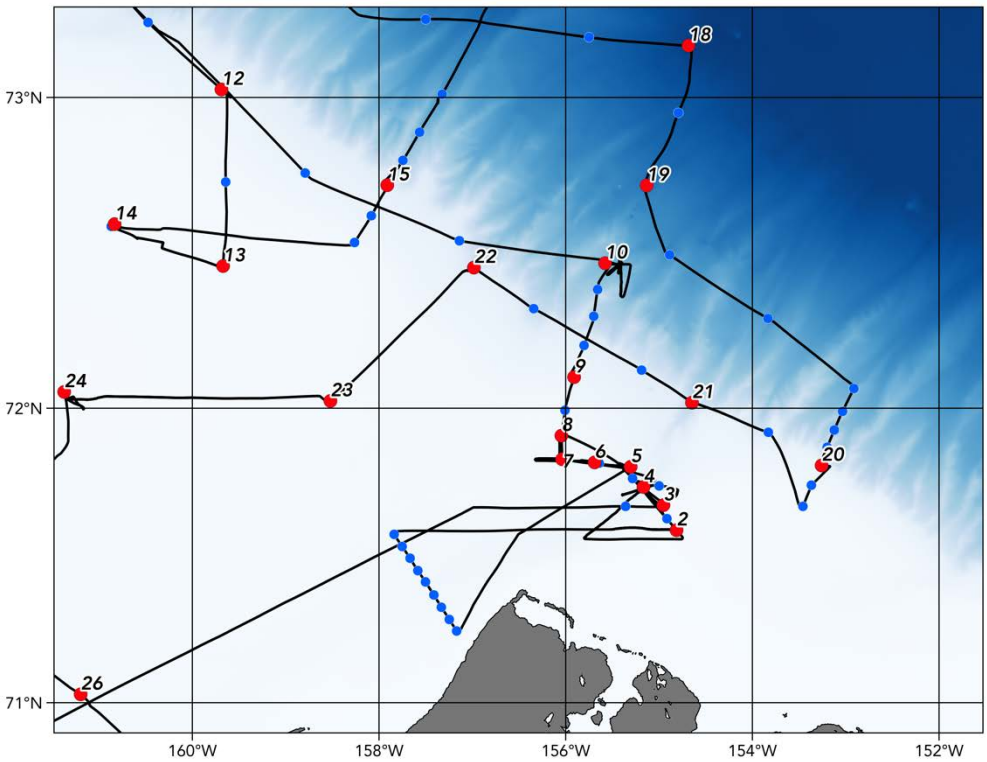

Figure 1.4-3: Detailed cruise track and CTD/XCTD stations for near the Pt. Barrow.

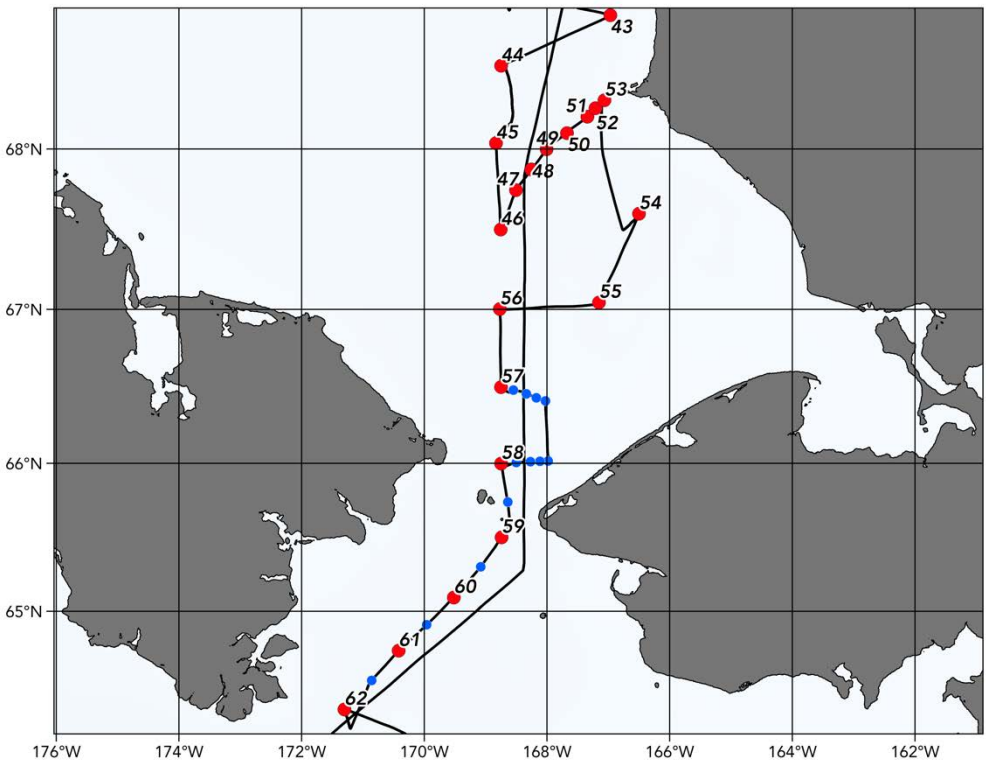

Figure 1.4-4: Detailed cruise track and CTD/XCTD stations around Bering Strait

1.5. List of participants

Table 1.5-1: List of participants of MR21-05C.

No.	Name	Organization	Position
1	Amane Fujiwara	Japan Agency for Marine-Earth Science and Technology (JAMSTEC)	Research Scientist
2	Motoyo Itoh	Japan Agency for Marine-Earth Science and Technology (JAMSTEC)	Assistant Professor
3	Jonotaro Onodera	Japan Agency for Marine-Earth Science and Technology (JAMSTEC)	Research Scientist
4	Mariko Hatta	Japan Agency for Marine-Earth Science and Technology (JAMSTEC)	Senior Scientist
5	Hiroshi Yoshida	Japan Agency for Marine-Earth Science and Technology (JAMSTEC)	Research Scientist
6	Kiyotaka Tanaka	Japan Agency for Marine-Earth Science and Technology (JAMSTEC)	Project Researcher
7	Makoto Sugesawa	Japan Agency for Marine-Earth Science and Technology (JAMSTEC)	Research Student/Graduate Student
8	Takeshi Kinase	Japan Agency for Marine-Earth Science and Technology (JAMSTEC)	Post-Doctoral Researcher
9	Takuhei Shiozaki	Atmosphere Ocean Research Institute, The University of Tokyo	Associate Professor
10	Yasushi Fujiwara	Graduate School of Frontier Sciences, The University of Tokyo	Research Scientist
11	Ryosuke Uchiyama	Graduate School of Frontier Sciences, The University of Tokyo	Graduate Student
12	Eun Yae Son	Atmosphere Ocean Research Institute, The University of Tokyo	Graduate Student
13	Daiki Nomura	Field Science Center for Northern Biosphere, Hokkaido University	Associate Professor
14	Manami Tozawa	Graduate School of Fisheries Silences, Hokkaido University	Graduate Student
15	Kohei Matsuno	Faculty of Fisheries Sciences, Hokkaido University	Associate Professor
16	Wakana Endo	Graduate School of Fisheries Silences, Hokkaido University	Graduate Student
17	Tatsuya Kawakami	Faculty of Fisheries Sciences, Hokkaido University	Research Scientist

18	Kohei Sumiya	Japan Agency for Marine-Earth Science and Technology (JAMSTEC)	Technical Staff
19	Makoto Ozaki	Japan Agency for Marine-Earth Science and Technology (JAMSTEC)	Technical Staff
21	Ryo Oyama	Nippon Marine Enterprises, Ltd.	Technical Staff
22	Ryo Kimura	Nippon Marine Enterprises, Ltd.	Technical Staff
23	Kazuho Yoshida	Nippon Marine Enterprises, Ltd.	Technical Staff
24	Satomi Ogawa	Nippon Marine Enterprises, Ltd.	Technical Staff
25	Masahiro Orui	Marine Works Japan Ltd.	Technical Staff
26	Rei Ito	Marine Works Japan Ltd.	Technical Staff
27	Akira So	Marine Works Japan Ltd.	Technical Staff
28	Katsunori Sagishima	Marine Works Japan Ltd.	Technical Staff
29	Hiroaki Sako	Marine Works Japan Ltd.	Technical Staff
30	Daiki Ushiromura	Marine Works Japan Ltd.	Technical Staff
31	Hiroyuki Nakajima	Marine Works Japan Ltd.	Technical Staff
32	Keita Hayashi	Marine Works Japan Ltd.	Technical Staff
33	Makoto Takada	Marine Works Japan Ltd.	Technical Staff
34	Noriyuki Kisen	Marine Works Japan Ltd.	Technical Staff
35	Minori Kamikawa	Marine Works Japan Ltd.	Technical Staff
36	Misato Kuwahara	Marine Works Japan Ltd.	Technical Staff
37	Tomoko Miyoshi	Marine Works Japan Ltd.	Technical Staff
38	Nagisa Fujiki	Marine Works Japan Ltd.	Technical Staff
39	Tomomi Sone	Marine Works Japan Ltd.	Technical Staff

40	Aine Yoda	Marine Works Japan Ltd.	Technical Staff
41	Erii Irie	Marine Works Japan Ltd.	Technical Staff
42	Airi Hara	Marine Works Japan Ltd.	Technical Staff
43	Yuta Oda	Marine Works Japan Ltd.	Technical Staff
44	Shintaro Amikura	Marine Works Japan Ltd.	Technical Staff
45	David Snider	Martech Polar	Ice Pilot

2. Meteorology

2.1. C-band weather radar

(1) Personnel

Fumikazu TAKETANI	(JAMSTEC)	(not on board)
Masaki KATSUMATA	(JAMSTEC)	(not on board)
Ryo OYAMA	(NME)	
Kazuho YOSHIDA	(NME)	
Satomi OGAWA	(NME)	
Ryo KIMURA	(NME)	
Yoichi INOUE	(Mirai Crew)	

(2) Objectives

The objective of weather radar observations is to investigate the structures and evolutions of precipitating systems over the high-latitude region including arctic ocean.

(3) Instrumentation and methods

i. Radar specifications

The C-band weather radar on board the R/V Mirai was used. Basic specifications of the radar are as follows:

Frequency:	5370 MHz (C-band)
Polarimetry:	Horizontal and vertical (simultaneously transmitted and received)
Transmitter:	Solid-state transmitter
Pulse Configuration:	Using pulse-compression
Output Power:	6 kW (H) + 6 kW (V)
Antenna Diameter:	4 meters
Beam Width:	1.0 degrees
Inertial Navigation Unit:	PHINS (IXBLUE S.A.S)

ii. Available radar variables

Radar variables, which were converted from the power and phase of the backscattered signal at vertically- and horizontally-polarized channels, were as follows:

Radar reflectivity:	Z
Doppler velocity:	Vr
Spectrum width of Doppler velocity:	SW
Differential reflectivity:	Z_{DR}
Differential propagation phase:	Φ_{DP}
Specific differential phase:	K_{DP}
Co-polar correlation coefficients:	ρ_{HV}

iii. Operation methodology

The antenna was controlled to point the commanded ground-relative direction, by controlling the azimuth and elevation to cancel the ship attitude (roll, pitch and yaw) detected by the laser gyro. The Doppler velocity was also corrected by subtracting the ship movement in beam direction.

For the maintenance, internal signals of the radar were checked and

calibrated at the beginning and the end of the cruise. Meanwhile, the following parameters were checked daily; (1) frequency, (2) mean output power, (3) pulse width, and (4) PRF (pulse repetition frequency).

During the cruise, the radar was operated as in Table 2.1-1. A dual PRF mode was used for a volume scan. For RHI and surveillance PPI scans, a single PRF mode was used.

(4) Preliminary results

The C-band weather radar observations were conducted through the cruise, except in the area where the operations were prohibited by Japanese license. The observation started at 04UTC on 01 Sep. 2021, and continued until 00UTC on 18 Oct. 2021.

The obtained data will be analyzed after the cruise.

(5) Data archive

All data obtained during this cruise will be submitted to the JAMSTEC Data Management Group (DMG).

Table 2.1-1: Scan modes of C-band weather radar

	Surveillance PPI Scan	Volume Scan						RHI Scan
Repeated Cycle (min.)	30	6						6
Times in One Cycle	1	1						3
PRF(s) (Hz)	400	dual PRF (ray alternative)						1250
		667	833	938	1250	1333	2000	
Azimuth (deg)	Full Circle							Option
Bin Spacing (m)	150							
Max. Range (km)	300	150		100		60		100
Elevation Angle(s) (deg.)	0.5	0.5		1.0, 1.8, 2.6, 3.4, 4.2, 5.1, 6.2, 7.6, 9.7, 12.2, 15.2		18.7, 23.0, 27.9, 33.5, 40.0		0.0 ~ 60.0

2.2. Optical Disdrometer

(1) Personnel

Fumikazu TAKETANI	(JAMSTEC)	(not on board)
Masaki KATSUMATA	(JAMSTEC)	(not on board)

(2) Objectives

The disdrometer can continuously obtain size distribution of raindrops. The objective of this observation is (a) to reveal microphysical characteristics of the rainfall, depends on the type, temporal stage, etc. of the precipitating clouds, (b) to retrieve the coefficient to convert radar reflectivity (especially from C-band radar in Section 5.3) to the rainfall amount, and (c) to validate the algorithms and the products of the satellite-borne precipitation radars; TRMM/PR and GPM/DPR.

(3) Instrumentations and Methods

Two “Laser Precipitation Monitor (LPM)” (Adolf Thies GmbH & Co) are utilized. It is an optical disdrometer. The instrument consists of the transmitter unit which emit the infrared laser, and the receiver unit which detects the intensity of the laser come thru the certain path length in the air. When a precipitating particle fall thru the laser, the received intensity of the laser is reduced. The receiver unit detect the magnitude and the duration of the reduction and then convert them onto particle size and fall speed. The sampling volume, i.e. the size of the laser beam “sheet”, is 20 mm (W) x 228 mm (D) x 0.75 mm (H).

The particles are categorized by the detected size and fall speed and counted the number in each category every minutes. The categories are shown in Table 2.2-1.

The LPMs are installed on the top (roof) of the anti-rolling system, as shown in Fig. 2.2-1. Both are installed at the corner at the bow side and the starboard side. One (in aft) equipped the "wind protection element" to reduce the effect of the wind on the measurement, and to estimate the effectiveness of the "element" by comparing data from two sensors.

(4) Preliminary Results

The data have been obtained all through the cruise, except non-permitted territorial waters and EEZs. The further analyses for the rainfall amount, drop-size-distribution parameters, etc., will be carried out after the cruise.

(5) Data Archive

All data obtained during this cruise will be submitted to the JAMSTEC Data Management Group (DMG).

(6) Acknowledgment

The operations are supported by Japan Aerospace Exploration Agency (JAXA) Precipitation Measurement Mission (PMM).

Fig. 2.2-1: Onboard LPM sensors. (Left) The location of the sensors, as designated by the red broken circle. (Right) The sensors. Right one (aft one) equipped wind protection element to reduce the effect of the wind, while left one (fore one) did not.

Table 2.2-1: Categories of the particle size and the fall speed.

Particle Size		
Class	Diameter [mm]	Class width [mm]
1	≥ 0.125	0.125
2	≥ 0.250	0.125
3	≥ 0.375	0.125
4	≥ 0.500	0.250
5	≥ 0.750	0.250
6	≥ 1.000	0.250
7	≥ 1.250	0.250
8	≥ 1.500	0.250
9	≥ 1.750	0.250
10	≥ 2.000	0.500
11	≥ 2.500	0.500
12	≥ 3.000	0.500
13	≥ 3.500	0.500
14	≥ 4.000	0.500
15	≥ 4.500	0.500
16	≥ 5.000	0.500
17	≥ 5.500	0.500
18	≥ 6.000	0.500
19	≥ 6.500	0.500
20	≥ 7.000	0.500
21	≥ 7.500	0.500
22	≥ 8.000	unlimited

Fall Speed		
Class	Speed [m/s]	Class width [m/s]
1	≥ 0.000	0.200
2	≥ 0.200	0.200
3	≥ 0.400	0.200
4	≥ 0.600	0.200
5	≥ 0.800	0.200
6	≥ 1.000	0.400
7	≥ 1.400	0.400
8	≥ 1.800	0.400
9	≥ 2.200	0.400
10	≥ 2.600	0.400
11	≥ 3.000	0.800
12	≥ 3.400	0.800
13	≥ 4.200	0.800
14	≥ 5.000	0.800
15	≥ 5.800	0.800
16	≥ 6.600	0.800
17	≥ 7.400	0.800
18	≥ 8.200	0.800
19	≥ 9.000	1.000
20	≥ 10.000	10.000

2.3. Micro Rain Radar

(1) Personnel

Fumikazu TAKETANI	(JAMSTEC)	(not on board)
Masaki KATSUMATA	(JAMSTEC)	(not on board)

(2) Objectives

The micro rain radar (MRR) is a compact vertically-pointing Doppler radar, to detect vertical profiles of rain drop size distribution. The objective of this observation is to understand detailed vertical structure of the precipitating systems.

(3) Instruments and Methods

The MRR-2 (METEK GmbH) was utilized. The specifications are in Table 2.3-1. The antenna unit was installed at the starboard side of the anti-rolling systems (see Fig. 2.3-1), and wired to the junction box and laptop PC inside the vessel.

The data was averaged and stored every 1 minute. The vertical profile of each parameter was obtained every 100 meters in range distance (i.e. height) up to 3100 meters. The recorded parameters were; Drop size distribution, radar reflectivity, path-integrated attenuation, rain rate, liquid water content and fall velocity.

Fig. 2.3-1: Onboard MRR sensor. (Left) The location of the sensors, as designated by the red broken circle. (Right) The antenna unit.

Table 2.3-1: Specifications of the MRR-2.

Transmitter power	50 mW
Operating mode	FM-CW
Frequency	24.230 GHz (modulation 1.5 to 15 MHz)
3dB beam width	1.5 degrees
Spurious emission	< -80 dBm / MHz
Antenna Diameter	600 mm
Gain	40.1 dBi

(4) Preliminary Results

The data have been obtained all through the cruise, except non-permitted territorial waters and EEZs. The further analyses will be after the cruise.

(5) Data Archive

All data obtained during this cruise will be submitted to the JAMSTEC Data Management Group (DMG).

(6) Acknowledgment

The operations are supported by Japan Aerospace Exploration Agency (JAXA) Precipitation Measurement Mission (PMM).

2.4. GNSS precipitable water

(1) Personnel

Fumikazu TAKETANI	(JAMSTEC)	(not on board)
Masaki KATSUMATA	(JAMSTEC)	(not on board)
Mikiko FUJITA	(JAMSTEC)	(not on board)

(2) Objectives

Getting the GNSS satellite data to estimate the total column integrated water vapor content of the atmosphere.

(3) Instruments and Methods

The GNSS satellite data was archived to the receiver (Trimble NetR9) with 5 sec interval. The GNSS antenna (Margrin) was set on the roof of aft wheel house. The observations were carried out all through the cruise.

(4) Preliminary Results

We will calculate the total column integrated water from observed GNSS satellite data after the cruise.

(5) Data Archive

Raw data is recorded as T02 format and stream data every 5 seconds. These raw datasets are available from Mikiko Fujita of JAMSTEC. Corrected data will be submitted to JAMSTEC Marine-Earth Data and Information Department and will be archived there.

2.5. Microwave Radiometer

(1) Personnel

Fumikazu TAKETANI	(JAMSTEC)	(not on board)
Masaki KATSUMATA	(JAMSTEC)	

(2) Objective

To retrieve total column integrated water vapor content of the atmosphere.

(3) Method

The microwave radiometer (hereafter MWR; manufactured by Furuno Electric Co., Ltd.) is used. The MWR received natural microwave within the angle of 20 deg. from zenith, at the frequencies around 22 GHz. The received signal can be converted to the column integrated water vapor (or precipitable water). The observation was made every 20 seconds except when periodic auto-calibration was on-going (once in several minutes). The rain sensor is equipped to identify the period of rainfall.

In addition to the MWR, the whole sky camera was installed beside the MWR. This is to monitor cloud cover, which also affects the microwave signals. The camera obtained the whole-sky image every 2 minutes.

Both instruments were installed at the top of the roof of aft wheelhouse, as in Fig. 2.5-1. The data were continuously obtained all through the cruise period.

(4) Results

The all data are archived in the sensor unit. The obtained data will be retrieved and analyzed after the end of the cruise.

(5) Data archive

The data will be submitted to the JAMSTEC Data Management Group (DMG).

(6) Acknowledgment

The observation was supported by the JSPS KAKENHI Grant 20H04306.

Fig. 2.5-1: Outlook of the microwave radiometer (right) and the whole-sky camera (left) installed at the roof of the aft wheelhouse.

2.6. Surface Meteorological Observations

(1) Personnel

Amane Fujiwara	JAMSTEC	-PI
Ryo Oyama	NME (Nippon Marine Enterprises, Ltd.)	
Kazuho Yoshida	NME	
Satomi Ogawa	NME	
Ryo Kimura	NME	
Yoichi Inoue	MIRAI Crew	

(2) Objectives

Surface meteorological parameters are observed as a basic dataset of the meteorology. These parameters provide the temporal variation of the meteorological condition surrounding the ship.

(3) Parameters

i. MIRAI Surface Meteorological (SMet) system measured parameters are listed in Table 2.6-1.

Table 2.6-1: Parameters of MIRAI SMet system

Parameter	Units	Remarks
1 Latitude	degree	
2 Longitude	degree	
3 Ship's speed	knot	MIRAI log
4 Ship's heading	degree	MIRAI gyro
5 Relative wind speed	m/s	6sec./10min. averaged
6 Relative wind direction	degree	6sec./10min. averaged
7 True wind speed	m/s	6sec./10min. averaged
8 True wind direction	degree	6sec./10min. averaged
9 Barometric pressure	hPa	adjusted to sea surface level 6sec. averaged
10 Air temperature (starboard)	degC	6sec. averaged
11 Air temperature (port)	degC	6sec. averaged
12 Dewpoint temperature (starboard)	degC	6sec. averaged
13 Dewpoint temperature (port)	degC	6sec. averaged
14 Relative humidity (starboard)	%	6sec. averaged
15 Relative humidity (port)	%	6sec. averaged
16 Sea surface temperature	degC	6sec. averaged
17 Precipitation intensity (optical rain gauge)	mm/hr	hourly accumulation
18 Precipitation (capacitive rain gauge)	mm/hr	hourly accumulation
19 Downwelling shortwave radiation	W/m^2	6sec. averaged
20 Downwelling infra-red radiation	W/m^2	6sec. averaged

21 Significant wave height (bow)	m	hourly
22 Significant wave height (stern)	m	hourly
23 Significant wave period (bow)	second	hourly
24 Significant wave period (stern)	second	hourly

ii. Shipboard Oceanographic and Atmospheric Radiation (SOAR) system measured parameters are listed in Table 2.6-2.

Table 2.6-2: Parameters of SOAR system (JamMet)

Parameter	Units	Remarks
1 Latitude	degree	
2 Longitude	degree	
3 SOG	knot	
4 COG	degree	
5 Relative wind speed	m/s	
6 Relative wind direction	degree	
7 Barometric pressure	hPa	
8 Air temperature	degC	
9 Relative humidity	%	
10 Precipitation intensity (optical rain gauge)	mm/hr	
11 Precipitation (capacitive rain gauge)	mm/hr	reset at 50 mm
12 Down welling shortwave radiation	W/m^2	
13 Down welling infra-red radiation	W/m^2	
14 Defuse irradiance	W/m^2	
15 "SeaSnake" raw data	mV	
16 SSST (SeaSnake)	degC	
17 PAR	$microE/cm^2/sec$	
18 UV 305 nm	$microW/cm^2/nm$	
19 UV 320 nm	$microW/cm^2/nm$	
20 UV 340 nm	$microW/cm^2/nm$	
21 UV 380 nm	$microW/cm^2/nm$	

(4) Instruments and methods

In this cruise, the two systems for the observation were used.

i. SMet system

Instruments of SMet system are listed in Table 2.6-3. Data were collected and processed by KOAC-7800 weather data processor made by Koshin-Denki, Japan. The data set consists of 6 seconds averaged data.

Table 2.6-3: Instruments and installation locations of SMet system

Sensors	Type	Manufacturer	Location (altitude from surface)
Anemometer	KS-5900	Koshin Denki,	Foremast (25 m)

		Japan	
Tair/RH with aspirated radiation shield	HMP155 43408 Gill	Vaisala, Finland R.M. Young, U.S.A.	Compass deck (21 m) starboard and port side
Thermometer: SST	RFN2-0	Koshin Denki, Japan	4th deck (-1m, inlet -5m)
Barometer	Model-370	Setra System, U.S.A.	Captain deck (13 m) Weather observation room
Capacitive rain gauge	50202	R. M. Young, U.S.A.	Compass deck (19 m)
Optical rain gauge	ORG-815DS	Osi, USA	Compass deck (19 m)
Radiometer (short wave)	MS-802	Eko Seiki, Japan	Radar mast (28 m)
Radiometer (long wave)	MS-202	Eko Seiki, Japan	Radar mast (28 m)
Wave height meter	WM-2	Tsurumi-seiki, Japan	Bow (10 m) Stern (8m)

ii. SOAR measurement system

SOAR system designed by BNL (Brookhaven National Laboratory, USA) consists of major five parts.

a) Analog meteorological data sampling with CR1000 logger manufactured by Campbell Scientific Inc. Canada – wind pressure, and rainfall (by a capacitive rain gauge) measurement.
b) Digital meteorological data sampling from individual sensors - air temperature, relative humidity and precipitation (by optical rain gauge (ORG)) measurement.
c) Radiation data sampling with CR1000X logger manufactured by Campbell Inc. and radiometers with ventilation unit manufactured by Hukseflux Thermal Sensors B.V. Netherlands – short and long wave downward radiation measurement.
d) Photosynthetically Available Radiation (PAR) sensor manufactured by Biospherical Instruments Inc. (USA) - PAR measurement.
e) Scientific Computer System (SCS) developed by NOAA (National Oceanic and Atmospheric Administration, USA) - centralized data acquisition and logging of all data sets.

SCS recorded radiation, air temperature, relative humidity, CR1000 and ORG data. SCS composed Event data (JamMet) from these data and ship's navigation data every 6 seconds. Instruments and their locations are listed in Table 2.6-4.

Table 2.6-4: Instruments and installation locations of SOAR system

Sensors (Meteorological)	Type	Manufacturer	Location (altitude from surface)
Anemometer	05106	R.M. Young, USA	Foremast (25 m)
Barometer with pressure port	PTB210 61002 Gill	VAISALA, Finland R.M. Young, USA	Foremast (23 m)
Rain gauge	50202	R.M. Young, USA	Foremast (24 m)
Tair/RH with aspirated radiation shield	HMP155 43408 Gill	VAISALA, Finland R.M. Young, USA	Foremast (23 m)
Optical rain gauge	ORG-815DR	Osi, USA	Foremast (24 m)

Sensors (Radiation)	Type	Manufacturer	Location *
Radiometer (short wave) with ventilation unit	SR20 VU01	Hukseflux Thermal Sensors B.V., Netherlands	Foremast (25 m)
Radiometer (long wave) with ventilation unit	IR20 VU01	Hukseflux Thermal Sensors B.V., Netherlands	Foremast (25 m)

Sensor (PAR&UV)	Type	Manufacturer	Location (altitude from surface)
PAR&UV sensor	PUV-510	Biospherical Instrum ents Inc., USA	Navigation deck (18m)

For the quality control as post processing, we checked the following sensors, before and after the cruise.

i. Young Rain gauge (SMet and SOAR)
   Inspect of the linearity of output value from the rain gauge sensor to change Input value by adding fixed quantity of test water.
ii. Barometer (SMet and SOAR)
   Comparison with the portable barometer value, PTB220, VAISALA
iii. Thermometer (air temperature and relative humidity) (SMet and SOAR)
   Comparison with the portable thermometer value, HM70, VAISALA

(5) Observation log

31 Aug. 2021 - 21 Oct. 2021

(6) Preliminary results

Figure. 2.6-1 shows the time series of the following parameters;

Wind (SOAR)

Air temperature (SMet)
Relative humidity (SMet)
Precipitation (SOAR, ORG)
Short / Long wave radiation (SOAR)
Pressure (SMet)
Sea surface temperature (SMet)
Significant wave height (SMet)

(7) Data archives

These data obtained in this cruise will be submitted to the Data Management Group of JAMSTEC, and will be opened to the public via "Data Research System for Whole Cruise Information in JAMSTEC (DARWIN)" in JAMSTEC web site.
<http://www.godac.jamstec.go.jp/darwin/e>

(8) Remarks (Times in UTC)

i) The following periods, Sea surface temperature of SMet data were available.
00:00UTC 01 Sep. 2021 - 23:00UTC 04 Oct. 2021
22:05UTC 06 Oct. 2021 - 06:00UTC 18 Oct. 2021

ii) The following time, increasing of SMet capacitive rain gauge data were invalid due to MF/HF radio transmission.
04:48UTC 05 Sep. 2021 - 05:06UTC 05 Sep. 2021
03:41UTC 16 Oct. 2021 - 03:51UTC 16 Oct. 2021
05:16UTC 20 Oct. 2021 - 05:23UTC 20 Oct. 2021

iii) The following periods, SMet wind speed/direction were measured by the ultrasonic anemometer on the aftermast.
01:04UTC 13 Sep. 2021 - 08:16UTC 14 Sep. 2021

iv) The following period, wind speed/direction data sometimes contain irregular value or large fluctuation due to sensor failure.
22:05UTC 15 Sep. 2021 - 22:06UTC 15 Sep. 2021
05:39UTC 19 Sep. 2021 - 09:24UTC 19 Sep. 2021
15:13UTC 29 Sep. 2021 - 15:51UTC 29 Sep. 2021
08:17UTC 11 Oct. 2021 - 11:40UTC 11 Sep. 2021

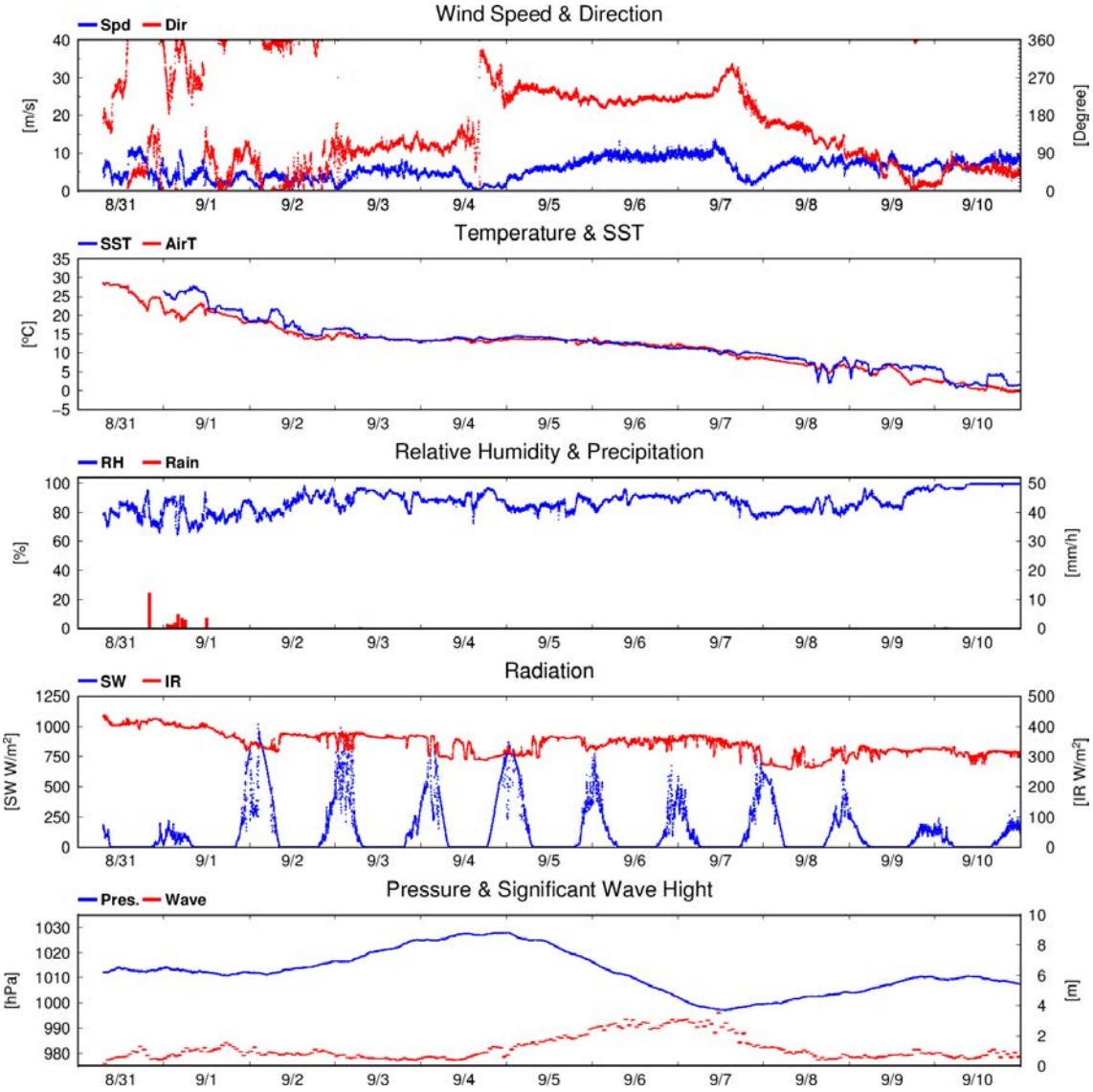

Figure 2.6-1: Time series of surface meteorological parameters during this cruise

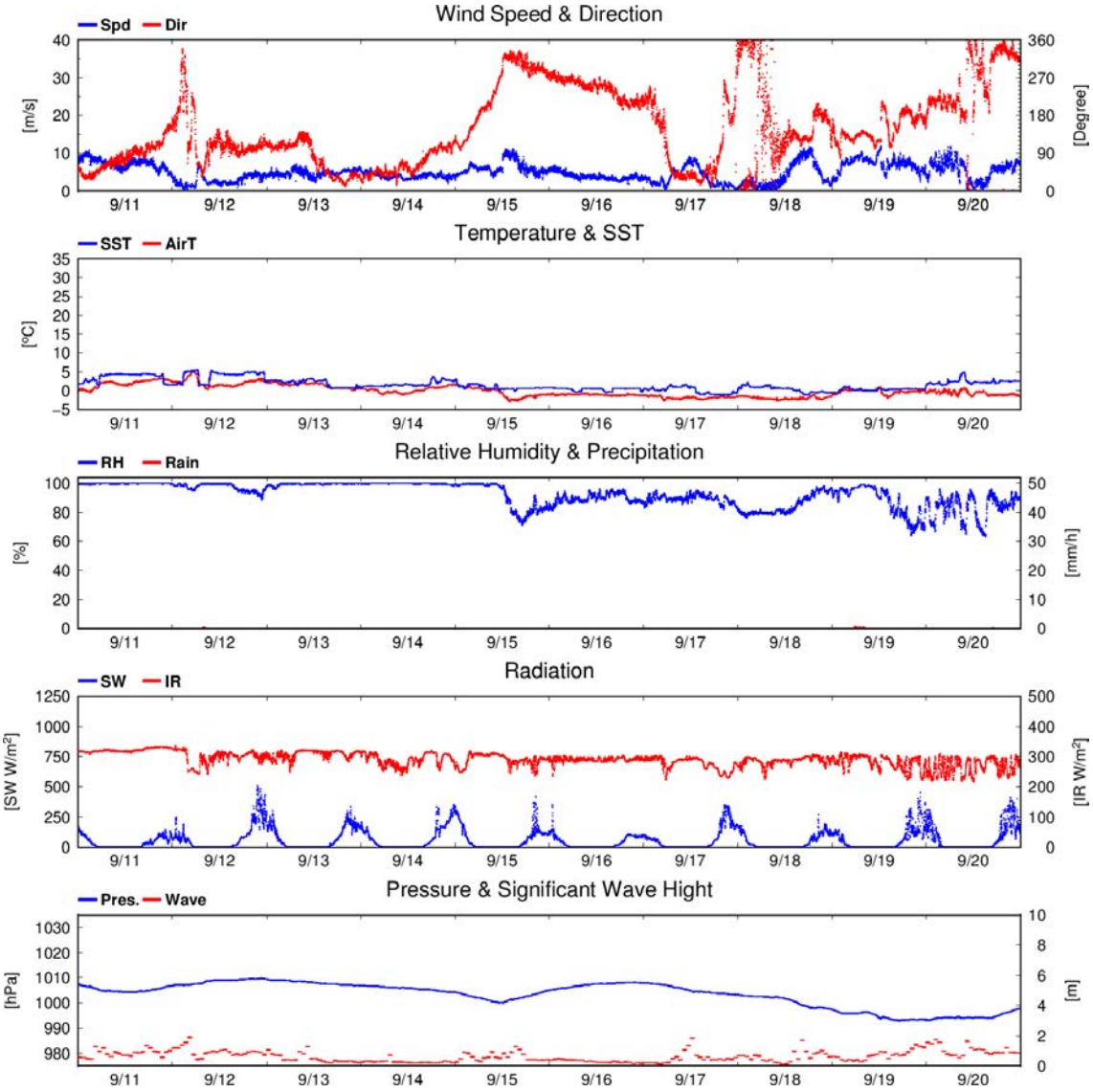

Figure 2.6-1: (Continued)

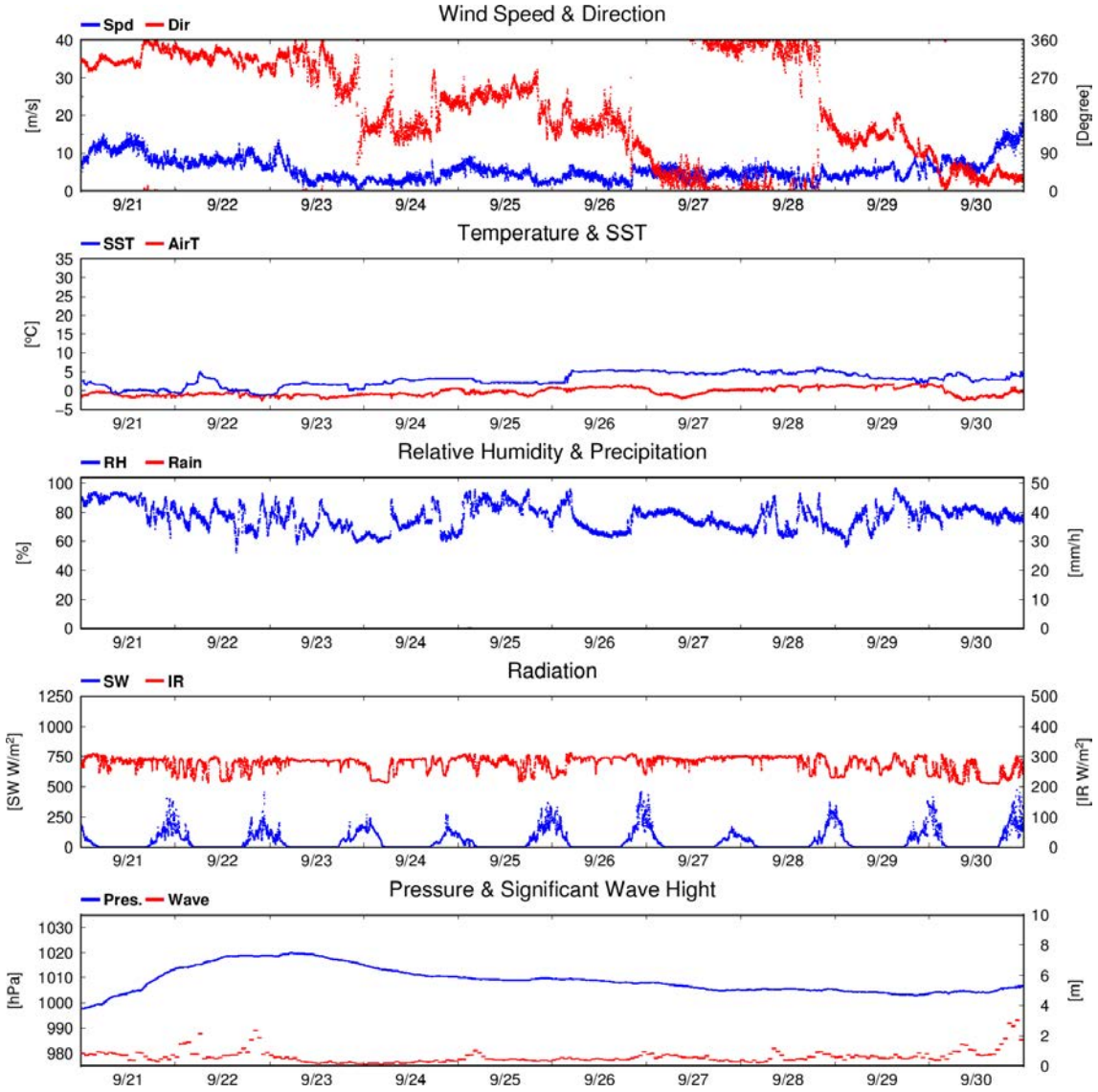

Figure 2.6-1: (Continued)

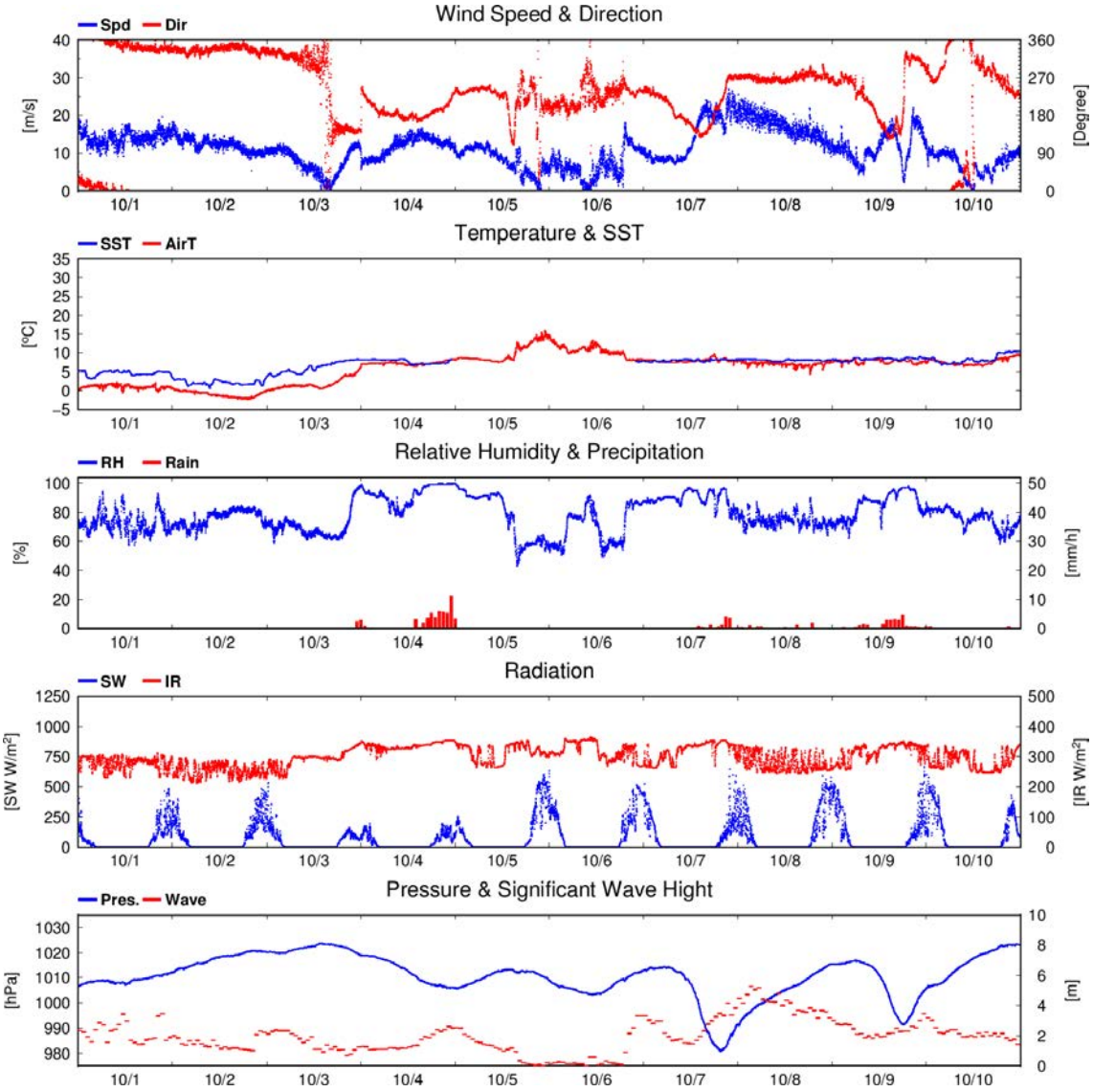

Figure 2.6-1: (Continued)

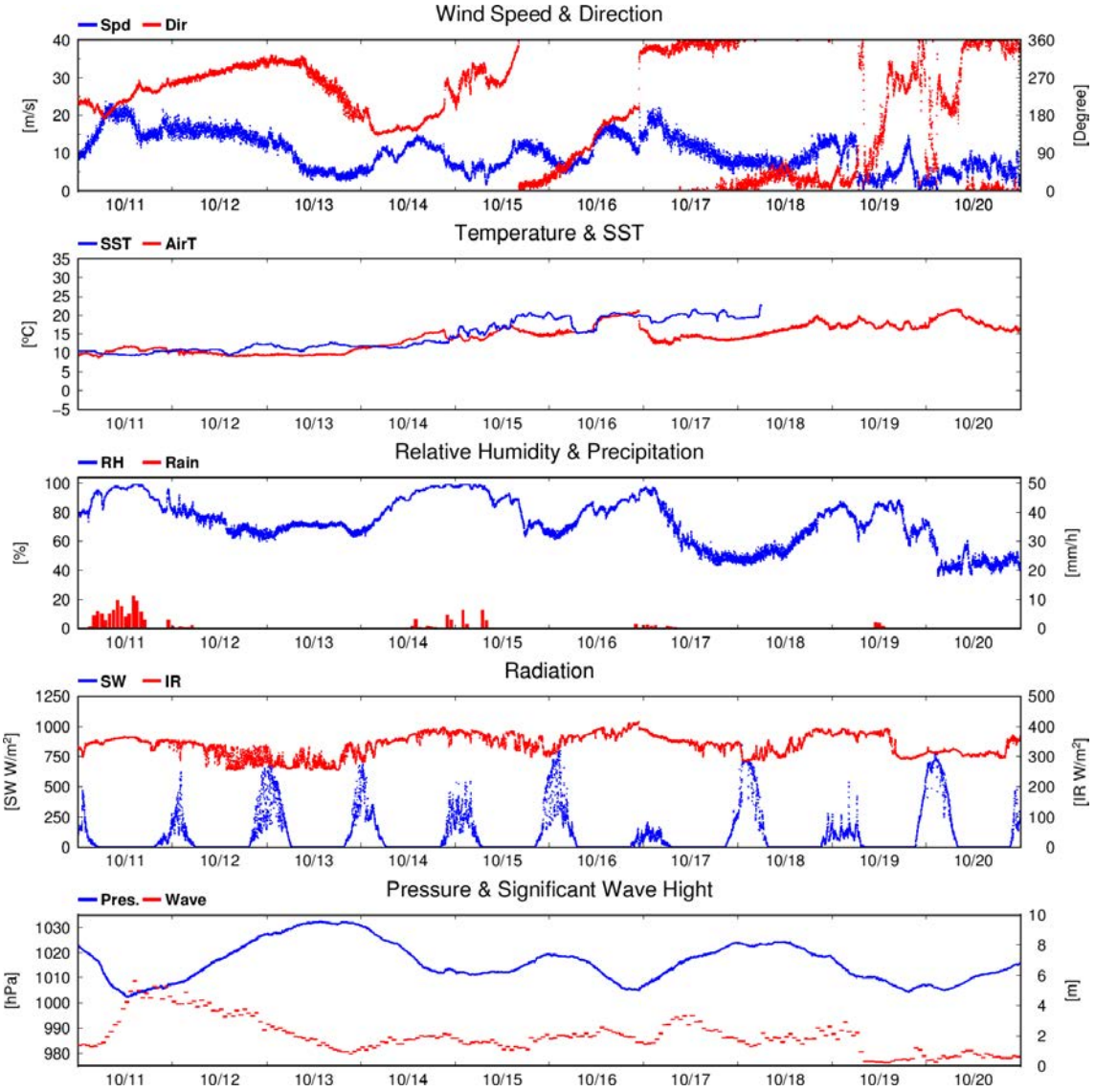

Figure 2.6-1: (Continued)

2.7. Ceilometer

(1) Personnel

Amane Fujiwara	JAMSTEC	-PI
Ryo Oyama	NME (Nippon Marine Enterprises, Ltd.)	
Kazuho Yoshida	NME	
Satomi Ogawa	NME	
Ryo Kimura	NME	
Yoichi Inoue	MIRAI Crew	

(2) Objectives

The information of cloud base height and the liquid water amount around cloud base is important to understand the process on formation of the cloud. As one of the methods to measure them, the ceilometer observation was carried out.

(3) Parameters

Cloud base height [m].

Backscatter profile, sensitivity and range normalized at 10 m resolution.

Estimated cloud amount [oktas] and height [m]; Sky Condition Algorithm.

(4) Instruments and methods

Cloud base height and backscatter profile were observed by ceilometer (CL51, VAISALA, Finland). The measurement configurations are shown in Table 2.7-1. On the archive dataset, cloud base height and backscatter profile are recorded with the resolution of 10 m.

Table 2.7-1: The measurement configurations

Property	Description
Laser source	Indium Gallium Arsenide (InGaAs) Diode
Transmitting center wavelength	910±10 nm at 25 degC
Transmitting average power	19.5 mW
Repetition rate	6.5 kHz
Detector	Silicon avalanche photodiode (APD)
Responsibility at 905 nm	65 A/W
Cloud detection range	0 ~ 13 km
Measurement range	0 ~ 15 km
Resolution	10 m in full range
Sampling rate	36 sec.
Sky Condition	Cloudiness in octas (0 ~ 9) 0 Sky Clear 1 Few 3 Scattered 5-7 Broken 8 Overcast

(5) Observation log

31 Aug. 2021 - 21 Oct. 2021

(6) Preliminary results

Figure 2.7-1 shows the time-series of the lowest, second and third cloud base height during the cruise.

(7) Data archives

These data obtained in this cruise will be submitted to the Data Management Group of JAMSTEC, and will be opened to the public via "Data Research System for Whole Cruise Information in JAMSTEC (DARWIN)" in JAMSTEC web site.
<http://www.godac.jamstec.go.jp/darwin/e>

(8) Remarks (Times in UTC)

Window cleaning

18:42UTC 07 Sep. 2021
19:02UTC 15 Sep. 2021
22:21UTC 22 Sep. 2021
19:30UTC 28 Sep. 2021
18:12UTC 05 Oct. 2021
01:42UTC 09 Oct. 2021
03:16UTC 13 Oct. 2021
04:27UTC 18 Oct. 2021

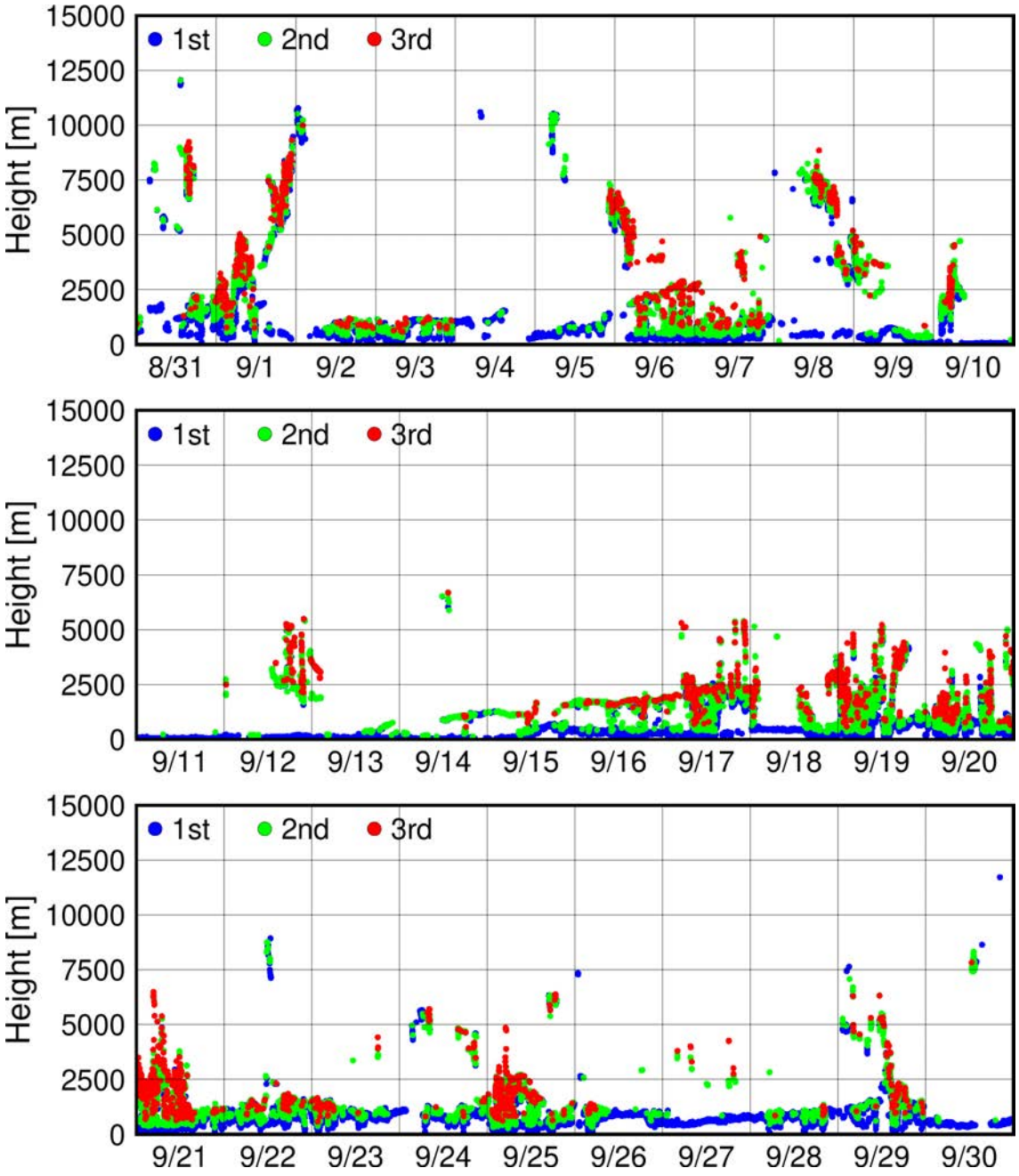

Figure 2.7-1: Time series of cloud base height during this cruise

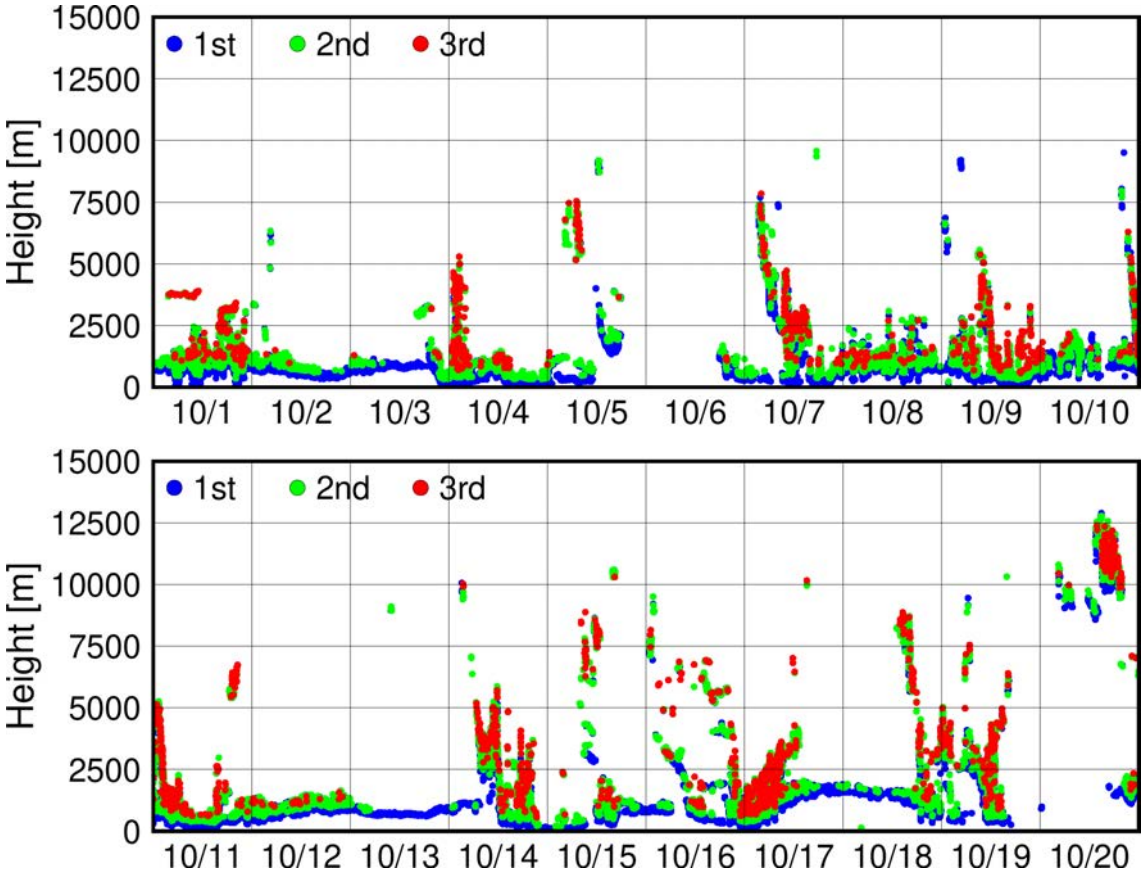

Figure 2.7-1: (Continued)

2.8 Tropospheric gas and particles observation

2.8.1. Atmospheric surface observation for trace gas and aerosols

(1) Personnel

Fumikazu Taketani	JAMSTEC(Principal Investigator)	
- not on board		
Takeshi Kinase	JAMSTEC	- on board
Masayuki Takigawa	JAMSTEC	- not on board
Yugo Kanaya	JAMSTEC	- not on board
Takuma Miyakawa	JAMSTEC	- not on board
Hisahiro Takashima	JAMSTEC/Fukuoka Univ.	- not on board
Kazuyo Yamaji	JAMSTEC/Kobe Univ.	- not on board
Yutaka Tobo	NIPR	- not on board
Zhu Chunmao	JAMSTEC	- not on board

(2) Objectives

・To investigate roles of gas and aerosols in the marine atmosphere in relation to climate change
・To investigate processes of biogeochemical cycles between the atmosphere and the ocean.
・To investigate gas and aerosol transports from anthropogenic activities
・To investigate physical and -chemical particle states of aerosols
・To investigate contribution of suspended particles to the rain, and snow

(3) Parameters

・Particle size distribution
・Black carbon(BC) and fluorescent particles
・Aerosol extinction coefficient (AEC)
・Composition of ambient particles
・Individual particle features of ambient particles
・Hygroscopicity and ice nucleation of ambient particles
・Composition of snow and rain
・Surface ozone(O_3), and carbon monoxide(CO) mixing ratios

(4) Instruments and methods

(4-1) Online aerosol observations:

(4-1-1) Particle size distribution

The size distribution of aerosol particles was measured by a scanning mobility particle sizer (SMPS) (Nano Scan model 3910, TSI), and a handheld optical particle counter (OPC) (KR-12A, Rion).

(4-1-2) Black carbon (BC)

Number and mass BC concentration and their size distribution were measured by an instrument based on laser-induced incandescence, single particle soot photometer (SP2) (model D, Droplet Measurement Technologies). The laser-induced incandescence technique based on intracavity Nd:YVO4 laser operating at 1064 nm were used for detection of single particles of BC.

(4-1-3) Fluorescent property

Fluorescent properties of aerosol particles were measured by a single particle fluorescence sensor, Waveband Integrated bioaerosol sensor (WIBS4) (WIBS-4A, Droplet Measurement Technologies). Two pulsed xenon lamps emitting UV light (280 nm and 370 nm) were used for excitation. Fluorescence emitted from a single particle within 310–400 nm and 420–650 nm wavelength windows was recorded.

(4-1-4) Aerosol extinction coefficient (AEC)

Multi-Axis Differential Optical Absorption Spectroscopy (MAX-DOAS), a passive remote sensing technique measuring spectra of scattered visible and ultraviolet (UV) solar radiation, was used for atmospheric aerosol and gas profile measurements. Our MAX-DOAS instrument consists of two main parts: an outdoor telescope unit and an indoor spectrometer (Acton SP-2358 with Princeton Instruments PIXIS-400B), connected to each other by a 14-m bundle optical fiber cable. The line of sight was in the directions of the portside of the vessel and the scanned elevation angles were 2, 3, 4, 6, 10, 20, 90 degrees in the 30-min cycle. The roll motion of the ship was measured to autonomously compensate for additional motion of the prism, employed for scanning the elevation angle.

For the selected spectra recorded with elevation angles with good accuracy, DOAS spectral fitting was performed to quantify the slant column density (SCD) of NO2 (and other gases) and O_4 (O_2-O_2, collision complex of oxygen) for each elevation angle. Then, the O_4 SCDs were converted to the aerosol optical depth (AOD) and the vertical profile of aerosol extinction coefficient (AEC) using an optimal estimation inversion method with a radiative transfer model. The tropospheric vertical column/profile of NO_2 and other gases (including IO) were retrieved using derived aerosol profiles.

The sample air for particle measurements was commonly drawn from the rooftop of the environmental research room through a custom-made concentric tube-type inlet at the sampling rate of 30 L/min for sampling total suspended particulate matters (TSP) (Miyakawa et al., in review) to the SMPS and SP2. A part of the sampler air (~1.5 L/min) was isokinetically extracted and was dehumidified using a large diameter Nafion dryer (MD-700, Perma Pure, Inc.) to eliminate water vapor and liquid water contents of airborne particles (typical values of relative humidity (RH) at the exit of the dryer were lower than ~18% over the Arctic Ocean), and was subsequently introduced via flow splitters to those instruments installed in the environmental research room.

(4-2) Ambient aerosol sampling

Ambient aerosol samplings were carried out by air samplers installed at the compass deck. Ambient particles were coll

These sampling logs are listed in Tables 2.8-1, 2.8-2, 2.8-3, 2.8-4, and 2.8-5. The samples are going to be analyzed in the laboratory.

(4-3) CO and O_3

Ambient air was continuously sampled on the compass deck and drawn through ~20-m-long Teflon tubes connected to a nondispersive infrared (NDIR) CO analyzer (Model 48i-TLE, Thermo Fisher Scientific) and a UV photometric ozone analyzer (model 205, 2B Technologies), located in the environmental research room. The data will be used for characterizing air mass origins

(5) Observation log

Table 2.8.1-1: Log of ambient particles sampling on the quartz filter by a high-volume air sampler.

ID	Data collected (Sampling end)				Latitude			Longitude		
	YYYY	MM	DD	hh:mm: (UTC)	Deg.	Min.	N/S	Deg.	Min.	E/W
MR2105C-HV-001	2021	9	3	7:12	46	52.86	N	159	47.3	E
MR2105C-HV-002	2021	9	5	22:05	53	7.19	N	170	15.9	E
MR2105C-HV-003	2021	9	8	20:30	65	33.34	N	168	22.72	W
MR2105C-HV-004	2021	9	10	18:24	71	43.95	N	155	9.3	W
MR2105C-HV-005	2021	9	12	17:26	71	40.66	N	154	56.92	W
MR2105C-HV-006	2021	9	14	19:45	72	28.12	N	155	25.53	W
MR2105C-HV-007	2021	9	16	22:38	74	31.45	N	161	55.74	W
MR2105C-HV-009	2021	9	18	20:23	73	23.83	N	158	42.81	W
MR2105C-HV-010	2021	9	20	23:37	72	30.49	N	154	55.7	W
MR2105C-HV-011	2021	9	22	23:07	71	44.93	N	163	23.58	W
MR2105C-HV-012	2021	9	24	20:32	70	59.57	N	166	37.1	W
MR2105C-HV-013	2021	9	26	21:03	70	0.23	N	166	38.17	W
MR2105C-HV-014	2021	9	28	19:58	68	53.27	N	168	6.22	W
MR2105C-HV-015	2021	9	30	5:13	68	11.63	N	167	20.92	W
MR2105C-HV-016	2021	10	2	16:59	64	18.35	N	171	17.92	W
MR2105C-HV-017	2021	10	5	0:52	56	21.26	N	166	57.29	W
MR2105C-HV-018	2021	10	9	0:40	53	22.06	N	178	4.64	W
MR2105C-HV-019	2021	10	11	4:02	49	53.46	N	169	27.01	E
MR2105C-HV-020	2021	10	12	22:25	47	21.3	N	164	0.51	E
MR2105C-HV-021	2021	10	15	3:56	42	25	N	153	27.81	E
MR2105C-HV-022	2021	10	18	0:05	37	25.09	N	143	44.16	E

Table 2.8.1-2: Log of ambient particles sampling on the nuclepore filter by a handmade air sampler.

ID	Data collected (Sampling end)				Latitude			Longitude		
	YYYY	MM	DD	hh:mm: (UTC)	Deg.	Min.	N/S	Deg.	Min.	E/W
MR2105C-IN-001	2021	9	3	7:12	46	52.86	N	159	47.3	E
MR2105C-IN-002	2021	9	5	22:05	53	7.19	N	170	15.9	E
MR2105C-IN-003	2021	9	8	20:30	65	33.34	N	168	22.72	W
MR2105C-IN-004	2021	9	10	18:24	71	43.95	N	155	9.3	W
MR2105C-IN-005	2021	9	12	17:26	71	40.66	N	154	56.92	W
MR2105C-IN-006	2021	9	14	19:45	72	28.12	N	155	25.53	W
MR2105C-IN-007	2021	9	16	22:38	74	31.45	N	161	55.74	W
MR2105C-IN-009	2021	9	18	20:23	73	23.83	N	158	42.81	W
MR2105C-IN-010	2021	9	20	23:37	72	30.49	N	154	55.7	W
MR2105C-IN-011	2021	9	22	23:07	71	44.93	N	163	23.58	W
MR2105C-IN-012	2021	9	24	20:32	70	59.57	N	166	37.1	W
MR2105C-IN-013	2021	9	26	21:03	70	0.23	N	166	38.17	W
MR2105C-IN-014	2021	9	28	19:58	68	53.27	N	168	6.22	W
MR2105C-IN-015	2021	9	30	5:13	68	11.63	N	167	20.92	W
MR2105C-IN-016	2021	10	2	16:59	64	18.35	N	171	17.92	W
MR2105C-IN-017	2021	10	5	0:52	56	21.26	N	166	57.29	W
MR2105C-IN-018	2021	10	9	0:40	53	22.06	N	178	4.64	W
MR2105C-IN-019	2021	10	11	4:02	49	53.46	N	169	27.01	E
MR2105C-IN-020	2021	10	12	22:25	47	21.3	N	164	0.51	E
MR2105C-IN-021	2021	10	15	3:56	42	25	N	153	27.81	E
MR2105C-IN-022	2021	10	18	0:05	37	25.09	N	143	44.16	E

Table 2.8.1-3: Log of ambient particles sampling on the Cu grid by an AS-24W sampler.

ID	Data collected (Sampling end)				Latitude			Longitude		
	YYYY	MM	DD	hh:mm: (UTC)	Deg.	Min.	N/S	Deg.	Min.	E/W
MR2105C-TEM-01	2021	9	5	2:20	53	45.15	N	171	6.09	E
MR2105C-TEM-02	2021	9	8	20:20	65	12.27	N	168	35.29	W
MR2105C-TEM-03	2021	9	10	18:20	71	42.64	N	155	4.87	W
MR2105C-TEM-04	2021	9	13	10:36	71	49.93	N	156	17.79	W
MR2105C-TEM-05	2021	9	16	2:30	74	31.64	N	161	59.25	W
MR2105C-TEM-06	2021	9	18	8:40	73	3.35	N	157	13.83	W
MR2105C-TEM-07	2021	9	20	10:40	71	55.49	N	153	47.4	W
MR2105C-TEM-08	2021	9	24	12:40	71	4.17	N	166	46.16	W
MR2105C-TEM-09	2021	9	28	12:40	68	53.47	N	168	40.31	W
MR2105C-TEM-10	2021	10	2	6:35	63	43.49	N	170	25.61	W
MR2105C-TEM-11	2021	10	6	0:30	53	54.19	N	166	31.61	W
MR2105C-TEM-12	2021	10	10	16:30	50	39.05	N	171	9.12	E
MR2105C-TEM-13	2021	10	14	4:30	44	58.11	N	158	4140	E
MR2105C-TEM-14	2021	10	18	4:30	37	23.14	N	143	41.44	E
MR2105C-TEM-15	2021	10	20	6:20	35	3.26	N	138	46.72	E

Table 2.8.1-4: Log of ambient particles sampling on the Cu grid and the Si wafer by an MPS-3 sampler.

ID	Data collected (Sampling end)				Latitude			Longitude		
	YYYY	MM	DD	hh:mm: (UTC)	Deg.	Min.	N/S	Deg.	Min.	E/W
MR2105C-ESEM-01	2021	9	3	4:18	44	10.76	N	155	6.29	E
MR2105C-ESEM-02	2021	9	3	7:30	44	39.32	N	155	54.47	E
MR2105C-ESEM-03	2021	9	4	6:56	47	4.36	N	160	8.32	E
MR2105C-ESEM-04	2021	9	5	3:32	49	46.25	N	165	27.81	E
MR2105C-ESEM-05	2021	9	6	3:15	53	55.14	N	171	20.66	E
MR2105C-ESEM-06	2021	9	7	19:13	60	57.98	N	171	31.86	W
MR2105C-ESEM-07	2021	9	8	0:38	61	55.93	N	175	49.67	W
MR2105C-ESEM-08	2021	9	8	6:24	62	58.85	N	173	54.55	W
MR2105C-ESEM-09	2021	9	8	15:38	64	32.31	N	170	25.72	W
MR2105C-ESEM-10	2021	9	8	20:47	65	16.43	N	168	24.19	W
MR2105C-ESEM-11	2021	9	9	5:29	67	23.01	N	168	21.79	W
MR2105C-ESEM-12	2021	9	9	16:02	69	45.84	N	167	9.4	W
MR2105C-ESEM-13	2021	9	9	23:30	70	38.77	N	163	12.47	W
MR2105C-ESEM-14	2021	9	10	15:50	71	40.2	N	155	0.38	W
MR2105C-ESEM-15	2021	9	12	4:03	71	25.52	N	156	49.37	W
MR2105C-ESEM-16	2021	9	13	5:15	71	48.23	N	155	19.78	W
MR2105C-ESEM-17	2021	9	13	22:46	72	14.89	N	155	45.22	W
MR2105C-ESEM-18	2021	9	15	1:59	72	32.53	N	157	4.26	W
MR2105C-ESEM-19	2021	9	15	5:59	73	2.11	N	159	40.99	W
MR2105C-ESEM-20	2021	9	15	10:01	73	41.22	N	161	31.46	W
MR2105C-ESEM-21	2021	9	15	16:20	74	31.18	N	161	55.04	W
MR2105C-ESEM-22	2021	9	15	19:32	74	31.63	N	161	56.88	W
MR2105C-ESEM-23	2021	9	16	23:35	74	24.9	N	162	7.27	W
MR2105C-ESEM-24	2021	9	17	10:05	72	54.33	N	159	37.92	W
MR2105C-ESEM-25	2021	9	18	0:07	72	33.86	N	159	37.84	W
MR2105C-ESEM-26	2021	9	18	6:47	72	50.86	N	157	39.07	W
MR2105C-ESEM-27	2021	9	18	8:59	73	7.29	N	157	7.29	W
MR2105C-ESEM-28	2021	9	18	20:48	73	23.7	N	158	43.16	W
MR2105C-ESEM-29	2021	9	19	11:09	73	9.56	N	154	39.46	W
MR2105C-ESEM-30	2021	9	19	22:49	72	43.12	N	155	8.71	W
MR2105C-ESEM-31	2021	9	20	8:53	71	42.54	N	153	24.71	W
MR2105C-ESEM-32	2021	9	21	0:33	72	26.09	N	157	8.38	W
MR2105C-ESEM-33	2021	9	21	4:17	72	1.43	N	158	31.73	W
MR2105C-ESEM-34	2021	9	21	17:04	72	3.3	N	161	22.68	W
MR2105C-ESEM-35	2021	9	22	3:46	70	59.86	N	161	6.6	W
MR2105C-ESEM-36	2021	9	22	16:26	71	26.44	N	164	57.03	W
MR2105C-ESEM-37	2021	9	22	23:39	71	44.64	N	163	24	W
MR2105C-ESEM-38	2021	9	23	6:53	71	43.06	N	166	36.86	W
MR2105C-ESEM-39	2021	9	24	0:47	71	56.17	N	168	9.29	W
MR2105C-ESEM-40	2021	9	24	5:20	71	24.61	N	168	19.55	W
MR2105C-ESEM-41	2021	9	25	17:59	70	59.73	N	168	44.95	W
MR2105C-ESEM-42	2021	9	26	3:22	70	0.06	N	167	50.37	W
MR2105C-ESEM-43	2021	9	27	17:49	69	60	N	167	27.9	W
MR2105C-ESEM-44	2021	9	27	23:34	69	21.03	N	166	14.09	W
MR2105C-ESEM-45	2021	9	28	7:20	69	27	N	168	31.37	W
MR2105C-ESEM-46	2021	9	29	4:46	68	29.48	N	168	41.66	W
MR2105C-ESEM-47	2021	9	29	22:37	67	31.61	N	168	42.8	W
MR2105C-ESEM-48	2021	9	30	5:10	68	11.36	N	167	21.8	W
MR2105C-ESEM-49	2021	9	30	22:38	67	1.73	N	167	9.73	W
MR2105C-ESEM-50	2021	10	1	3:16	67	0.15	N	168	46.36	W
MR2105C-ESEM-51	2021	10	1	17:20	65	59.84	N	168	45.09	W
MR2105C-ESEM-52	2021	10	2	17:29	64	18.93	N	171	18.22	W
MR2105C-ESEM-53	2021	10	9	1:13	53	21.44	N	178	12.93	W
MR2105C-ESEM-54	2021	10	10	3:33	52	6.5	N	174	28.23	E

(6) Preliminary results

(6-1) Secondary aerosol particle formation

Although aerosol concentrations are generally low in the Arctic region (Figure 2.8.1-1), marine secondary aerosol particle formation (such as sulfate related to DMS and secondary organic aerosol (SOA)) can be a key factor for climate change via the process of cloud production because these particles can form cloud condensation nuclei (CCN). However, their occurrence, particle composition, and hygroscopicity are not still understood well. We observed several aerosol events of new particle formations and their

growth during this Arctic cruise such as the fog production (Figure 2.8.1-2 and Photo 2.8.1-1). At the same time, we succeeded to collect aerosol samples for EM analysis. We will analyze individual particle composition, mixing state, and hygroscopicity of these samples using TEM and ESEM after the cruise.

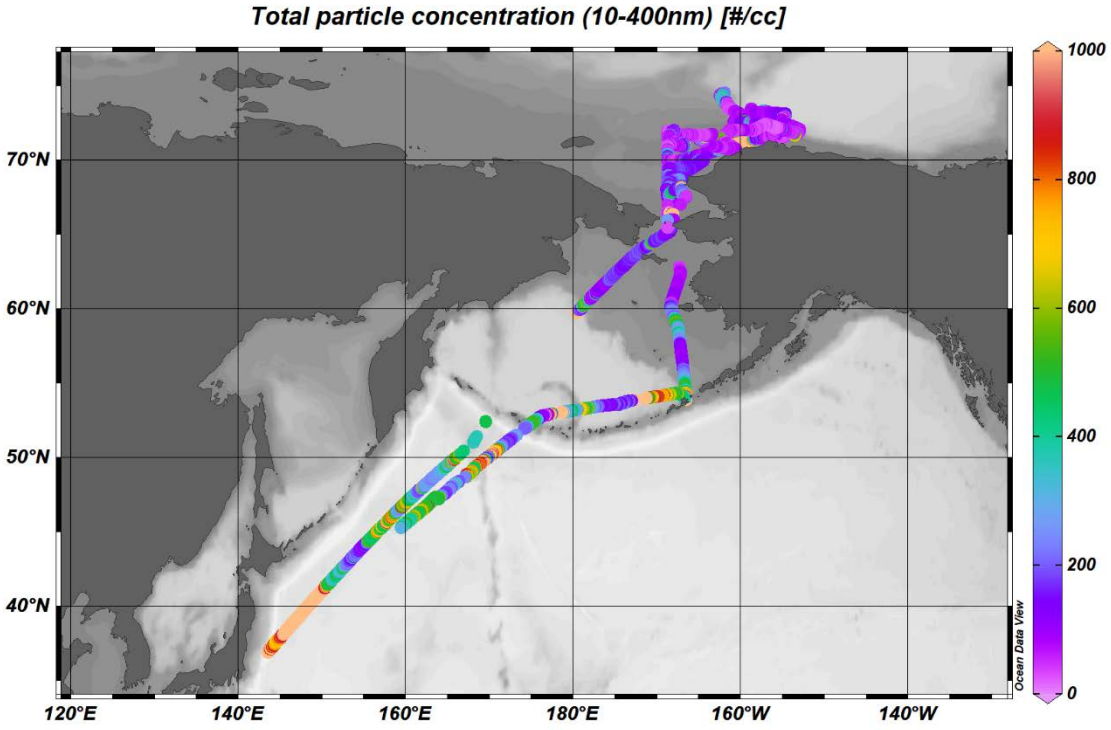

Figure 2.8.1-1: Spatial distribution of particle concentration which size of between 10 and 400 nm.

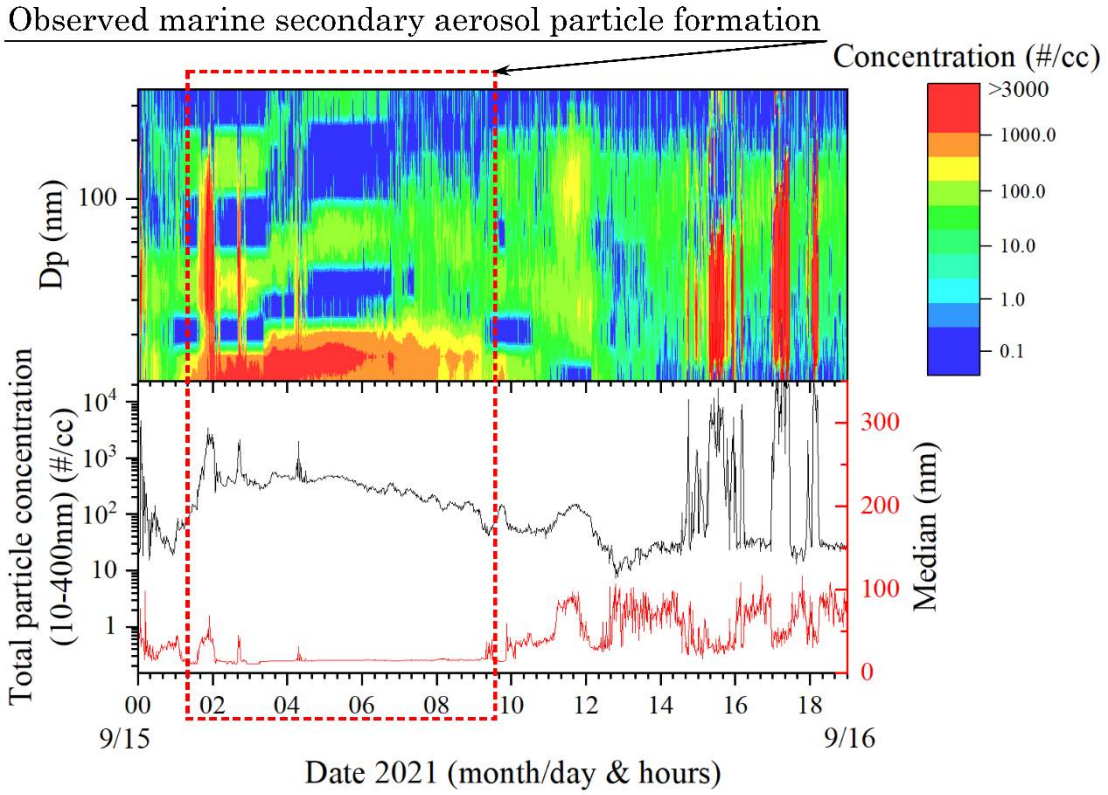

Figure 2.8.1-2: An example of the particle concentration, median diameter, and size distribution between 10 and 400 nm of particles when the marine secondary aerosol particle formation occurred (September 15-16).

Photo 2.8.1-1: Fogbow which was observed on September 15th, 1:30. At that time, we observed the marine secondary aerosol particle formation and their growth (Figure 2.8.1-2), indicating that formed marine secondary aerosol became CCN and contributed to the production of fogs.

(7) Data archives

These data obtained in this cruise will be submitted to the Data Management Group of JAMSTEC, and will be opened to the public via "Data Research System for Whole Cruise Information in JAMSTEC (DARWIN)" in JAMSTEC web site.
<http://www.godac.jamstec.go.jp/darwin/e>

2.8.2. Precipitation sampling

(1) Personnel

Fumikazu Taketani	JAMSTEC(PI)	-not on board
Hotaek Park	JAMSTEC	-not on board

(2) Objectives

・To investigate contribution of suspended particles to the rain, and snow
・To investigate isotope ratio of Hydrogen and Oxygen in the rain and snow

(3) Parameters

・Chemical composition of snow and rain
・Isotope ratio of Oxygen in the rain and snow

(4) Instruments and methods

Snow and rain samples were corrected using hand-made rain/snow sampler. These sampling logs are listed in Table 2.10.3-1. To investigate the isotope ratio in the rain/snow and interaction from aerosols to rain/snow, these samples are going to be analyzed in laboratory.

(5) Observation log

Table 2.8.2-1: Log of precipitation sampling.

ID	Data collected (Sampling start)				Latitude			Longitude		
	YYYY	MM	DD	hh:mm: (UTC)	Deg.	Min.	N/S	Deg.	Min.	E/W
MR2105C-RS-001	2021	8	30	8:35	36	29.8	N	142	49.66	E
MR2105C-RS-002	2021	8	31	23:03	37	49.63	N	144	51.36	E
MR2105C-RS-003	2021	9	1	8:00	43	37.28	N	154	25.50	E
MR2105C-RS-004	2021	9	3	0:30	46	52.72	N	159	47.47	E
MR2105C-RS-005	2021	9	8	20:40	71	40.39	N	155	0.39	E
MR2105C-RS-006	2021	9	10	15:55	71	42.32	N	155	21.99	W
MR2105C-RS-007	2021	9	11	17:46	71	39.26	N	154	57.87	W
MR2105C-RS-008	2021	9	12	18:17	72	28.12	N	155	25.53	W
MR2105C-RS-009	2021	9	15	17:39	74	31.53	N	161	55.14	W
MR2105C-RS-010	2021	9	16	17:00	74	31.41	N	161	55.46	W
MR2105C-RS-011	2021	9	17	15:28	72	32.98	N	160	29.06	W
MR2105C-RS-012	2021	9	18	21:12	72	43.19	N	155	8.29	W
MR2105C-RS-013	2021	9	19	18:40	72	43.38	N	155	7.83	W
MR2105C-RS-014	2021	9	24	17:30	70	35.3	N	168	44.58	W
MR2105C-RS-015	2021	9	28	20:35	68	51.7	N	167	45.46	W
MR2105C-RS-016	2021	10	3	17:30	56	21.26	N	166	57.29	W
MR2105C-RS-017	2021	10	6	19:10	52	52.31	N	176	34.6	E
MR2105C-RS-018	2021	10	9	1:22	52	51.62	N	176	28.74	E
MR2105C-RS-019	2021	10	10	20:30	50	14.28	N	170	13.59	E
MR2105C-RS-020	2021	10	14	0:15	45	18.41	N	159	25.57	E
MR2105C-RS-021	2021	10	16	7:39	39	58.48	N	148	35.45	E

(6) Data archives

These data obtained in this cruise will be submitted to the Data Management Group of JAMSTEC, and will be opened to the public via "Data Research System for Whole Cruise Information in JAMSTEC (DARWIN)" in JAMSTEC web site.
<http://www.godac.jamstec.go.jp/darwin/e>

2.9. Greenhouse gases observation

(1) Personnel

Yasunori Tohjima	NIES	-PI, not on board
Hideki Nara	NIES	-not on board
Shigeyuki Ishidoya	AIST	-not on board
Takeshi Kinase	JAMSTEC	on board
Fumikazu Taketani	JAMSTEC	-not on board
Shinji Morimoto	Tohoku Univ.	-not on board
Daisuke Goto	NIPR	-not on board
Prabir Patra	JAMSTEC	-not on board

(2) Objectives

(2-1) Continuous observations of CO_2, CH_4 and CO mixing ratios

The Arctic region is warming about twice as fast as the global average. Additionally, several studies suggested that the global warming would potentially enhance emissions of the greenhouse gases including CO_2 and CH_4 from the carbon pools in the Arctic permafrost into the atmosphere. The recent accelerated increase rate of the atmospheric CH4 might be attributed to the enhanced emissions from the Arctic region. Therefor there are growing concerns about feedback mechanism between the global warming and the greenhouse gas emissions from the Arctic region. The objective of this study is to detect the increases in the atmospheric greenhouse gas levels associated with the ongoing global warming in the Arctic region in the early stage. The continuous observations of the atmospheric CO_2 and CH_4 mixing ratios during this MR21-05C cruise would allow us to detect the enhanced mixing ratios associated with the regional emissions and to estimate the distribution of the regional emission sources. The atmospheric CO mixing ratios, which were also observed at the same time, can be used as an indicator of the anthropogenic emissions associated with the combustion processes.

Photo 2.9-1: Continuous measurement system of the atmospheric CO_2, CH_4, and CO based on a cavity ring-down spectrometer (CRDS) used during MR21-05C cruise.

(2-2) Discrete flask sampling

In order to clarify spatial variations and air-sea exchanges of the greenhouse gases at northern high latitude, whole air samples were corrected into 40 stainless-steel flasks on-board R/V MIRAI (MR21-05C). The collected air samples will be analyzed for the mixing ratios of CO_2, O_2, Ar, CH_4, CO, N_2O and SF_6 and the stable isotope ratios of CO_2 and CH_4.

(3) Parameters

(3-1) Continuous observations of CO_2, CH_4 and CO mixing ratios

Mixing ratios of atmospheric CO_2, CH_4, and CO.

(3-2) Discrete flask sampling

Mixing ratios of atmospheric CO_2, O_2 (O_2/N_2 ratio), Ar (Ar/N_2 ratio), CH_4, CO, N_2O and SF_6, □^{13}C and □^{18}O of CO_2, □^{13}C and□□D of CH_4.

(4) Instruments and methods

(4-1) Continuous observations of CO_2, CH_4 and CO mixing ratios

Atmospheric CO_2, CH_4, and CO mixing ratios were measured by a wavelength-scanned cavity ring-down spectrometer (WS-CRDS, Picarro, G2401, see Photo 1). An air intake, capped with an inverted stainless-steel beaker covered with stainless steel mesh, was placed on the right-side of the upper deck. A diaphragm pump (GAST, MOA-P108) was used to draw in the outside air at a flow rate of ~8 L min^{-1}. Water vapor in the sample air was removed to a dew pint of about 2°C and about -35°C by passing it through a thermoelectric dehumidifier (KELK, DH-109) and a Nafion drier (PERMA PURE, PD-50T-24), respectively. Then, the dried sample air was introduced into the WS-CRDS at a flow rate of 100 ml min^{-1}. The WS-CRDS were automatically calibrated every 49 hours by introducing 3 standard airs with known CO_2, CH_4 and CO mixing ratios. The analytical precisions for CO_2, CH_4 and CO mixing ratios are about 0.02 ppm, 0.3 ppb and 3 ppb, respectively.

(4-2) Discrete flask sampling

The air sampling equipment consisted of an air intake, a diaphragm pump (GAST MOA), a Stirling cooler (Twinbird) with a water trap, solenoid valves (CKD), a flow meter and a back pressure valve. Ambient air was pumped using the diaphragm pump from an air intake, dried cryogenically and filled into a 1 L stainless-steel flask at a pressure of 0.27 MPa.

(5) Observation log

The continuous observations of CO_2, CH_4 and CO mixing ratios were conducted during the entire cruise. Sampling logs of the discrete flask sampling are listed in Table 2.9-1.

Table 2.9-1 : List of logs of the discrete flask sampling

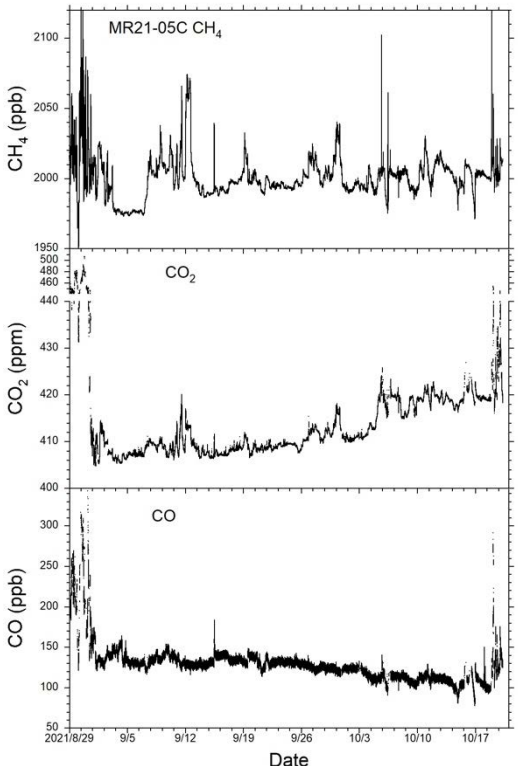

Figure 2.9-1: The time series of the atmospheric (top) CH_4, (middle) CO_2, and (bottom) CO mixing ratios observed during the entire period of MR21-05C cruise.

On board ID	Date Collected				
	YYYY	MM	DD	hh:mm	UTC/JST
MR2105-F001	2021	09	04	7:46	UTC
MR2105-F002	2021	09	04	2:13	UTC
MR2105-F003	2021	09	06	5:54	UTC
MR2105-F004	2021	09	06	22:37	UTC
MR2105-F005	2021	09	07	19:23	UTC
MR2105-F006	2021	09	08	19:22	UTC
MR2105-F007	2021	09	09	19:05	UTC
MR2105-F008	2021	09	10	22:55	UTC
MR2105-F009	2021	09	11	20:02	UTC
MR2105-F010	2021	09	13	1:12	UTC
MR2105-F011	2021	09	13	23:30	UTC
MR2105-F012	2021	09	15	6:08	UTC
MR2105-F013	2021	09	15	20:37	UTC
MR2105-F014	2021	09	17	0:59	UTC
MR2105-F015	2021	09	18	0:31	UTC
MR2105-F016	2021	09	18	22:56	UTC
MR2105-F017	2021	09	19	20:14	UTC
MR2105-F018	2021	09	20	20:57	UTC
MR2105-F019	2021	09	21	4:40	UTC
MR2105-F020	2021	09	22	20:17	UTC
MR2105-F021	2021	09	24	1:31	UTC
MR2105-F022	2021	09	25	0:26	UTC
MR2105-F023	2021	09	27	2:08	UTC
MR2105-F024	2021	09	28	7:49	UTC
MR2105-F025	2021	09	28	20:21	UTC
MR2105-F026	2021	09	30	1:51	UTC
MR2105-F027	2021	10	01	3:03	UTC
MR2105-F028	2021	10	02	1:39	UTC
MR2105-F029	2021	10	03	19:40	UTC
MR2105-F030	2021	10	04	17:45	UTC
MR2105-F031	2021	10	07	1:30	UTC
MR2105-F032	2021	10	08	3:54	UTC
MR2105-F033	2021	10	09	2:44	UTC
MR2105-F034	2021	10	10	2:11	UTC
MR2105-F035	2021	10	10	22:23	UTC
MR2105-F036	2021	10	12	4:32	UTC
MR2105-F037	2021	10	13	5:10	UTC
MR2105-F038	2021	10	14	4:30	UTC
MR2105-F039	2021	10	15	7:55	UTC

(6) Preliminary results

The time series of the atmospheric CH_4, CO_2, and CO mixing ratios observed during the entire cruise are shown in Fig. 2.9-1.

(7) Data archives

These data obtained in this cruise will be submitted to the Data Management Group of JAMSTEC, and will be opened to the public via "Data Research System for Whole Cruise Information in JAMSTEC (DARWIN)" in JAMSTEC web site.
<http://www.godac.jamstec.go.jp/darwin/e>

2.10. Isotope analysis for water vapor

(1) Personnel

Hotaek Park (JAMSTEC) Principle investigator

(2) Background and objective

The warming climates enforce the retreat of the Arctic sea ice, with earlier ice melt and longer warming season period. The Arctic sea ice has reached its minimum extent for the year, at 4.72 million square kilometers on September 16, 2021, reported by the National Snow and Ice Data Center (NSIDC) at the University of Colorado Boulder. The 2021 minimum is the twelfth lowest in the nearly 43-year satellite record. The opened sea surface further enhances the Arctic warming through positive ice albedo feedbacks and the warming effect of the evaporated water vapor, especially significant in autumn and early winter. The resultant wetter and warming atmosphere likely results in an increase of precipitation in the Arctic region, including the neighbor terrestrial region caused by the moisture transport through the atmospheric dynamics, consequently strengthening water cycle in the Arctic regions. The increased autumnal moisture induced by the declined sea ice is able to bring higher snow depth in the winter season. The snow is likely correlated to the increased spring discharge. In reality, the observations of the Arctic river discharges show significant increases in spring snowmelt season and the autumn, suggesting a close association with the declined Arctic sea ice. Moreover, the snow has an insulation function, warming permafrost. The permafrost warming combined with the warming air temperature can increase the melting of ground ice within the permafrost, thus increasing the connectivity of the melted water to river discharge. Likewise, these linkages suggest the potential impacts of the declining sea ice on the terrestrial hydrologic processes.

The observed data during this MR21 cruise likely provide important information for the spatial and temporal variability of the isotopic ratios along the cruise route in the opened Arctic Ocean surface. However, they have some constraints in identifying the implication of the declined sea ice to the intensified terrestrial water cycle. Numerical models are a useful tool to identify the linkage of the declining sea ice and the terrestrial hydrology. The modeling requires the validation of the simulated results against observations. The combination of numerical model simulation and isotope observation makes it possible to explore the relationship of the declining sea ice and the terrestrial water cycle. Therefore, the observation of the isotope of atmospheric water vapor was consecutively conducted in this year since the MR19-03C Arctic cruise. This document reports the isotopic properties observed at the cruise of this year.

(3) Parameters

Isotope ratios of Oxygen and Hydrogen and water vapor concentration

(4) Instrument and method

The isotope of atmosphere water vapor was monitored by a Cavity Ringdown Spectrometer (L2130-i, Isotopic H_2O, Picarro, Figure 2.10-1), which simultaneously observes the isotope ratios of oxygen and hydrogen with 1–2 Hz frequency, including water vapor concentration. The observed data are archived on the storage of the spectrometer, operated by Windows system. Two standard liquids, for example with isotope values of -0.21 permil and -30.76 permil in oxygen, are individually injected for 15 minutes every 12-hour, in which the derived linear regression equation is used to calibrate the monitored values by the spectrometer.

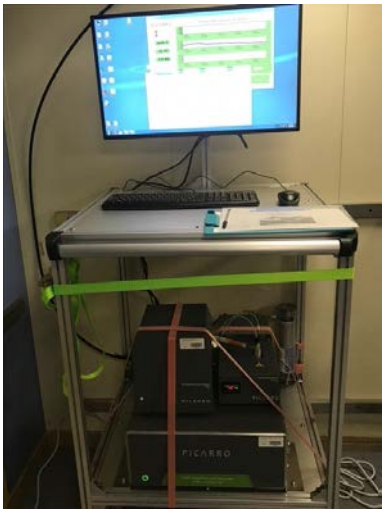

Figure 2.10-1: Isotope spectrometer system

(5) Preliminary results

The observed isotope ratios were averaged to hourly time steps, and Figure 2.10-2 exhibits their variability in the Arctic Ocean observed during the period of September 6 to October 4, 2021, including air and sea surface temperature. The isotope ratios are generally decreasing, responding to the variations of air temperature after entering to the Arctic Ocean of MIRAI. During the period from Sep. 10 to Oct. 2 when the vessel stayed over the Arctic Ocean, the air temperature showed variations at the range of -2 ~ 3℃. Meanwhile, the sea surface temperature showed larger daily variations than the air temperature, which represents the spatial variability of the sea surface heat condition along the ship cruising routes across north to south and east to west. In reality, the isotope of oxygen significantly correlated with air temperature, as identified in the data analysis observed at 2019 and 2020 MIRAI cruises. The isotopes show large diurnal and daily variability (Figure 2.10-2). In particular, d-excess (= $-8\times\delta^{18}O + \delta^{2}H$) displayed the largest daily variability compared to $\delta^{18}O$ and $\delta^{2}H$. The d-excess was significantly correlated to the difference between sea surface and air temperature (Figure 2.10-3). The d-excess represents the property of evaporation. Evaporated water vapor generally records lower $\delta^{18}O$ value, which results in higher d-excess. The larger difference between sea surface and air temperature is an efficient condition for larger evaporation from the ocean surface. In reality, the d-excess revealed higher value at the larger temperature difference, which indicates that the observations had caught the isotope ratios of the evaporated water vapor from the warmer ocean surface.

Both oxygen and hydrogen indicated significantly high correlation. Their relationship yielded the slope of 5.0, which is considerably lower than 6.1 and 5.9 in 2019 and 2020, respectively. The slopes distribute within the ranges of 5 and 7 obtained at the northernmost terrestrial sites. However, the slopes derived by the three-year cruise is lower than the value 8 of global meteoric water line (GMWL), which represent the

sensitivity of isotope to air temperature.

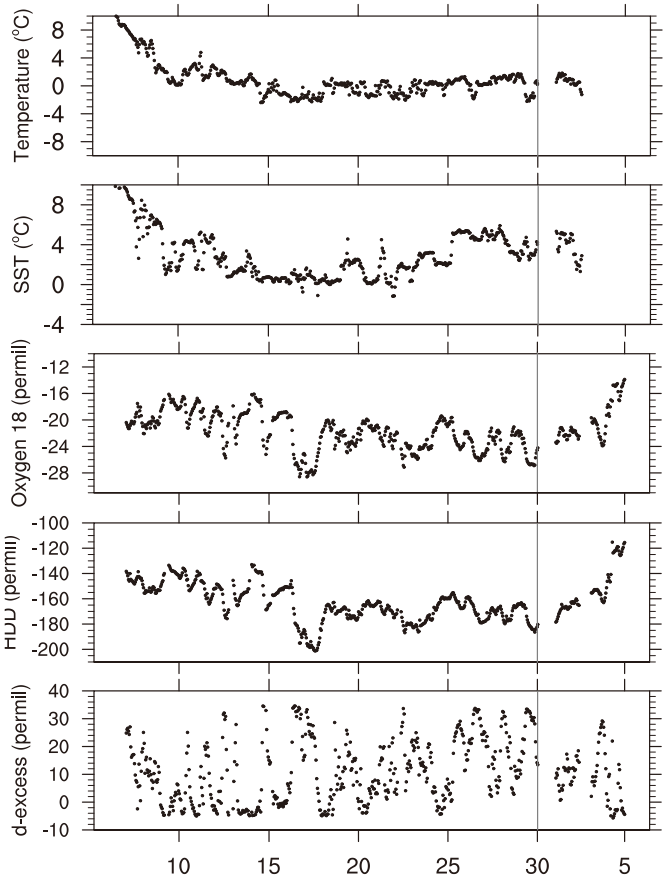

Figure 2.10-2: Variability of hourly averaged air temperature, sea surface temperature (SST), and isotopic variables during MR21-05C cruise. The gray line indicates the boundary of September and October.

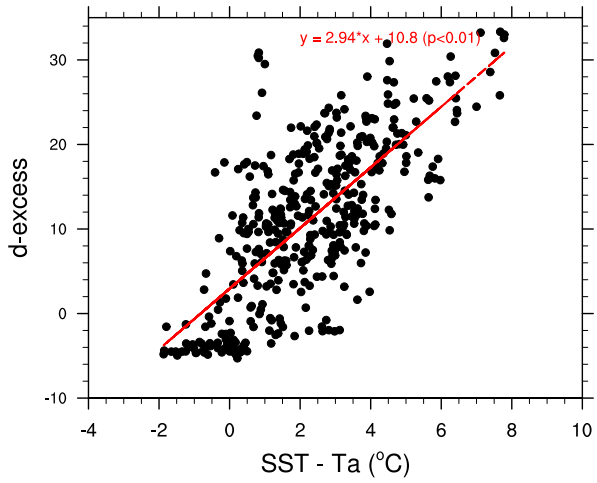

Figure 2.10-3: Relationship between d-excess and difference between sea surface and air temperature.

(6) Data archive

The data obtained in this cruise will be submitted to the Data Management Group of JAMSTEC, and will be opened to the public via “Data Research System for Whole Cruise Information in JAMSTEC (DARWIN)” in JAMSTEC web site. <http://www.godac.jamstec.go.jp/darwin/e>

3. Physical Oceanography

3.1. CTD cast and water sampling

(1) Personnel

Amane Fujiwara (JAMSTEC)	-PI
Motoyo Ito (JAMSTEC)	-CoPI
Rei Ito (MWJ)	*Operation leader
Hiroyuki Nakajima (MWJ)	
Airi Hara (MWJ)	
Aine Yoda (MWJ)	
Keita Hayashi (MWJ)	
Makoto Ozaki (JAMSTEC)	

(2) Objective

Investigation of oceanic structure and water sampling.

(3) Parameters

Temperature (Primary and Secondary)
Salinity (Primary and Secondary)
Pressure
Dissolved Oxygen (Primary "RINKO III" and Secondary "SBE43")
Fluorescence
Beam Transmission
Turbidity
Nitrate
Photosynthetically Active Radiation
Altimeter
Deep Ocean Standards Thermometer

(4) Instruments and Methods

CTD/Carousel Water Sampling System, which is a 36-position Carousel Water Sampler (CWS) with Sea-Bird Electronics, Inc. 12-liter sample Bottles were used for sampling seawater (#1 - #10 aced washed and Viton O-ring.). The sensors attached on the CTD were temperature (primary and secondary), conductivity (primary and secondary), pressure, dissolved oxygen (primary: RINKO III, secondary: SBE43), fluorescence, beam transmission, turbidity, nitrate, photosynthetically active radiation, altimeter and Deep Ocean Standards Thermometer. Salinity was computed by measured values of pressure, conductivity and temperature. The CTD/CWS was deployed from starboard on working deck.

Specifications of the sensors are listed below.

CTD: SBE911plus CTD system
Under water unit:

SBE9plus (S/N: 09P54451-1027, Sea-Bird Electronics, Inc.)
Pressure sensor: Digiquartz pressure sensor (S/N:117457)
Calibrated Date: 08 Jul 2020

Carousel water sampler:
SBE32 (S/N: 3254451-0826, Sea-Bird Electronics, Inc.)

Temperature sensors:
Primary: SBE03-04/F (S/N: 031525, Sea-Bird Electronics, Inc.)
Calibrated Date: 01 Jun. 2019
Secondary: SBE03-04/F (S/N: 031464, Sea-Bird Electronics, Inc.)
Calibrated Date: 05 Jun. 2021

Conductivity sensors:
Primary: SBE04C (S/N: 042435, Sea-Bird Electronics, Inc.)
Calibrated Date: 25 Jun. 2019
Secondary: SBE04C (S/N: 042854, Sea-Bird Electronics, Inc.)
Calibrated Date: 08 Jun. 2021

Dissolved Oxygen sensor:
Primary: RINKOIII (S/N: 0287_163011BA, JFE Advantech Co., Ltd.)
Calibrated Date: 28 May. 2021

Secondary: SBE43 (S/N: 430401 Sea-Bird Electronics, Inc.)
Calibrated Date: 02 Jul. 2019

Fluorescence:
Primary:
Chlorophyll Fluorometer (S/N: 3618, Seapoint Sensors, Inc.)
Gain setting: 10X, 0-15 ug/l
Calibrated Date: None
Offset: 0.000

Transmission meter:
C-Star (S/N CST-1363DR, WET Labs, Inc.)
Calibrated Date: 13 Aug. 2021

Turbidity:
Turbidity Meter (S/N: 14953)
Gain setting: 100X
Scale factor: 1.000
Calibrated Date: None

Nitrate:
Deep SUNA (S/N 1613, Satlantic, Inc.)
Calibration Date: None
Casts used: 001M001 – 015M001, 020M001 – 063M001

Photosynthetically Active Radiation:
PAR sensor (S/N: 1025, Satlantic Inc.)
Calibrated Date: 06 Jul. 2015

Altimeter:
Benthos PSA-916T (S/N: 1100, Teledyne Benthos, Inc.)

Submersible Pump:
Primary: SBE5T (S/N: 055816, Sea-Bird Electronics, Inc.)
Secondary: SBE5T (S/N: 054598, Sea-Bird Electronics, Inc.)

Bottom contact switch: (Sea-Bird Electronics, Inc.)

Deep ocean standards thermometer:
SBE35 (S/N: 0053, Sea-Bird Electronics, Inc.)
Calibrated Date: 15 Jun. 2021

Deck unit: SBE11plus (S/N 11P54451-0872, Sea-Bird Electronics, Inc.)

Configuration file: MR2105C_A.xmlcon
001M001 – 015M001, 020M001 – 063M001
MR2105C_B.xmlcon
016M001 – 019M001

The CTD raw data were acquired on real time using the Seasave-Win32 (ver.7.26.7.121) provided by Sea-Bird Electronics, Inc. and stored on the hard disk of the personal computer. Seawater was sampled during the up cast by sending fire commands from the personal computer.

For depths where vertical gradients of water properties were exchanged to be large, the bottle was exceptionally fired after waiting from the stop for 60 seconds to enhance exchanging the water between inside and outside of the bottle. 30 seconds below thermocline to stabilize then fire.

Data processing procedures and used utilities of SBE Data Processing-Win32 (ver.7.26.7.129) and SEASOFT were as follows:

(The process in order)

DATCNV: Convert the binary raw data to engineering unit data. DATCNV also extracts bottle information where scans were marked with the bottle confirm bit during acquisition. The duration was set to 4.4 seconds, and the offset was set to 0.0 seconds.

TCORP (original module): Corrected the pressure sensitivity of the temperature (SBE3) sensor.
S/N 031525: 1.714e-008 (degC/dbar)
S/N 031464: 7.75293156e-009 (degC/dbar)

RINKOCOR (original module): Corrected the time dependent, pressure induced effect (hysteresis) of the RINKOIII profile data.

RINKOCORROS (original module): Corrected the time dependent, pressure induced effect (hysteresis) of the RINKOIII bottle information data by using the hysteresis corrected profile data.

BOTTLESUM: Create a summary of the bottle data. The data were averaged over 4.4 seconds.

ALIGNCTD: Convert the time-sequence of sensor outputs into the pressure sequence to ensure that all calculations were made using measurements from the same parcel of water. Dissolved oxygen data are systematically delayed with respect to depth mainly because of the long time constant of the dissolved oxygen sensor and of an additional delay from the transit time of water in the pumped pluming line. This delay was compensated by 5 seconds advancing dissolved oxygen sensor (SBE43) output (dissolved oxygen voltage) relative to the temperature data. RINKOIII voltage (User polynomial 0) was advanced 1 second and transmission data was advanced 2 seconds.

WILDEDIT: Mark extreme outliers in the data files. The first pass of WILDEDIT obtained the accurate estimate of the true standard deviation of the data. The data were read in blocks of 1000 scans. Data greater than 10 standard deviations were flagged. The second pass computed a standard deviation over the same 1000 scans excluding the flagged values. Values greater than 20 standard deviations were marked bad. This process was applied to pressure, depth, temperature (primary and secondary), conductivity (primary and secondary), dissolved oxygen voltage (SBE43).

CELLTM: Remove conductivity cell thermal mass effects from the measured conductivity. Typical values used were thermal anomaly amplitude alpha = 0.03 and the time constant 1/beta = 7.0.

FILTER: Perform a low pass filter on pressure and depth data with a time constant of 0.15 second. In order to produce zero phase lag (no time shift) the filter runs forward first then backward

WFILTER: Performed a median filter to remove spikes. The window length is determined for a specific data value and the median value is calculated for each specified window, and the data value at the window's center point is replaced by the median value. The window length is specified as 49 scans for the fluorescence data, beam transmission data, beam attenuation data, output voltage of Transmissometer and turbidity data. The window length is specified as 73 scans for nitrate data.

SECTIONU (original module of SECTION): Select a time span of data based on scan number in order to reduce a file size. The minimum number was set to be the starting time when the CTD package was beneath the sea-surface after activation of the pump. The maximum number of was set to be the end time when the package came up from the surface.

LOOPEDIT: Mark scans where the CTD was moving less than the minimum velocity of 0.0 m/s (traveling backwards due to ship roll).

DESPIKE (original module): Remove spikes of the data. A median and mean absolute deviation was calculated in 1-dbar pressure bins for both down and up cast, excluding the flagged values. Values greater than 4 mean absolute deviations from the median were marked bad for each bin. This process was performed twice for temperature, conductivity and dissolved oxygen (RINKOIII and SBE43) voltage.

DERIVE: Compute dissolved oxygen (SBE43).

BINAVG: Average the data into 1 dbar bins and 1 sec bins.

BOTTOMCUT (original module): Deletes discontinuous scan bottom data, when it's created by BINAVG.

DERIVE: Compute salinity, potential temperature, and sigma-theta.

SPLIT: Separate the data from the input .cnv file into down cast and up cast files.

(5) Station list

During this cruise, 65casts of CTD observation were carried out. Date, time and locations of the CTD casts are listed in Table 3.1-1.

(6) Preliminary Results

During this cruise, we judged noise, spike or shift in the data of some casts. These were as follows.

001M001: Secondary Temperature, Secondary Salinity
down 1090 dbar: spike

011M001: Primary Temperature, Primary Salinity
up 200 dbar: spike

SBE43 voltage
down 1121 - 1181 dbar: noise

011M002: SBE43 voltage
down 461 - 463 dbar: spike

016M001: SBE43 voltage
down 2047 - 2049 dbar: spike
down 2231 - 2580 dbar: noise
down 2900 - 2922 dbar: spike

017M001: SBE43 voltage
down 1412 - 2228 dbar: noise shift
up 2227 - 1302 dbar: noise shift

018M001: SBE43 voltage
down 2354 - 2355 dbar: spike

019M001: Secondary Temperature, Secondary Salinity
up 1669 - 1 dbar: shift

020M001: Secondary Salinity
down 33 - 46 dbar: shift

021M001: Secondary Temperature
down 1067 - 1069 dbar: spike

Secondary Salinity
down 550 dbar: spike

023M001: Secondary Temperature, Secondary Salinity
down 39 dbar: shift

024M001: fluorescence
down 19 - 21 dbar: out of range
up 19 - 18 dbar: out of range

032M001: Secondary Salinity
down 6 - 7 dbar: spike

034M001: transmission
up 28 - 23 dbar: shift

035M001: Primary Salinity
down 13 dbar: spike

040M001: Primary Salinity
down 41 dbar: spike

043M001: Primary Salinity
down 19 dbar: spike

052M001: Turbidity
down 23 - 26 dbar: spike

062M001: transmission
up 15 - 14 dbar: spike

063M001: Primary Temperature, Primary Salinity
down 122 dbar: spike

Secondary Temperature, Secondary Salinity
down 115 dbar: spike

nitrate

down 899 - 2000 dbar: out of range
up 1999 - 150 dbar: out of range

(7) Data archive

These data obtained in this cruise will be submitted to the Data Management Group of JAMSTEC, and will be opened to the public via "Data Research System for Whole Cruise Information in JAMSTEC (DARWIN)" in JAMSTEC web site.
<http://www.godac.jamstec.go.jp/darwin/e>

Table 3.1-1: MR21-05C CTD cast table

Stnnbr	Castno	Date(UTC)	Time(UTC)		BottomPosition		Depth	Wire	HT Above	Max	Max	CTD	Remark
		(mmddyy)	Start	End	Latitude	Longitude	(m)	Out (m)	Bottom (m)	Depth	Pressure	Filename	
001	1	090321	23:25	03:05	46-52.71N	159-47.49E	5089.0	1980.5	-	1976.9	2003.0	001M001	
002	1	091221	17:10	17:16	71-35.47N	154-48.60W	39.2	31.1	4.0	33.7	34.0	002M001	
003	1	091221	18:54	19:13	71-40.74N	154-56.38W	98.9	47.8	-	49.5	50.0	003M001	
003	2	091221	20:20	20:53	71-40.61N	154-57.61W	100.9	93.7	5.3	95.0	96.0	003M002	
004	1	091321	01:26	02:21	71-44.39N	155-08.14W	285.8	282.6	5.1	282.9	286.0	004M001	
005	1	091321	06:08	06:49	71-48.27N	155-17.66W	194.3	189.1	5.7	189.9	192.0	005M001	
006	1	091321	09:14	09:22	71-49.51N	155-49.88W	89.1	83.1	5.3	84.1	85.0	006M001	
007	1	091321	13:37	13:44	71-49.82N	156-02.42W	84.7	78.6	5.1	80.2	81.0	007M001	
008	1	091321	14:55	15:02	71-54.77N	156-02.69W	73.8	66.3	4.9	68.3	69.0	008M001	
009	1	091321	17:03	17:43	72-06.12N	155-54.76W	209.0	202.1	5.3	202.8	205.0	009M001	
010	1	091421	02:55	04:42	72-28.48N	155-35.13W	1829.0	1826.0	9.7	1821.0	1848.0	010M001	
011	1	091521	22:35	00:12	74-31.52N	161-55.16W	1688.0	1680.3	9.3	1675.6	1700.0	011M001	
011	2	091621	17:04	18:01	74-31.42N	161-55.70W	1688.0	502.2	-	501.1	507.0	011M002	
012	1	091721	08:06	08:21	73-00.26N	159-35.48W	275.0	266.3	5.0	266.1	269.0	012M001	
013	1	091721	12:22	12:26	72-27.35N	159-40.05W	48.4	39.3	4.9	42.6	43.0	013M001	
014	1	091721	19:39	20:01	72-35.90N	160-49.95W	49.2	41.2	4.5	43.5	44.0	014M001	
015	1	091821	04:14	05:10	72-43.40N	157-54.52W	376.7	370.1	10.1	368.8	373.0	015M001	
016	1	091821	10:10	11:50	73-17.87N	156-47.89W	3325.0	3318.6	9.3	3309.9	3371.0	016M001	
017	1	091821	19:03	20:58	73-23.86N	158-42.83W	2214.0	2199.7	10.1	2193.4	2228.0	017M001	
018	1	091921	09:14	11:08	73-09.60N	154-40.07W	3785.0	3778.0	9.8	3767.3	3841.0	018M001	
019	1	091921	17:09	19:28	72-43.37N	155-07.91W	2969.0	2955.2	10.5	2949.2	3001.0	019M001	
020	1	092021	06:43	07:23	71-48.46N	153-14.95W	247.0	214.4	5.0	216.6	219.0	020M001	
021	1	092021	13:08	13:52	72-01.10N	154-38.68W	1146.0	1134.0	10.2	1131.1	1146.0	021M001	
022	1	092021	19:16	20:16	72-27.56N	156-59.38W	466.0	450.2	9.8	449.8	455.0	022M001	
023	1	092121	04:05	04:25	72-01.45N	158-31.55W	56.1	47.8	4.9	50.5	51.0	023M001	
024	1	092121	16:56	17:10	72-03.25N	161-22.59W	31.2	23.5	4.7	25.7	26.0	024M001	
025	1	092121	23:10	23:25	71-31.34N	162-27.59W	43.0	34.2	5.8	36.6	37.0	025M001	
026	1	092221	03:27	03:46	70-59.87N	161-06.60W	46.2	38.8	5.5	40.6	41.0	026M001	
027	1	092221	17:35	17:50	71-26.29N	164-56.99W	42.2	33.1	5.1	36.6	37.0	027M001	
028	1	092221	22:45	23:06	71-45.13N	163-23.57W	41.4	32.9	5.1	35.6	36.0	028M001	
029	1	092321	05:35	05:52	71-45.83N	166-21.53W	44.9	37.1	4.9	39.6	40.0	029M001	
030	1	092321	17:01	17:17	72-00.24N	168-45.29W	51.0	42.3	4.7	45.5	46.0	030M001	
031	1	092321	22:08	22:32	72-03.92N	167-54.20W	50.3	42.3	4.7	44.5	45.0	031M001	
032	1	092421	03:52	04:08	71-30.10N	168-44.66W	48.6	40.2	5.3	42.6	43.0	032M001	
033	1	092421	17:55	18:17	71-00.00N	166-38.72W	44.8	36.9	5.5	38.6	39.0	033M001	
034	1	092521	17:17	17:33	71-00.00N	168-44.95W	44.5	36.0	5.3	38.6	39.0	034M001	
035	1	092521	20:43	21:03	70-29.97N	168-44.98W	38.7	30.1	5.3	32.7	33.0	035M001	
036	1	092621	01:27	01:43	69-59.91N	168-43.92W	40.9	32.2	4.7	35.6	36.0	036M001	
037	1	092621	05:35	05:52	70-00.00N	166-39.99W	47.0	35.5	7.6	38.6	39.0	037M001	
038	1	092721	17:52	18:15	70-00.01N	164-27.87W	35.7	28.8	3.8	30.7	31.0	038M001	
039	1	092721	23:32	23:49	69-21.03N	166-14.07W	37.5	28.8	4.6	31.7	32.0	039M001	
040	1	092821	02:39	02:45	69-25.78N	167-27.60W	48.6	40.8	5.1	42.6	43.0	040M001	
041	1	092821	05:38	05:57	69-29.98N	168-44.95W	51.7	44.1	5.3	45.5	46.0	041M001	
042	1	092821	17:29	17:54	69-00.03N	168-45.16W	53.2	44.1	5.7	46.5	47.0	042M001	
043	1	092821	22:12	22:28	68-48.04N	166-57.42W	41.6	32.9	5.0	35.6	36.0	043M001	
044	1	092921	03:18	03:35	68-30.25N	168-44.80W	53.8	45.2	5.3	47.5	48.0	044M001	
045	1	092921	17:47	18:15	68-02.00N	168-49.90W	59.2	49.8	6.5	51.5	52.0	045M001	
046	1	092921	21:32	21:46	67-30.00N	168-44.67W	49.7	41.7	5.4	43.6	44.0	046M001	
047	1	093021	00:01	00:05	67-45.04N	168-30.02W	50.3	41.3	5.6	43.6	44.0	047M001	
048	1	093021	01:10	01:16	67-52.54N	168-14.77W	56.7	48.0	4.5	51.5	52.0	048M001	
049	1	093021	02:24	02:40	68-00.04N	168-00.17W	54.2	46.3	5.3	48.5	49.0	049M001	
050	1	093021	04:09	04:15	68-06.02N	167-40.24W	52.8	44.7	4.6	47.5	48.0	050M001	
051	1	093021	05:27	05:33	68-12.11N	167-20.29W	47.5	39.0	4.7	42.6	43.0	051M001	
052	1	093021	06:15	06:21	68-15.09N	167-12.49W	44.8	37.3	4.8	39.6	40.0	052M001	
053	1	093021	07:05	07:20	68-18.11N	167-03.37W	39.1	32.0	5.0	33.7	34.0	053M001	
054	1	093021	18:02	18:24	67-36.07N	166-30.03W	46.8	36.9	5.2	40.6	41.0	054M001	
055	1	093021	22:18	22:31	67-01.76N	167-09.71W	40.5	30.0	4.8	34.6	35.0	055M001	
056	1	100121	03:17	03:36	67-00.17N	168-46.37W	46.6	36.8	5.0	40.6	41.0	056M001	
057	1	100121	06:41	06:59	66-29.87N	168-45.59W	52.3	44.5	5.3	47.5	48.0	057M001	
058	1	100121	17:59	18:26	65-59.77N	168-44.99W	53.4	42.3	5.2	47.5	48.0	058M001	
059	1	100121	21:55	22:10	65-29.90N	168-45.06W	54.8	45.4	5.5	48.5	49.0	059M001	
060	1	100221	01:59	02:16	65-05.67N	169-31.11W	50.3	40.2	5.8	44.6	45.0	060M001	
061	1	100221	05:52	06:10	64-43.51N	170-25.58W	50.4	40.1	4.8	44.6	45.0	061M001	
062	1	100221	18:45	19:06	64-18.92N	171-18.20W	46.2	36.9	5.2	40.6	41.0	062M001	
063	1	101121	02:04	03:40	49-54.75N	169-29.36E	5416.0	1976.1	-	1973.4	2000.0	063M001	

3.2. LADCP

(1) Personnel
Yusuke Kawaguchi, University of Tokyo (PI) -not on board
Shigeto Nishino, JAMSTEC
Eun Yae Son, University of Tokyo
Ito Rei, MWJ (Operation leader)
Hiroyuki Nakajima, MWJ
Airi Hara, MWJ
Yoda Aine, MWJ
Makoto Ozaki, Hokkaido University

(2) Objective
To investigate ocean current velocity and vertical shear of the deep sea

(3) Parameters
The device retrieves depth, horizontal velocity (u), meridional velocity (v).

(4) Objectives and methodology
The lowered ADCP (LADCP), Workhorse Monitor WHM300 (Teledyne RD Instrument, San Diego, California, USA) was utilized at the CTD points where is deeper than 300 m in MR21-05C to get a shear data at the same time. LADCP system consists of two ADCP of upward-and downward looking transducer and a 43V battery package. The LADCP system was set for recording before the CTD cast and its data was recovered right after the cast. Velocity conversion from the two transducers were done by LDEO LADCP software (version 10; Visbeck 2002). For the data conversion, navigation data and CTD data were applied for the improvement of data quality.
Detailed configuration is below:

Bin size: 8.0 m

Number of bins: 25

Pings per ensemble: 1

Ping interval: 1.0 sec

(5) Station log
Station number is match with CTD files. Each station has 2 data with separated folder named MASTR (down-looking ADCP) and SLAVE (up-looking ADCP). In total, 10 profiles were obtained in the ChukChi and Beaufort Seas. Note 001M001 is test cast

which is obtained at the K2 mooring position in the northern Pacific.

(6) Data format and quality

The data has the extension of .000 which is the raw format of the RDI software.

The quality of acquired data were checked using LDEO LADCP software. Heading, pitching, and roll during down/up cast was in stable range (Figure 3.2-1). Also the beam performance and correlation among the four beams showed above 98% and 115 m, respectively (Figure 3.2-2).

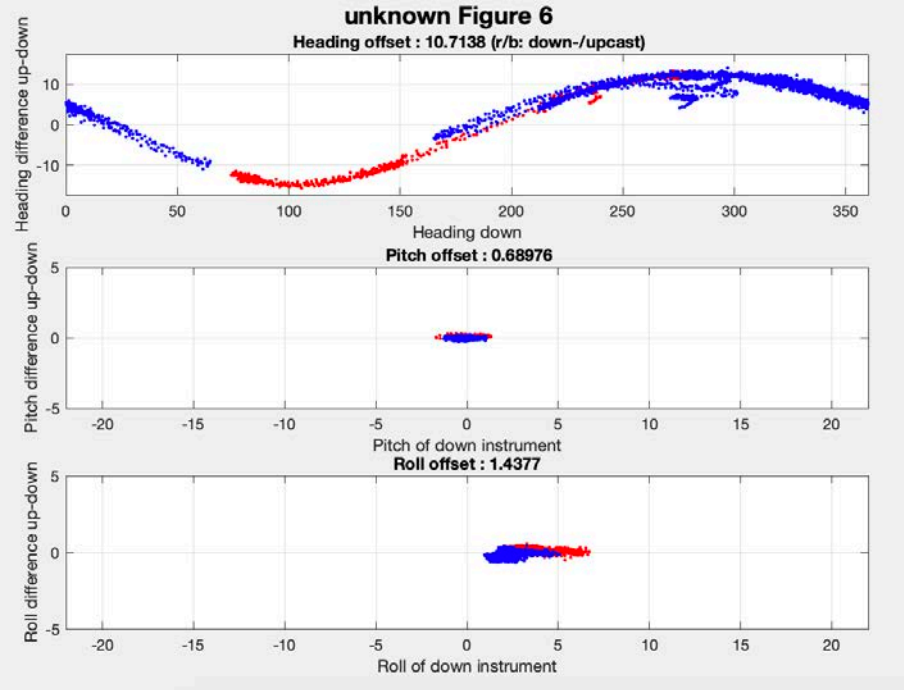

Figure 3.2-1: Offset of heading (upper panel), pitch (middle panel), and roll (lower panel) during the cast.

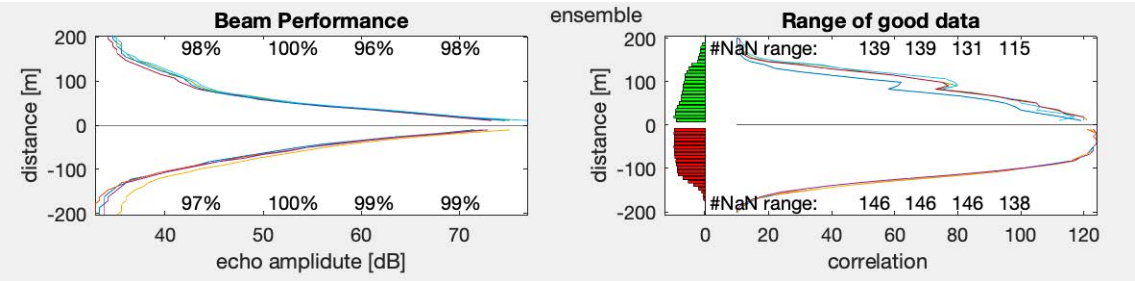

Figure 3.2-2: Beam performance (left panel) and correlation (right panel) of up-looking and down-looking ADCP.

(7) Data archive

These data obtained in this cruise will be submitted to the Data Management Group of JAMSTEC, and will be opened to the public via "Data Research System for Whole Cruise Information in JAMSTEC (DARWIN)" in JAMSTEC web site.
http://www.godac.jamstec.go.jp/darwin/e

(8) Reference

Visbeck, M. (2002): Deep velocity profiling using Acoustic Doppler Current Profilers: Bottom track and inverse solutions, J. Atmos. Oceanic Technol., 19, 794–807.

3.3. XCTD

(1) Personnel

Amane Fujiwara (JAMSTEC) -PI
Motoyo Itoh (JAMSTEC) -CoPI
Yusuke Kawaguchi (The University of Tokyo) – Not on board
Eun-Yae Son (The University of Tokyo)
Ryo Oyama (Nippon Marine Enterprises, Ltd.; NME) – Operation leader
Kazuho Yoshida (NME)
Satomi Ogawa (NME)
Ryo Kimura (NME)
Yoichi Inoue (MIRAI Crew)

(2) Objective

To obtain vertical profiles of sea water temperature and salinity (calculated from temperature, pressure (depth), and conductivity).

(3) Parameters

The ranges and accuracies of parameters measured by the XCTD (eXpendable Conductivity, Temperature & Depth profiler) are as follows; Parameter Range Accuracy Conductivity 0 ~ 60 [mS/cm] +/- 0.03 [mS/cm] Temperature -2 ~ 35 [deg-C] +/- 0.02 [deg-C] Depth 0 ~ 1000 [m] 5 [m] or 2 [%] (either of them is major)

(4) Instruments and Methods

We observed vertical profiles of sea water temperature and salinity measured by XCTD-1 and XCTD-1N probes manufactured by Tsurumi-Seiki Co. (TSK). The electric signal from the probe was converted by MK-150N (TSK), and was recorded by AL-12B software (Ver.1.1.4, TSK). We launched 64 probes by using the automatic launcher. The XCTD observation log is shown in Table 3.3-1

(5) Observation log

Table 3.3-1: XCTD observation log

No.	Station No.	Date [YYYY/MM/DD]	Time [hh:mm]	Latitude [deg]	Longitude [deg]	Depth [m]	SST [deg-C]	SSS [PSU]	Probe S/N
1	K2	2021/09/04	03:48	46-57.6886N	159-56.4552E	5166	13.343	32.761	21044200
2	BC	2021/09/10	14:58	71-40.3429N	155-21.5598W	225	3.832	30.237	20015336
3	X003(DBO5)	2021/09/12	05:11	71-14.8826N	157-10.1739W	47	5.257	30.385	19018619
4	X004(DBO5)	2021/09/12	05:27	71-17.2670N	157-14.8914W	55	5.187	30.424	19018623
5	X005(DBO5)	2021/09/12	05:44	71-19.7749N	157-19.9957W	89	5.259	30.291	19018620
6	X006(DBO5)	2021/09/12	06:01	71-22.3031N	157-24.7953W	109	5.388	30.178	19018626
7	X007(DBO5)	2021/09/12	06:19	71-24.9830N	157-30.2144W	122	5.582	30.099	19018621
8	X008(DBO5)	2021/09/12	06:35	71-27.2879N	157-35.1177W	110	4.694	30.241	19018700
9	X009(DBO5)	2021/09/12	06:52	71-29.8136N	157-40.1005W	84	1.717	29.297	19018698
10	X010(DBO5)	2021/09/12	07:08	71-32.2094N	157-45.2069W	71	1.525	28.998	19018699
11	X011(DBO5)	2021/09/12	07:25	71-34.6724N	157-50.3281W	64	1.487	29.075	19018697
12	MID(St02-St03)	2021/09/12	18:08	71-37.8552N	154-54.9683W	55	4.390	30.030	19018693
13	MID(St03-St04)	2021/09/12	23:25	71-44.4634N	155-00.0645W	202	4.675	30.192	19018691
14	MID(St04-St05)	2021/09/13	04:42	71-45.9504N	155-17.0705W	203	2.690	29.733	20015342
15	XCTD+TM_1	2021/09/13	08:39	71-49.0447N	155-38.5068W	114	2.224	29.059	19018622
16	MID(St08-St09)	2021/09/13	15:34	71-59.5823N	156-00.5051W	112	1.014	26.719	20015345
17	MID(St09-StTM)	2021/09/13	22:34	72-12.3891N	155-48.2441W	347	0.720	26.026	20121375
18	XCTD+TM_2	2021/09/13	23:42	72-18.0986N	155-41.9993W	1123	1.245	26.968	20121376
19	MID(StTM-St10)	2021/09/14	00:09	72-23.3124N	155-39.5217W	1372	1.003	26.318	20015339
20	NBC to NAP_1	2021/09/15	02:06	72-32.7410N	157-08.3932W	398	1.056	26.337	20121379
21	NBC to NAP_2	2021/09/15	04:23	72-45.7139N	158-47.5199W	207	1.808	28.198	20121382
22	from NAP_1	2021/09/17	00:25	74-15.0117N	162-17.7254W	1204	0.536	27.105	20111245
23	from NAP_2	2021/09/17	00:58	74-09.0131N	162-11.0936W	987	0.260	26.935	20111248
24	from NAP_3	2021/09/17	01:23	74-05.0094N	162-03.6654W	807	0.240	26.901	20121377
25	from NAP_4	2021/09/17	01:49	74-01.0193N	161-53.2427W	380	0.472	26.792	20121378
26	from NAP_5	2021/09/17	02:27	73-54.9992N	161-44.5231W	328	0.479	26.983	20121383
27	from NAP_6	2021/09/17	03:37	73-41.0154N	161-31.9640W	330	0.143	26.759	20121380
28	from NAP_7	2021/09/17	04:40	73-26.7918N	161-21.9767W	263	0.247	26.689	20121385
29	from NAP_8	2021/09/17	06:15	73-13.9998N	160-28.5481W	496	0.917	27.017	20121386
30	MID(St12-St13)	2021/09/17	10:53	72-44.0096N	159-38.6215W	80	1.573	28.327	20121384
31	WaveBuoy1	2021/09/17	17:08	72-35.5091N	160-52.2108W	48	-0.929	28.387	20121381
32	St14-St15_1	2021/09/18	02:15	72-32.4088N	158-15.8030W	121	1.580	28.800	20111253
33	St14-St15_2	2021/09/18	02:46	72-37.5552N	158-05.0122W	214	1.555	28.468	20111250
34	St15-St16_1	2021/09/18	06:32	72-48.1223N	157-44.7049W	1202	1.078	26.904	20111247
35	St15-St16_2	2021/09/18	07:02	72-53.4573N	,157-33.9703W	1876	1.348	27.003	20111244
36	XCTD+TM_3	2021/09/18	08:24	73-00.5999N	157-19.4580W	2402	0.833	26.317	20111251
37	WaveBouy_2	2021/09/18	17:07	73-28.7720N	158-44.9933W	2463	-1.036	26.571	20111254
38	St17-St18_1	2021/09/19	03:37	73-14.5717N	157-30.0615W	2901	0.996	27.052	20111243
39	St17-St18_2	2021/09/19	06:09	73-11.2364N	155-45.0544W	3262	0.088	25.696	20111249
40	St18-St19	2021/09/19	12:28	72-57.1032N	154-47.6030W	3461	0.382	26.971	20111246
41	St19-St20_1	2021/09/20	00:44	72-30.0254N	154-53.2441W	2666	2.028	26.915	20111256
42	St19-St20_2	2021/09/20	02:41	72-17.6600N	153-50.0267W	2391	1.889	25.540	20111260
43	St19-St20_3	2021/09/20	04:29	72-03.8990N	152-54.7781W	2091	1.657	25.615	20111259
44	St19-St20_4	2021/09/20	04:55	71-59.3682N	153-02.0492W	1524	1.501	25.568	20111262
45	St19-St20_5	2021/09/20	05:16	71-55.6561N	153-07.3609W	1397	1.707	26.147	20111258
46	St19-St20_6	2021/09/20	05:36	71-52.2140N	153-11.9387W	743	2.384	29.518	20111264
47	St20-St21_1	2021/09/20	08:42	71-44.6132N	153-22.0878W	128	4.119	29.902	20111261
48	St20-St21_2	2021/09/20	09:06	71-40.3460N	153-27.5228W	53	4.513	29.834	20111252
49	St20-St21_3	2021/09/20	10:46	71-55.2015N	153-49.7556W	484	2.066	27.360	20111255
50	St21-St22_1	2021/09/20	15:37	72-02.5308N	155-11.2499W	425	2.043	29.203	20111257
51	St21-St22_2	2021/09/20	17:36	72-19.5835N	156-20.6132W	855	2.225	28.993	20111263
52	MID(St36-St37)	2021/09/26	03:35	70-00.0308N	167-42.6145W	48	3.704	30.922	20111265
53	MID(St37-St38)	2021/09/27	02:56	69-59.9191N	165-32.4098W	41	5.314	30.764	20121674
54	St57-St58_1	2021/10/01	08:18	66-28.8233N	168-32.9467W	52	5.329	30.392	20121676
55	St57-St58_2	2021/10/01	08:51	66-27.3400N	168-20.2147W	48	4.861	29.643	20121679
56	St57-St58_3	2021/10/01	09:20	66-25.7983N	168-10.4607W	36	5.102	30.228	20121677
57	St57-St58_4	2021/10/01	09:47	66-24.5773N	168-01.5447W	26	5.248	29.627	20121683
58	St57-St58_5	2021/10/01	11:57	66-00.8921N	167-58.8730W	33	5.050	29.419	20111266
59	St57-St58_6	2021/10/01	12:15	66-00.7705N	168-06.9349W	44	4.950	29.194	20121681
60	St57-St58_7	2021/10/01	12:35	66-00.6191N	168-16.2182W	52	5.233	28.895	20121680
61	St57-St58_8	2021/10/01	13:06	66-00.2761N	168-30.1086W	51	5.104	29.284	20121400
62	St58-St59	2021/10/01	20:08	65-44.4947N	168-38.3654W	51	5.038	29.282	20121682
63	St59-St60	2021/10/01	23:51	65-18.2363N	169-04.8580W	54	3.714	31.402	20121399
64	St60-St61	2021/10/02	04:14	64-54.3951N	169-57.7654W	48	1.490	32.615	20121675

(6) Data archives

These data obtained in this cruise will be submitted to the Data Management Group (DMG) of JAMSTEC, and will be opened to the public via "Data Research System for Whole Cruise Information in JAMSTEC (DARWIN)" in JAMSTEC web site.
<http://www.godac.jamstec.go.jp/darwin/e>

3.4. Shipboard ADCP

(1) Personnel

Amane Fujiwara	JAMSTEC	-PI
Motoyo Itoh	JAMSTEC	-CoPI
Ryo Oyama	NME (Nippon Marine Enterprises, Ltd.)	
Kazuho Yoshida	NME	
Satomi Ogawa	NME	
Ryo Kimura	NME	
Yoichi Inoue	MIRAI Crew	

(2) Objectives

To obtain continuous measurement data of the current profile along the ship's track.

(3) Parameters

Upper ocean current velocity: horizontal velocity, vertical velocity and depth.

(4) Instruments and methods

Upper ocean current measurements were made during this cruise, using the hull-mounted Acoustic Doppler Current Profiler (ADCP) system. For most of its operation, the instrument was configured for water-tracking mode. Bottom-tracking mode, interleaved bottom-ping with water-ping, was made to get the calibration data for evaluating transducer misalignment angle in the shallow water. The system consists of following components;

1. R/V MIRAI has installed the Ocean Surveyor for vessel-mount ADCP (frequency 76.8 kHz; Teledyne RD Instruments, USA). It has a phased-array transducer with single ceramic assembly and creates 4 acoustic beams electronically. We mounted the transducer head rotated to a ship-relative angle of 45 degrees azimuth from the keel.
2. For heading source, we use ship's gyro compass (Tokyo Keiki, Japan), continuously providing heading to the ADCP system directory. Additionally, we have Inertial Navigation Unit (Phins, Ixblue, France) which provide high-precision heading, attitude information, pitch and roll. They are stored in ".N2R" data files with a time stamp.
3. Differential GNSS system (StarPack-D, Fugro, Netherlands) providing precise ship's position.
4. We used VmDas software version 1.50.19(TRDI) for data acquisition.
5. To synchronize time stamp of ping with Computer time, the clock of the logging computer is adjusted to GPS time server by using NTP (Network Time Protocol).
6. Fresh water is charged in the sea chest to prevent bio fouling at transducer face.
7. The sound speed at the transducer does affect the vertical bin mapping and

vertical velocity measurement, and that is calculated from temperature, salinity (constant value; 35.0 PSU) and depth (6.5 m; transducer depth) by equation in Medwin (1975).

Data were configured for "8 m" layer intervals starting about 19m below sea surface. Data were recorded every ping as raw ensemble data (.ENR). Additionally, 15 seconds averaged data were recorded as short-term average (.STA). 300 seconds averaged data were long-term average (.LTA), respectively.
Major acquisition parameters for the measurement, Direct Command, are shown in Table 3.4-1.
Table 3.4-1: Major parameters

Bottom-Track Commands
BP = 001 Pings per Ensemble (almost less than 1,300m depth)
Environmental Sensor Commands
EA = 04500 Heading Alignment (1/100 deg)
ED = 00065 Transducer Depth (0 - 65535 dm)
EF = +001 Pitch/Roll Divisor/Multiplier (pos/neg) [1/99 - 99]
EH = 00000 Heading (1/100 deg)
ES = 35 Salinity (0-40 pp thousand)
EX = 00000 Coordinate Transform (Xform:Type; Tilts; 3Bm; Map)
EZ = 10200010 Sensor Source (C; D; H; P; R; S; T; U)
C (1): Sound velocity calculates using ED, ES, ET (temp.)
D (0): Manual ED
H (2): External synchro
P (0), R (0): Manual EP, ER (0 degree)
S (0): Manual ES
T (1): Internal transducer sensor
U (0): Manual EU
EV = 0 Heading Bias(1/100 deg)
Timing Commands
TE = 00:00:02.00 Time per Ensemble (hrs:min:sec.sec/100)
TP = 00:02.00 Time per Ping (min:sec.sec/100)
Water-Track Commands
WA = 255 False Target Threshold (Max) (0-255 count)

WC = 120 Low Correlation Threshold (0-255)
WD = 111 100 000 Data Out (V; C; A; PG; St; Vsum; Vsum^2; #G; P0)
WE = 1000 Error Velocity Threshold (0-5000 mm/s)
WF = 0800 Blank After Transmit (cm)
WN = 100 Number of depth cells (1-128)

WP = 00001 Pings per Ensemble (0-16384)
WS = 800 Depth Cell Size (cm)
WV = 0390 Radial Ambiguity Velocity (cm/s)

(5) Observation log
31 Aug. 2021 - 21 Oct. 2021 (UTC)

(6) Preliminary results
Figure 3.4-1 shows the current velocity of Barrow Canyon line.

(7) Data archives
These data obtained in this cruise will be submitted to the Data Management Group of JAMSTEC, and will be opened to the public via "Data Research System for Whole Cruise Information in JAMSTEC (DARWIN)" in JAMSTEC web site.
< http://www.godac.jamstec.go.jp/darwin/e >

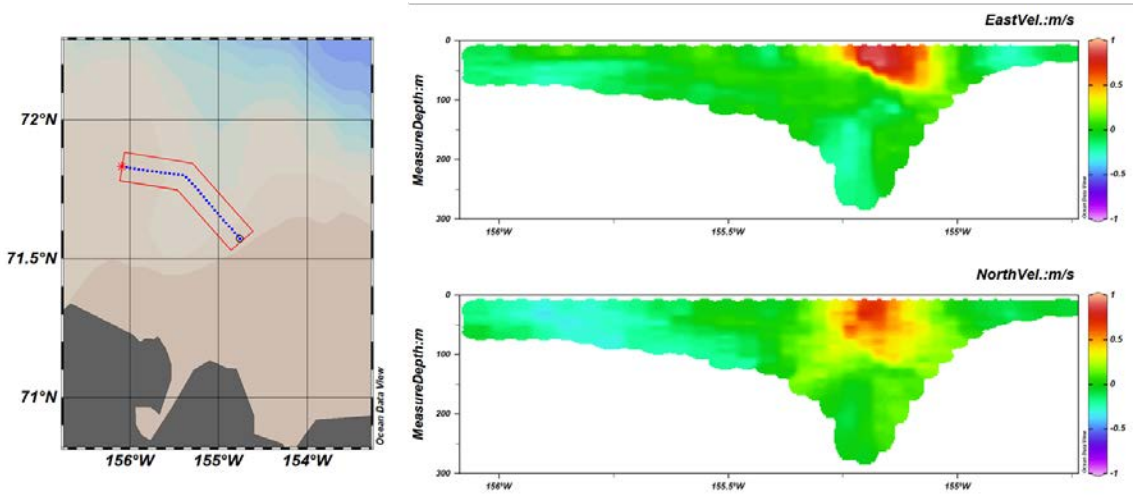

Figure 3.4-1: The current velocity of Barrow Canyon line.

3.5. TurboMap

(1) Personnel

Yusuke Kawaguchi, University of Tokyo (PI) -not on board
Eun Yae Son, University of Tokyo
Ryo Oyama, NME (Operation leader)
Yoshida Kazuho, NME
Kimura Ryo, NME
Ogawa Satomi, NME
Inoue Yoichi, NME
Shigeto Nishino, JAMSTEC

(2) Objectives

Investigate on turbulent mixing in the western Arctic including marginal ice zone.
Quantify the diapycnal heat flux from the Pacific Summer Water by the turbulent mixing

(3) Parameter

According to the manufacture's nominal specifications, the range, accuracy and sampling rates of acquisition parameters are shown in Table 3.5-1.

Table. 3.5-1: Parameters and accuracy for each sensor

Parameter	Sensor type	Measurable range	Accuracy	Sampling rate
∂u/∂z (primary)	Shear probe	0~10 /s	5%	512Hz
T+∂T/∂z	FPO-7 thermistor	±0.01°C	±0.01°C	512Hz
T	Platinum wire thermometer	−5~45°C	±0.01°C	64 Hz
Conductivity	Inductive Cell	0~70 mS	±0.01 mS	64 Hz
Depth	Semiconductor strain gauge	0~1000 m	±0.2%	64Hz
x- acceleration	Solid-state fixed mass	±2 G	±1%	256 Hz
y- acceleration	Solid-state fixed mass	±2 G	±1%	256 Hz
z- acceleration	Solid-state fixed mass	±2 G	±1%	64Hz
Chlorophyll	Solid-state fixed mass	0~100 µg/Lm	0.5 µg/L or ±1%	256 Hz
Turbidity	Backscatter	0~100 ppm	1ppm or ±2%	256 Hz

∂u/∂z (Secondary)	∂u/∂z Shear	0~10 s^{-1}	5%	512 Hz

(4) Instruments and methodology

Turbulence Ocean Microstructure Acquisition Profiler (TurboMAP-L, manufactured by JFE Alec Co Ltd.) was used to measure turbulence-scale temperature and shear. TurboMap is a quasi-free-falling instrument that obtains turbulent mixing parameters (∂u/∂z and ∂T/∂z), bio-optical parameters (in vivo fluorescence and back scatter) and hydrographic parameters (conductivity, temperature, and pressure). The TurboMAP is a loosely tethered free-fall profiler that carries two airfoil shear probes, a fast-response thermistor (FP07), a light-emitting diode fluorescence/turbidity probe, and a CTD package (Wolk et al. 2002). The TurboMAP collects vertical profiles of microscale velocity shear, high- and low-resolution temperature, conductivity, and pressure, as the underwater device descends from the surface to maximum depth. The free-falling speed of the instrument is roughly at 0.5–0.6 m s^{-1}. Operation of the ship's side thrusters is halted under operation of micro-data acquisition so that they may not create any artificial noise corruption or disturbance in the micro-scale data. The microscale data within 5 m depth are not recommended for the use in analysis as they may include potential noise due to the instrument's initial adjustment to free-falling.

(5) Station log

We conducted 108 casts in total including test casts of MR2105C-1.BIN, MR2105C-3.BIN, and MR2105C-3.BIN. The raw data has a format of MR2105C-No.BIN, where No. is written in Table. 3.5-2, the data log. Data acquisition location is marked as orange reversed triangles in Figure 3.5-1.

Table. 3.5-2: Lists of stations and filename

Cast	Date (UTC)	Latitude	Longitude	Depth (m)	Obs. Depth (m)	File name
01	2021/09/04	46-58.4245N	159-58.4079E	5195	592	MR2105C-1.BIN
02	2021/09/04	46-58.4245N	159-58.4079E	5195	528	MR2105C-2.BIN
03	2021/09/04	46-58.4245N	159-58.4079E	5195	540	MR2105C-3.BIN
04	2021/09/12	71-35.4654N	154-48.6813W	39	36	MR2105C-4.BIN
05	2021/09/12	71-35.4654N	154-48.6813W	39	36	MR2105C-5.BIN
06	2021/09/12	71-35.4654N	154-48.6813W	39	36	MR2105C-6.BIN
07	2021/09/12	71-42.3885N	154-49.4290W	101	76	MR2105C-7.BIN
08	2021/09/12	71-42.3885N	154-49.4290W	101	83	MR2105C-8.BIN
09	2021/09/13	71-44.6157N	155-05.4506W	261	238	MR2105C-9.BIN

10	2021/09/13	71-44.6157N	155-05.4506W	261	217	MR2105C-10.BIN
11	2021/09/13	71-48.2784N	155-16.4573W	202	188	MR2105C-11.BIN
12	2021/09/13	71-48.2784N	155-16.4573W	202	192	MR2105C-12.BIN
13	2021/09/13	71-49.0165N	155-36.0931W	120	101	MR2105C-13.BIN
14	2021/09/13	71-49.0165N	155-36.0931W	120	109	MR2105C-14.BIN
15	2021/09/13	71-49.8723N	156-02.3357W	84	81	MR2105C-15.BIN
16	2021/09/13	71-49.8723N	156-02.3357W	84	81	MR2105C-16.BIN
17	2021/09/13	71-49.8723N	156-02.3357W	84	79	MR2105C-17.BIN
18	2021/09/13	72-06.2810N	155-55.4625W	213	193	MR2105C-18.BIN
19	2021/09/13	72-06.2810N	155-55.4625W	213	184	MR2105C-19.BIN
20	2021/09/13	72-17.8919N	155-41.8209W	1123	570	MR2105C-20.BIN
21	2021/09/14	72-28.5949N	155-35.6301W	1819	580	MR2105C-21.BIN
22	2021/09/16	74-31.3424N	161-55.7946W	1684	267	MR2105C-22.BIN
23	2021/09/16	74-31.3424N	161-55.7946W	1684	252	MR2105C-23.BIN
24	2021/09/17	73-00.4866N	159-35.9734W	286	262	MR2105C-24.BIN
25	2021/09/17	73-00.4866N	159-35.9734W	286	257	MR2105C-25.BIN
26	2021/09/17	72-35.8656N	160-49.9041W	49	46	MR2105C-26.BIN
27	2021/09/17	72-35.8656N	160-49.9041W	49	46	MR2105C-27.BIN
28	2021/09/17	72-35.8656N	160-49.9041W	49	46	MR2105C-28.BIN
29	2021/09/18	72-43.7292N	157-54.7171W	393	345	MR2105C-29.BIN
30	2021/09/18	72-43.7292N	157-54.7171W	393	378	MR2105C-30.BIN
31	2021/09/18	72-59.0516N	157-22.2466W	2287	511	MR2105C-31.BIN
32	2021/09/18	73-23.5594N	158-43.7523W	2198	596	MR2105C-32.BIN
33	2021/09/19	73-09.5975N	154-42.0277W	3775	537	MR2105C-33.BIN
34	2021/09/19	72-43.3769N	155-07.3090W	2972	541	MR2105C-34.BIN
35	2021/09/20	71-48.3817N	153-12.7596W	260	196	MR2105C-35.BIN
36	2021/09/20	71-48.3817N	153-12.7596W	260	221	MR2105C-36.BIN
37	2021/09/20	72-01.1000N	154-38.6802W	1149	573	MR2105C-37.BIN
38	2021/09/20	72-27.5422N	156-59.9513W	457	447	MR2105C-38.BIN
39	2021/09/21	72-01.3328N	158-32.2595W	56	34	MR2105C-39.BIN
40	2021/09/21	72-01.3328N	158-32.2595W	56	37	MR2105C-40.BIN
41	2021/09/21	72-01.3328N	158-32.2595W	56	30	MR2105C-41.BIN
42	2021/09/21	72-01.3328N	158-32.2595W	56	44	MR2105C-42.BIN
43	2021/09/21	71-31.2786N	162-27.6640W	43	39	MR2105C-43.BIN
44	2021/09/21	71-31.2556N	162-27.6620W	43	36	MR2105C-44.BIN
45	2021/09/21	71-31.2296N	162-27.6563W	43	39	MR2105C-45.BIN

46	2021/09/21	70-59.6277N	161-06.1686W	45	35	MR2105C-46.BIN
47	2021/09/21	70-59.6277N	161-06.1686W	45	42	MR2105C-47.BIN
48	2021/09/21	70-59.6277N	161-06.1686W	45	38	MR2105C-48.BIN
49	2021/09/22	71-26.3755N	164-57.0709W	42	38	MR2105C-49.BIN
50	2021/09/22	71-26.3755N	164-57.0709W	42	38	MR2105C-50.BIN
51	2021/09/22	71-26.3755N	164-57.0709W	42	37	MR2105C-51.BIN
52	2021/09/22	71-44.7162N	163-23.9965W	40	30	MR2105C-52.BIN
53	2021/09/22	71-44.7162N	163-23.9965W	40	35	MR2105C-53.BIN
54	2021/09/22	71-44.7162N	163-23.9965W	40	36	MR2105C-54.BIN
55	2021/09/23	71-45.8694N	166-21.4395W	45	38	MR2105C-55.BIN
56	2021/09/23	71-45.8694N	166-21.4395W	45	39	MR2105C-56.BIN
57	2021/09/23	71-45.8694N	166-21.4395W	45	39	MR2105C-57.BIN
58	2021/09/23	72-00.2295N	168-45.3683W	51	47	MR2105C-58.BIN
59	2021/09/23	72-00.2295N	168-45.3683W	51	45	MR2105C-59.BIN
60	2021/09/23	72-00.2295N	168-45.3683W	51	41	MR2105C-60.BIN
61	2021/09/23	72-03.8588N	167-57.4794W	50	46	MR2105C-61.BIN
62	2021/09/23	72-03.8588N	167-57.4794W	50	43	MR2105C-62.BIN
63	2021/09/23	72-03.8588N	167-57.4794W	50	43	MR2105C-63.BIN
64	2021/09/24	71-30.2633N	168-44.3210W	48	39	MR2105C-64.BIN
65	2021/09/24	71-30.2633N	168-44.3210W	48	41	MR2105C-65.BIN
66	2021/09/24	71-30.2633N	168-44.3210W	48	41	MR2105C-66.BIN
67	2021/09/24	71-30.2633N	168-44.3210W	45	37	MR2105C-67.BIN
68	2021/09/24	71-30.2633N	168-44.3210W	45	40	MR2105C-68.BIN
69	2021/09/24	71-30.2633N	168-44.3210W	45	41	MR2105C-69.BIN
70	2021/09/25	70-59.9910N	168-44.9423W	44	37	MR2105C-70.BIN
71	2021/09/25	70-59.9910N	168-44.9423W	44	38	MR2105C-71.BIN
72	2021/09/25	70-59.9910N	168-44.9423W	44	40	MR2105C-72.BIN
73	2021/09/25	70-29.9281N	168-44.6235W	39	30	MR2105C-73.BIN
74	2021/09/25	70-29.9281N	168-44.6235W	39	32	MR2105C-74.BIN
75	2021/09/25	70-29.9281N	168-44.6235W	39	33	MR2105C-75.BIN
76	2021/09/26	70-00.1353N	166-39.5095W	47	38	MR2105C-76.BIN
77	2021/09/26	70-00.1353N	166-39.5095W	47	39	MR2105C-77.BIN
78	2021/09/26	70-00.1353N	166-39.5095W	47	40	MR2105C-78.BIN
79	2021/09/28	69-25.7930N	167-27.5882W	48	42	MR2105C-79.BIN
80	2021/09/28	69-25.7930N	167-27.5882W	48	43	MR2105C-80.BIN
81	2021/09/28	69-25.7930N	167-27.5882W	48	44	MR2105C-81.BIN

82	2021/09/28	69-29.9932N	168-45.0280W	51	41	MR2105C-82.BIN
83	2021/09/28	69-29.9932N	168-45.0280W	51	42	MR2105C-83.BIN
84	2021/09/28	69-29.9932N	168-45.0280W	51	47	MR2105C-84.BIN
85	2021/09/28	69-00.1480N	168-45.1918W	53	43	MR2105C-85.BIN
86	2021/09/28	69-00.1480N	168-45.1918W	53	46	MR2105C-86.BIN
87	2021/09/28	69-00.1480N	168-45.1918W	53	45	MR2105C-87.BIN
88	2021/09/28	68-48.0635N	166-57.1802W	41	36	MR2105C-88.BIN
89	2021/09/28	68-48.0635N	166-57.1802W	41	36	MR2105C-89.BIN
90	2021/09/28	68-48.0635N	166-57.1802W	41	36	MR2105C-90.BIN
91	2021/09/29	68-30.4428N	168-44.8893W	53	47	MR2105C-91.BIN
92	2021/09/29	68-30.4428N	168-44.8893W	53	45	MR2105C-92.BIN
93	2021/09/29	68-30.4428N	168-44.8893W	53	48	MR2105C-93.BIN
94	2021/09/29	68-02.0567N	168-49.9505W	59	49	MR2105C-94.BIN
95	2021/09/29	68-02.0567N	168-49.9505W	59	54	MR2105C-95.BIN
96	2021/09/29	68-02.0567N	168-49.9505W	59	55	MR2105C-96.BIN
97	2021/09/29	67-30.0270N	168-44.3620W	49	45	MR2105C-97.BIN
98	2021/09/29	67-30.0270N	168-44.3620W	49	43	MR2105C-98.BIN
99	2021/09/29	67-30.0270N	168-44.3620W	49	42	MR2105C-99.BIN
100	2021/10/02	65-05.5834N	169-31.2331W	51	34	MR2105C-100.BIN
101	2021/10/02	65-05.5834N	169-31.2331W	51	40	MR2105C-101.BIN
102	2021/10/02	65-05.5834N	169-31.2331W	51	42	MR2105C-102.BIN
103	2021/10/02	64-43.4031N	170-25.6422W	49	41	MR2105C-103.BIN
104	2021/10/02	64-43.4031N	170-25.6422W	49	44	MR2105C-104.BIN
105	2021/10/02	64-43.4031N	170-25.6422W	49	42	MR2105C-105.BIN
106	2021/10/02	64-18.8991N	171-18.1887W	46	41	MR2105C-106.BIN
107	2021/10/02	64-18.8991N	171-18.1887W	46	36	MR2105C-107.BIN
108	2021/10/02	64-18.8991N	171-18.1887W	46	39	MR2105C-108.BIN

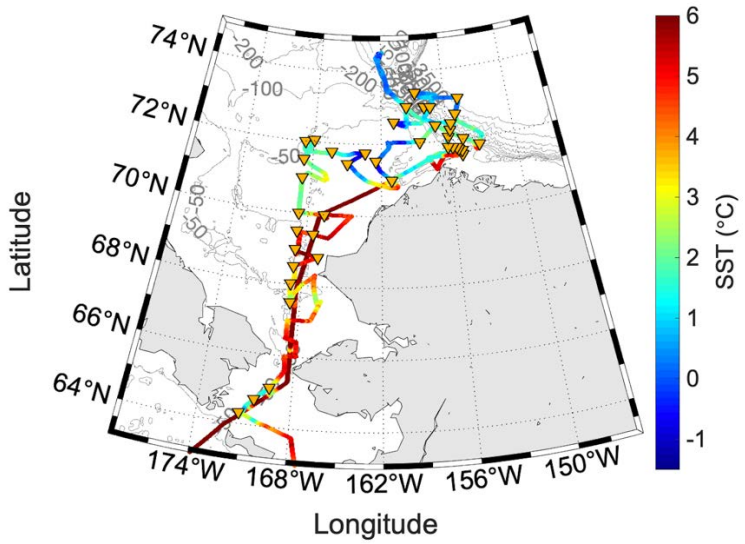

Figure 3.5-3: Map of the western Arctic with TurboMap observation station during MR21-05C cruise. The colored line shows sea surface temperature along the cruise track of Mirai.

Preliminary results

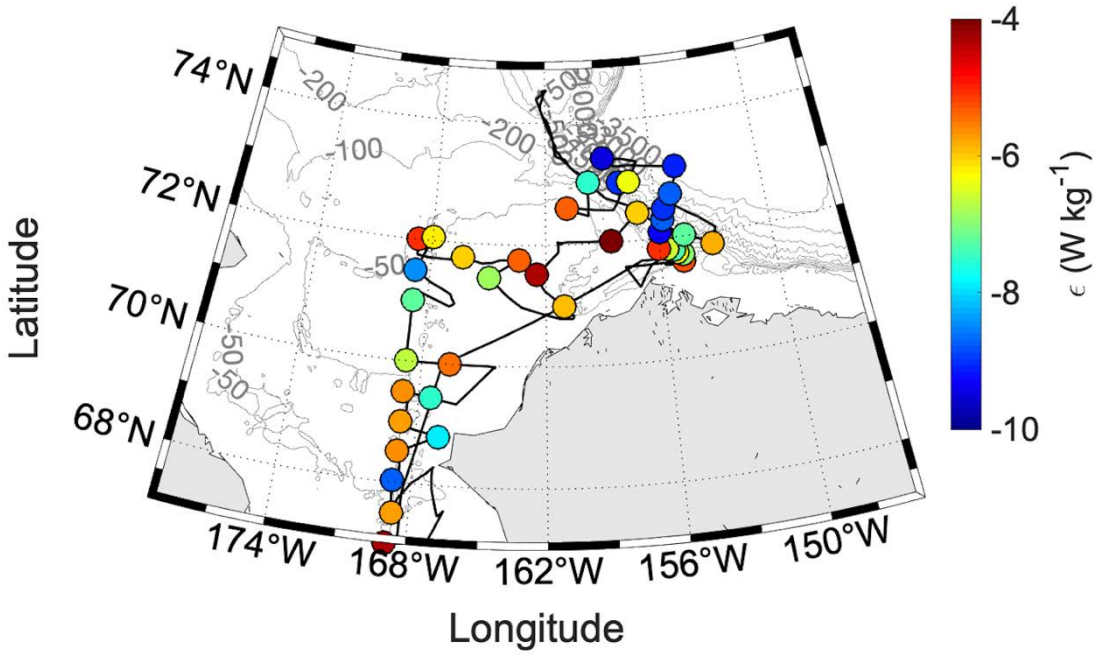

Figure 3.5-2: Averaged turbulence dissipation rate over salinity range of 29–32 psu. The black solid line shows cruise track of R/V *Mirai*.

To quantify the turbulence strength within the Pacific Summer Water, we take an average of turbulence dissipation rate (e) between the salinity range of 29–32 psu (Figure 3.5-2). It showed less turbulent mixing in the Canada Basin area near the values at O(-

9 W kg^{-1}). On the other hand, it showed elevated values in the shelf area. Especially, it showed the highest value near Hanna Shoal area rather than other Chukchi area. Over the Barrow Canyon area showed the values near O(-7 W kg^{-1}).

(6) Remarks

TurboMAP consists of 2 shear probes for checking shear data validity. It is able to be utilized with only one shear probe, however, a pair of shear sensor is recommended. Figure 3.5-3 is turbulence dissipation rate that obtained by each shear sensors to see the validation among sensors. During MR21-05C, we utilized two set of shear probe (Cast No. 3~20: shear1: S/N 505 shear2: S/N 1233; Cast No. 21~108: shear1: S/N 505, shear2: S/N 1233). Throughout the observation, we utilized FP07 which has a S/N of 147. The detailed information is written in observation log.

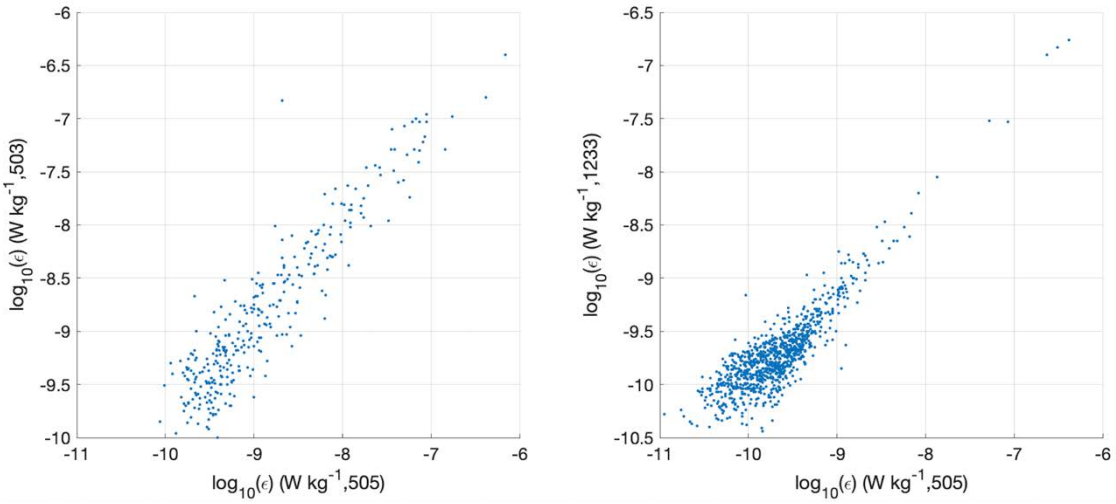

Figure 3.5-3: Correlation between the two shear sensors that used for MR21-05C.

(7) Data archive

These data obtained in this cruise will be submitted to the Data Management Group of JAMSTEC, and will be opened to the public via "Data Research System for Whole Cruise Information in JAMSTEC (DARWIN)" in JAMSTEC web site.

<http://www.godac.jamstec.go.jp/darwin/e>

3.6. Buoys

3.6.1. Drifting buoy

(1) Personnel

Yusuke Kawaguchi, University of Tokyo (PI) - not on board

Eun Yae Son, University of Tokyo

(2) Objectives

Investigation on the heat variation of the incoming Pacific Summer Water from the Barrow canyon

(3) Parameter

IceBTC100/40-17T3P (IMEI: 300234061169620)

GPS positions and air pressure of drifting buoy

Water temperature and hydrostatic pressure at certain depth

(4) Instruments and methodology

We deployed ice buoy for investigating heat variability of the Pacific Summer Water by following the Alaskan coastal current. IceBTC100/40 is designed for utilization in the sea ice covered area which has a 100 m-long thermistor chain with the pressure sensors. It measures upper ocean temperature with the accuracy of +/-0.1°C (resolution of 0.04°C) and air pressure with the accuracy of +/-1 hPa (resolution of 0.1 hPa). IceBTC40/60 has 17 thermistors and three hydrostatic pressure sensors. We deployed the buoy in the deepest station in the Barrow canyon near the mooring station BCC (St.04).

Table. 3.6.1-1: Deployment information

Type	Argos ID	Deploy time (UTC)	Deploy location [deg-min]	Data interval	Depth (m)	denotes
IceBTC100/40	206617	15:11 Sep 13, 2021	71-44.10N, 143-16.151W	hourly	261	Barrow Canyon

(5) Preliminary result

The buoy drifts along the current to western part of the Barrow Canyon. However, it stopped to move since September 23 at the western part of the Barrow Canyon (Figure 3.6.1-1). The deepest pressure sensor showed pressure near 74.3 dbar which supposed to be 110 m. The temperature timeseries shows the semi-diurnal pattern, which is suspected to tidal motion (Figure 3.6.1-2).

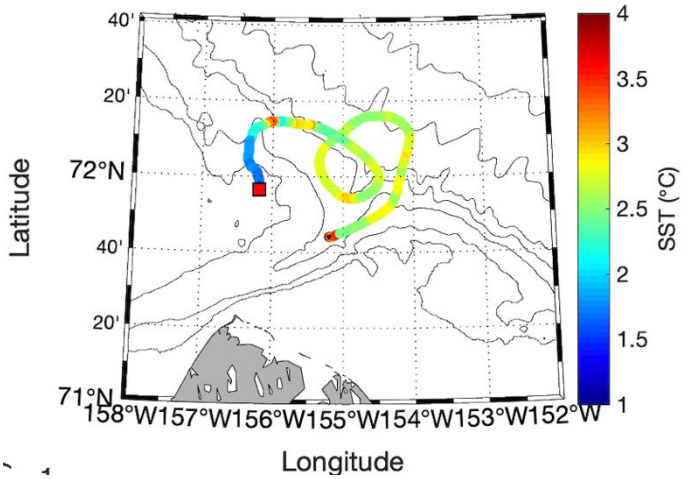

Figure 3.6.1-1: Bottom topography of near Barrow Canyon area with the buoy's drift track. The color represents the sea surface temperature that is measured by the buoy. The red square shows the location since September 23.

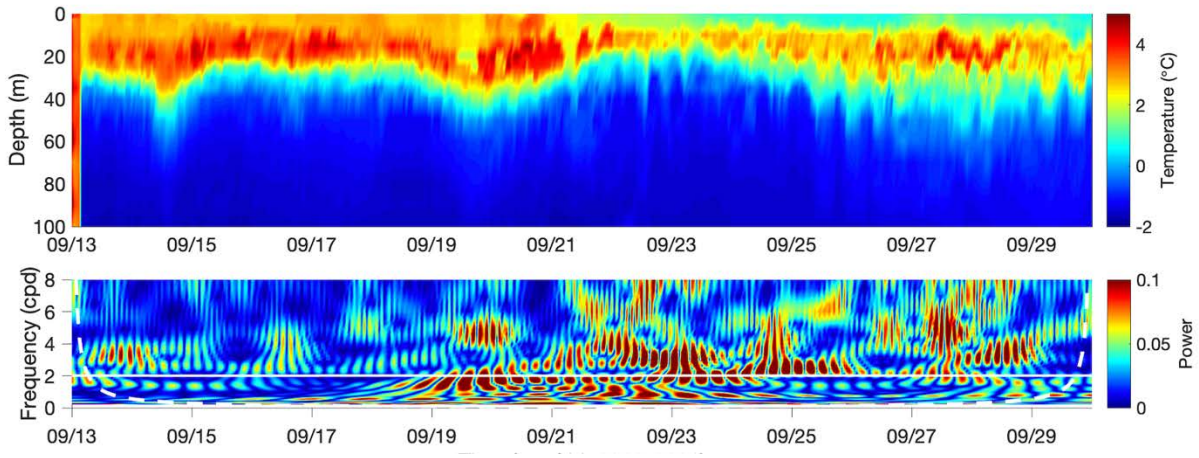

Figure 3.6.1-2: Timeseries of water temperature from IceBTC100/40 (upper panel) and morlet wavelet analysis of temperature at 20 m depth (lower panel). The white dashed line shows 95% of confidence line of wavelet analysis and Inertial frequency line is shown as white solid line.

(6) Data archive

The raw data obtained in this cruise will be submitted to the Data Management Group (DMG) of JAMSTEC.

3.6.2. Wave buoys

(1) Personnel
Takuji Waseda (Principal Investigator, the University of Tokyo, not on board)
Tsubasa Kodaira (the University of Tokyo, not on board)
Takehiko Nose (the University of Tokyo, not on board)
Yasushi Fujiwara (the University of Tokyo)
Ryosuke Uchiyama (the University of Tokyo)
Tomotaka Katsuno (the University of Tokyo, not on board)

(2) Objectives
Interaction processes between ocean waves and sea ice, which are becoming more important in the Arctic Sea, are not fully understood. To deepen their understandings, two drifting buoys were deployed near the ice edge to measure the waves in the water near the old ice and in the freezing season. Another buoy was used for tethered measurement, aiming for calibration of other wave measurement instruments.

(3) Parameters
The following statistical parameters are calculated and sent via satellite every hour.
Significant wave height, peak wave period, peak wave direction, peak wave directional spread, mean wave period, mean wave direction, mean wave directional spread, sea surface temperature, frequency-directional variance density spectrum, GPS location, wind speed, and wind direction
In tethered measurement, raw timeseries of 3-dimensional GPS location is also retrieved.

(4) Instruments and methods
The type of drifting wave buoy used was a Spotter device manufactured by Sofar Ocean Technologies. They are battery- and solar-powered and have a two-way communication function via Iridium satellite communication.
Three buoys were used. SPOT-1391 and SPOT-1218 were deployed near the ice edge, and SPOT-1216 was used for tethered measurements.
In tethered observations, the buoy was tied to a 400-meter-long rope and released from the stern. Then the ship slowly moved away so that the rope would become straight. Then the ship stayed at the location for 1-2 hours, keeping distance from the buoy.

(5) Observation log
Time and locations of wave buoy deployment are listed in Table 3.6.2-1. At both stations, the buoys were deployed at about 3 km away from the ice edge. Two buoys have been sending measured data each hour until 10-05-2021, when this report is written.

Table 3.6.2-1: Time and locations of wave buoy deployment.

Station #	Spotter ID	Time (UTC)	Location
ICE1	SPOT-1391	09-17-2021 17:00	72-35.48N ,160-52.33W
ICE2	SPOT-1218	09-18-2021 17:08	73-28.77N ,158-44.99W

Time and locations of wave buoy tethered observation are listed in Table 3.6.2-2.

Table 3.6.2-2: Time and locations of tethered measurement.

Start time (UTC)	End time (UTC)	Location
09-04-2021 22:21	09-05-2021 00:15	49-21.48N ,164-37.87E
09-13-2021 04:19	09-13-2021 05:41	71-48.17N ,155-21.59W
10-10-2021 23:47	10-11-2021 01:41	49-54.30N ,169-29.67E
10-12-2021 22:12	10-13-2021 00:10	47-21.58N ,164-00.41E

(6) Preliminary results

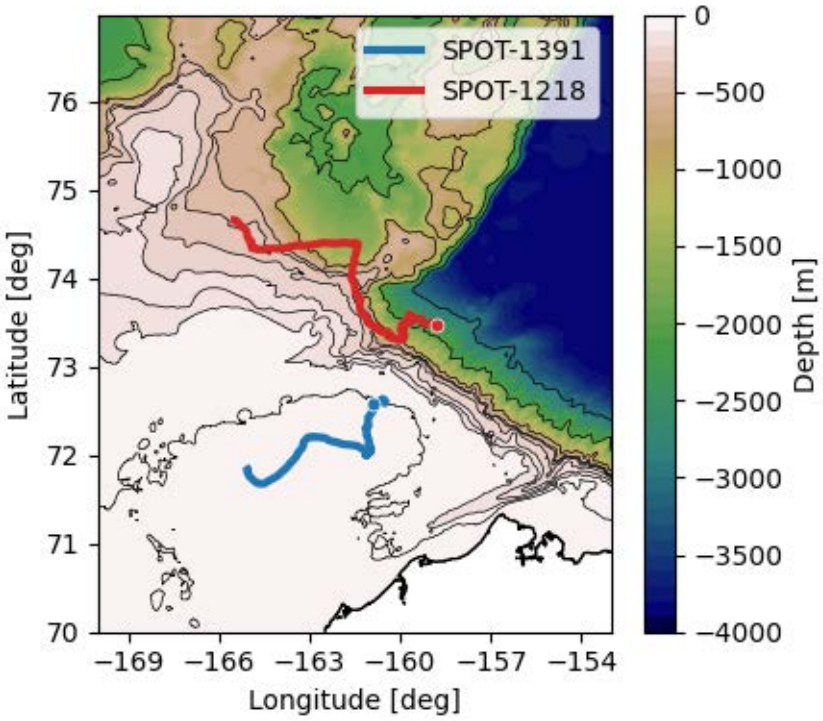

Figure 3.6.2-1: Map showing trajectories of deployed wave buoys. Points with white edges indicate the locations where the buoys were deployed.

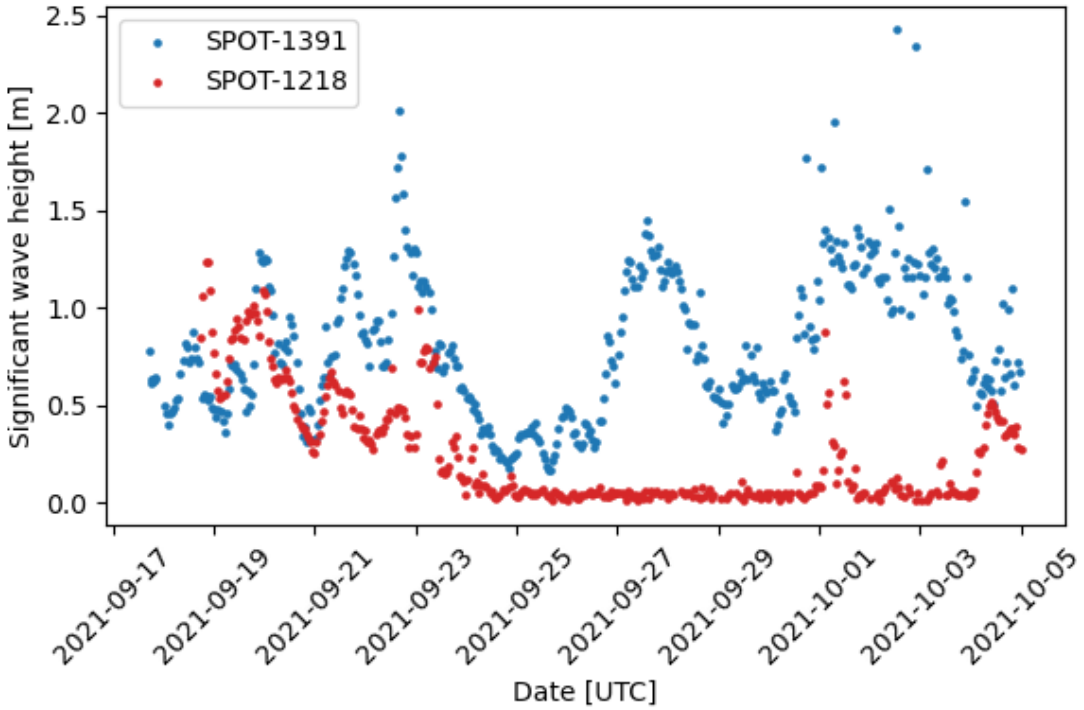

Figure 3.6.2-2: Timeseries of significant wave height observed by the deployed wave buoys.

(7) Data archives

These data obtained in this cruise will be submitted to the Data Management Group of JAMSTEC, and will be opened to the public via "Data Research System for Whole Cruise Information in JAMSTEC (DARWIN)" in JAMSTEC web site.
<http://www.godac.jamstec.go.jp/darwin/e>

3.7. Microwave wave gauge

(1) Personnel
Takuji Waseda (Principal Investigator, not on board)
Tsubasa Kodaira (not on board)
Takehiko Nose (not on board)
Yasushi Fujiwara
Ryosuke Uchiyama

(2) Objectives
Microwave wave gauge was installed at the bow to obtain a continuous and detailed wave data at the ship location.

(3) Parameters
Relative speed of the instrument and the water surface, three-component acceleration, and three-component angular velocity

(4) Instruments and methods
Doppler wave sensor system (SJM-001), produced by Japan Radio Co. Ltd., was installed at the bow (Figure 3.7-1). It is connected to a computer via ethernet, where the data is continuously recorded.

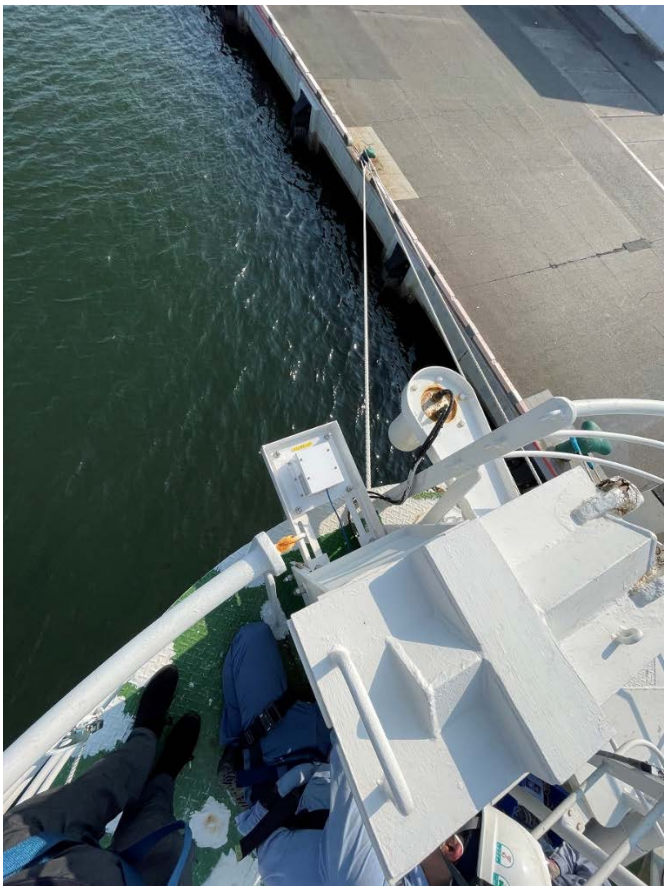

Figure 3.7-1: Microwave wave gauge installed at the bow.

The sensor radiates microwave signal to the water and measures the Doppler shift frequency of the reflected signal. Doppler shift frequency is converted to the relative speed, and then the accelerometer and the gyro sensor data is used to correct for ship motion to obtain the absolute motion of the water surface.
The data is obtained at 10 Hz frequency, and spectral analysis for noise removal is conducted for every 20 minutes record. Data quality is checked by using the ship heading direction, ship speed, and wind direction.

(5) Station list or Observation log

Data is continuously collected, starting from 08-29-2021 04:40 to 10-20-2021 03:40 (both in UTC). The data recording software failed between 09-09-2021 18:30 to 09-10-2021 17:20. The ethernet cable was broken down due to bad weather, and the measurement stopped between 10-12-2021 00:00 to 10-12-2021 23:20.

(6) Preliminary results

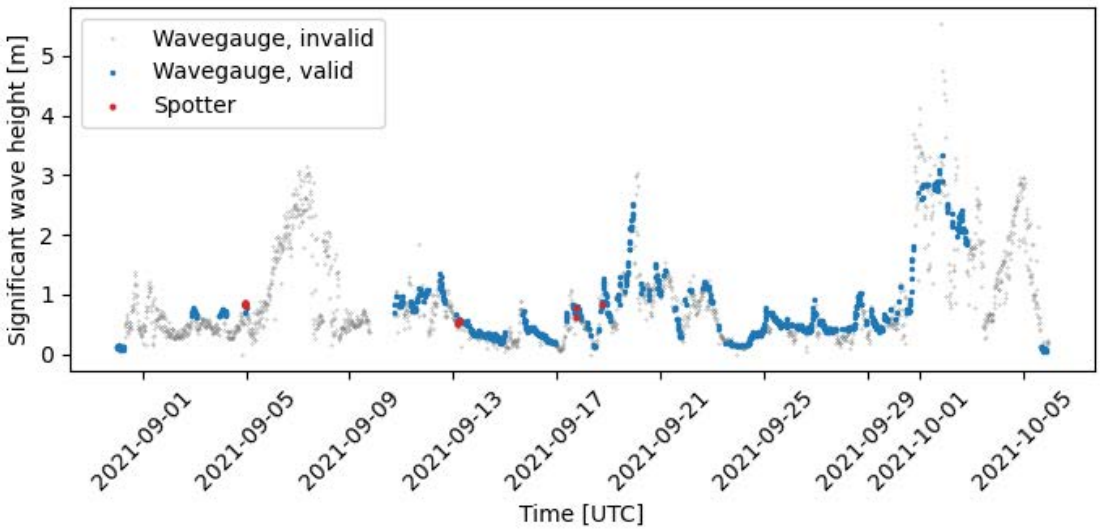

Figure 3.7-2: Time series of the significant wave height (H_m0) up to 10-05-2021. Valid and invalid data are shown with blue and gray markers, respectively. Wave heights measured by Spotter wave buoys, when they were tethered from the ship or near the ship after deployment, are shown with red markers.

(7) Data archives

These data obtained in this cruise will be submitted to the Data Management Group of JAMSTEC, and will be opened to the public via "Data Research System for Whole Cruise Information in JAMSTEC (DARWIN)" in JAMSTEC web site.
<http://www.godac.jamstec.go.jp/darwin/e>

3.8. Stereo and Network cameras

(1) Personnel

Takuji Waseda (Principal Investigator, the University of Tokyo, not on board)
Tsubasa Kodaira (the University of Tokyo, not on board)
Takehiko Nose (the University of Tokyo, not on board)
Yasushi Fujiwara (the University of Tokyo)
Ryosuke Uchiyama (the University of Tokyo)
Alberto Alberello (?, not on board)

(2) Objectives

Stereo cameras – to obtain a spatio-temporal variation of water surface elevation and ice motion
Network cameras – to obtain a continuous record of waves, ice, and sea splay (see also section 3.9)

(3) Parameters

Stereo cameras - Monochrome images (4064 x 4064 pixels), acceleration (3-axis), gyro (3-axis) and geomagnetism (3-axis).
Network cameras – Camera record in asf format.

(4) Instruments and methods

Stereo cameras - The two cameras, mounted in separate housing on the compass deck of the R/V Mirai, were synchronized to allow stereo reconstruction of the captured images of surface ocean waves. (Figure 3.8-1) Both cameras were connected via USB cables to a laptop computer placed in a watertight black plastic box (Figure 3.8-1). HDD storage device in total were also installed in the box. The system was directly connected to the environmental research lab with ethernet cables, which enable us to access the system from inside the vessel. A 9-axis inertial moment unit (ZMP-IMUZ) was also placed in the box to measure the motion of the cameras.

Figure 3.8-1: Installed stereo camera system. Cameras are indicated with orange circles, and the logger box is indicated with blue circle.

Network cameras – Four cameras (AXIS M2026-LE Mk II) are installed and recorded the whole footage of the cruise. They are connected to two recorders (AXIS S3008, 2TB) placed indoor, and the saved movies are transferred to external HDDs for backup. The locations and the directions of the cameras and their targets are listed in Table 3.8-1. The installed four cameras are shown in Figure 3.8-2.

Camera #	Location and direction	Target
1	Compass deck, looking bowside	Footage of sea splays on the deck
2	Compass deck, looking starboard side	General record of sea state and sea ice
3	Foremast top, looking back and downward	Footage of sea splays on the deck
4	Foremast top, looking bowside and downward	Waves that the ship encountered

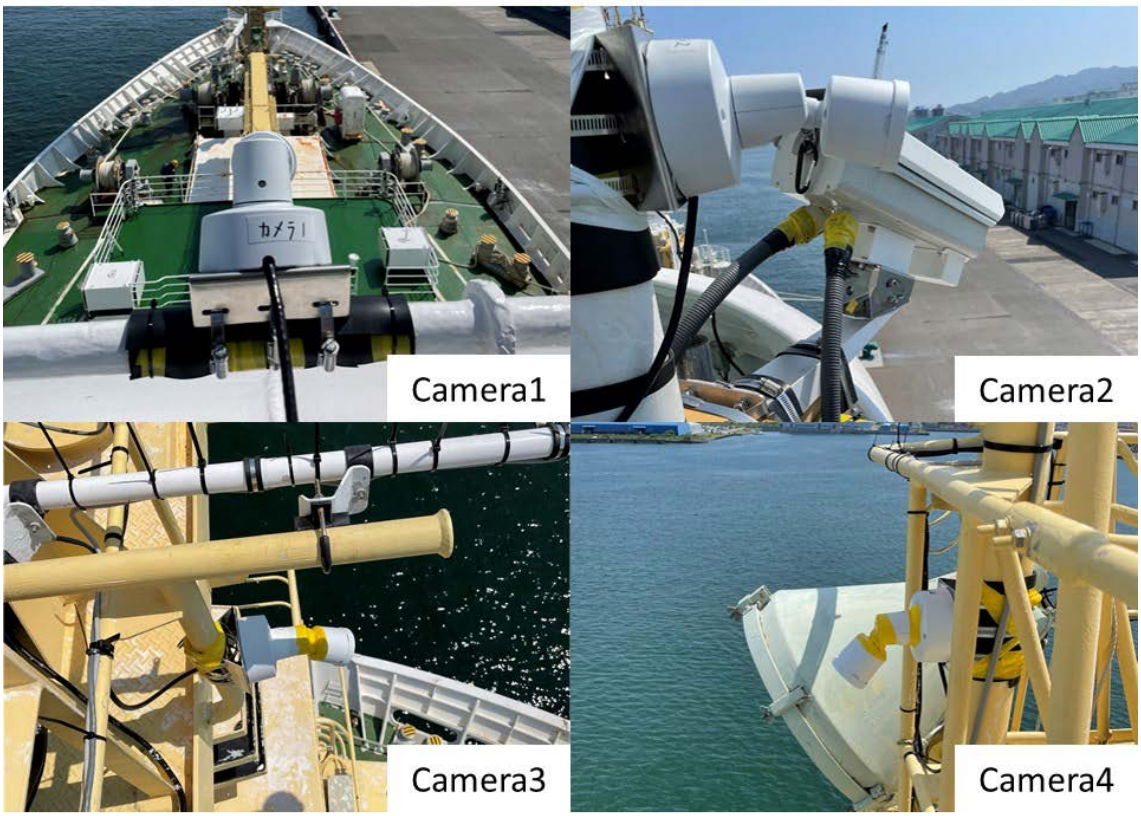

Figure 3.8-2: Installed network cameras.

(5) Station list or Observation log

Stereo cameras – Images were collected with 4Hz frequency for 20 minutes of each hour, only in daytime. They started recording in 08-31-2021 and stopped recording in 10-19-2021.

Network cameras – The four cameras continuously recorded from 08-31-2021 to 10-19-2021.

(6) Preliminary results

Figures 3.8-3 and 3.8-4 shows sample images of the stereo cameras and the network cameras, respectively.

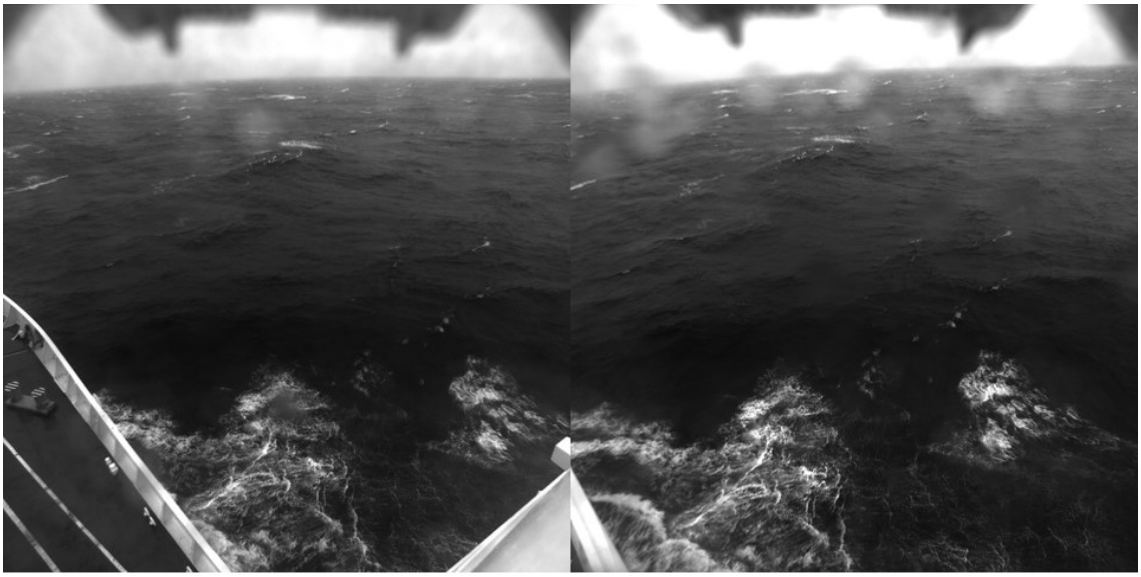

Figure 3.8-3: Sample images of the stereo cameras (left: left camera, right: right camera).

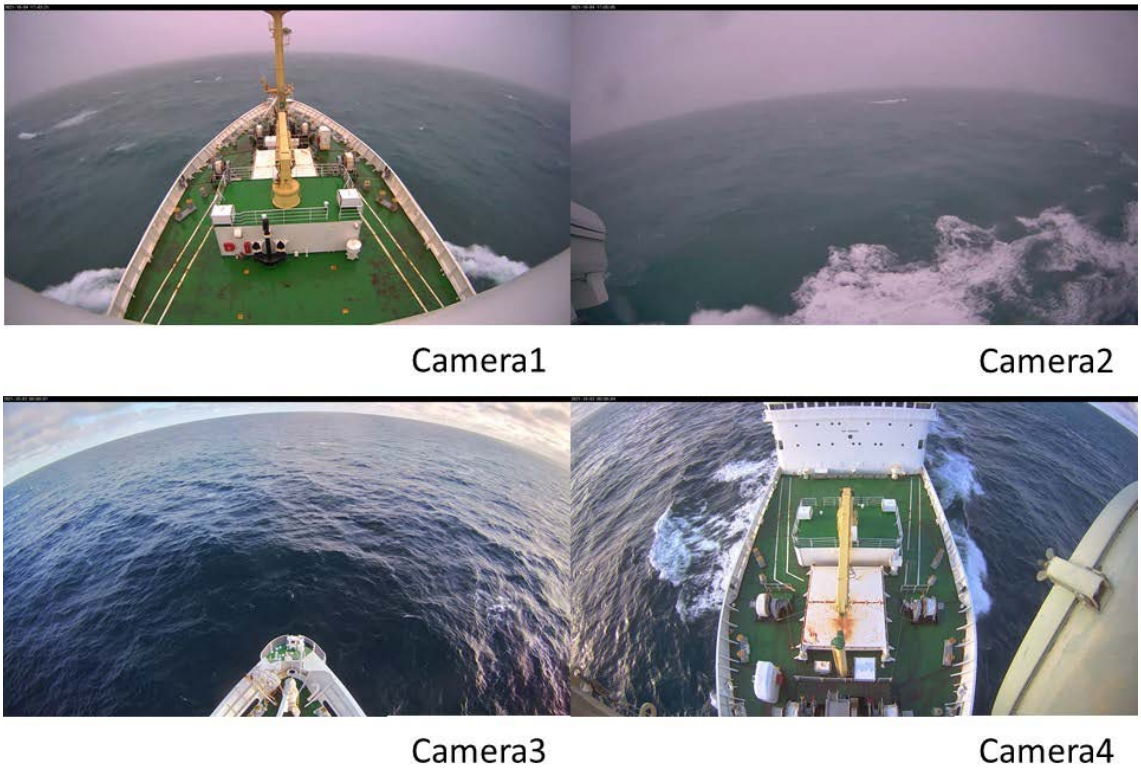

Figure 3.8-4: Sample images of the network cameras.

(7) Data archives

These data obtained in this cruise will be submitted to the Data Management Group of JAMSTEC, and will be opened to the public via "Data Research System for Whole Cruise Information in JAMSTEC (DARWIN)" in JAMSTEC web site.
<http://www.godac.jamstec.go.jp/darwin/e>

3.9. Radar

3.9.1. Ice analysis

(1) Personnel

Amane Fujiwara	JAMSTEC	-PI
Ryo Oyama	NME (Nippon Marine Enterprises, Ltd.)	
Kazuho Yoshida	NME	
Satomi Ogawa	NME	
Ryo Kimura	NME	
Yoichi Inoue	MIRAI Crew	

(2) Objectives

In the sea ice areas, marine radar provides an important tool for the detection of sea ice and icebergs. It is importance to monitor the sea ice daily and produce ice forecasts to assist ship traffic and other marine operations. In order to select route optimally, ice condition prediction technology is necessary, and image information of ice-sea radar is used for constructing a route selection algorithm.

(3) Parameters

Capture format: JPEG
Capture interval: 60 seconds
Resolution: 1,024×768 pixel
Color tone: 256 gradation

(4) Instruments and methods

R/V MIRAI is equipped with an Ice Navigation Radar, “sigma S6 Ice Navigator (Rutter Inc.)”. The ice navigation radar, the analog signal from the x-band radar is converted by a modular radar interface and displayed as a digital video image (Figure 3.9.1-1). The sea ice radar is equipped with a screen capture function and saves at arbitrary time intervals.

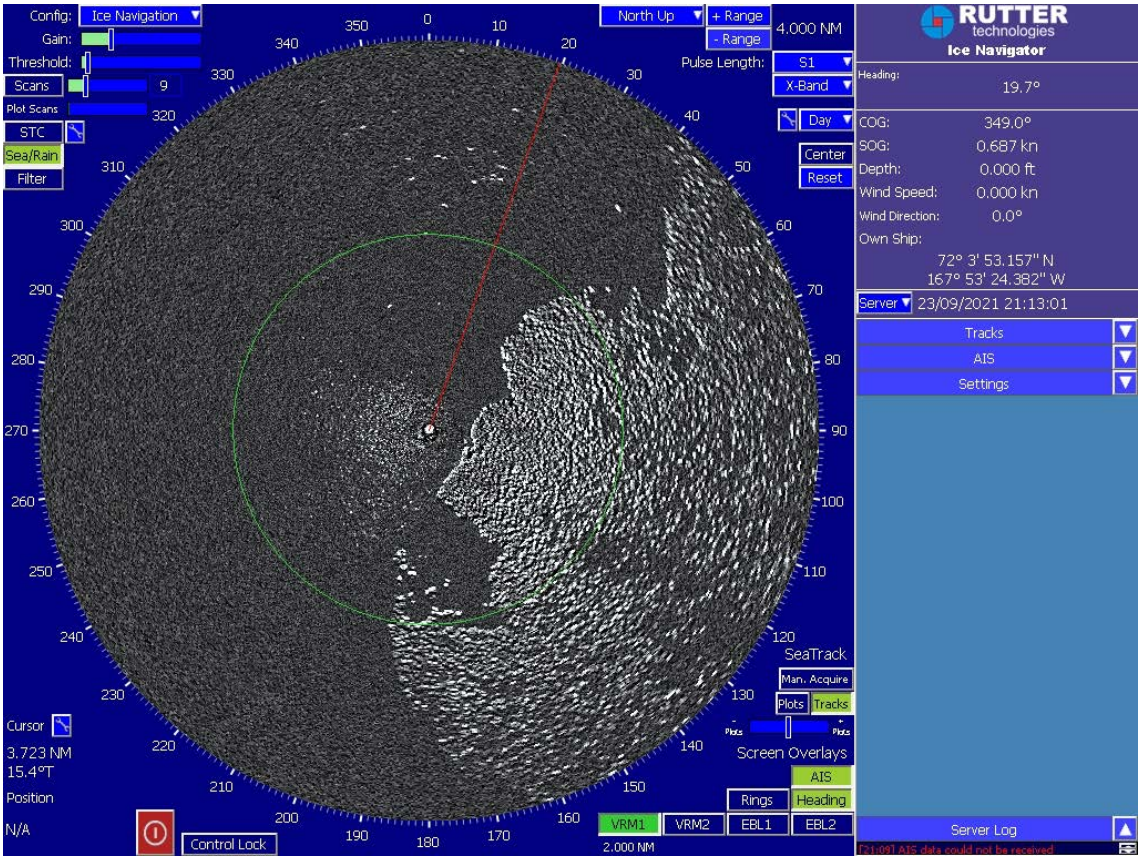

Figure 3.9.1-1: Image of sea ice analysis

(5) Observation log

08 Sep. 2021 - 01 Oct. 2021

(6) Data archives

These data obtained in this cruise will be submitted to the Data Management Group of JAMSTEC, and will be opened to the public via "Data Research System for Whole Cruise Information in JAMSTEC (DARWIN)" in JAMSTEC web site.

< http://www.godac.jamstec.go.jp/darwin/e >

3.9.2. Wave analysis

(1) Personnel

Takuji Waseda (Principal Investigator, the University of Tokyo, not on board)
Tsubasa Kodaira (the University of Tokyo, not on board)
Takehiko Nose (the University of Tokyo, not on board)
Yasushi Fujiwara (the University of Tokyo)
Ryosuke Uchiyama (the University of Tokyo)

(2) Objectives

The objective of this observation is to collect radar images in the various sea state throughout the expedition. The imagery data can be utilized to conduct following analysis.
Calibrate the significant wave height derived from SNR (signal to noise ratio) of the wave-like signal in the radar image by comparing with the buoy data during the buoy deployment. (See 3.6.2 for the detail.)
Compare the wave directional spectra derived from the radar imagery with the buoy.
Observe spatial distribution of sea ice in the marginal ice zone.

(3) Parameters

SWP file (raw radar video), OBW file (bulk parameters, such as significant wave height, SNR, wave period, etc.), PNG file (analyzed radar image), CSV file (2-D wave spectra)

(4) Instruments and methods

The X-band radar (MR) installed in R/V Mirai is used. The signal strength of the wave and sea ice from MR is recorded via the radar video logging system (JRC) and the PC which has the wave analyzing software (JRC) installed.
For the calibration of significant wave height derived from the wave analyzing software, the Spotter buoy (Sofar) is used, which is described in 3.6.2.

(5) Observation log

Both the radar video logging system and the radar analyzing PC records the file described in (3) during the period of entire cruise, except for when the ship is in port at Dutch Harbor and the radar transmit is turned off. (2021/10/5 17:00 ~ 10/6 18:00 UTC)

(6) Preliminary results

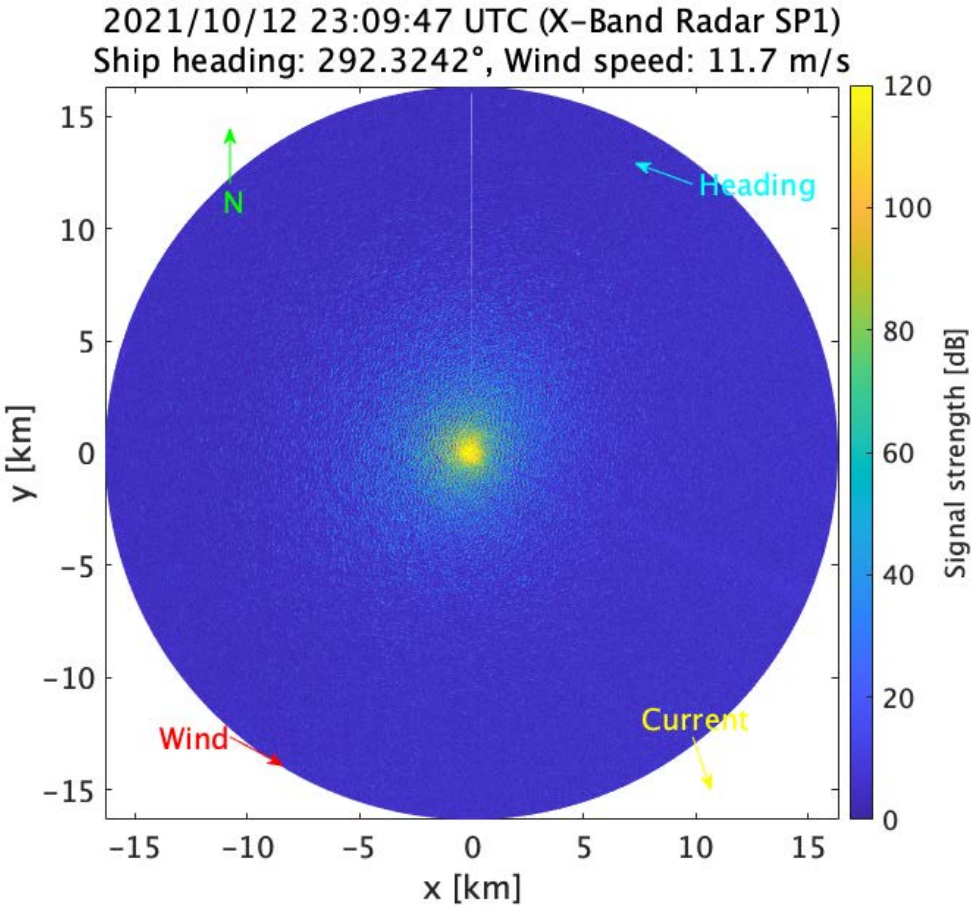

Figure 3.9.2-1: A snapshot of the radar sweep video recorded via the radar video logging system on 12th October 2021 UTC.

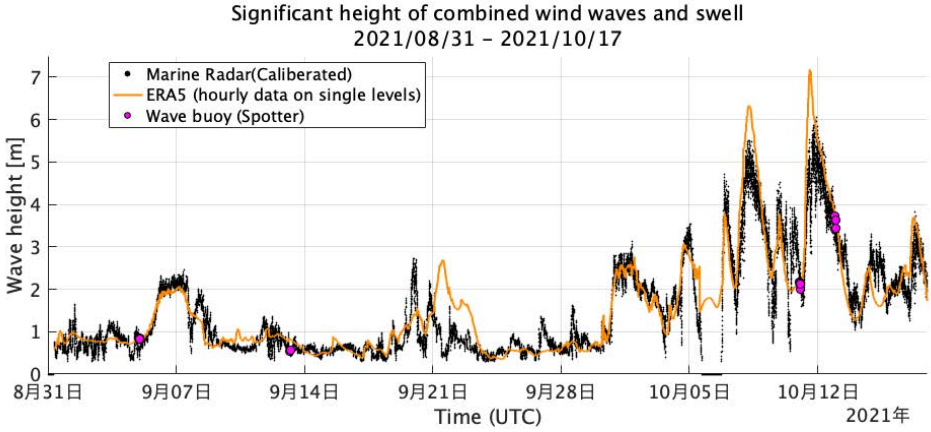

Figure 3.9.2-2: The time series of significant wave height derived by the radar during the period of 2021/8/31 to 10/17 UTC. The significant wave height derived from the buoy, which is used for the calibration, is shown in magenta color. ERA5 is also shown in orange line for a comparison.

(7) Data archives

These data obtained in this cruise will be submitted to the Data Management Group of JAMSTEC, and will be opened to the public via "Data Research System for Whole Cruise Information in JAMSTEC (DARWIN)" in JAMSTEC web site.
<http://www.godac.jamstec.go.jp/darwin/e>

3.10. Sea spray

(1) Personnel

Takuji Waseda (Principal Investigator, the University of Tokyo, not on board)
Tsubasa Kodaira (the University of Tokyo, not on board)
Takehiko Nose (the University of Tokyo, not on board)
Yasushi Fujiwara (the University of Tokyo)
Ryosuke Uchiyama (the University of Tokyo)
Toshihiro Ozeki (Hokkaido University of Education, not on board)
Takatoshi Matsuzawa (National Marine Research Institute, not on board)

(2) Objectives

Marine disasters caused by ship icing occur frequently in cold regions. The typical growth mechanism of sea spray icing is as follows. First, sea spray is generated from the bow of the ship. Next, the spray drifts and impinges upon the superstructure, after which there is a wet growth of ice from the brine water flow. To address icing on the ship, we focus on the impinging seawater spray. We investigated the liquid water contents (LWC) of seawater spray impinges on R/V Mirai, especially in front of the deck area at the bow.

(3) Parameters

CSV file (voltage)

(4) Instruments and methods

The amount of seawater spray LWC is measured by 4 sets of marine rain gauge type spray gauge (MRS). MRS is composed of a marine rain gauge (Young 50202) with a simple modification of a cylindrical spray trap installed on top of its head to collect seawater spray that will come fly in horizontally. The MRS can measure the water volume as voltage (0 ~ 500ml, 0 ~ 5V), and it will automatically flush the water when its capacity reaches full at 500ml.

Addition to the measurement of naturally encountered seawater spray, controlled measurement was conducted. In the controlled measurement, ship ran into 5 different direction (25 minutes each) heading the main wave direction: 0°(head sea), ±30°, and ±60°.

(5) Observation log

Because there was no seawater spray event in the beginning of the cruise, the data was recorded from 11th September 2021 to 17th October 2021, until the measurement units were removed. Table 3.9 shows the time and location during the controlled measurement.

Table 3.10-1: Time and locations of controlled measurement.

Start time (UTC)	End time (UTC)	Location
10-07-2021 22:00	10-08-2021 00:50	53.705N ,185.898E
10-11-2021 21:00	10-11-2021 23:55	48.738N ,167.113E
10-13-2021 00:10	10-13-2021 03:00	47.393N ,163.621E

(6) Preliminary results

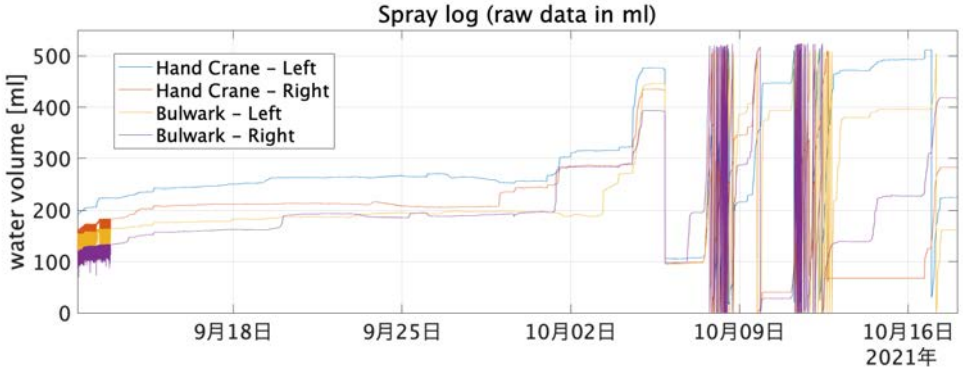

Figure 3.10-1: The time series of measured water volume in each MRS unit.

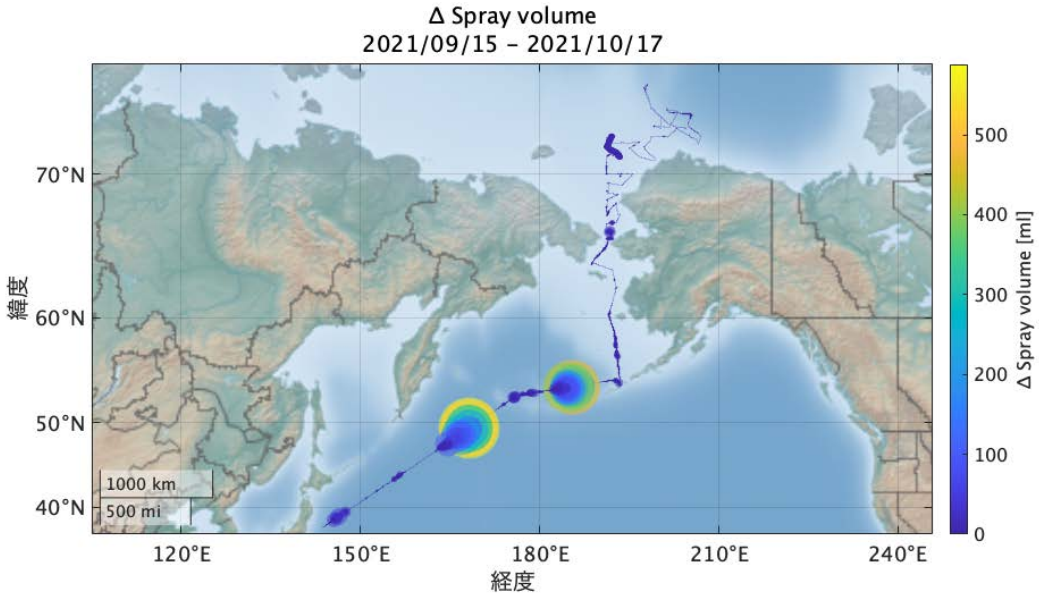

Figure 3.10-2: The bubble map of measured water volume (sum of 4 MRS unit) along the ship track.

(7) Data archives

These data obtained in this cruise will be submitted to the Data Management Group of JAMSTEC, and will be opened to the public via "Data Research System for Whole Cruise Information in JAMSTEC (DARWIN)" in JAMSTEC web site.
<http://www.godac.jamstec.go.jp/darwin/e>

3.11. Sea ice observation from aircrafts

(1) Personnel

Takuji Waseda (Principal Investigator, the University of Tokyo, not on board)
Tsubasa Kodaira (the University of Tokyo, not on board)
Takehiko Nose (the University of Tokyo, not on board)
Yasushi Fujiwara (the University of Tokyo)
Ryosuke Uchiyama (the University of Tokyo)
Jun Inoue (National Institute for Polar Research, not on board)
Kazutoshi Sato (Kitami Institute of Technology, not on board)

(2) Objectives

Since R/V Mirai cannot enter into packed sea ice region, its visual light observation from nearby is valuable. Especially because we collected radar data at the ice edge, its visual imagery to compare with is fruitful. To achieve these, we flew an unmanned aircraft (drone) equipped with a high-resolution camera near the ice edge.
Here, the test flight at the Pacific Ocean is also described.

(3) Parameters

Movies with 4-K resolution (3840 x 2160)

(4) Instruments and methods

The drone that we used is Mavic 2 Pro produced by DJI.
The deck above the anti-rolling system is chosen for the take-off/landing place. To avoid the error in IMU calibrations, the take-off and the landing was not done from the floor, but from hand-held state (Figure 3.11-1).
After the take-off, the drone flew towards the ice edge (or floating ice) to capture its close-shot movies and flew back to R/V Mirai before the battery goes low.
Considering severe conditions in the Arctic sea and the operators' skills, its horizontal distance and height were limited to 500m and 120m, respectively.

Figure 3.11-1: Hand-held landing (Photo provided by Mr. Ryo Kimura, NME)

(5) Observation log

Table 3.11-1 shows the time, location, and target of the flights.

Flight #	Time (UTC)	Location	Target
1	09-02-2021 23:15-23:45	43-45.71N ,154-22.64E	Test flight
2	09-17-2021 17:27-17:41, 18:45-19:05	72-35.78N ,160-51.74W (ICE1)	Ice edge
3	09-22 2021 22:30-22:45	71-45.28N ,163-23.31W (ICE3)	Floating ice
4	09-23-2021 17:30-17:45	72-00.27N ,168-45.36W (St.30)	Floating ice
5	09-23-2021 20:15-20:30 20:40-20:55	72-03.26N ,167-54.20W (ICE4)	Ice edge

(6) Preliminary results

Figure 3.11-2 shows an example of the image obtained at flight 2.

Figure 3.11-2: An image obtained at flight 2.

(7) Data archives

These data obtained in this cruise will be submitted to the Data Management Group of JAMSTEC, and will be opened to the public via "Data Research System for Whole Cruise Information in JAMSTEC (DARWIN)" in JAMSTEC web site.
<http://www.godac.jamstec.go.jp/darwin/e>

3.12. Moorings

Oceanographic moorings continuously measure oceanographic parameters (temperature, salinity, currents, oxygen, chlorophyll, pH, ice thickness) through the year. Three physical oceanographic moorings (BCE-19, BCC-19, BCW-19) in the Barrow Canyon and one sediment trap mooring (NAP-20t) in the Northwind Abyssal Plain are recovered. Three physical oceanographic moorings (BCE-21, BCC-21, BCW-21) are re-deployed in the Barrow Canyon and one sediment trap mooring (NBC-21t) is deployed in the northwest of Barrow Canyon.

3.12.1 Barrow Canyon Moorings

(1) Personnel

Motoyo Itoh (JAMSTEC) Principal Investigator
Amane Fujiwara (JAMSTEC) Chief Scientist
Hiroki Ushiromura (Marine Works Japan Ltd., MWJ)
as the leader of technical team for mooring operation of MWJ
(Sagishima, K., So, A., Oorui, M., Ito, R., and Hayashi, K.)
Ryo Ohyama (Nippon Marine Enterprises, Ltd.; NME)
as the leader for SSBL acoustic survey team of NME
(Ogawa, S., Yoshida, K, and Kimura, R.)
Jonaotaro Onodera (JAMSTEC)
Yasushi Fujiwara (The University of Tokyo)
Ryosuke Uchiyama (The University of Tokyo)
Shigeto Nishino* (JAMSTEC)
Eiji Watanabe* (JAMSTEC)
Takashi Kikuchi* (JAMSTEC)
Michiyo Yamamoto Kawai* (Tokyo University of Marine Science and Technology)
Takuji Waseda* (The University of Tokyo)
Tsubasa Kodaira* (The University of Tokyo)
*: onshore members

(2) Objectives

The objective of mooring measurements in the Barrow Canyon is to monitor the variations of volume, heat and fresh water fluxes of Pacific-origin water through the Barrow Canyon. Barrow Canyon, in the northeast Chukchi Sea, is a major conduit through which the Pacific water enters the Arctic basin. JAMSTEC has conducted subsurface oceanographic mooring observations in the mouth of the Barrow Canyon since 2000.

We recovered three moorings (BCE-19, BCC-19, BCW-19) and re-deployed three similar configuration moorings (BCE-21, BCC-21, BCW-21) in the Barrow Canyon.

(3) Parameters

Oceanic velocities
Pressure, Temperature and Conductivity
Dissolved oxygen
Chlorophyll-a and turbidity
Wave height
Water sampling

(4) Instruments and methods

1) CTD, CT, T, P sensors
SBE37-SM (Sea-Bird Electronics Inc.)
A7CT-USB (JFE Advantech)
DEFI-T (JFE Advantech)

2) Current meters
Workhorse ADCP 300 kHz Sentinel (Teledyne RD Instruments, Inc.)
Aquadopp Current Meter 2MHz (NORTEK AS)

3) Dissolved oxygen sensor
AROW-USB (JFE Advantech)

4) Chlorophyll-a and turbidity sensor
ACLW-USB (JFE Advantech)
MFL50W-USB (JFE Advantech)

5) Acoustic transponder
XT-6000, XT6001 (Teledyne Benthos, Inc.)

6) Acoustic releaser
Model-L, LGC (Nichiyu giken kogyo co., LTD)
8242XS (ORE offshore /EdgeTech)
865-A (Teledyne Benthos, Inc.)

7) Water sampler
RAS500 (McLANE)

8) Nitrate sensor
SUNA (Sea-Bird Electronics Inc.)

9) Wave height and current meter
Signature500 (NORTEK AS)

(5) Station list

Table 3.12.1-1: Moorings recovered by MR21-05C

Mooring Name	Recovered Time (UTC)	Latitude	Longitude
BCW-19	2021/09/10	71-47.766'N	155-20.777'W
BCC-19	2021/09/10	71-44.049'N	155-09.624'W
BCE-19	2021/09/10	71-40.368'N	154-59.923'W

Table 3.12.1-2: Moorings deployed by MR21-05C

Mooring Name	Deployed Time (UTC)	Latitude	Longitude	Depth (m)
BCW-21	2021/09/11	71-47.7727'N	155-20.7602'W	171
BCC-21	2021/09/11	71-44.0519'N	155-09.7849'W	289
BCE-21	2021/09/11	71-40.3778'N	154-59.9817'W	108

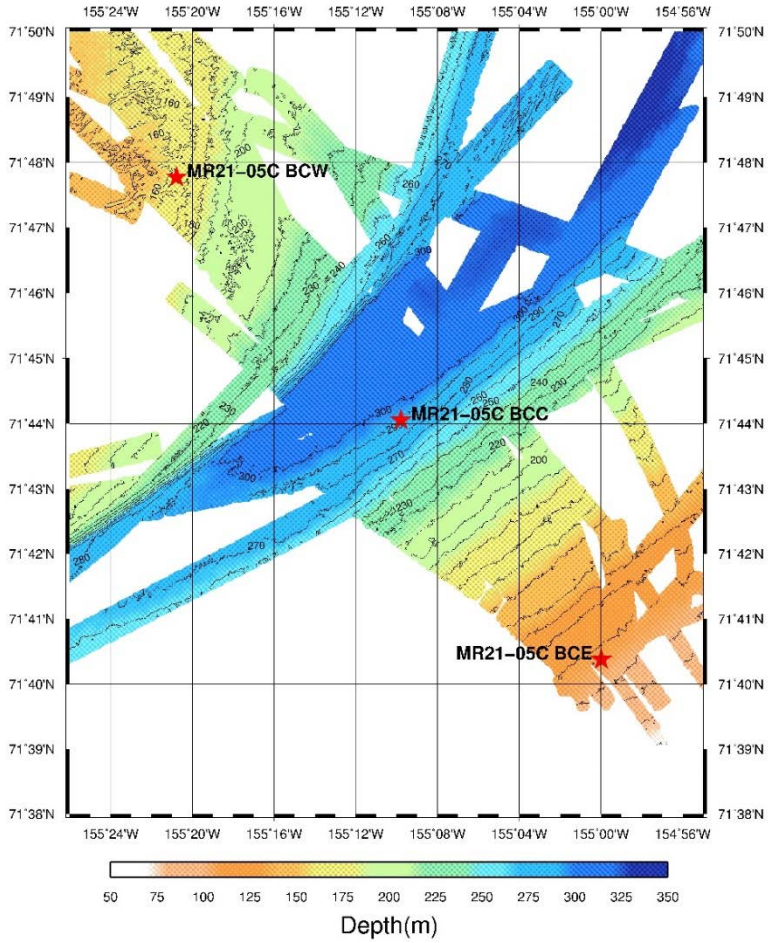

Figure 3.12.1-1: Positions of deployed moorings (BCE-21, BCC-21, and BCW-21).

(7) Data archives

These mooring data will be opened to the public via a web site below.

<http://www.jamstec.go.jp/arctic/data_archive/mooring/mooring_index.html>

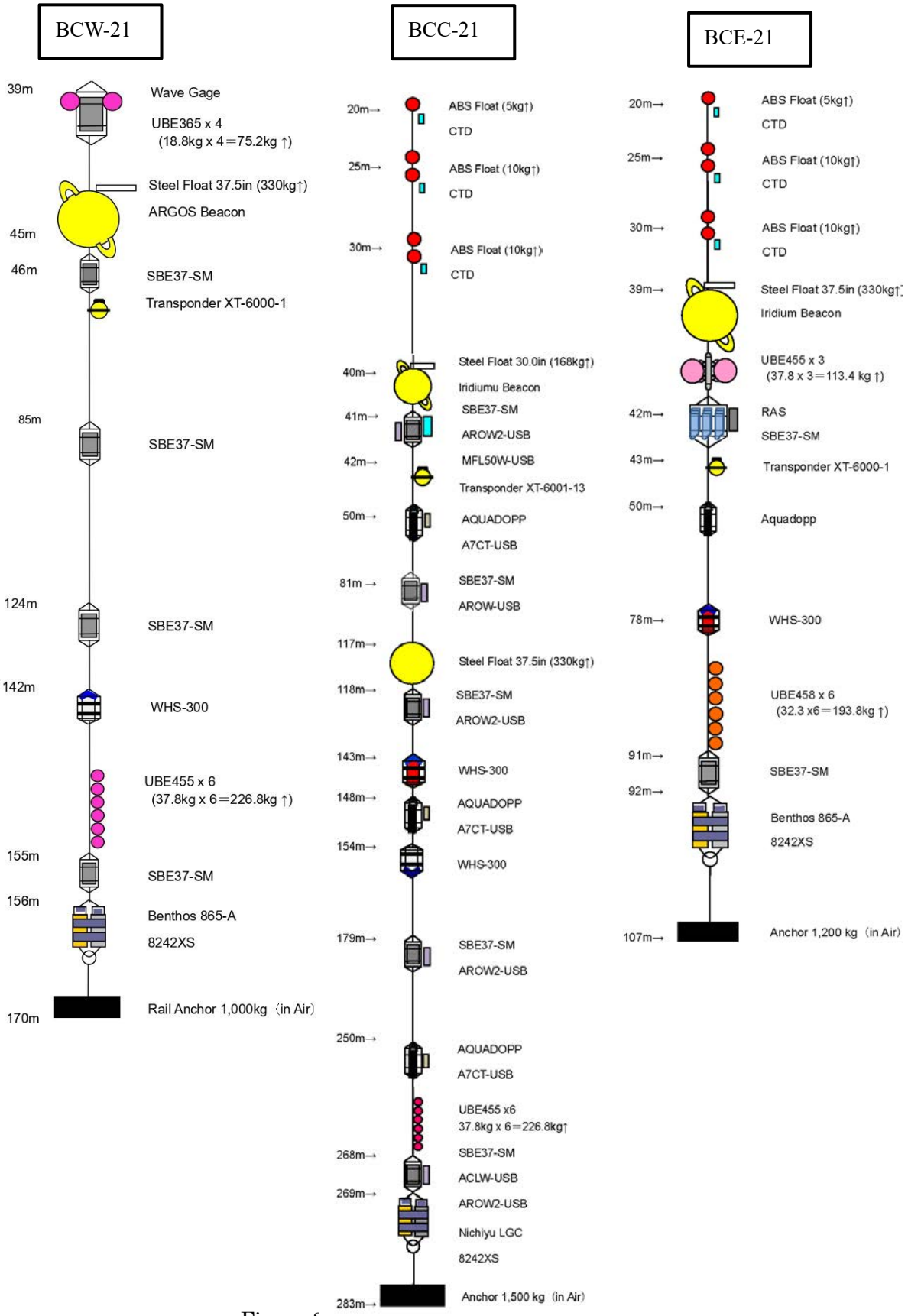

Figure 3.12.1-2. Mooring diagrams.

3.12.2 Sediment trap

(1) Personnel

Naomi Harada* JAMSTEC - Principal Investigator
Jonaotaro Onodera JAMSTEC
Yuichiro Tanaka* AIST
Atsushi Suzuki* AIST
Motoyo Itoh JAMSTEC
Katsunori Kimoto* JAMSTEC
Eiji Watanabe* JAMSTEC
Takuhei Shiozaki Tokyo Univ. AORI
Daiki Ushiromura as the leader of technical team for mooring operation of MWJ
(Ushiromura, D., Sagishima, K., So, A., Oorui, M., Ito, R., and Hayashi, K.)
Ryo Ohyama as the leader for SSBL acoustic survey team of NME
(Ogawa, S., Yoshida, K, and Kimura, R.).
*: onshore members

(2) Objectives

To monitor hydrographic condition regarding to ocean acidification and warming.
To understand lateral transportation of shelf materials to basin with physical oceanographic condition from northern off Barrow Canyon to the Chukchi Borderland.
To investigate biodiversity in the study region.

(3) Parameters

Settling particles, water temperature, salinity, current, ice thickness, dissolved oxygen, turbidity, chlorophyll-a, PAR, pH

(4) Instruments and methods

<Instruments>

All instruments on recovered and deployed moorings are listed in Tables 3.12.2-1 and -2. The designs of recovered and deployed mooring are shown in Figures 3.12.2-1, -2, and -3. The all required procedure for export/reimport control at the Shimizu custom was performed by the Suzuyo, Co. Ltd.

<Methods>

Acoustic communication of releasers to be deployed were examined at 2000 m depth near Station K2 in the northwestern North Pacific Ocean. For the deployment sensors, log file or photograph of configuration process were taken. Sample cups of sediment trap were filled-with filtered sea water taken at 1000 m depth in the southwestern Canada Basin in previous Mirai cruise. The water contains formalin (4v/v%) and sodium hydroborate for pH adjustment (pH ~8.2). The time-series sediment trap was scheduled with 13 days

interval from 00:00 of September 16, 2021 to 00:00 of August 20, 2022 (UTC), and then 12 days interval from July 12 to September 10, 2021. The battery of acoustic releasers is for continuous two-years deployment.

Safety briefing by chief officer was conducted for all related staffs working on stern deck just before the start of mooring deployment and recovery operations. All staffs working on stern deck worn floating jackets, hard hat, safety shoes, and gloves. The "A" frame and capstan winch was applied for the mooring operation on the deck. Just in case, dragging tools, which are composed of hooks, weights, chains, shackles, TRITON wires and ropes, were loaded for mooring recovery in this cruise.

For deployment, all serial numbers of deploying equipment and connection of all parts were checked just before the deployment and/or during the deployment operation. Mooring deployment started from the throw-in of top buoy into water (Table 3.12.2-1, Figure 3.12.2-4). The ships go forward with slow speed (~1.0knot). Before the dropping sinker, the slow towing of mooring continued until the ship reaches at the planned target position of the mooring. Deepening and vanish of top buoy from sea surface was confirmed, and then reaching of sinker at ser floor was confirmed by ship's acoustic ranging system. The mooring position was determined using SSBL and transducer of Benthos 865A releaser. The water depth was determined by the depth value of the position in MBES topography map (Figure 3.12.2-4). The position, water depth, top depth, and recovery plan (season and ship) of the NBC21t will be noticed to AOOS and related persons in the world.

Recovery operation for NAP20t started from acoustic communication between ship's transducer and the transducer of acoustic releaser. Both two releasers of Nichiyu LGC were enabled from the ship's transducer although the moored depth of Nichiyu releasers was out of useable range for ship's transducer communication on the Nichiyu (<~1000m). Thus, ranging was not successful due to the longer distance and louder sound noise from vessel. Ranging and sending release command was successfully performed by throwing-in of the Nichiyu transducer to sea from the lower deck of stern. The ship's zodiac went to the drifting top buoy, and connected a rope from stern to the top buoy. The rope was spooled on deck, and the mooring equipment was recovered on deck from the top buoy to acoustic releasers.

(5) Tables of sediment trap mooring operation.

Table 3.12.2-1: Deployment of NBC21t on September 14, 2021.

NBC21t Planned Coordinates: 72°28.32' N 155°24.51' W Water Depth: 1995 m				
Start of mooring deployment (72°26.2115'N 155°32.4384'W, 1768 m water depth)				17:09
Weather Condition Air temp. 0.9°C, Atmospheric pressure 1005.4hPa, Wind direction 83°, Wind speed 5.4 m/s, SST 1.4°C, Wave height 0.30 m at stern, Current direction 254°, Current speed 0.7 knot				
Time of instruments and anchor in water				
Item#	Type	Model	Serial Number	Time
1	Float Ice profiler CT DO Multi-Exciter PAR Iridium Beacon LED Flasher	77F00A00 IPS-5 MN-IP113 A7CT2-USB ARO-USB MFL50W-USB DEFI2-L iBCN-7 (MMI-513-32000) MMF-523-12000	1002 5113 310 130 20 0BKB023 J09-008 J09-007	17:11
2	Transponder Floats	XT6000 Benthos 17" x4	47196 -	17:11
3	CT	SBE37SM	6934	17:12
4	Float	Steel 30"	-	17:14
5	CT	SBE37SM	8858	17:19
6	ADCP	WH-300 (w/ BT)	15385	17:20
7	CT DO pH	SBE37SM ARO-USB SPS-14Ti Battery Unit of SPS	8860 135 40306167001 40340067001	17:24
8	Float	Benthos 17" x5	-	17:29
9	Logger ├ ADCP ├ Pressure ├ DO └ CO2	SeaGuard II 5650IW DCPS5402 4117E 4330IW CO2	1958 165 1272 2709 78	17:33
10	Sediment trap CT	SMD26S-6000 A7CT-USB	26S032 626	17:43
11	Floats	Benthos 17" x5	-	18:08
12	Sediment trap	SMD26S-6000	26S033	18:24
13	Floats	Benthos 17" x5	-	18:58
14	Releaser Releaser	Benthos 865A Nichiyu LGC	537 0021	18:58
(Towing for ~5min. to planned mooring position)				

15	Anchor (72°28.229'N 155°24.550'W, 1997 m)	1000kg in air	-	19:12
Confirmation of anchor arrival at sea floor				19:30
Releaser ranging (Item#16) Slant range: 2744 m, 2681 m, 2289 m (865A) Communication with Nichiyu LGC			537 0021	19:48
SSBL transponder survey for Benthos 865A Position Water Depth Estimated Top-buoy Depth		72°28.1770'N 1989 m 33 m	155°25.3433'W	

Table 3.12.2-2: Recovery of NAP20t on September 15, 2021.

NAP20t Coordinates: 74°31.37' N 161°55.88' W Water depth: 1685 m	
Weather Condition Air Temp. -1.6°C, Atmospheric Press. 1002.5hPa Wind Direction 319°, Wind Speed 7.3 m/s, SST 0.7°C	18:00
Call to releaser (Nichiyu LGC S/N 0078) from lower stern deck	18:07
Ranging at 74°31.1290'N 161°55.6351'W (0.25nm away from NAP20t position) Acoustic slant range: 1764m, 1764m (as sound speed 1500 m s^{-1})	18:08
Transmission of release command at 74°31.1448'N 161°55.5633'W (0.24nm away from NAP20t)	18:10
Finding of top buoy at sea surface from bridge	18:11
Connection of ship's rope to top buoy by clue on zodiac	19:16

Recovered Mooring Instruments				
Frame#	Type	Model	Serial Number	Time
1	Float Ice profiler CT DO Multi-Exciter PAR Iridium Beacon LED Flasher	MN-IP123 IPS-5 A7CT2-USB ARO-USB MFL50W-USB DEFI2-L iBCN-7 (MMI-513-32000) MMF-523-12000	ASL-SFFC-001 51032 613 136 44 0BKB022 H01-001 J01-055	19:34
-	Transponder Floats	XT6001-17" Benthos 17" x4	75683 -	
2	CT	SBE37SM	13678	
3	CT	SBE37SM	13677	
4	CT DO pH	SBE37SM ARO-USB SPS-14	15456 131 40306166001	
5	ADCP	WHS-300	24534	
-	Floats	Benthos 17" x5	-	

6	Sediment Trap CT	SMD26S-6000 A7CT-USB	98063 691	19:57
7	ADCP	Aquadopp DW	AQD15193	
-	Floats	Benthos 17” x5		
8	Sediment Trap	SMD26S-6000	98057	20:39
-	Floats	Benthos 17” x5	-	
-	Releaser Releaser	Nichiyu LGC Nichiyu LGC	0078 0079	20:59
End of recovery operation at 74°32.3798’N 162°00.3676’W				21:00

(6) Preliminary Results

The CT (A7CT2-USB S/N613) on top buoy was recovered with broken sensor guard (Figure 3.12.2-5). Other recovered sensors look good. All sensor’s data and sediment trap samples were obtained without operational trouble. Roughly estimated sedimentation rate based on sediment thickness in the bottles of sediment trap showed that higher particle flux occurred in fall 2010 and summer 2021 (Table 3.12.2-3). The high accumulation rate for shallow trap in May-June 2021 is due to swimmers. Low accumulation rate at shallow trap for #01-03 may be because of low trapping efficiency in strong current condition and/or temporal deepening of the sediment trap.

Table 3.12.2-3: The accumulation rate (mm day^{-1}) of trapped particles composed of settling particles and swimmers in the sediment traps of NAP20t. Date is UTC.

#	Initial Date YY-MM-DD	Shallow Trap	Deep Trap	#	Initial Date YY-MM-DD	Shallow Trap	Deep Trap
01	20-10-12	0.0022	0.0066	14	21-03-30	0.0034	0.0020
02	20-10-25	0.0020	0.0066	15	21-04-12	0.0078	0.0022
03	20-11-07	0.0015	0.0046	16	21-04-25	0.0037	0.0015
04	20-11-20	0.0051	0.0064	17	21-05-08	0.0174	0.0012
05	20-12-03	0.0037	0.0042	18	21-05-21	0.0076	0.0010
06	20-12-16	0.0039	0.0039	19	21-06-03	0.0108	0.0010
07	20-12-29	0.0034	0.0037	20	21-06-16	0.0100	0.0012
08	21-01-11	0.0054	0.0029	21	21-06-29	0.0007	0.0012
09	21-01-24	0.0049	0.0037	22	21-07-12	0.0024	0.0013
10	21-02-06	0.0042	0.0034	23	21-07-24	0.0040	0.0024
11	21-02-19	0.0022	0.0024	24	21-08-05	0.0072	0.0074
12	21-03-04	0.0020	0.0029	25	21-08-17	0.0066	0.0080
13	21-03-17	0.0010	0.0017	26	21-08-29	0.0040	0.0066
				(Open hole state at 21-09-10)			

(7) Data archives

These data obtained in this cruise will be submitted to the Data Management Group of JAMSTEC, and will be opened to the public via “Data Research System for Whole Cruise Information in JAMSTEC (DARWIN)” in JAMSTEC web site.

<http://www.godac.jamstec.go.jp/darwin/e>

NAP20t (Recovery)
74°31.37' N 161°55.88' W

NBC21t (Deployment)
72°28.1770'N 155°25.3433'W

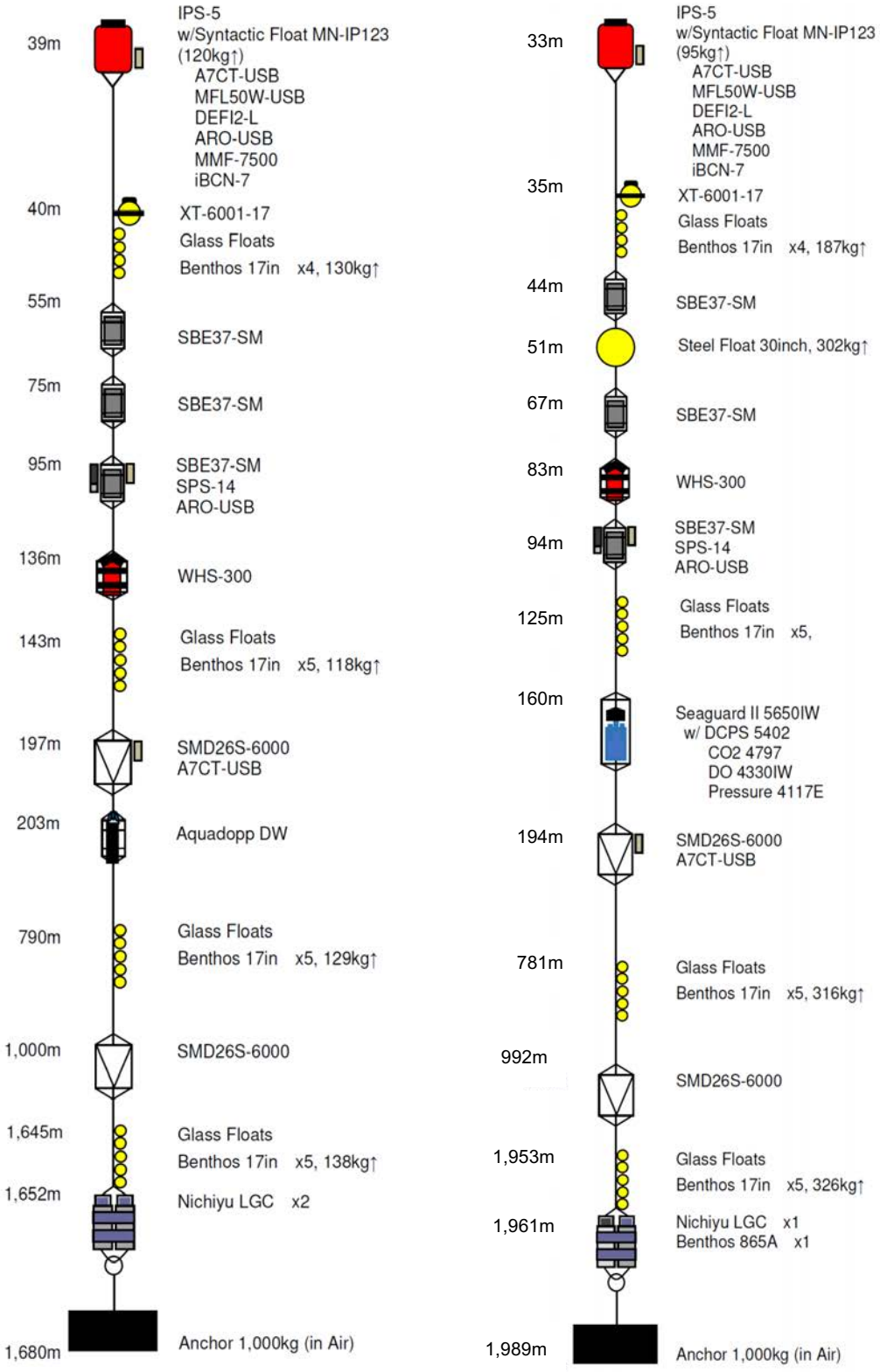

Figure 3.12.2-1: The summary of mooring design for NAP20t and NBC21t.

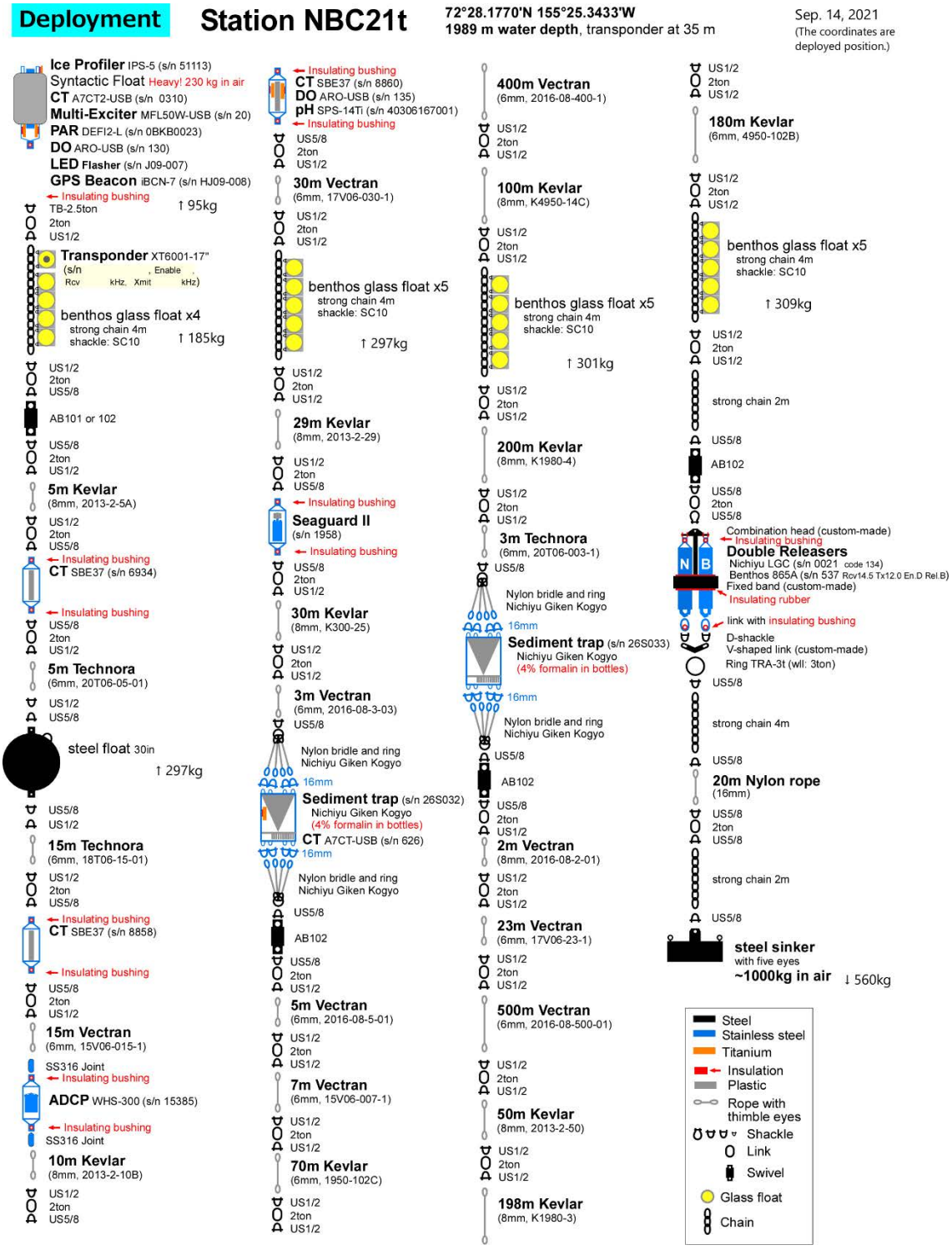

Figure 3.12.2-2: Diagram of deployed sediment trap mooing NBC21t.

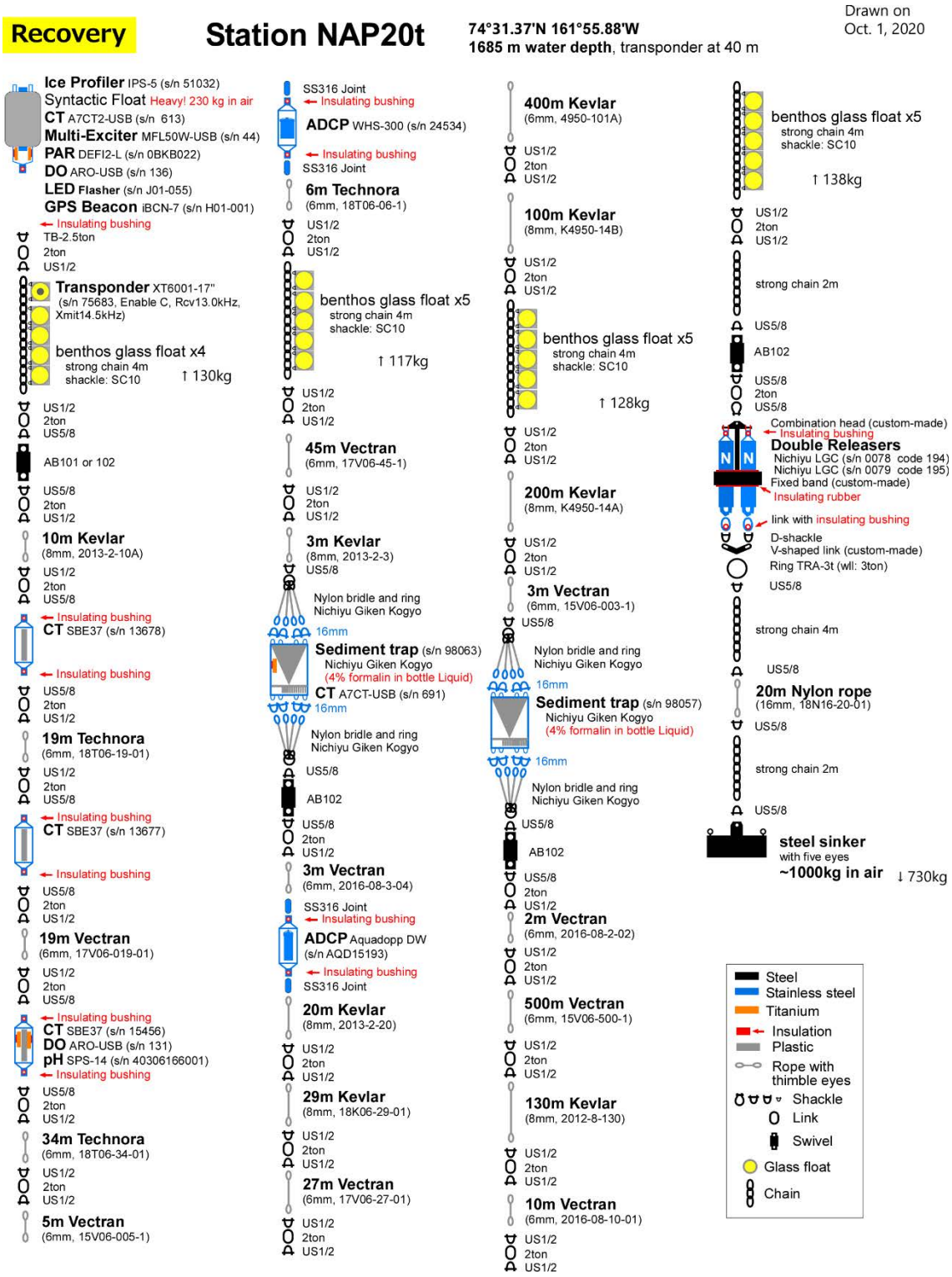

Figure 3.12.2-3: Diagram of recovered sediment trap mooing NAP20t.

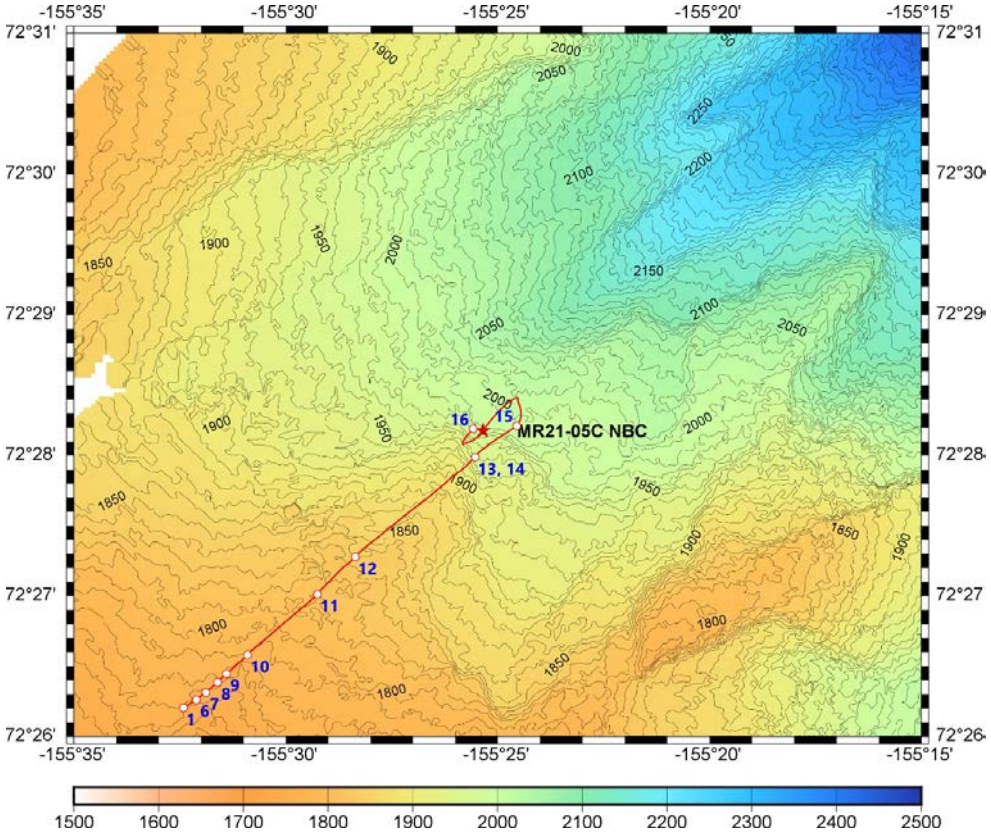

Figure 3.12.2-4: The MBES topography map showing the mooing NBC21t position (star symbol in red) with vessel's track during the deployment operation. The numbers in blue for white dot symbol represent the position of item# in Table 3.12.2-1.

Figure 3.12.2-5: The photograph showing sensor guard of A7CT-USB (S/N613) recovered as the broken state, which had been attached on the mooring frame (lower part) of ice profiling sonar of NAP20t.

3.13. Salinity measurements

(1) Personnel

Amane Fujiwara	(JAMSTEC)	- Principal Investigator
Katsunori Sagishima	(MWJ)	-Operation leader

(2) Objective

To provide calibrations for the measurements of salinity collected from CTD casts, bucket sampling, and underway surface water monitoring system.

(3) Parameters

Salinity

(4) Instruments and methods

a. Sampling

Seawater samples were collected with 12-liter water sampling bottles, clean sampling bottles, marine snow catcher system and underway surface water monitoring system. The salinity sample bottle of the 250ml brown glass bottle with screw cap was used for collecting the sample water. Each bottle was rinsed 3 times with the sample water, and was filled with sample water to the bottle shoulder. The salinity sample bottles for underway surface water monitoring system were sealed with a plastic septum and screw cap because we took into consideration the possibility of storage for about one month. The caps were rinsed 3 times with the sample seawater before its use. Each bottle was stored for more than 24 hours in the laboratory before the salinity measurement.
The kind and number of samples taken are shown as follows ;

Table 3.13.-1: Kind and number of samples

Kind of Samples	Number of Samples
Samples for CTD	530
Samples for Bucket	47
Samples for underway surface water monitoring system	43
Sample for crean sample bottol	58
Sample for marine snow catcher	21
Total	699

b. Instruments and Method

The salinity analysis was carried out on R/V MIRAI during the cruise of MR21-05C using the salinometer (Model 8400B “AUTOSAL” ; Guildline Instruments Ltd.: S/N 62556) with an additional peristaltic-type intake pump (Ocean Scientific International, Ltd.). A pair of precision digital thermometers (1502A; FLUKE: S/N B78466 and B81549) were used for monitoring the ambient temperature and the bath temperature of the

salinometer.
The specifications of the AUTOSAL salinometer and thermometer are shown as follows ;

Salinometer (Model 8400B "AUTOSAL": Guildline Instruments Ltd.)
Measurement Range : 0.005 to 42 (PSU)
Accuracy : Better than ±0.002 (PSU) over 24 hours
Maximum Resolution : Better than ±0.0002 (PSU) at 35 (PSU)
Thermometer (1502A: FLUKE)
Measurement Range : 16 to 30 deg C (Full accuracy)
Resolution : 0.001 deg C
Accuracy : 0.006 deg C (@ 0 deg C)

The measurement system was almost the same as Aoyama *et al.* (2002). The salinometer was operated in the air-conditioned ship's laboratory at a bath temperature of 24 deg C. The ambient temperature varied from approximately 22 deg C to 24 deg C, while the bath temperature was very stable and varied within +/- 0.002 deg C on rare occasion. The measurement for each sample was done with a double conductivity ratio and defined as the median of 33 readings of the salinometer. Data were taken after rinsed 5 times with the sample water. The double conductivity ratio of sample was calculated from average value of two measurements. And it was used to calculate the bottle salinity with the algorithm for the practical salinity scale, 1978 (UNESCO, 1981). In the case of the difference between the double conductivity ratio of these two measurements being greater than or equal to 0.00003, continue to be measured up to 3 times. The difference between the double conductivity ratio of these two measurements being smaller than 0.00002 were selected. The measurement was conducted in about 8 hours per day and the cell was cleaned with neutral detergent after the measurement of the day.

(5) Station list
Table.3.13-2 shows the sampling locations for the salinity analysis in this cruise.

Table. 3.13-2: List of sampling locations of the salinity samples collected from CTD

Station	Cast	Date (UTC)	Bottom position		Depth (m)
		(mmddyy)	Latitude	Longitude	
001	1	090321	46-52.71N	159-47.49E	5089.0
003	2	091221	71-40.61N	154-57.61W	100.9
004	1	091321	71-44.39N	155-08.14W	285.8
005	1	091321	71-48.27N	155-17.66W	194.3
009	1	091321	72-06.12N	155-54.76W	209.0
010	1	091421	72-28.48N	155-35.13W	1829.0
011	1	091521	74-31.52N	161-55.16W	1688.0
011	2	091621	74-31.42N	161-55.70W	1688.0
014	1	091721	72-35.90N	160-49.95W	49.2

015	1	091821	72-43.40N	157-54.52W	376.7
017	1	091821	73-23.86N	158-42.83W	2214.0
019	1	091921	72-43.37N	155-07.91W	2969.0
020	1	092021	71-48.46N	153-14.95W	247.0
022	1	092021	72-27.56N	156-59.38W	466.0
023	1	092121	72-01.45N	158-31.55W	56.1
024	1	092121	72-03.25N	161-22.59W	31.2
025	1	092121	71-31.34N	162-27.59W	43.0
026	1	092221	70-59.87N	161-06.60W	46.2
027	1	092221	71-26.29N	164-56.99W	42.2
028	1	092221	71-45.13N	163-23.57W	41.4
029	1	092321	71-45.83N	166-21.53W	44.9
030	1	092321	72-00.24N	168-45.29W	51.0
031	1	092321	72-03.92N	167-54.20W	50.3
032	1	092421	71-30.10N	168-44.66W	48.6
033	1	092421	71-00.00N	166-38.72W	44.8
034	1	092521	71-00.00N	168-44.95W	44.5
035	1	092521	70-29.97N	168-44.98W	38.7
036	1	092621	69-59.91N	168-43.92W	40.9
037	1	092621	70-00.00N	166-39.99W	47.0
038	1	092721	70-00.01N	164-27.87W	35.7
039	1	092721	69-21.03N	166-14.07W	37.5
041	1	092821	69-29.98N	168-44.95W	51.7
042	1	092821	69-00.03N	168-45.16W	53.2
043	1	092821	68-48.04N	166-57.42W	41.6
044	1	092921	68-30.25N	168-44.80W	53.8
045	1	092921	68-02.00N	168-49.90W	59.2
046	1	092921	67-30.00N	168-44.67W	49.7
049	1	093021	68-00.04N	168-00.17W	54.2
053	1	093021	68-18.11N	167-03.37W	39.1
054	1	093021	67-36.07N	166-30.03W	46.8
055	1	093021	67-01.76N	167-09.71W	40.5
056	1	100121	67-00.17N	168-46.37W	46.6
057	1	100121	66-29.87N	168-45.59W	52.3
058	1	100121	65-59.77N	168-44.99W	53.4
059	1	100121	65-29.90N	168-45.06W	54.8
060	1	100221	65-05.67N	169-31.11W	50.3
061	1	100221	64-43.51N	170-25.58W	50.4
062	1	100221	64-18.92N	171-18.20W	46.2
063	1	101121	49-54.75N	169-29.36E	5416.0

(6) Preliminary results

a. Standard Seawater

Standardization control of the salinometer was set to 614(from 2021/09/13 to 09/ 26) and 625 (from 2021/09/27 to 2021/10/18). The value of STANDBY was 24+5138 and 24+5146 and that of ZERO was 0.0+0000. The IAPSO Standard Seawater (SSW) batch P164 was used as the standard for salinity. 24 bottles of P164 were measured.

Fig.3.13-1 shows the time series of the double conductivity ratio of the Standard

Seawater batch P164. The average of the double conductivity ratio was 1.99969 and the standard deviation was 0.00003 which is equivalent to 0.0006 in salinity.

Fig.3.13-2 shows the time series of the double conductivity ratio of the Standard Seawater batch P164 after correction. The average of the double conductivity ratio after correction was 1.99970 and the standard deviation was 0.00001, which is equivalent to 0.0002 in salinity.
The specifications of SSW batch P164 used in this cruise are shown as follows ;

Batch	:	P164
Conductivity ratio	:	0.99970
Salinity	:	34.994
Use by	:	23rd March. 2023

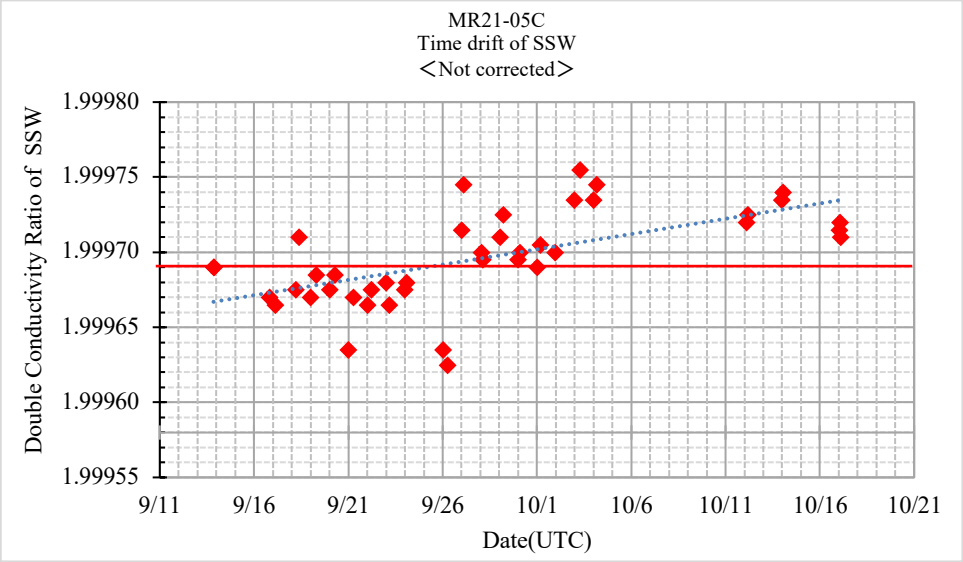

Fig. 3.13-1: Time series of double conductivity ratio for the Standard Seawater (before correction)

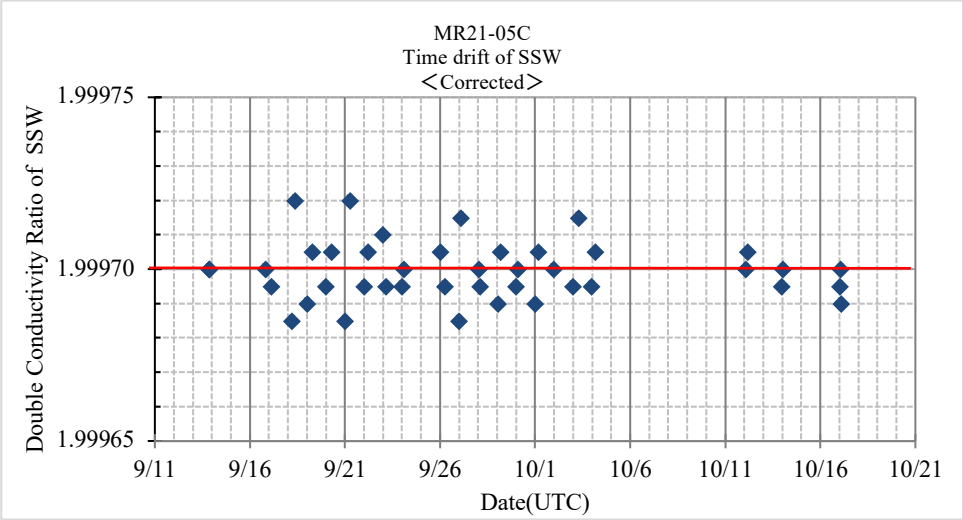

Fig. 3.13-2: Time series of double conductivity ratio for the Standard Seawater (after correction)

b. Sub-Standard Seawater

Sub-standard seawater was made from surface sea water filtered by a pore size of 0.2 micrometer and stored in a 20 liter container made of polyethylene and stirred for at least 24 hours before measuring. It was measured about every 10 samples in order to check for the possible sudden drifts of the salinometer.

c. Replicate Samples

We estimated the precision of this method using 88 pairs of replicate samples taken from the same water sampling bottle. Fig.3.12-3 shows the histogram of the absolute difference between each pair of the replicate samples. The average and the standard deviation of absolute difference among 88 pairs of replicate samples were 0.0017 and 0.0028 in salinity, respectively.

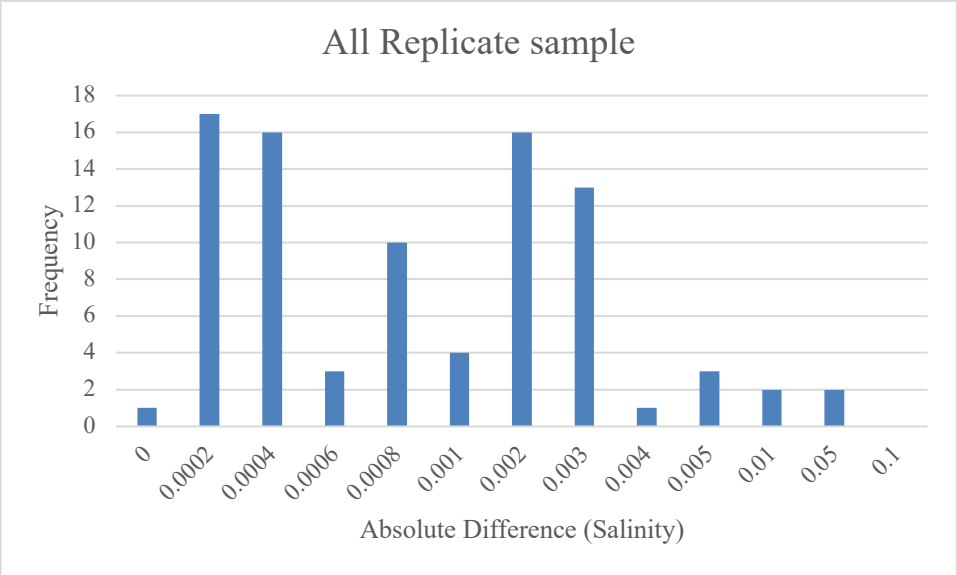

Fig. 3.13-3: The histogram of the salinity for the absolute difference of all replicate samples

(7) Data archive

These data obtained in this cruise will be submitted to the Data Management Group of JAMSTEC, and will be opened to the public via "Data Research System for Whole Cruise Information in JAMSTEC (DARWIN)" in JAMSTEC web site.
<http://www.godac.jamstec.go.jp/darwin/e>

(8) Reference

Aoyama, M., T. Joyce, T. Kawano and Y. Takatsuki : Standard seawater comparison up to P129. Deep-Sea Research, I, Vol. 49, 1103-1114, 2002

UNESCO : Tenth report of the Joint Panel on Oceanographic Tables and Standards. UNESCO Tech. Papers in Mar. Sci., 36, 25 pp., 1981

3.14 Density and Refractive Index

(1) Personnel

Hiroshi Uchida (JAMSTEC) (not onboard)
Amane Fujiwara (JAMSTEC)
Misato Kuwahara (MWJ)
Shintaro Amikura (MWJ)

(2) Objective

The objective of this study is to collect absolute salinity (also called "density salinity") data and to evaluate the algorithm to estimate absolute salinity anomaly provided along with TEOS-10 (the International Thermodynamic Equation of Seawater 2010) (IOC et al., 2010).

(3) Instruments and method

Seawater density for water samples was measured with a vibrating-tube density meter (DMA 5000M [serial no. 80570578], Anton-Paar GmbH, Graz, Austria) and a sample changer (Xsample 122 [serial no. 8548492], Anton-Paar GmbH). The sample changer is used to load samples automatically from up to ninety-six 12-mL glass vials.

Seawater refractive index was also simultaneously measured for the same water samples with a laboratory refractometer (Abbemat 650 [serial no. 99058548], Anton-Paar GmbH) by connected to the density meter. Light source of the refractometer is LED (wavelength of 589.3 nm).

Practical salinity for water samples was measured with a salinometer (AUTOSAL 8400B [serial no. 60132], Guildline Instruments, Ltd., Ontario, Canada). The bath temperature of the salinometer was set to 24 °C. The salinometer was standardized by using IAPSO Standard Seawater batch P164.

The water samples collected in 200 mL borosilicate glass bottles for IAPSO Standard Seawater were measured by taking the water sample into two 12-mL glass vials for each bottle just before practical salinity measurement. The glass vial was sealed with Parafilm M (Pechiney Plastic Packaging, Inc., Menasha, Wisconsin, USA) immediately after filling. Densities of the samples were measured at 20 °C by the density meter and refractometer two times (two vials) for each bottle and averaged to estimate the density and refractive index, respectively. It takes about 5 minutes and 15 seconds for one measurement of the density and refractive index, respectively. Resolution of the density meter is 0.001 kg/m^3, and resolution of the refractometer is 0.000001 nD which is equivalent to 0.004 kg/m^3 in density.

The density meter was initially calibrated by measuring air and pure water according to the instrument manual. However, measured density for the IAPSO Standard Seawater deviates from density of TEOS-10 calculated from practical salinity and composition of seawater, probably due to non-linearity of the density meter (Uchida et al., 2011). The

non-linearity can be corrected by measuring a reference sample simultaneously as:

$$\rho_{corr} = \rho - (\rho_{ref} - \rho_{ref\_true}) + c\,(\rho - \rho_{ref\_true}),$$

where ρ_{corr} is the corrected density of the sample, ρ is measured density of the sample, ρ_{ref} is measured density of the reference, ρ_{ref_true} is true density of the reference, and c is non-linearity correction factor. The non-linearity correction factor is estimated to be 0.000341 for the density meter (serial no. 80570578). This factor was estimated from the density of the IAPSO Standard Seawater measured in the MR21-04 cruise and changed from the previous value (0.000411).

Time drift of the density meter and refractometer was corrected by periodically measuring the density of ultra-pure water (Milli-Q water, Millipore, Billerica, Massachusetts, USA) prepared from Yokosuka (Japan) tap water in October 2014 as the reference. The true density of the Milli-Q water at 20 ºC was estimated to be 998.2041 kg m^{-3} from the isotopic composition (δD = –8.86 ‰, $\delta^{18}O$ = –59.9 ‰) and International Association for the Properties of Water and Steam (IAPWS)-95 standard. The ultra-pure water was measured at the beginning, the middle and the end of the day of measurement (October 30, 2021).

For the refractometer, refractive index anomalies from the ultra-pure water measurement were calculated for each day of measurement. Refractive index for pure water is about 1.332987 nD.

The IAPSO Standard Seawater (batch P164) and the Multi-parametric Standard Seawater (MSSW) (lot PRE19) (Uchida et al. 2020) were also measured to check the non-linearity correction. The IAPSO Standard Seawater was measured at the beginning, the middle and the end of the day of measurement. The MSSW was measured at every about 20 measurements (11 times). The measured densities are listed in Table 3.14.1. The measured refractive index anomalies are also listed in Table 3.14.2.

Surface water density was also measured with a refractive index density sensor (prototype 1, JAMSTEC [serial no. 4D020050 (SI-F80SO [55095]), cell no. 1-2]) (Uchida et al., 2019) by attaching the density sensor to the Continuous Sea Surface Water Monitoring System (between SBE 45 and HGTD-Pro).

Table 3.14.1: Measured density at 20 °C of the IAPSO Standard Seawater and the Multi-parametric Standard Seawater (MSSW). True densities estimated from practical salinity and composition of seawater using TEOS-10 are also shown.

Standard Seawater	True density (kg/m^3)	Measured density (kg/m^3)	Number of measurements
P164	1024.7624	1024.7630±0.0009	4
PRE19	1024.2171	1024.2187±0.0007	11

Table 3.14.2: Measured refractive index anomaly from pure water measurement at 20 °C of the IAPSO Standard Seawater and the Multi-parametric Standard Seawater (MSSW).

Standard Seawater	Refractive index anomaly (10^5 nD)	Number of measurements
P164	646.05±0.02	4
PRE19	633.05±0.03	11

(4) Results

Density and refractive index were measured for samples collected from two CTD/water sampling casts (stations 10 and 19) and from the Continuous Sea Surface Water Monitoring System once in a day during the cruise. A total of 90 samples were measured. Density salinity (DNSSAL) can be back calculated from the measured density and temperature (20 °C) with TEOS-10.

The measured practical salinities for the CTD/water sampling casts are shown in Fig. 3.14.1. Practical salinities measured on board for station 010 might be biased for about -0.003.

The measured density salinity anomalies (δS_A) for the CTD/water sampling casts are shown in Fig. 3.14.2. The measured δS_A was well agree with the δS_A estimated from Pawlowicz et al. (2011) which exploits the correlation between δS_A and nutrient concentrations (silicate and nitrate) and carbonate system parameters (total alkalinity and dissolved inorganic carbon) based on mathematical investigation.

The measured density salinity anomalies (δS_A) for the Continuous Sea Surface Water Monitoring System are shown in Fig. 3.14.3.

The measured density salinity was well correlated with the measured refractive index anomaly (Fig. 3.14.4). The root-mean-square difference from the regression line (offset = -0.1247, slope = 0.05461) was 0.0055 g/kg.

Post-cruise calibration for the refractive index density sensor is not yet finished.

(5) References

IOC, SCOR and IAPSO (2010): The international thermodynamic equation of seawater – 2010: Calculation and use of thermodynamic properties. Intergovernmental Oceanographic Commission, Manuals and Guides No. 56, UNESCO (English), 196 pp.

Pawlowicz, R., D.G. Wright and F. J. Millero (2011): The effects of biogeochemical processes on ocean conductivity/salinity/density relationships and the characterization of real seawater. Ocean Science, 7, 363-387.

Uchida, H., T. Kawano, M. Aoyama and A. Murata (2011): Absolute salinity measurements of standard seawaters for conductivity and nutrients. La mer, 49, 237-244.

Uchida, H., T. Kawano, T. Nakano, M. Wakita, T. Tanaka and S. Tanihara (2020): An expanded batch-to-batch correction for IAPSO standard seawater. J. Atmos. Oceanic Technol., doi:10.1175/JTECH-D-19-0184.1.

Uchida, H., Y. Kayukawa and Y. Maeda (2019): Ultra high-resolution seawater density sensor based on a refractive index measurement using the spectroscopic interference method. Sci. Rep., doi:10.1038/s41598-019-52020-z.

(6) Data archive

These obtained data will be submitted to JAMSTEC Data Management Group (DMG).

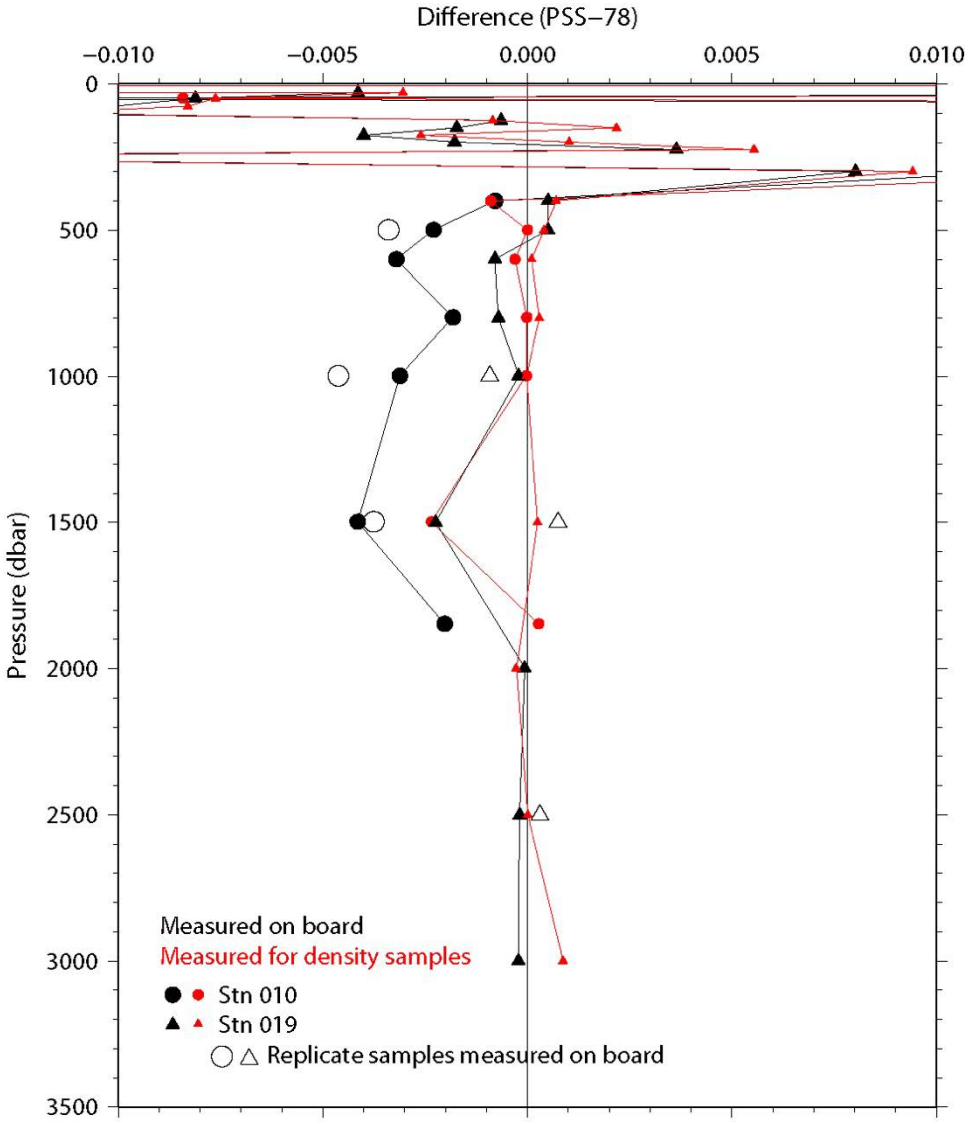

Figure 3.14.1: Vertical distribution of difference between the CTD salinity and sampled salinity. The CTD salinity data was preliminary calibrated by using the sampled salinity data measured for the density samples (red dots).

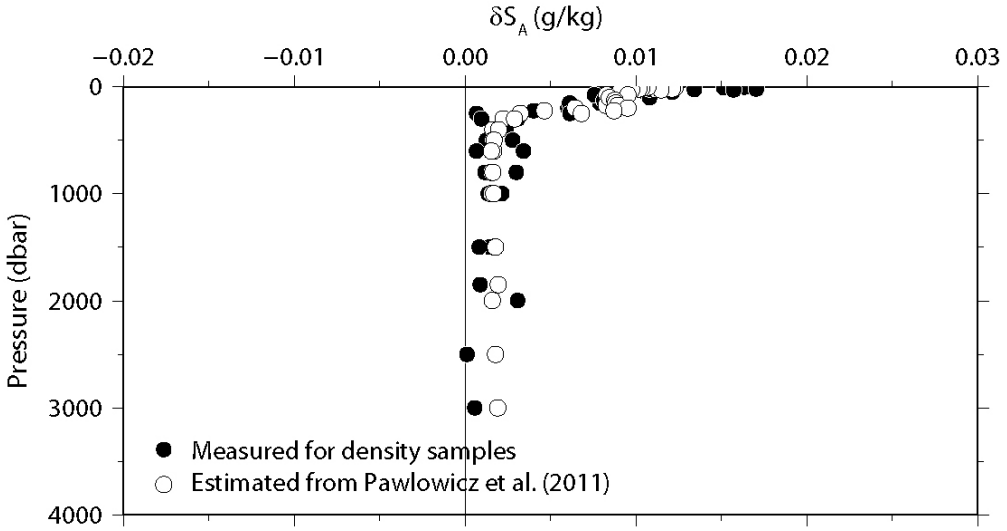

Figure 3.14.2: Vertical distribution of density salinity anomaly measured by the density meter (closed circles). Absolute salinity anomaly estimated from nutrients and carbonate system parameters (Pawlowicz et al., 2011) are also shown (open circles).

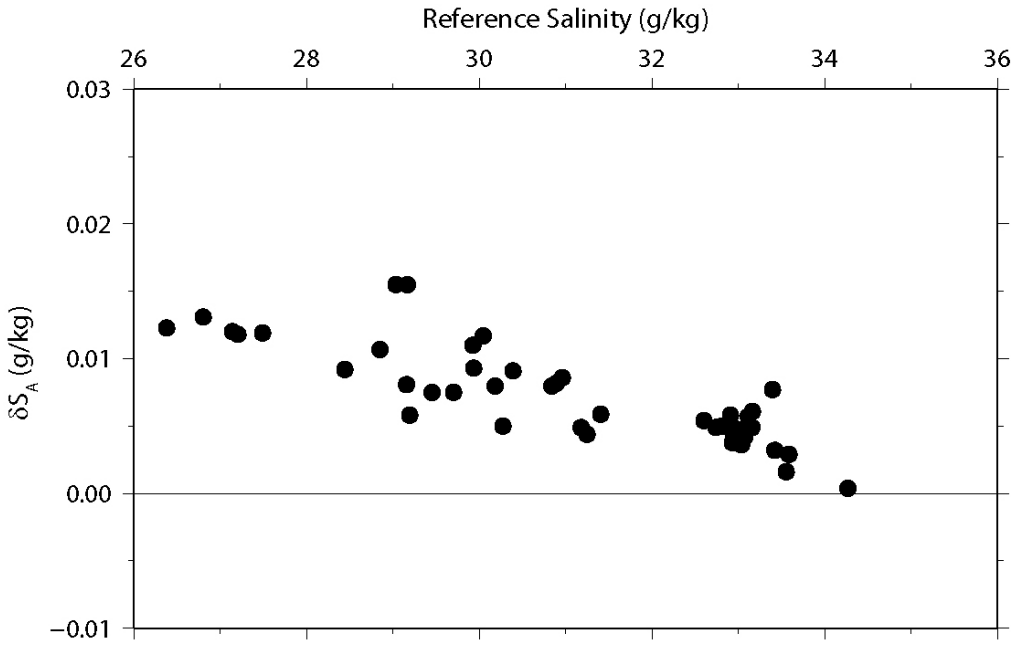

Figure 3.14.3: Surface water density salinity anomaly plotted against practical salinity.

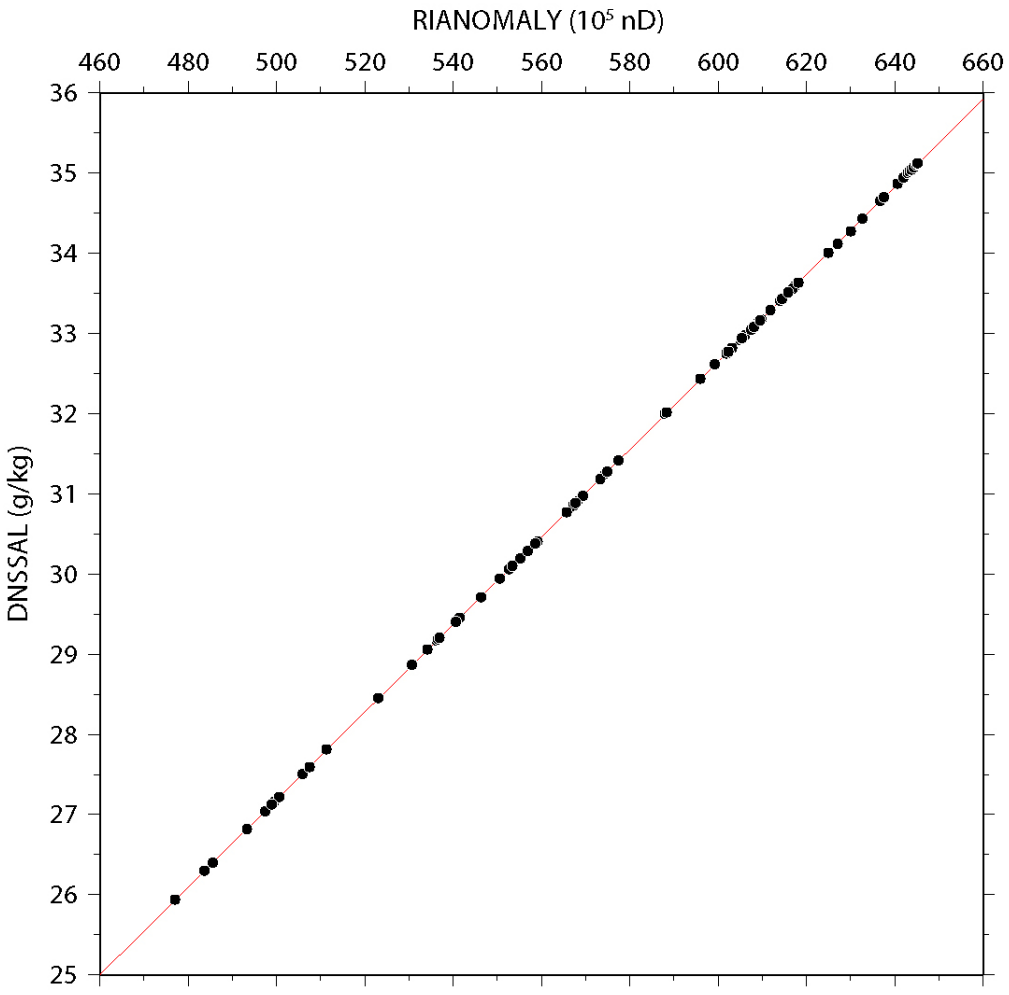

Figure 3.14.4: Comparison between density salinity (DNSSAL) measured by the density meter and refractive index anomaly (RIANOMALY) from pure water measurement. Red line shows the regression line.

4. Biogeochemical Oceanography
4.1. Dissolved Oxygen

(1) Personnel

Amane Fujiwara (JAMSTEC): Principal Investigator
Motoyo Itoh (JAMSTEC)
Hiroaki Sakoh (MWJ): Operation Leader
Misato Kuwahara(MWJ)
Shintaro Amikura(MWJ)

(2) Objective

Determination of dissolved oxygen in seawater by Winkler titration.

(3) Parameters

Dissolved Oxygen

(4) Instruments and methods

Following procedure is based on winkler method (Dickson, 1996; Culberson, 1991).

a. Instruments

Burette for sodium thiosulfate and potassium iodate;
Automatic piston burette (APB-510 / APB-620) manufactured by Kyoto Electronics Manufacturing Co., Ltd. / 10 cm^3 of titration vessel

Detector;
Automatic photometric titrator (DOT-15X) manufactured by Kimoto Electric Co., Ltd.

Software;
DOT_Terminal Ver. 1.3.1

b. Reagents

Pickling Reagent I:
Manganese(II) chloride solution (3 mol dm^{-3})

Pickling Reagent II:
Sodium hydroxide (8 mol dm^{-3}) / Sodium iodide solution (4 mol dm^{-3})

Sulfuric acid solution (5 mol dm^{-3})

Sodium thiosulfate (0.025 mol dm^{-3})

Potassium iodate (0.001667 mol dm^{-3})

c. Sampling

Seawater samples were collected with Niskin bottle attached to the CTD/Carousel Water Sampling System (CTD system). Seawater for oxygen

measurement was transferred from the bottle to a volume calibrated flask (ca. 100 cm^3), and three times volume of the flask was overflowed. Temperature was simultaneously measured by digital thermometer during the overflowing. After transferring the sample, two reagent solutions (Reagent I and II) of 1 cm^3 each were added immediately and the stopper was inserted carefully into the flask. The sample flask was then shaken vigorously to mix the contents and to disperse the precipitate finely throughout. After the precipitate has settled at least halfway down the flask, the flask was shaken again vigorously to disperse the precipitate. The sample flasks containing pickled samples were stored in a laboratory until they were titrated.

d. Sample measurement

For over two hours after the re-shaking, the pickled samples were measured on board. Sulfuric acid solution with its volume of 1 cm^3 and a magnetic stirrer bar were put into the sample flask and the sample was stirred. The samples were titrated by sodium thiosulfate solution whose morality was determined by potassium iodate solution. Temperature of sodium thiosulfate during titration was recorded by a digital thermometer. Dissolved oxygen concentration (μmol kg^{-1}) was calculated by sample temperature during seawater sampling, salinity measured by salinometer or the sensor on CTD system in accordance with the situation (ex. bottle salinity flag is 9), flask volume, and titrated volume of sodium thiosulfate solution without the blank. During this cruise, 2 sets of the titration apparatus were used.

e. Standardization and determination of the blank

Concentration of sodium thiosulfate titrant was determined by potassium iodate solution. Pure potassium iodate was dried in an oven at 130 ºC, and 1.7835 g of it was dissolved in deionized water and diluted to final weight of 5 kg in a flask. After 10 cm^3 of the standard potassium iodate solution was added to another flask using a volume-calibrated dispenser, 90 cm^3 of deionized water, 1 cm^3 of sulfuric acid solution, and 1 cm^3 of pickling reagent solution II and I were added in order. Amount of titrated volume of sodium thiosulfate for this diluted standard potassium iodate solution (usually 5 times measurements average) gave the morality of sodium thiosulfate titrant.

The oxygen in the pickling reagents I (1 cm^3) and II (1 cm^3) was assumed to be 7.6×10^{-8} mol (Murray et al., 1968). The blank due to other than oxygen was determined as follows. First, 1 and 2 cm^3 of the standard potassium iodate solution were added to each flask using a calibrated dispenser. Then 100 cm^3 of deionized water, 1 cm^3 of sulfuric acid solution, 1 cm^3 of pickling II reagent solution, and same volume of pickling I reagent solution were added into the flask in order. The blank was determined by difference between the first (1 cm^3 of potassium iodate) titrated volume of the sodium thiosulfate and the second (2 cm^3 of potassium iodate) one. The titrations were conducted for 3 times and their average was used as the blank value.

(5) Observation log

a. Standardization and determination of the blank

Table 4.1-1 shows results of the standardization and the blank determination during this cruise.

Table 4.1-1: Results of the standardization and the blank determinations during cruise

Date (yyyy/mm/dd)	Potassium iodate ID	Sodium thiosulfate ID	DOT-15X (No.9)		DOT-15X (No.10)		Station
			E.P. (cm^3)	Blank (cm^3)	E.P. (cm^3)	Blank (cm^3)	
2021/09/01	K21B03	T-21C	3.957	-0.005	3.965	0.002	001
2021/09/01	reference 21-06	T-21C	3.955	-0.005	3.963	0.002	
2021/09/05	K21B04	T-21C	3.954	-0.006	3.964	0.003	
2021/09/09	K21B05	T-21C	3.954	-0.007	3.962	0.002	003-009
2021/09/14	K21B06	T-21C	3.955	-0.007	3.962	0.002	010-015
2021/09/19	K21B07	T-21C	3.957	-0.005	3.962	0.000	017-020
2021/09/21	K21B08	T-21C	3.957	-0.003	3.962	0.003	022
2021/09/21	K21B08	T-21D	3.954	-0.006	3.962	0.001	023-033
2021/09/25	K21B09	T-21D	3.954	-0.007	3.961	0.002	034-042
2021/09/29	K21B10	T-21D	3.955	-0.005	3.960	0.001	043-062
2021/10/03	K21B11	T-21D	3.955	-0.005	3.960	0.000	
2021/10/07	K21C01	T-21D	3.956	-0.005	3.960	0.000	
2021/10/07	K21C01	T-21E	3.952	-0.006	3.958	0.001	063
2021/10/12	K21C02	T-21E	3.953	-0.006	3.958	0.000	
2021/10/16	K21C03	T-21E	3.954	-0.005	3.961	0.002	

b. Repeatability of sample measurement

Replicate samples were taken at every CTD casts. The standard deviation of the replicate measurement (Dickson et al., 2007) was 0.17 μmol kg^{-1} (n= 104). Results of replicate samples were shown in Table 4.1-2 and this diagram shown in Figure 4.1-1. These data use the preliminary data. The standard deviation (s) is given by the expression,

$$s = \sqrt{\frac{\sum_{i=1} {d_i}^2}{2k}}$$

where d and k are the difference of replicate measurements and the number of replicate samples, respectively.

Table 4.1-2: Results of the replicate sample measurements

Layer	Number of replicate sample pairs	Oxygen concentration (μmol kg^{-1}) Standard Deviation
< 200m	87	0.18
>=200m	17	0.09
All	104	0.17

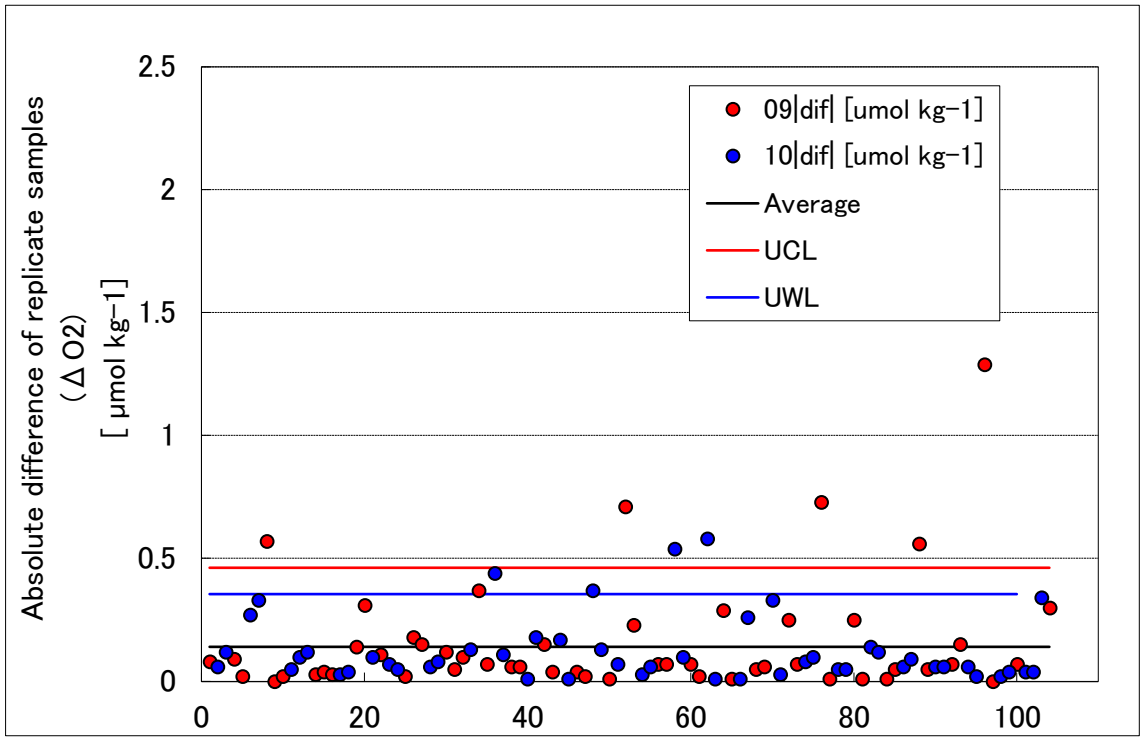

Figure 4.1-1: Difference of replicate samples against sequence number
UCL:upper control limit, UWL:upper warning limit (Dickson et al., 2007)

(6) Data archives

These data obtained in this cruise will be submitted to the Data Management Group (DMG) of JAMSTEC, and will opened to the public via "Data Research System for Whole Cruise Information in JAMSTEC (DARWIN)" in JAMSTEC web site.
<http://www.godac.jamstec.go.jp/darwin/e>

(7) References

Culberson, C. H. (1991). *Dissolved Oxygen.* WHPO Publication 91-1.

Dickson, A. G. (1996). Determination of dissolved oxygen in sea water by Winkler titration. In *WOCE Operations Manual*, Part 3.1.3 Operations & Methods, WHP Office Report WHPO 91-1.

Dickson, A. G., Sabine, C. L., & Christian, J. R.(Eds.), (2007). *Guide to best practices for ocean CO_2 measurements, PICES Special Publication 3*: North Pacific Marine Science Organization.

Murray, C. N., Riley, J. P., & Wilson, T. R. S. (1968). The solubility of oxygen in Winklerreagents used for the determination of dissolved oxygen. *Deep Sea Res.*, 15, 237-238.

4.2. Nutrients

(1) Personnel

Michio AOYAMA (JAMSTEC/University of Tsukuba/University of Fukushima)
: Principal Investigator
Mariko HATTA (JAMSTEC)
Amane Fujiwara (JAMSTEC)
Tomomi SONE (MWJ): Operation Leader
Yuta ODA (MWJ)
Yuko MIYOSHI (MWJ)
Makoto TAKADA (MWJ)

(2) Objectives

The objective of this document is to show the present status of the nutrient concentrations during the R/V Mirai MR21-05C cruise (EXPOCODE: 49NZ20210831) in the Arctic Ocean and Pacific Ocean, and then evaluate the comparability of this obtained data set during this cruise using the certified reference materials of the nutrients in seawater.

(3) Parameters

The parameters are nitrate, nitrite, silicate, phosphate and ammonia in seawater.

(4) Instruments and methods

(4-1) Analytical detail using QuAAtro 39 systems (BL TEC K.K.)

As the analytical systems for this cruise, two new systems of "QuAAtro 39" were used, which were purchased and delivered in March 2021. In order to identify those units, the system was labeled as #5 and #6, respectively.

Nitrate + nitrite and nitrite were analyzed by the following methodology that was modified from the original method of Grasshoff (1976). The flow diagrams were shown in Figure 4.2-1 for nitrate + nitrite and Figure 4.2-2 for nitrite. For the nitrate + nitrite analysis, the sample were mixed with the alkaline buffer (Imidazole) and then the mixture was pushed through a cadmium coil which was coated with a metallic copper. This step was conducted due to reduce from nitrate to nitrite in the sample, which allowed us to determine nitrate + nitrite in the seawater sample. For the nitrite analysis, the sample was mixed with reagents without this reduction step. In the flow system, seawater sample with or without the reduction step was mixed with an acidic sulfanilamide reagent through a mixing coil to produce a diazonium ion. And then, the mixture was mixed with the N-1-naphthylethylenediamine dihydrochloride (NED) to produce a red azo dye. The azo dye compound was injected into the spectrophotometric detection to monitor the signal at 545 nm. Thus, for the nitrite analysis, sample was determined without passing thought the Cd coil. Nitrate was computed by the difference

between nitrate+nitrite concentration and nitrite concentration.
The silicate method is analogous to that described for phosphate (see below). The method is essentially that of Grasshoff et al. (1999). The flow diagrams were shown in Figure 4.2-3. Silicomolybdic acid compound was first formed by mixing silicate in the sample with the molybdic acid. The silicomolybdic acid compound was then reduced to silicomolybdous acid, "molybdenum blue," using L-ascorbic acid as the reductant. And then the signal was monitored at 630 nm.
The methodology for the phosphate analysis is a modified procedure of Murphy and Riley (1962). The flow diagrams were shown in Figure 4.2-4. Molybdic acid was added to the seawater sample to form the phosphomolybdic acid compound, and then it was reduced to phosphomolybdous acid compound using L-ascorbic acid as the reductant. And then the signal was monitored at 880 nm.
The ammonia in seawater was determined using the flow diagrams shown in Figure 4.2-5. Sample was mixed with an alkaline solution containing EDTA, which ammonia as gas state was formed from seawater. The ammonia (gas) is absorbed in a sulfuric acid by way of 0.5 μm pore size membrane filter (ADVANTEC PTFE) at the dialyzer attached to the analytical system. And then the ammonia absorbed in sulfuric acid was determined by coupling with phenol and hypochlorite to form indophenols blue, and the signal was determined at 630 nm.
The details of a modification of analytical methods for four parameters, nitrate, nitrite, silicate and phosphate, are also compatible with the methods described in nutrients section in the new GO-SHIP repeat hydrography nutrients manual (Becker et al., 2019). This manual is a revised version of the GO-SHIP repeat hydrography nutrients manual (Hydes et al., 2010). The analytical method of ammonium is compatible with the determination of ammonia in seawater using a vaporization membrane permeability method (Kimura, 2000).

(4-2) Nitrate + Nitrite reagents
50 % Triton solution
50 mL of Triton™ X-100 (CAS No. 9002-93-1) were mixed with 50 mL of ethanol (99.5 %).

Imidazole (buffer), 0.06 M (0.4 % w/v)
Dissolved 4 g of the imidazole (CAS No. 288-32-4) in 1000 mL ultra-pure water, and then added 2 mL of the hydrogen chloride (CAS No. 7647-01-0). After mixing, 1 mL of the 50 % triton solution was added.

Sulfanilamide, 0.06 M (1 % w/v) in 1.2 M HCl
Dissolved 10 g of 4-aminobenzenesulfonamide (CAS No. 63-74-1) in 900 mL of ultra-pure water, and then add 100 mL of the hydrogen chloride (CAS No. 7647-01-0). After mixing, 2 mL of the 50 % triton solution was added.

NED, 0.004 M (0.1 % w/v)
Dissolved 1 g of N-(1-naphthalenyl)-1,2-ethanediamine dihydrochloride (CAS No. 1465-25-4) in 1000 mL of ultra-pure water and then added 10 mL of hydrogen chloride (CAS No. 7647-01-0). After mixing, 1 mL 50 % of the Triton solution was added. This reagent was stored in a dark bottle.

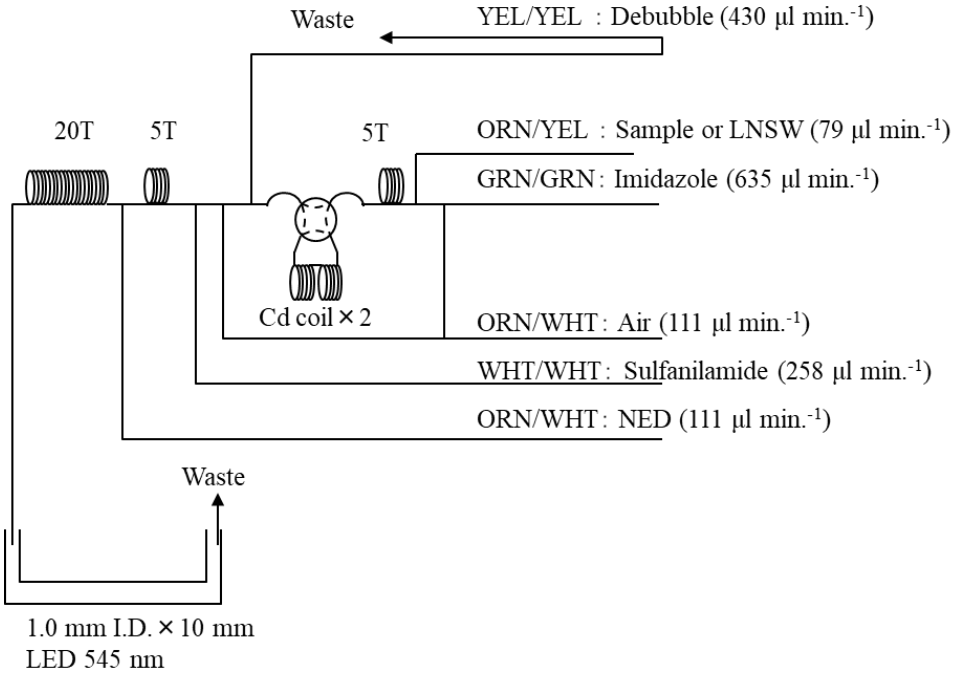

Figure 4.2-1: NO_3+NO_2 (1ch.) flow diagram.

(4-3) Nitrite reagents
50 % Triton solution
50 mL of the Triton™ X-100 (CAS No. 9002-93-1) were mixed with 50 mL ethanol (99.5 %).

Sulfanilamide, 0.06 M (1 % w/v) in 1.2 M HCl
Dissolved 10 g of 4-aminobenzenesulfonamide (CAS No. 63-74-1) in 900 mL of ultra-pure water, and then added 100 mL of hydrogen chloride (CAS No. 7647-01-0). After mixing, 2 mL of the 50 % triton solution were added.

NED, 0.004 M (0.1 % w/v)
Dissolved 1 g of N-(1-naphthalenyl)-1,2-ethanediamine dihydrochloride (CAS No. 1465-25-4) in 1000 mL of ultra-pure water and then added 10 mL of hydrogen chloride (CAS No. 7647-01-0). After mixing, 1 mL of the 50 % triton solution was added. This reagent

was stored in a dark bottle.

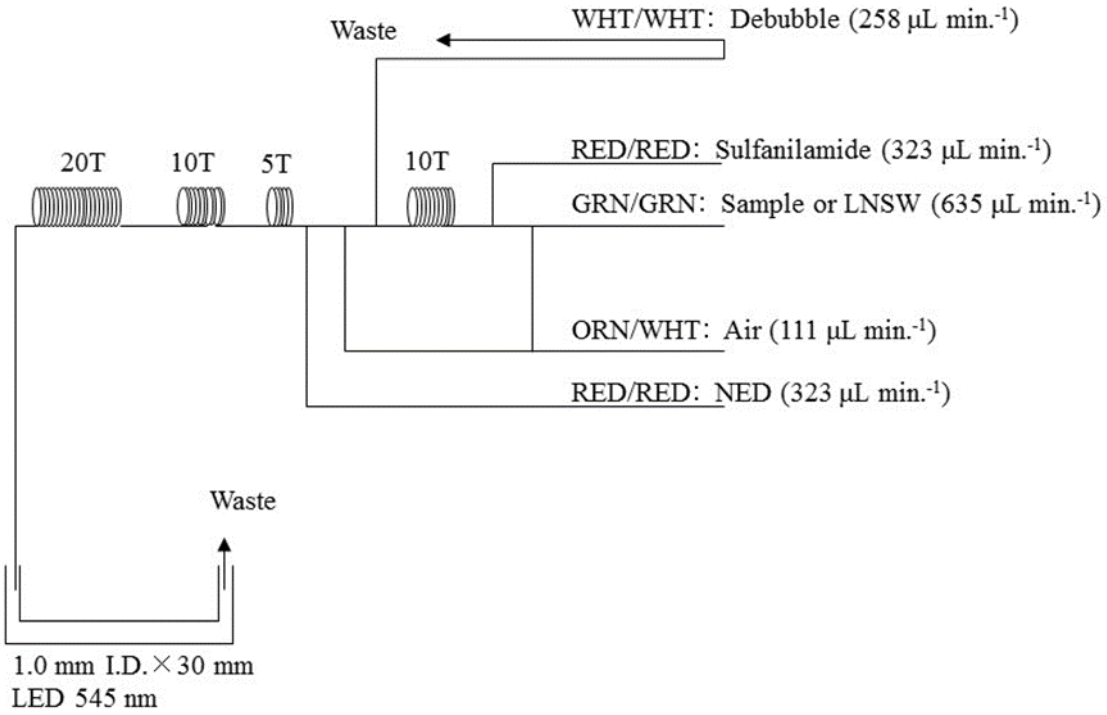

Figure 4.2-2: NO_2 (2ch.) flow diagram.

(4-4) Silicate reagents

15 % Sodium dodecyl sulfate solution

75 g of sodium dodecyl sulfate (CAS No. 151-21-3) was mixed with 425 mL ultra-pure water.

Molybdic acid, 0.03 M (1 % w/v)

Dissolved 7.5 g of sodium molybdate dihydrate (CAS No. 10102-40-6) in 980 mL ultra-pure water, and then added 12 mL of a 4.5M sulfuric acid. After mixing, 20 mL of the 15 % sodium dodecyl sulfate solution was added. Note that the amount of sulfuric acid was reduced from the previous report (MR19-03C) since we have modified the method of Grasshoff et al. (1999).

Oxalic acid, 0.6 M (5 % w/v)

Dissolved 50 g of oxalic acid (CAS No. 144-62-7) in 950 mL of ultra-pure water.

Ascorbic acid, 0.01 M (3 % w/v)

Dissolved 2.5 g of L-ascorbic acid (CAS No. 50-81-7) in 100 mL of ultra-pure water. This reagent was freshly prepared every day.

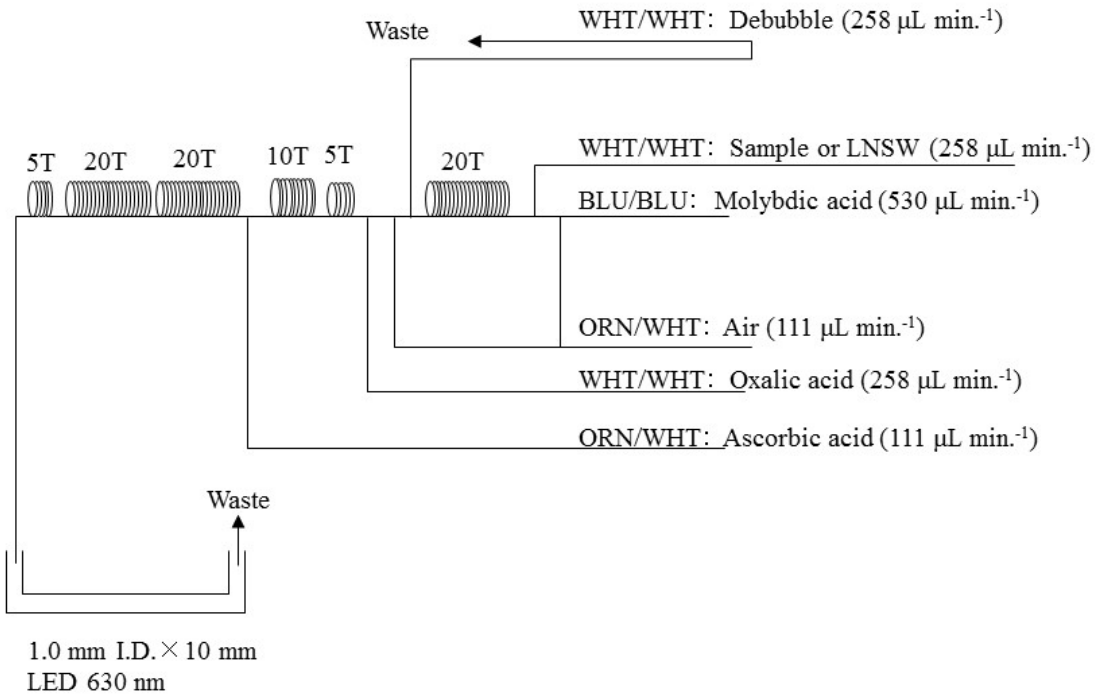

Figure 4.2-3: SiO_2 (3ch.) flow diagram.

(4-5) Phosphate reagents

15 % Sodium dodecyl sulfate solution

75 g of sodium dodecyl sulfate (CAS No. 151-21-3) were mixed with 425 mL of ultra-pure water.

Stock molybdate solution, 0.03 M (0.8 % w/v)

Dissolved 8 g of sodium molybdate dihydrate (CAS No. 10102-40-6) and 0.17 g of antimony potassium tartrate trihydrate (CAS No. 28300-74-5) in 950 mL of ultra-pure water, and then added 50 mL of sulfuric acid (CAS No. 7664-93-9).

PO_4 color reagent

Dissolved 1.2 g of L-ascorbic acid (CAS No. 50-81-7) in 150 mL of the stock molybdate solution. After mixing, 3 mL of the 15 % sodium dodecyl sulfate solution was added. This reagent was freshly prepared before every measurement.

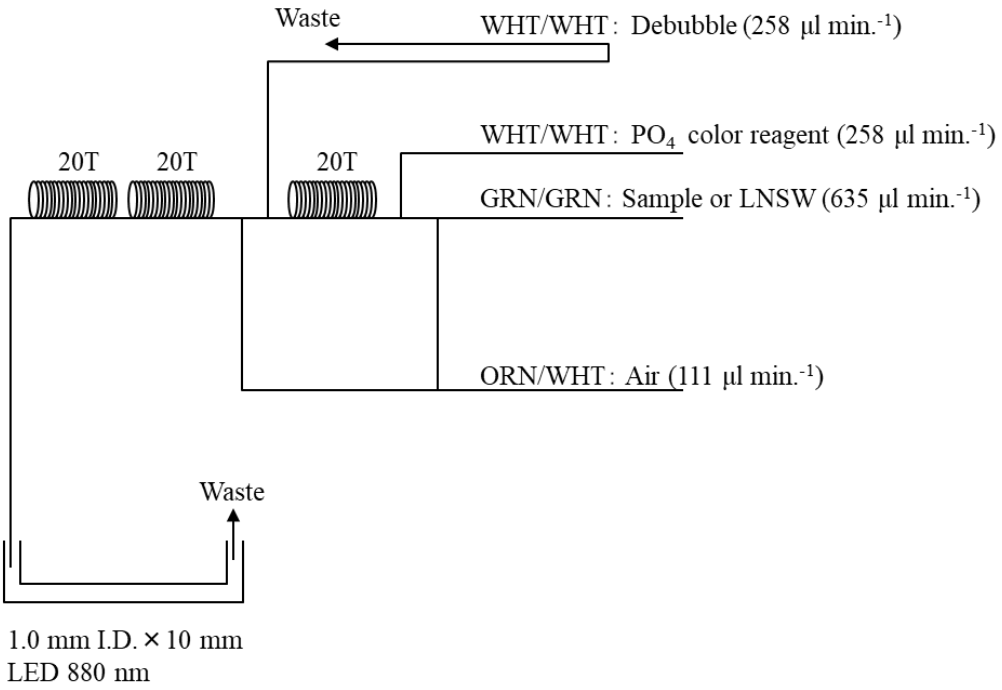

Figure 4.2-4: PO_4 (4ch.) flow diagram.

(4-6) Ammonia reagents

30 % Triton solution

30 mL of a Triton™ X-100 (CAS No. 9002-93-1) were mixed with 70 mL ultra-pure water.

EDTA

Dissolved 41 g of a tetrasodium; 2-[2-[bis(carboxylatomethyl)amino]ethyl-(carboxylatemethyl)amino]acetate;tetrahydrate (CAS No. 13235-36-4) and 2 g of a boric acid (CAS No. 10043-35-3) in 200 mL of ultra-pure water. After mixing, a 1 mL of the 30 % triton solution was added. This reagent is prepared every week.

NaOH liquid

Dissolved 1.5 g of a sodium hydroxide (CAS No. 1310-73-2) and 16 g of a tetrasodium; 2-[2-[bis(carboxylatomethyl) amino]ethyl - (carboxylatomethyl) amino]acetate; tetrahydrate (CAS No. 13235-36-4) in 100 mL of ultra-pure water. This reagent was prepared every week. Note that we reduced the amount of a sodium hydroxide from 5 g to 1.5 g because pH of C standard solutions has been lowered 1 pH unit due to the change of recipe of B standards solution (the detailed of those standard solution, see 7.2.4).

Stock nitroprusside

Dissolved 0.25 g of a sodium nitroferricyanide dihydrate (CAS No. 13755-38-9) in 100 mL of ultra-pure water, and then added 0.2 mL of a 1M sulfuric acid. Stored in a dark bottle and prepared every month.

Nitroprusside solution

Added 4 mL of the stock nitroprusside and 4 mL of a 1M sulfuric acid in 500 mL of ultra-pure water. After mixing, 2 mL of the 30 % triton solution was added. This reagent was stored in a dark bottle and prepared every 2 or 3 days.

Alkaline phenol

Dissolved 10 g of a phenol (CAS No. 108-95-2), 5 g of a sodium hydroxide (CAS No. 1310-73-2) and 2 g of a sodium citrate dihydrate (CAS No. 6132-04-3) in 200 mL of ultra-pure water. Stored in a dark bottle and prepared every week.

NaClO solution

Mixed 3 mL of a sodium hypochlorite (CAS No. 7681-52-9) in 47 mL of ultra-pure water. Stored in a dark bottle and fleshly prepared before every measurement. This reagent need be 0.3 % available chlorine.

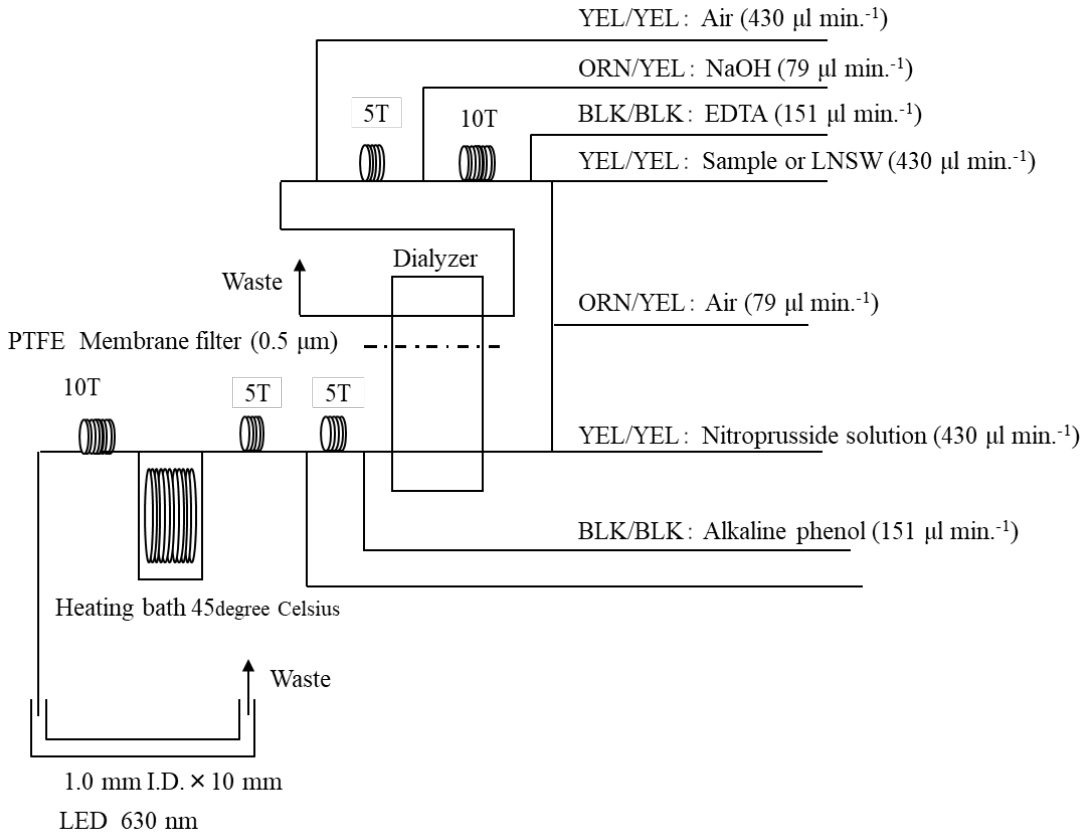

Figure 4.2-5: NH_4 (5ch.) flow diagram.

(4-7) Sampling procedures

Sampling for nutrient samples was conducted right after the sampling for other parameters (oxygen, salinity and trace gases). Samples were collected into two new 10

mL polyacrylates vials without any sample drawing tube that usually used for the oxygen samples. Each vial was rinsed three times before filling and then was sealed without any head-space immediately after the collection. The vials were put into a water bath that was adjusted to the ambient temperature at 22.4 ± 0.7 degree Celsius, for more than 30 minutes to keep the constant temperature of samples before measuring. When the transmissometer signal (Xmiss) of the sample was less than 95 % or comfirmed the presence of particles in the vial, we basically carried out centrifuging the sample by using a centrifuge (type: CN-820, Hsiang Tai). The conditions of centrifuge were set about 3400 rpm for 2.5 minute. The treated samples were listed in Table 4.2-1.
No transfer from the vial to another container was made and the vials were set an autosampler tray directly. Samples were analyzed after collection within 24 hours.

(4-8) Data processing
Raw data from QuAAtro 39 were treated as follows:
- Checked if there were any baseline shift.
- Checked the shape of each peak and positions of peak values. If necessary, a change was made for the positions of peak values.
- Conducted carry-over correction and baseline drift correction followed by sensitivity correction to apply to the peak height of each sample.
- Conducted baseline correction and sensitivity correction using the linear regression.
- Using the pressure and the salinity from uncalibrated CTD data and the laboratory room temperature (20 degree Celsius), the density of each sample had been calculated tentatively. The obtained density was used to calculate the final nutrient concentration with the unit of umol kg^{-1}.
- Calibration curves to obtain the nutrients concentrations were assumed second order equations.

(4-9) Summary of nutrients analysis
During this cruise, 28 runs were conducted to obtain the values for the samples collected by 49 casts at 48 stations. The total number of the seawater samples were 982. For each sample depth, we collected duplicate samples, and then determined all of the samples. The sampling locations for the nutrients was shown in Figure 4.2-6(a) and (b).

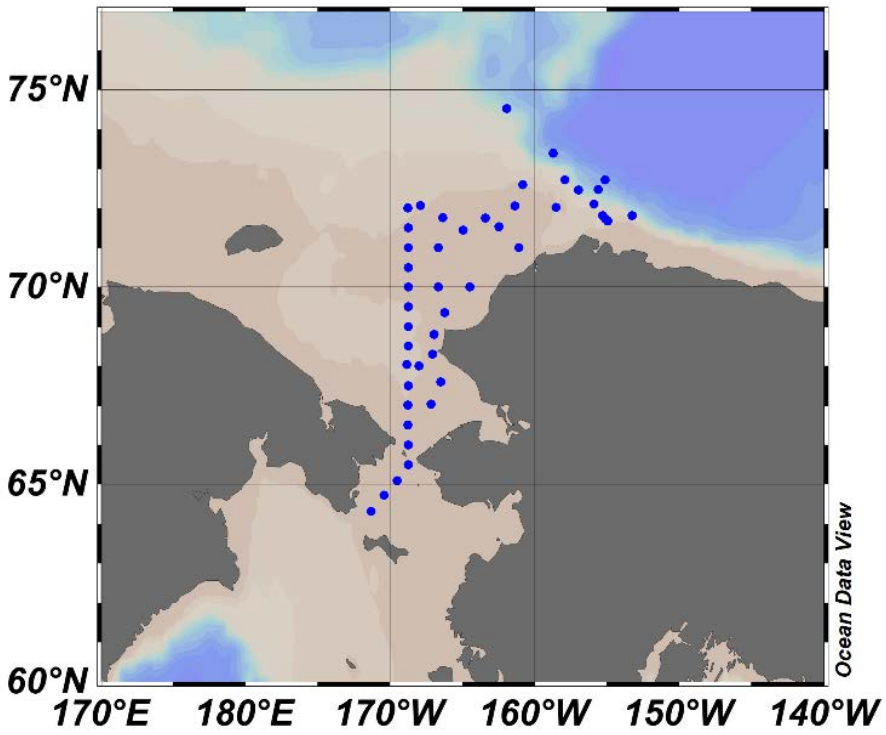

Figure 4.2-6(a) Sampling positions of nutrients sample in the Arctic Ocean.

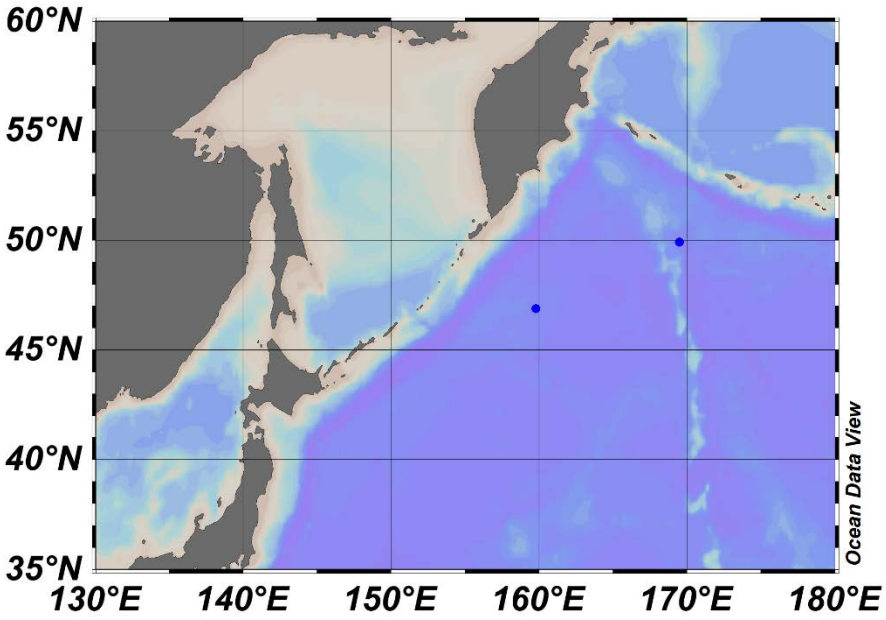

Figure 4.2-6(b) Sampling positions of nutrients sample in the Pacific Ocean.

Table 4.2-1: Centrifuged samples

Station	Cast	Bottle	Depth (dbar)	Trans (%)
3	2	0	0.0	-
3	2	34	4.9	89.2
3	2	33	10.0	93.8
3	2	35	16.0	93.2
3	2	32	19.9	87.1
3	2	31	30.2	92.7
3	2	27	42.9	90.7
3	2	30	49.7	89.1
3	2	29	75.2	86.4
3	2	1	96.5	79.2
4	1	0	0.0	-
4	1	34	4.8	95.7
4	1	33	9.9	95.6
4	1	35	15.8	96.3
4	1	32	19.7	97.3
4	1	31	30.1	98.8
4	1	30	50.0	95.4
4	1	29	75.1	92.6
4	1	28	99.7	89.1
4	1	27	125.1	86.8
4	1	26	150.4	88.8
4	1	25	175.0	85.4
4	1	24	199.5	81.5
4	1	23	224.4	78.9
4	1	22	249.8	58.2
4	1	1	285.7	55.8
5	1	0	0.0	-
5	1	34	4.5	96.1
5	1	35	6.8	96.5
5	1	33	9.7	96.7
5	1	32	20.0	97.0
5	1	31	30.1	96.7
5	1	30	50.1	97.6
5	1	29	74.9	97.5
5	1	28	100.0	98.4
5	1	27	124.8	96.6
5	1	1	191.9	82.1

Station	Cast	Bottle	Depth (dbar)	Trans (%)
9	1	0	0.0	-
9	1	34	5.1	97.8
9	1	33	10.0	97.5
9	1	32	20.0	97.7
9	1	35	21.9	97.7
9	1	31	30.1	98.8
9	1	30	50.1	98.4
9	1	29	75.1	98.2
9	1	28	100.2	97.5
9	1	27	124.9	98.2
9	1	26	149.9	97.8
9	1	25	175.0	85.8
9	1	24	200.0	76.8
9	1	23	205.0	76.2
14	1	33	9.9	94.3
14	1	35	17.9	92.5
14	1	1	43.5	68.1
15	1	28	100.0	94.2
15	1	27	125.1	94.3
15	1	21	299.8	86.0
15	1	1	373.2	83.5
20	1	31	30.0	92.4
20	1	30	49.9	85.1
20	1	29	75.1	89.9
20	1	28	100.0	92.0
20	1	27	125.0	92.3
20	1	1	219.2	94.8
22	1	29	75.3	92.7
22	1	27	125.3	92.7
23	1	32	20.0	93.3
23	1	31	30.1	91.7
23	1	30	50.1	83.1
23	1	1	50.8	83.4
24	1	35	20.4	65.4
24	1	32	20.4	65.1
24	1	1	25.6	78.6

Station	Cast	Bottle	Depth (dbar)	Trans (%)
25	1	34	5.1	93.9
25	1	33	9.8	94.1
25	1	31	30.2	68.5
25	1	1	37.4	66.9
26	1	32	20.0	93.3
26	1	31	30.1	55.1
26	1	1	41.0	53.5
27	1	31	30.2	70.4
27	1	1	36.8	65.2
28	1	34	5.1	94.1
28	1	33	10.3	94.4
28	1	31	30.3	70.4
28	1	1	35.9	67.4
29	1	31	30.0	77.5
29	1	1	39.8	67.0
30	1	1	45.6	72.7
31	1	31	30.1	83.8
31	1	1	44.5	71.0
32	1	31	30.1	87.2
32	1	1	43.0	72.5
33	1	31	30.0	59.1
33	1	1	39.4	61.4
34	1	31	30.0	81.9
34	1	1	39.1	75.2
35	1	32	20.2	94.7
35	1	31	30.0	71.8
35	1	1	33.1	66.7
36	1	31	30.1	75.4
36	1	1	35.6	69.2
37	1	0	0.0	-
37	1	34	4.9	89.2
37	1	33	10.0	89.1
37	1	35	18.0	88.1
37	1	32	20.1	88.0
37	1	31	30.0	86.0
37	1	1	38.4	40.6

Station	Cast	Bottle	Depth (dbar)	Trans (%)
38	1	0	0.0	-
38	1	34	5.2	91.8
38	1	33	9.9	92.3
38	1	35	12.3	92.6
38	1	32	20.1	94.1
38	1	31	29.6	67.7
38	1	1	31.2	58.7
39	1	0	0.0	-
39	1	34	4.9	89.9
39	1	35	7.0	90.3
39	1	33	10.0	90.0
39	1	32	20.1	89.9
39	1	31	30.8	76.3
39	1	1	31.4	74.9
41	1	0	0.0	-
41	1	34	4.8	93.8
41	1	33	9.9	93.9
41	1	35	11.9	93.8
41	1	31	30.1	90.4
41	1	1	46.2	56.4
42	1	0	0.0	-
42	1	34	4.9	94.1
42	1	33	10.3	89.9
42	1	35	14.2	93.1
42	1	31	30.2	91.1
42	1	1	47.3	61.7
43	1	0	0.0	-
43	1	34	5.0	78.7
43	1	33	10.1	78.7
43	1	35	15.0	77.0
43	1	32	20.2	87.1
43	1	31	30.1	89.4
43	1	1	35.7	66.7
44	1	33	10.1	94.9
44	1	32	20.0	87.0
44	1	31	30.1	85.9
44	1	1	48.2	67.8

Station	Cast	Bottle	Depth (dbar)	Trans (%)
45	1	0	0.0	-
45	1	34	5.1	91.8
45	1	31	29.8	90.0
45	1	30	49.9	35.5
45	1	1	52.4	31.3
46	1	0	0.0	-
46	1	34	4.9	93.3
46	1	31	30.4	88.2
46	1	1	44.3	74.3
49	1	0	0.0	-
49	1	34	4.8	92.2
49	1	35	6.6	92.9
49	1	33	10.0	92.9
49	1	32	19.9	97.7
49	1	31	29.9	89.2
49	1	1	49.2	73.6
53	1	33	10.3	84.9
53	1	35	12.0	86.1
53	1	32	20.4	94.6
53	1	1	34.0	80.0
54	1	32	20.2	71.1
54	1	31	30.3	71.6
54	1	1	40.9	73.0
55	1	0	0.0	-
55	1	34	5.7	94.4
55	1	33	10.0	94.5
55	1	31	30.6	80.7
55	1	1	34.4	69.9
56	1	33	14.4	94.7
56	1	32	20.4	94.5
56	1	31	30.3	85.4
56	1	1	40.2	73.9

Station	Cast	Bottle	Depth (dbar)	Trans (%)
57	1	0	0.0	-
57	1	34	5.4	93.0
57	1	35	7.6	93.1
57	1	33	10.0	93.4
57	1	32	20.2	94.3
57	1	31	30.2	80.6
57	1	1	48.3	71.8
58	1	32	20.5	91.2
58	1	35	21.8	91.8
58	1	31	30.2	86.7
58	1	1	47.3	83.1
59	1	0	0.0	-
59	1	34	5.6	86.6
59	1	35	8.6	86.6
59	1	33	10.9	86.9
59	1	31	30.5	91.1
59	1	1	49.1	74.7
60	1	35	28.8	91.8
60	1	31	30.3	91.6
60	1	1	44.9	74.6
61	1	0	0.0	-
61	1	34	5.8	89.3
61	1	33	10.4	89.3
61	1	35	17.1	89.3
61	1	32	20.3	89.2
61	1	31	30.1	89.3
61	1	1	44.5	75.1
62	1	0	0.0	-
62	1	34	4.8	92.6
62	1	33	9.9	92.5
62	1	35	15.0	92.3
62	1	32	20.3	92.3
62	1	31	30.5	92.7
62	1	1	41.0	92.0

(5) Station list

The sampling stations were listed as shown in Table 4.2-2.

Table 4.2-2: List of stations

Run serial	Station	Cast	Date (UTC)	Position*		Depth (m)
			(mmddyy)	Latitude	Longitude	
1	001	1	090321	46-52.72N	159-47.49E	5089
2	003	2	091221	71-40.61N	154-57.61W	101
3	004	1	091321	71-44.39N	155-08.15W	286
3	005	1	091321	71-48.28N	155-17.66W	194

4	009	1	091321	72-06.13N	155-54.77W	209
5	010	1	091421	72-28.49N	155-35.14W	1829
6	011	1	091521	74-31.52N	161-55.17W	1688
7	011	2	091621	74-31.43N	161-55.70W	1688
8	014	1	091721	72-35.90N	160-49.95W	49
8	015	1	091821	72-43.41N	157-54.52W	377
9	017	1	091821	73-23.87N	158-42.83W	2214
10	019	1	091921	72-43.37N	155-07.91W	2969
11	020	1	092021	71-48.46N	153-14.95W	247
12	022	1	092021	72-27.56N	156-59.39W	466
12	023	1	092121	72-01.46N	158-31.55W	56
13	024	1	092121	72-03.26N	161-22.60W	31
13	025	1	092121	71-31.35N	162-00.01W	43
13	026	1	092221	70-59.87N	161-00.01W	46
14	027	1	092221	71-26.29N	164-00.03W	42
14	028	1	092221	71-45.13N	163-23.57W	41
15	029	1	092321	71-45.83N	166-21.53W	45
15	030	1	092321	72-00.25N	168-00.00W	51
15	031	1	092321	72-03.92N	167-54.20W	50
16	032	1	092421	71-30.11N	168-44.66W	49
16	033	1	092421	71-00.43N	166-38.73W	45
17	034	1	092521	71-00.01N	168-44.96W	45
17	035	1	092521	70-29.97N	168-44.98W	39
18	036	1	092621	69-59.92N	168-00.00W	41
18	037	1	092621	70-00.01N	166-40.00W	47
19	038	1	092721	70-00.01N	164-27.88W	36
19	039	1	092721	69-21.03N	166-14.08W	38
20	041	1	092821	69-29.98N	168-44.95W	52
20	042	1	092821	69-00.03N	168-45.17W	53
21	043	1	092821	68-48.04N	166-00.01W	42
21	044	1	092921	68-30.25N	168-44.81W	54
22	045	1	092921	68-02.01N	168-49.90W	59
22	046	1	092921	67-30.01N	168-44.67W	50
23	049	1	093021	68-00.05N	168-00.17W	54
23	053	1	093021	68-18.11N	167-03.38W	39
23	054	1	093021	67-36.08N	166-30.04W	47

24	055	1	093021	67-01.77N	167-09.71W	41
24	056	1	100121	67-00.17N	168-00.00W	47
25	057	1	100121	66-29.87N	168-45.59W	52
25	058	1	100121	65-59.77N	168-44.99W	53
26	059	1	100121	65-29.90N	168-00.00W	55
26	060	1	100221	65-05.68N	169-31.12W	50
27	061	1	100221	64-43.51N	170-25.58W	50
27	062	1	100221	64-18.92N	171-18.20W	46
28	063	1	101121	49-54.76N	169-29.36E	5416

* Position indicates latitude and longitude where CTD reached maximum depth at the cast.

(6) Certified Reference Material of nutrients in seawater

KANSO certified reference materials (CRMs, Lot: CE, CL, CO, CG) were used to ensure the comparability and traceability of nutrient measurements during this cruise. The details of CRMs are shown below.

Production

KANSO CRMs for inorganic nutrients in seawater were produced by KANSO Co.,Ltd. This CRM has been produced using autoclaved natural seawater based on the quality control system under ISO Guide 34 (JIS Q 0034).

KANSO Co.,Ltd. has been accredited under the Accreditation System of National Institute of Technology and Evaluation (ASNITE) as a CRM producer since 2011. (Accreditation No.: ASNITE 0052 R)

Property value assignment

The certified values were the arithmetic means of the results of 30 bottles from each batch (measured in duplicates) analyzed by both KANSO Co.,Ltd. and Japan Agency for Marine-Earth Science and Technology (JAMSTEC) using the colorimetric method (continuous flow analysis, CFA, method). The salinity of the calibration standards solution to obtain each calibration curve was adjusted to the salinity of the used CRMs within ± 0.5.

Metrological Traceability

Each certified value of nitrate, nitrite, and phosphate of KANSO CRMs were calibrated using one of Japan Calibration Service System (JCSS) standard solutions for each nitrate ions, nitrite ions, and phosphate ions. JCSS standard solutions were calibrated using the secondary solution of JCSS for each of these ions. The secondary solution of JCSS was calibrated using the specified primary solution produced by Chemicals

Evaluation and Research Institute (CERI), Japan. CERI specified primary solutions were calibrated using the National Metrology Institute of Japan (NMIJ) primary standards solution of nitrate ions, nitrite ions and phosphate ions, respectively.
For the certified value of silicate of KANSO CRM was calibrated using a newly established silicon standards solution named "exp64" produced by JAMSTEC and KANSO. This silicon standard solution was produced by a dissolution technique with an alkaline solution. The mass fraction of Si in the produced solution was calibrated based on NMIJ CRM 3645-a Si standard solution by a technology consulting system of National Institute of Advanced Industrial Science and Technology (AIST), and this value is traceable to the International System of Units (SI).
The certified values of nitrate, nitrite, and phosphate of KASNO CRM are thus traceable to the SI through the unbroken chain of calibrations, JCSS, CERI and NMIJ solutions as stated above, each having stated uncertainties. The certified values of silicate of KANSO CRM are traceable to the SI through the unbroken chain of calibrations, NMIJ CRM 3645-a02 Si standard solution, having stated uncertainties.
As stated in the certificate of NMIJ CRMs, each certified value of dissolved silica, nitrate ions, and nitrite ions was determined by more than one method using one of NIST SRM of silicon standard solution and NMIJ primary standards solution of nitrate ions and nitrite ions. The concentration of phosphate ions as stated information value in the certificate was determined NMIJ primary standards solution of phosphate ions. Those values in the certificate of NMIJ CRMs are traceable to the SI.
One of the analytical methods used for certification of NMIJ CRM for nitrate ions, nitrite ions, phosphate ions and dissolved silica was a colorimetric method (continuous mode and batch mode). The colorimetric method is the same as the analytical method (continuous mode only) used for certification of KANSO CRM. For certification of dissolved silica, exclusion chromatography/isotope dilution-inductively coupled plasma mass spectrometry and ion exclusion chromatography with post-column detection was used. For certification of nitrate ions, ion chromatography by direct analysis and ion chromatography after halogen-ion separation was used. For certification of nitrite ions, ion chromatography by direct analysis was used.
NMIJ CRMs were analyzed at the time of certification process for CRM and the results were confirmed within expanded uncertainty stated in the certificate of NMIJ CRMs.

(6.1) CRM for this cruise

23 sets of CRM lots CE, CL, CO, and CG were used, which almost cover a range of nutrients concentrations in the Arctic Ocean.
Each CRM's serial number was randomly selected. The CRM bottles were stored at a room named "BIOCHEMICAL LABORATORY" on the ship, where the temperature was maintained around 19.99 degree Celsius – 23.81 degree Celsius.

(6.2) CRM concentration

Nutrients concentrations for the CRM lots CE, CL, CO and CG were shown in Table 4.2-3.

Table 4.2-3: Certified concentration and the uncertainty (k=2) of CRMs.

unit: μmol kg^{-1}

Lot	Nitrate	Nitrite**	Silicate	Phosphate	Ammonia***
CE*	0.01 ± 0.03	0.031 ± 0.03	0.06 ± 0.09	0.012 ±0.006	0.69
CL	5.47 ± 0.15	0.017 ± 0.006	13.8 ± 0.3	0.425 ± 0.019	1.68
CO	15.86 ± 0.15	0.047 ± 0.04	34.72 ± 0.16	1.177 ± 0.014	0.54
CG	23.7 ± 0.2	0.073 ± 0.03	56.4 ± 0.5	1.70 ± 0.02	0.61

*Nitrate, silicate and phosphate values of CRM lot CE are below quantifiable detection limit and shown as only reference values.

**Nitrite concentration values are measured on the ship before MR21-04 cruise in July 2021.

***Ammonia values are not certified and shown as only reference values.

(7) Nutrients standards

(7.1) Volumetric laboratory-ware of in-house standards

All volumetric glassware and polymethylpentene (PMP)-ware used were gravimetrically calibrated. Plastic volumetric flasks were gravimetrically calibrated at the temperature of use within 3 K at around 20 degree Celsius.

(7.1.1) Volumetric flasks

Volumetric flasks of Class quality (Class A) are used because their nominal tolerances are 0.05 % or less over the size ranges likely to be used in this work. Since Class A flasks are made of borosilicate glass, the standard solutions were transferred to plastic bottles as quickly as possible after the solutions were made up to volume and well mixed in order to prevent the excessive dissolution of silicate from the glass. PMP volumetric flasks were gravimetrically calibrated and used only within 3 K of the calibration temperature. The computation of volume contained by the glass flasks at various temperatures other than the calibration temperatures were conducted by using the coefficient of linear expansion of borosilicate crown glass.

The coefficients of cubical expansion of each glass and PMP volumetric flask was determined by actual measurement in 2018 and 2019. The coefficients of cubical expansion of glass volumetric flask (SHIBATA HARIO) was 0.0000110 to 0.0000172 K^{-1} and that of PMP volumetric flask (NALGEN PMP) was 0.00039 to 0.00045 K^{-1}. The weights obtained in the calibration weightings were corrected for the density of water and air buoyancy.

(7.1.2) Pipettes

All glass pipettes have nominal calibration tolerances of 0.1 % or better. These were gravimetrically calibrated to verify and improve upon this nominal tolerance.

(7.2) Reagents, general considerations

(7.2.1) Specifications

For nitrate standard, "potassium nitrate 99.995 suprapur®" provided by Merck, Batch B1706365, CAS No. 7757-79-1, was used.

For nitrite standard solution, we used a nitrite ion standard solution (NO_2^- 1000) provided by Wako, Lot ESG1055, Code. No. 146-06453. This standard solution was certified by Wako using the ion chromatography method. Calibration result is 1004 mg L^{-1} at 20 degree Celsius. Expanded uncertainty of calibration (k=2) is 0.8 % for the calibration result.

For the silicate standard solution, we used our in-house Si standard solution "exp64" which was produced by alkali fusion technique from 5N SiO_2 powder produced jointly by JAMSTEC and KANSO. The mass fraction of Si in the "exp64" solution was calibrated based on NMIJ CRM 3645-a02 Si standard solution.

For phosphate standard, we used a potassium dihydrogen phosphate anhydrous 99.995 suprapur®" provided by Merck, Batch B1781408, CAS No.: 7778-77-0, was used.

For ammonia standard, ammonium chloride (CRM 3011-a) provided by NMIJ, CAS No. 12125-02-9 was used. The purity of this standard was reported as >99.9 % by the manufacture. Expanded uncertainty of calibration (k=2) was 0.022 %.

(7.2.2) Ultra-pure water

Ultra-pure water (Milli-Q water) freshly drawn was used for the preparation of reagents, standard solutions and for measurements of the reagent and the system blanks.

(7.2.3) Low nutrients seawater (LNSW)

Surface water having low nutrient concentration was taken and filtered using 0.20 μm pore capsule cartridge filter around 17S and 100E during MR19-04 cruise in February 2020. This water was drained into 20 L cubitainers and stored in a cardboard box.

Nutrients concentrations in LNSW were measured on August 2020. The averaged nutrient concentrations in the LNSW were 0.00 μmol L^{-1} for nitrate, 0.00 μmol L^{-1} for nitrite, 1.93 μmol L^{-1} for silicate and 0.00 μmol L^{-1} for ammonia. We observed phosphate concentration values were different in each cardboard box, so we measured the values for each box. The phosphate concentration value in the LNSW we used in this cruise was 0.072 to 0.096 μmol L^{-1}. The concentrations of nitrate, nitrite and ammonia were lower than detection limit as stated in chapter (8.5).

(7.2.4) Concentrations of nutrients for A, D, B and C standards

Concentrations of nutrients for A, D, B and C standards were adjusted as shown in Table 4.2-4(a) to (c).

We used JAMSTEC-KANSO in-house Si standard solution for A standard of silicate, which doesn't need to neutralize by the hydrochloric acid. B standard was diluted from A standard with the following recipes shown in Table 4.2-5(a) to (c). In order to match the salinity and the density of the stock solution (B standard) to the LNSW, during this dilution step, 15.30 g of a sodium chloride powder was dissolved in B standard, and then the final volume was adjusted to 500 mL.
The C standard solution was prepared in the LNSW following the recipes shown in Table 4.2-6(a) to (c). All volumetric laboratory tools were calibrated prior the cruise as stated in chapter (7.1). Then the actual concentrations of nutrients in each fresh standard solution were calculated based on the solution temperature, together with the determined factors of volumetric laboratory wares.
The calibration curves for each run were obtained using 4 or 5 levels, C-1 (LNSW), C-2, C-3, C-4 and C-5 that were diluting using the B standard solution.
The D standard solutions were made to calculate the reduction rate of Cd coil. The D standard was diluted from the A standard solution into the pure water.

Table 4.2-4(a): Nominal concentrations of nutrients for A, D, B and C standards for station 001.

Unit: $\mu mol\ kg^{-1}$

	A	B	D	C-1	C-2	C-3	C-4	C-5
NO_3	45000	900	900	LNSW	8.9	18	36	54
NO_2	21800	26	870	LNSW	0.3	0.5	1.0	1.6
SiO_2	35600	2850		LNSW	30	59	116	172
PO_4	6000	60		LNSW	0.7	1.3	2.5	3.7
NH_4	2000	160		LNSW	1.6	3.2	6.4	9.6

Table 4.2-4(b): Nominal concentrations of nutrients for A, D, B and C standards for station 003 to 062.

Unit: μmol kg^{-1}

	A	B	D	C-1	C-2	C-3	C-4
NO_3	22500	670	900	LNSW	13	27	40
NO_2	21800	26	870	LNSW	0.5	1.0	1.6
SiO_2	35600	1425		LNSW	30	59	87
PO_4	6000	60		LNSW	1.3	2.5	3.7
NH_4	4000	160		LNSW	3.2	6.4	9.6

Table 4.2-4(c): Nominal concentrations of nutrients for A, D, B and C standards for station 063.

Unit: μmol kg^{-1}

	A	B	D	C-1	C-2	C-3	C-4	C-5
NO_3	22500	900	900	LNSW	8.9	18	36	54
NO_2	21800	26	870	LNSW	0.3	0.5	1.0	1.6
SiO_2	35600	2850		LNSW	30	59	116	172
PO_4	6000	60		LNSW	0.7	1.3	2.5	3.7
NH_4	4000	160		LNSW	1.6	3.2	6.4	9.6

Table 4.2-5(a): B standard recipes for station 001. Final volume was 500 mL.

	A Std.
NO_3	10 mL
NO_2*	15 mL
SiO_2	40 mL
PO_4	5 mL
NH_4	40 mL

*NO2 was D standard solution which was diluted from A standard.

Table 4.2-5(b): B standard recipes for station 003 to 062. Final volume was 500 mL.

	A Std.
NO_3	15 mL
NO_2*	15 mL
SiO_2	20 mL
PO_4	5 mL
NH_4	20 mL

*NO2 was D standard solution which was diluted from A standard.

Table 4.2-5(c): B standard recipes forstation 063. Final volume was 500 mL.

	A Std.
NO_3	20 mL
NO_2*	15 mL
SiO_2	40 mL
PO_4	5 mL
NH_4	20 mL

*NO2 was D standard solution which was diluted from A standard.

Table 4.2-6(a): Working calibration standard recipes for station 001 and 063. Final volume was 500 mL.

C Std.	B Std.
C-2	5 mL
C-3	10 mL
C-4	20 mL
C-5	30 mL

Table 4.2-6(b): Working calibration standard recipes for other stations. Final volume was 500 mL.

C Std.	B Std.
C-2	10 mL
C-3	20 mL
C-4	30 mL

(7.2.5) Renewal of in-house standard solutions

In-house standard solutions as stated in paragraph (7.2.4) were remade by each "renewal time" shown in Table 4.2-7(a) to (c).

Table 4.2-7(a): Timing of renewal of in-house standards.

NO_3, NO_2, SiO_2, PO_4, NH_4	Renewal time
A-1 Std. (NO_3)	maximum a month
A-2 Std. (NO_2)	commercial prepared solution
A-3 Std. (SiO_2)	JAMSTEC-KANSO Si standard solution
A-4 Std. (PO_4)	maximum a month
A-5 Std. (NH_4)	maximum a month
D-1 Std.	maximum 8 days
D-2 Std.	maximum 8 days
B Std. (mixture of A-1, D-2, A-3, A-4 and A-5 std.)	maximum 8 days

Table 4.2-7(b): Timing of renewal of working calibration standards.

Working standards	Renewal time
C Std. (diluted from B Std.)	every 24 hours

Table 4.2-7(c): Timing of renewal of in-house standards for reduction estimation.

Reduction estimation	Renewal time
36 µM NO_3 (diluted D-1 Std.)	when C Std. renewed
35 µM NO_2 (diluted D-2 Std.)	when C Std. renewed

(8) Quality control

(8.1) The precision of the nutrient analyses during the cruise

The highest standard solution (C-4 or C-5) was repeatedly determined every 4 to 15 samples to obtain the analytical precision of the nutrient analyses during this cruise. During each run, the total number of the C-4 or C-5 determination was 8-13 times depending on the run. Each run, we obtained the analytical precision based on this C-4 or C-5 results, shown in Figures 4.2-7 to 4.2-11. In this cruise, there was total 28 runs. Except for a few runs, the analytical precisions were less than 0.2% for nitrate, silicate, and phosphate.

The overall precisions throughout this cruise were calculated based on the analytical precisions obtained from all of the runs, and shown in Table 4.2-8. During this cruise, overall median precisions were 0.14 % for nitrate, 0.20 % for nitrite, 0.14 % for silicate, 0.15 % for phosphate and 0.28 % for ammonia, respectively. The overall median precision for each parameter during this cruise was comparable to the previously published the precisions during the R/V Mirai cruises conducted in 2009 - 2020.

Table 4.2-8: Summary of overall precision based on the replicate analyses (k=1)

	Nitrate CV %	Nitrite CV %	Silicate CV %	Phosphate CV %	Ammonia CV %
Median	0.14	0.20	0.14	0.15	0.28
Mean	0.15	0.20	0.14	0.14	0.29
Maximum	0.25	0.47	0.21	0.23	0.46
Minimum	0.08	0.09	0.08	0.06	0.11
N	28	28	28	28	28

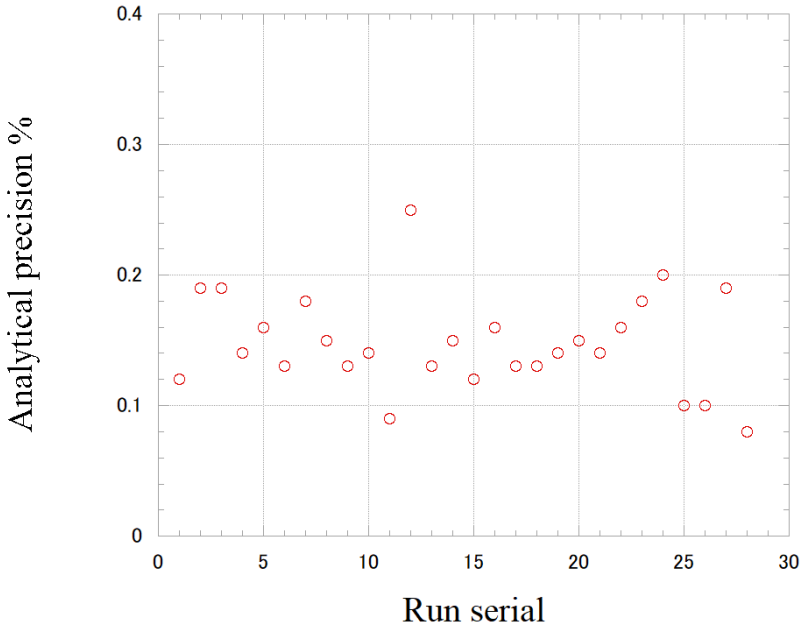

Figure 4.2-7: Time series of precision of nitrate in MR21-05C.

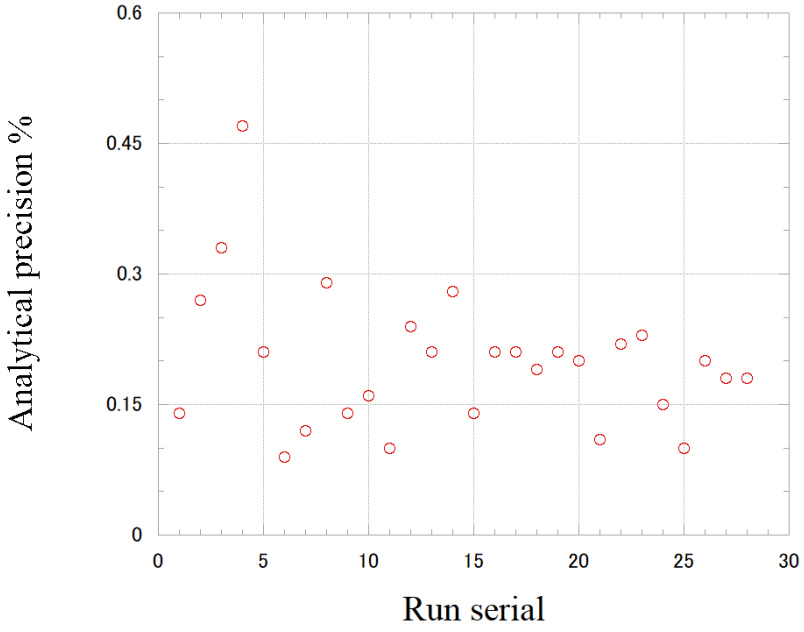

Figure 4.2-8: Same as 4.2-7 but for nitrite.

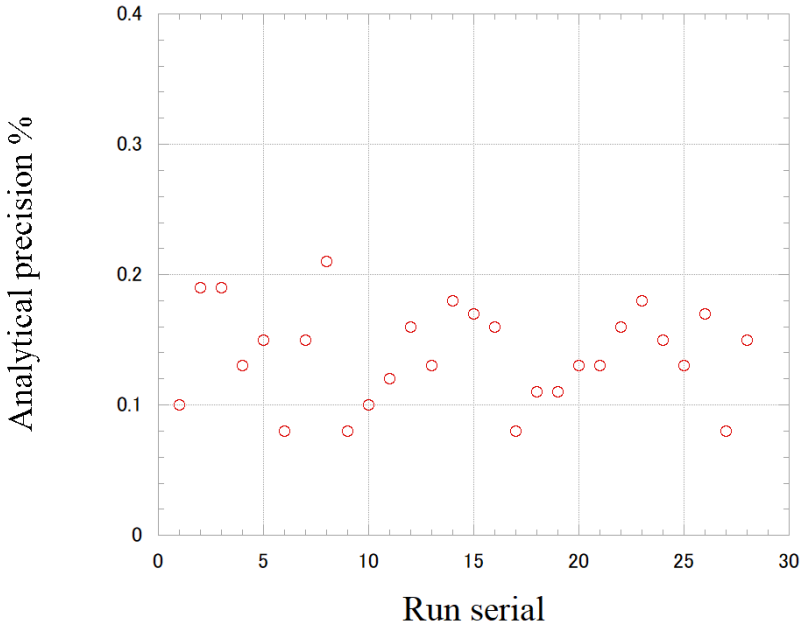

Figure 4.2-9: Same as 4.2-7 but for silicate.

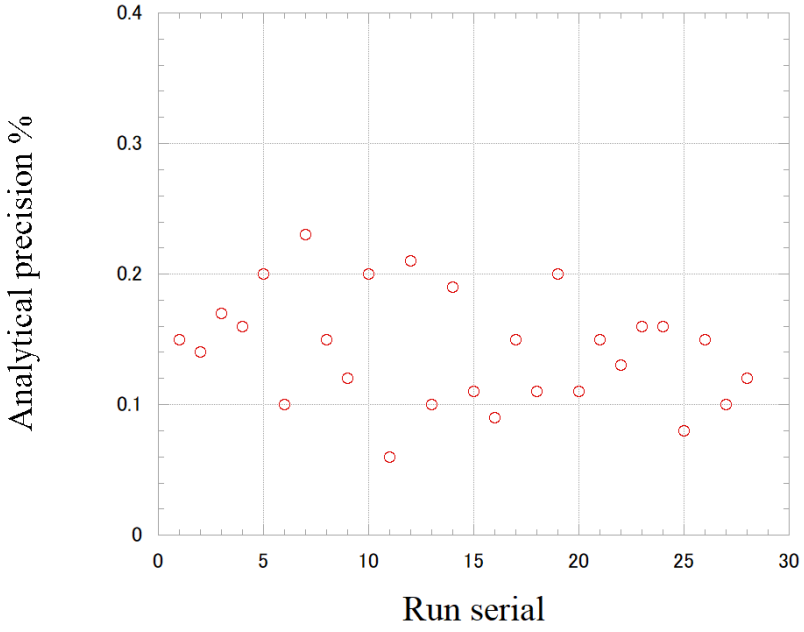

Figure 4.2-10: Same as 4.2-7 but for phosphate.

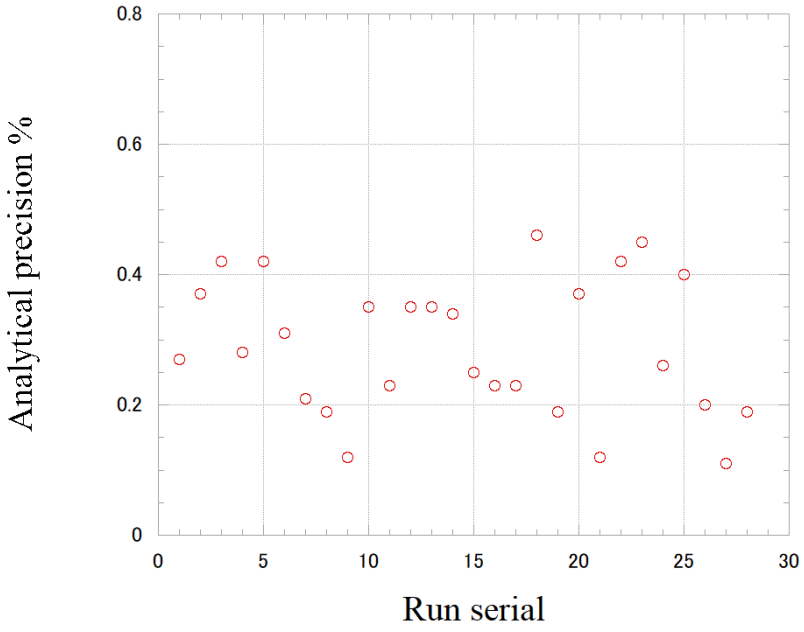

Figure 4.2-11: Same as 4.2-7 but for ammonia.

(8.2) CRM lot. CG measurement during this cruise

CRM lot. CG was measured every run to evaluate the comparability throughout the cruise. The all of the results of lot. CG during this cruise were shown as Figures 4.2-12 to 4.2-16. All of the measured concentrations of CRM lot. CG was within the uncertainty of certified values for nitrate, nitrite, silicate and phosphate. The reported CRM values were shown in Table 4.2-3.

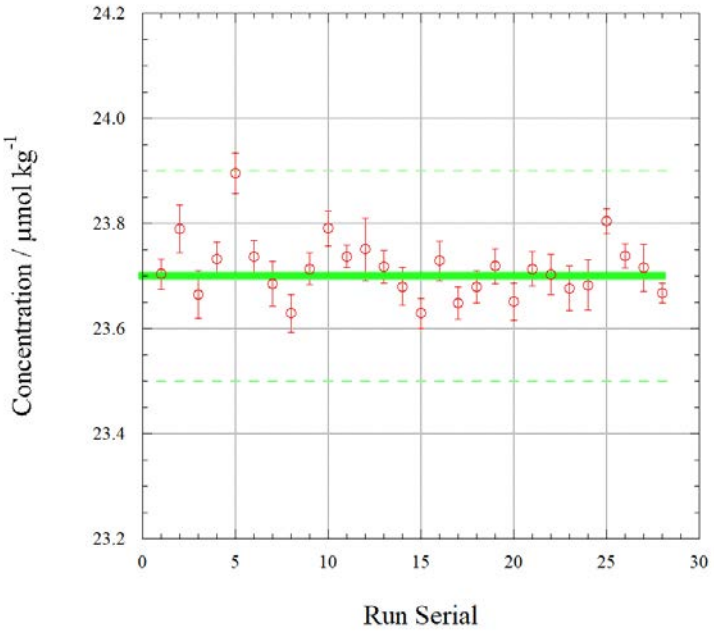

Figure 4.2-12: Time series of CRM-CG of nitrate in MR21-05C. Solid green line is certified nitrate concentration of CRM and broken green line show uncertainty of certified value at k=2.

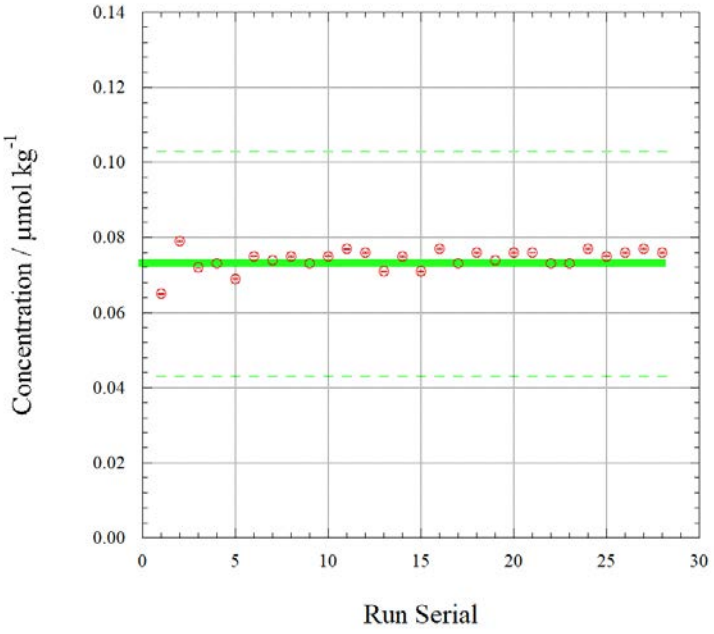

Figure 4.2-13: Same as Figure 4.2-12, but for nitrite.

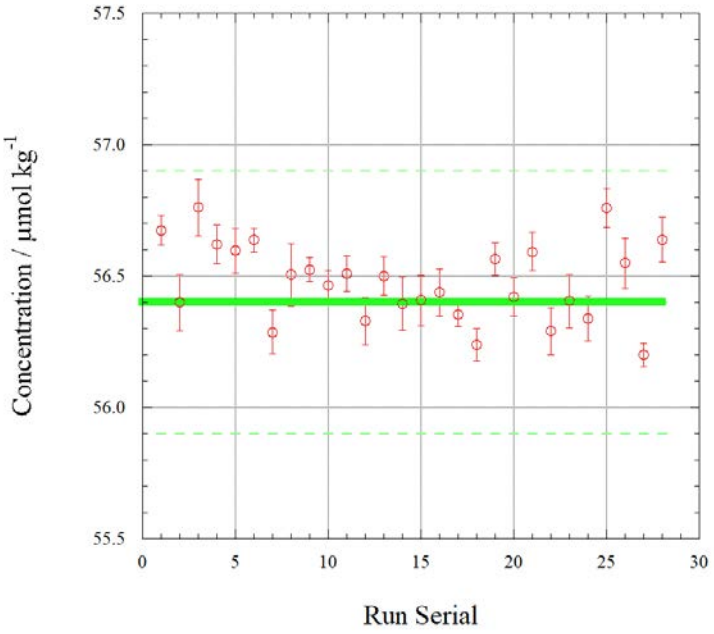

Figure 4.2-14: Same as Figure 4.2-12, but for silicate.

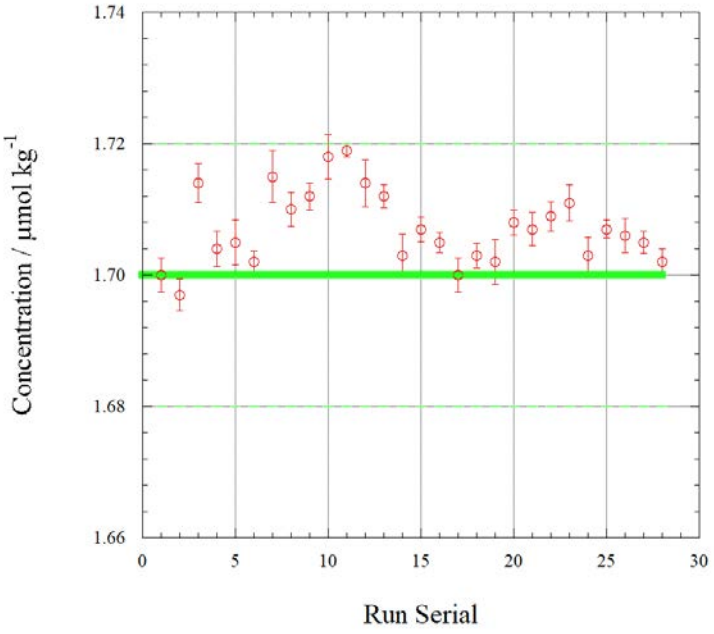

Figure 4.2-15: Same as Figure 4.2-12, but for phosphate.

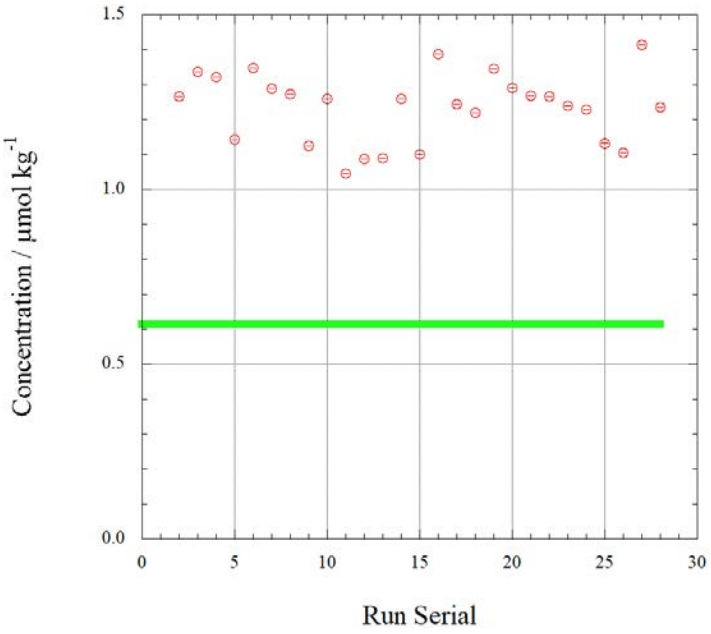

Figure 4.2-16: Time series of CRM-CG of ammonia in MR21-05C. Solid green line is reference value for ammonia concentration of CRM-CG.

(8.3) Carryover

We also summarized the magnitudes of carry over throughout the cruise. In order to evaluate carryover in each run, we conducted determinations of C-4 or C-5 followed by determination of LNSW twice. The difference from LNSW-1 to LNSW-2 was obtained and used for this "carryover" evaluation. The Carryover (%) was obtained from the following equation.

Carryover (%) = (LNSW-1 – LNSW-2) / (C-4 – LNSW-2) * 100 (%)

The summary of the carryover (%) was shown in Table 4.2-9 and Figure 4.2-17 to 4.2-21. The results were low % (<0.2 % for nitrite and phosphate; <0.3% for nitrate and silicate; <1% for ammonia). The low % indicates that there is no significant issue during this cruise.

Table 4.2-9: Summary of carryover throughout MR21-05C.

	Nitrate %	Nitrite %	Silicate %	Phosphate %	Ammonia %
Median	0.21	0.16	0.23	0.19	0.88
Mean	0.21	0.16	0.23	0.20	0.83
Maximum	0.36	0.33	0.33	0.35	1.21
Minimum	0.13	0.00	0.17	0.05	0.14
N	28	28	28	28	28

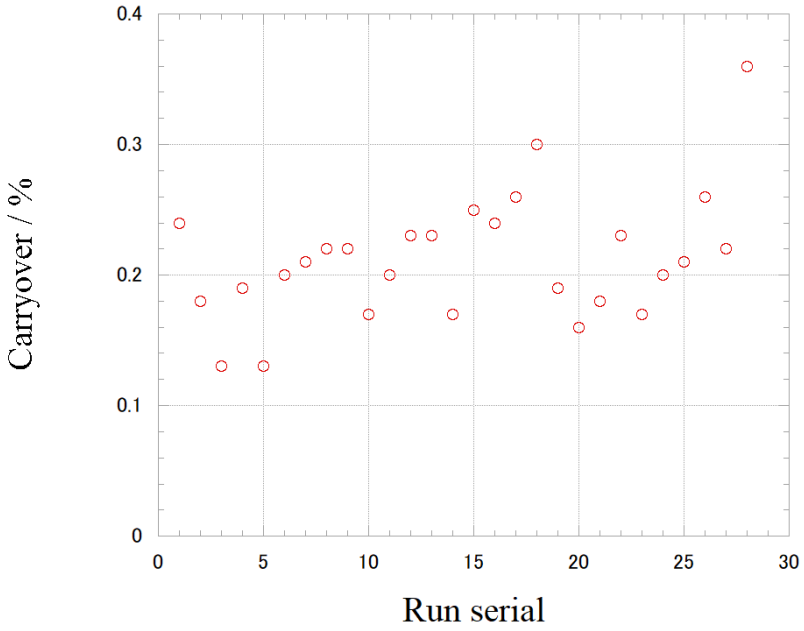

Figure 4.2-17: Time series of carry over of nitrate in MR21-05C.

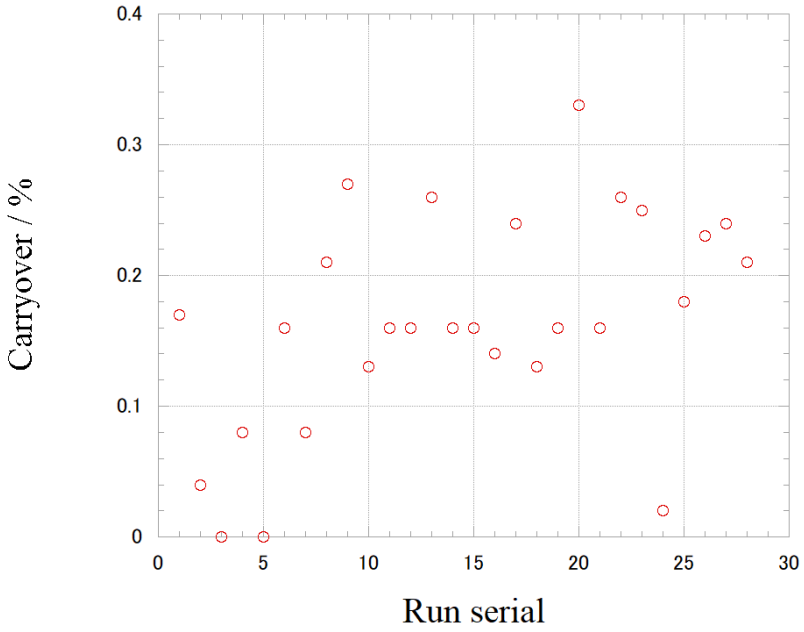

Figure 4.2-18: Same as 4.2-17 but for nitrite.

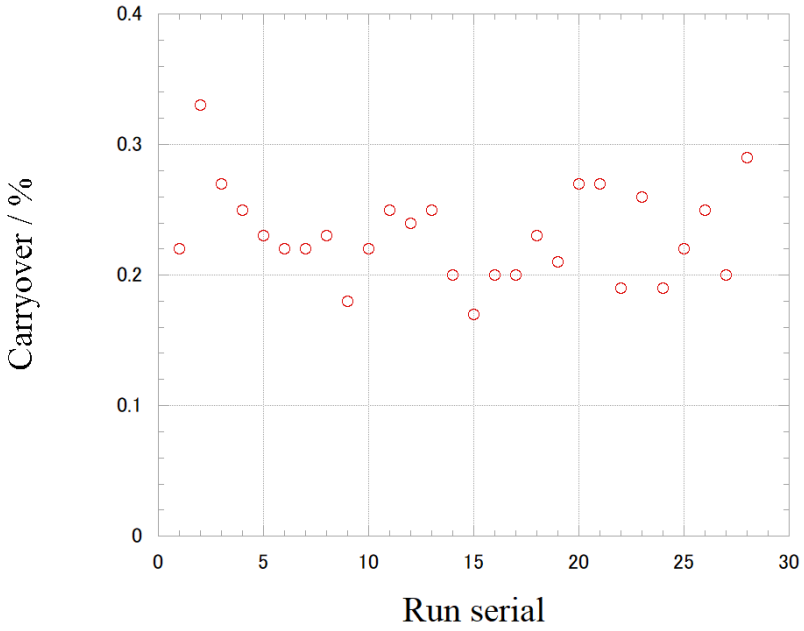

Figure 4.2-19: Same as 4.2-17 but for silicate

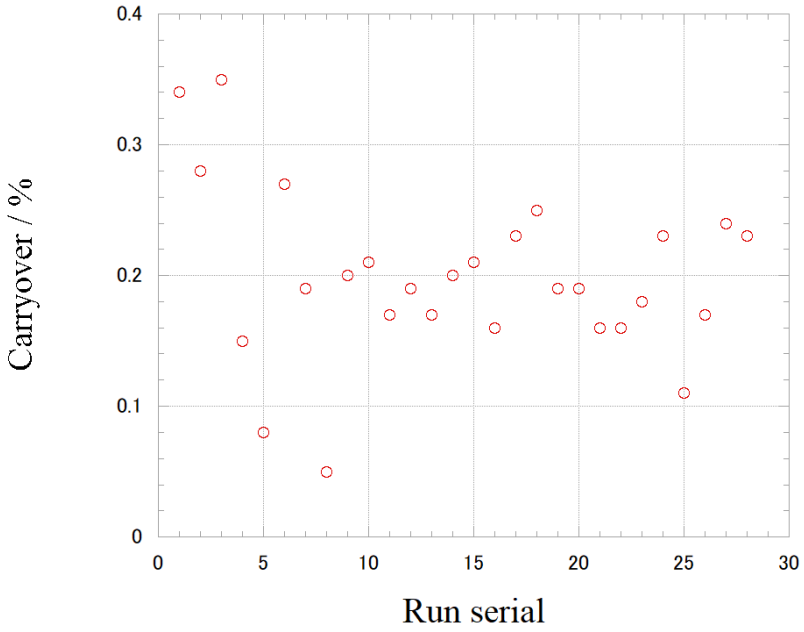

Figure 4.2-20: Same as 4.2-17 but for phosphate.

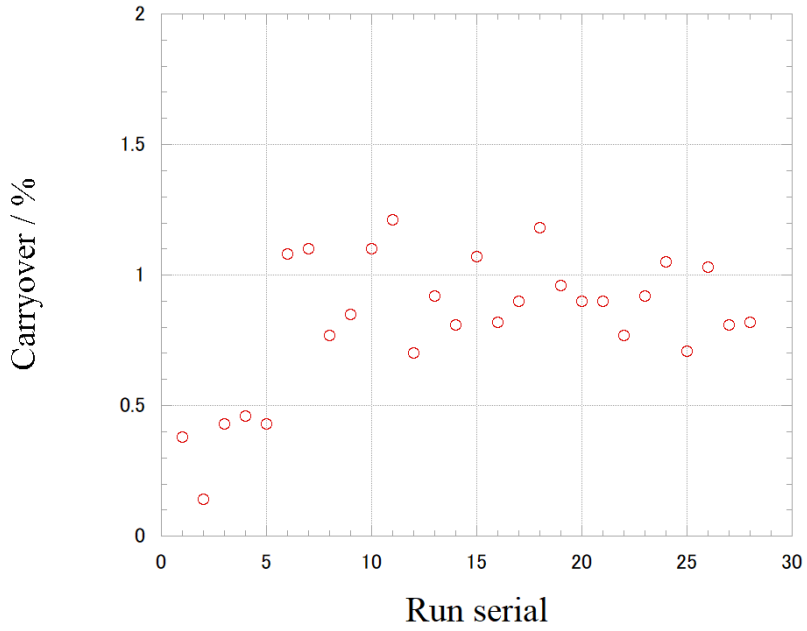

Figure 4.2-21: Same as 4.2-17 but for ammonia.

(8.4) Estimation of uncertainty of nitrate, silicate, phosphate, nitrite and ammonia concentrations

Empirical equations, eq. (1), (2) and (3) to estimate the uncertainty of measurement of nitrate, silicate and phosphate were obtained based on 28 measurements of 23 sets of CRMs (Table 4.2-3). These empirical equations are as follows, respectively.

Nitrate Concentration C_{NO3} in µmol kg^{-1}:

Uncertainty of measurement of nitrate (%) = $0.23527 + 0.81135 * (1 / C_{NO3})$ --- (1)

where C_{NO3} is nitrate concentration of sample.

Silicate Concentration C_{SiO2} in µmol kg^{-1}:

Uncertainty of measurement of silicate (%) = $0.1706 + 3.1797 * (1 / C_{SiO2})$ --- (2)

where C_{SiO2} is silicate concentration of sample.

Phosphate Concentration C_{PO4} in µmol kg^{-1}:

Uncertainty of measurement of phosphate (%) = $0.11543 + 0.28024 * (1 / C_{PO4})$ --- (3)

where C_{PO4} is phosphate concentration of sample.

Empirical equations, eq. (4) and (5) to estimate the uncertainty of measurement of nitrite and ammonia were obtained based on duplicate measurements of the samples.

Nitrite Concentration C_{NO2} in µmol kg^{-1}:

Uncertainty of measurement of nitrite (%) =

$0.14301 + 0.13125 * (1 / C_{NO2}) + 0.0.00019371 * (1 / C_{NO2}) * (1 / C_{NO2})$ --- (4)

where C_{NO2} is nitrite concentration of sample.

Ammonia Concentration C_{NH4} in µmol kg^{-1}:
Uncertainty of measurement of ammonia (%) =
$0.084338 + 1.2646 * (1 / C_{NH4}) - 0.003906 * (1 / C_{NH4}) * (1 / C_{NH4})$ --- (5)
where C_{NH4} is ammonia concentration of sample.

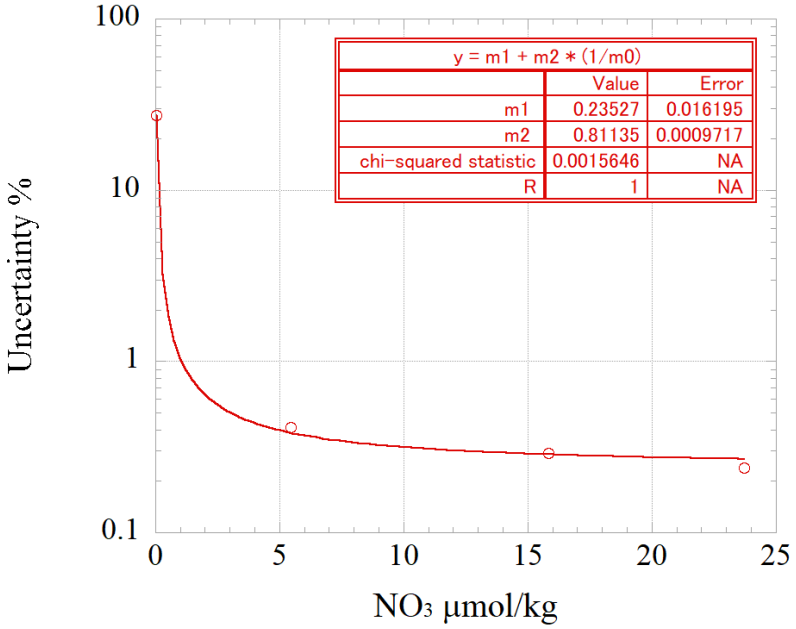

Figure 4.2-22: Estimation of uncertainty for nitrate.

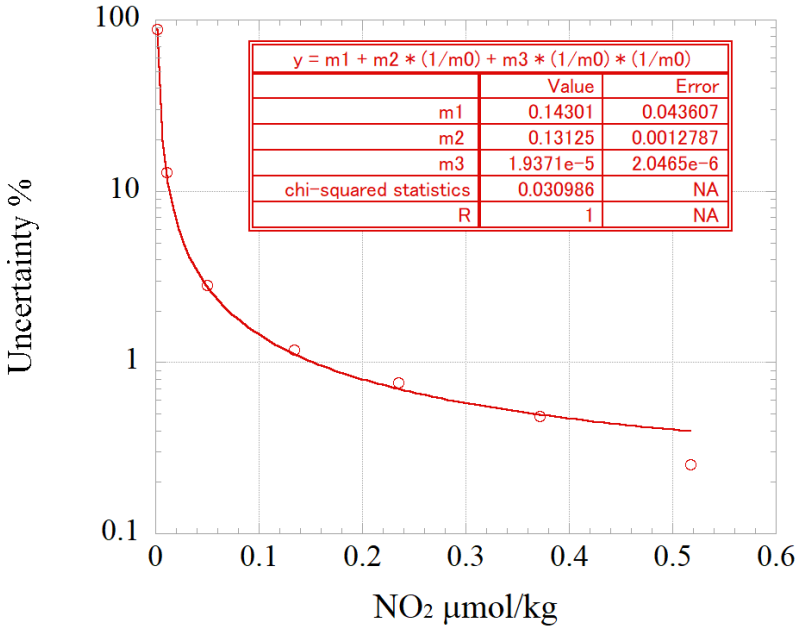

Figure 4.2-23: Estimation of uncertainty for nitrite.

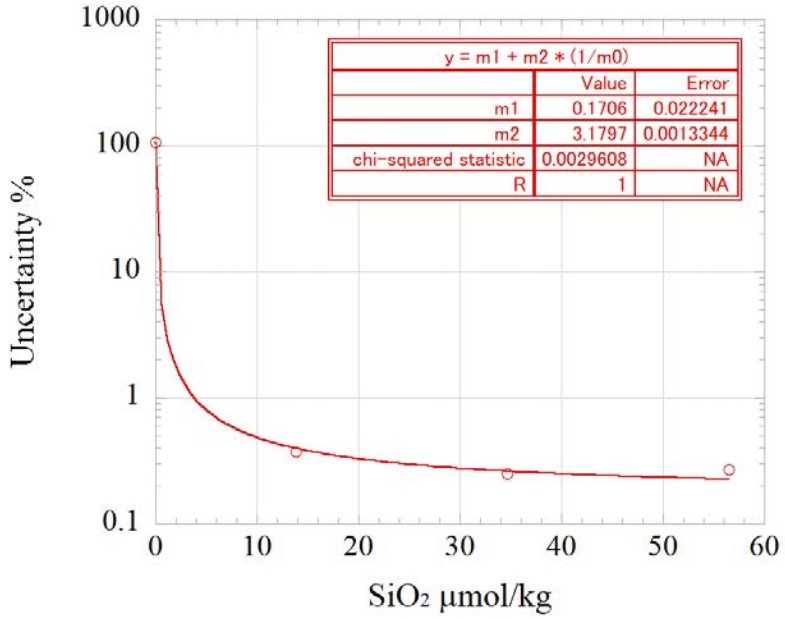

Figure 4.2-24: Estimation of uncertainty for silicate.

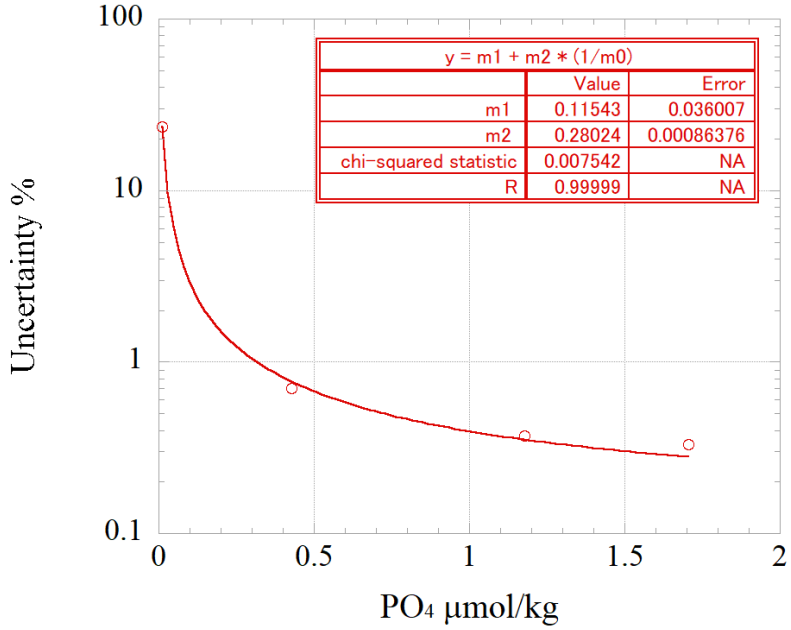

Figure 4.2-25: Estimation of uncertainty for phosphate.

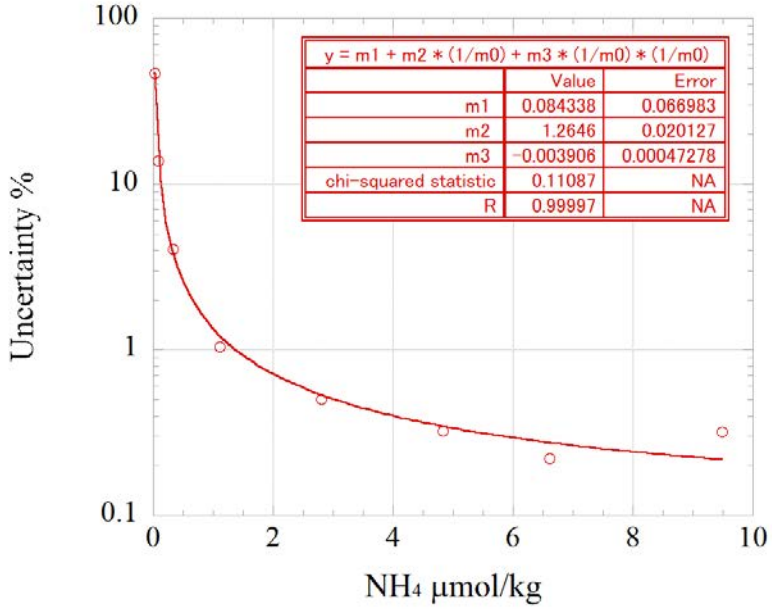

Figure 4.2-26: Estimation of uncertainty for ammonia.

(8.5) Detection limit and quantitative determination of nutrients analyses during the cruise

The LNSW was determined every 4 to 15 samples to obtain detection limit of the nutrient analyses during this cruise. During each run, the total number of the LNSW determination was 7-12 times depending on the run. The detection limit was calculated based on the LNSW results obtained from all the runs by the following equation.

Detection limit = 3 * standard deviation of repeated measurement of LNSW

The summary of detection limit is shown in Table 4.2-10. During in this cruise, detection limit is 0.03 µmol kg^{-1} for nitrate, 0.005 µmol kg^{-1} for nitrite, 0.10 µmol kg^{-1} for silicate, 0.010 µmol kg^{-1} for phosphate and 0.04 µmol kg^{-1} for ammonia, respectively.

The quantitative determination of nutrient analyses is the concentration of which uncertainty is 33 % in the empirical equations, eq. (1) to (5) in chapter (8.4). The summary of quantitative determination is shown in Table 4.2-10. During in this cruise, the quantitative determination was 0.02 µmol kg^{-1} for nitrate, 0.010 µmol kg^{-1} for nitrite, 0.10 µmol kg^{-1} for silicate, 0.009 µmol kg^{-1} for phosphate and 0.04 µmol kg^{-1} for ammonia, respectively.

Table 4.2-10: Summary of detection limit and quantitative determination.

	Nitrate µmol kg^{-1}	Nitrite µmol kg^{-1}	Silicate µmol kg^{-1}	Phosphate µmol kg^{-1}	Ammonia µmol kg^{-1}
Detection limit	0.03	0.005	0.10	0.010	0.04
Quantitative determination*	0.02	0.010	0.10	0.009	0.04

* Due to the large baseline variability over the daily analysis, the detection limit was calculated to be greater than the calculated quantitative determination.

(9) Problems and our actions/solutions

(9.1) Significant baseline drift of silicate and phosphate

During this cruise, we had faced significant baseline drift issues for silicate and phosphate analysis, which was conducted by unit #6. The baseline went lower significantly with the function of the time, the examples were shown in Figure 4.2-27 and Figure 4.2-28. We inspected unit#6 and found obvious damage on the two metal rails attached with the platen, as shown in Picture 4.2-1. This component should have supported the constant flows of the solutions of samples and reagents. This damage of the metal rail might result in a significant decrease of the transport volume of the solutions into the mixing zone, and then the baseline was reduced significantly. In case the normal baseline correction procedure could not apply to this data set since the obtained baseline drift was too large, we flagged those data as "3" (questionable). In case that one of the duplicate samples or both were found within the baseline issue, we flagged those both samples as "3". Finally, 41 paired samples of silicate and 13 paired samples of phosphate were flagged as "3".

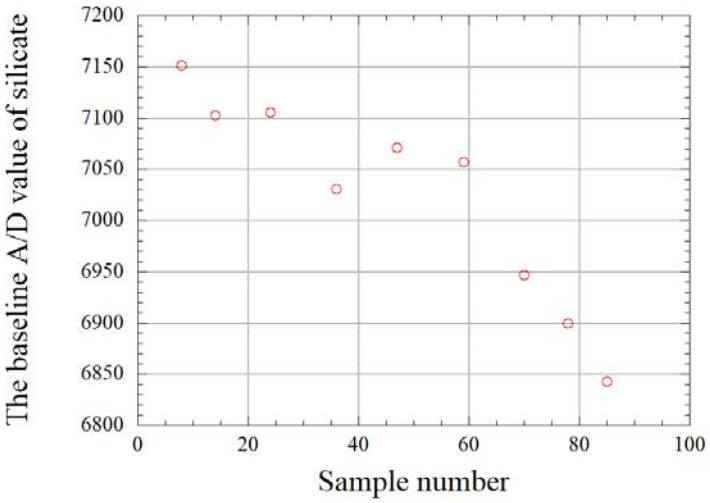

Figure 4.2-27: The baseline A/D value of silicate during an analysis of station 045 and 046 samples in run 22.

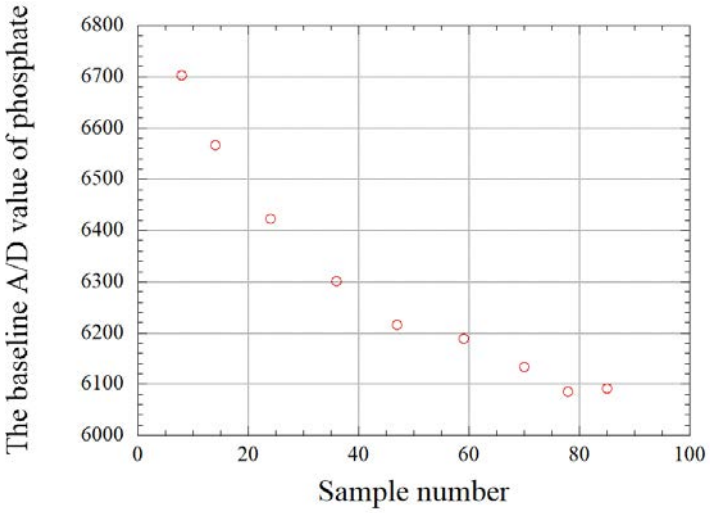

Figure 4.2-28: The baseline A/D value of phosphate during analysis of station 045 and 046 samples in run 22.

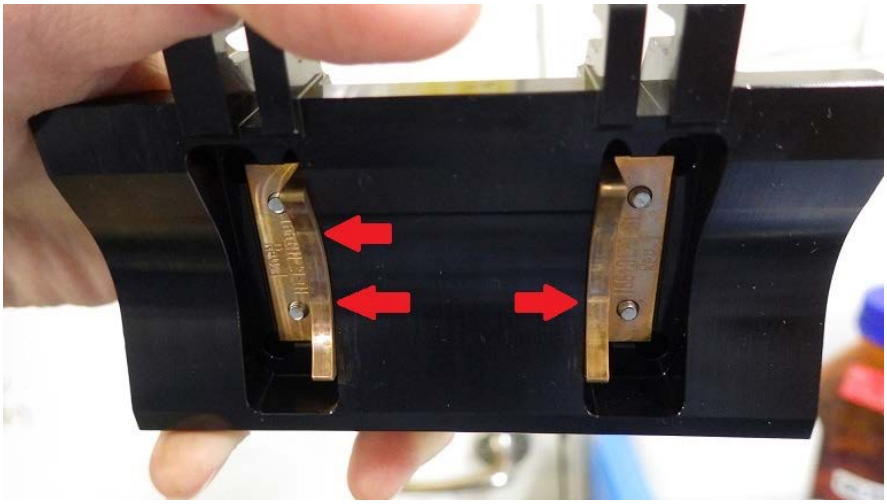

Picture 4.2-1: Damage on the metal rails attached with the platen.

(9.2) Nitrate contamination

Five paired samples collected at station 63 showed a significantly large difference, which exceeded the uncertainty of analysis. Although those samples were reanalyzed, the difference remained the same. Therefore, those samples were probably contaminated during the sampling procedure or during the storage step. Furthermore, the N/P (nitrate: phosphate ratio) calculated by the obtained nitrate values were also outlier from the upper/deeper samples (or the values at the similar depth near stations). Thus, we concluded that those samples were most likely contaminated.

One of the possibilities of this nitrate contamination at station 63 might be from the nitrile gloves. This is because those samples have been collected by the nitrile gloves during the water sampling due to the shortage of the usual gloves that with low nitrate

elution. Note that we had washed the surface of the nitrile globes with low nutrients sea water before sampling to prevent nitrate contamination. We flagged “3” to the higher valued sample within the pair.

(10) List of reagents

List of reagents is shown in Table 4.2-11.

Table 4.2-11: List of reagent in MR21-05C.

IUPAC name	CAS Number	Formula	Compound Name	Manufacture	Grade
4-Aminobenzenesulfonamide	63-74-1	$C_6H_8N_2O_2S$	Sulfanilamide	FUJIFILM Wako Pure Chemical Corporation	JIS Special Grade
Ammonium chloride	12125-02-9	NH_4Cl	Ammonium Chloride	FUJIFILM Wako Pure Chemical Corporation	JIS Special Grade
Antimony potassium tartrate trihydrate	28300-74-5	$K_2(SbC_4H_2O_6)_2 \cdot 3H_2O$	Bis[(+)-tartrato]diantimonate(III) Dipotassium Trihydrate	FUJIFILM Wako Pure Chemical Corporation	JIS Special Grade
Boric acid	10043-35-3	H_3BO_3	Boric Acid	FUJIFILM Wako Pure Chemical Corporation	JIS Special Grade
Hydrogen chloride	7647-01-0	HCl	Hydrochloric Acid	FUJIFILM Wako Pure Chemical Corporation	JIS Special Grade
Imidazole	288-32-4	$C_3H_4N_2$	Imidazole	FUJIFILM Wako Pure Chemical Corporation	JIS Special Grade
L-Ascorbic acid	50-81-7	$C_6H_8O_6$	L-Ascorbic Acid	FUJIFILM Wako Pure Chemical Corporation	JIS Special Grade
N-(1-Naphthalenyl)-1,2-ethanediamine, dihydrochloride	1465-25-4	$C_{12}H_{16}Cl_2N_2$	N-1-Naphthylethylenediamine Dihydrochloride	FUJIFILM Wako Pure Chemical Corporation	for Nitrogen Oxides Analysis
Oxalic acid	144-62-7	$C_2H_2O_4$	Oxalic Acid	FUJIFILM Wako Pure Chemical Corporation	Wako Special Grade
Phenol	108-95-2	C_6H_6O	Phenol	FUJIFILM Wako Pure Chemical Corporation	JIS Special Grade
Potassium nitrate	7757-79-1	KNO_3	Potassium Nitrate	Merck KGaA	Suprapur®
Potassium dihydrogen phosphate	7778-77-0	KH_2PO_4	Potassium dihydrogen phosphate anhydrous	Merck KGaA	Suprapur®
Sodium chloride	7647-14-5	NaCl	Sodium Chloride	FUJIFILM Wako Pure Chemical Corporation	TraceSure®
Sodium citrate dihydrate	6132-04-3	$Na_3C_6H_5O_7 \cdot 2H_2O$	Trisodium Citrate Dihydrate	FUJIFILM Wako Pure Chemical Corporation	JIS Special Grade
Sodium dodecyl sulfate	151-21-3	$C_{12}H_{25}NaO_4S$	Sodium Dodecyl Sulfate	FUJIFILM Wako Pure Chemical Corporation	for Biochemistry
Sodium hydroxide	1310-73-2	NaOH	Sodium Hydroxide for Nitrogen Compounds Analysis	FUJIFILM Wako Pure Chemical Corporation	for Nitrogen Analysis
Sodium hypochlorite	7681-52-9	NaClO	Sodium Hypochlorite Solution	Kanto Chemical co., Inc.	Extra pure
Sodium molybdate dihydrate	10102-40-6	$Na_2MoO_4 \cdot 2H_2O$	Disodium Molybdate(VI) Dihydrate	FUJIFILM Wako Pure Chemical Corporation	JIS Special Grade
Sodium nitroferricyanide dihydrate	13755-38-9	$Na_2[Fe(CN)_5NO] \cdot 2H_2O$	Sodium Pentacyanonitrosylferrate(III) Dihydrate	FUJIFILM Wako Pure Chemical Corporation	JIS Special Grade
Sulfuric acid	7664-93-9	H_2SO_4	Sulfuric Acid	FUJIFILM Wako Pure Chemical Corporation	JIS Special Grade
tetrasodium;2-[2-[bis(carboxylatomethyl)amino]ethyl-(carboxylatomethyl)amino]acetate;tetrahydrate	13235-36-4	$C_{10}H_{12}N_2Na_4O_8 \cdot 4H_2O$	Ethylenediamine-N,N,N',N'-tetraacetic Acid Tetrasodium Salt Tetrahydrate (4NA)	Dojindo Molecular Technologies, Inc.	-
Synonyms: t-Octylphenoxypolyethoxyethanol 4-(1,1,3,3-Tetramethylbutyl)phenyl-polyethylene glycol Polyethylene glycol tert-octylphenyl ether	9002-93-1	$(C_2H_4O)_nC_{14}H_{22}O$	Triton™ X-100	Sigma-Aldrich Japan G.K.	-

(11) Data archives

These data obtained in this cruise will be submitted to the Data Management Group of JAMSTEC, and will be opened to the public via "Data Research System for Whole Cruise Information in JAMSTEC (DARWIN)" in JAMSTEC web site.
<http://www.godac.jamstec.go.jp/darwin/e>

(12) References

Susan Becker, Michio Aoyama E. Malcolm S. Woodward, Karel Bakker, Stephen Coverly, Claire Mahaffey, Toste Tanhua, (2019) The precise and accurate determination of dissolved inorganic nutrients in seawater, using Continuous Flow Analysis methods, n: The GO-SHIP Repeat Hydrography Manual: A Collection of Expert Reports and Guidelines. Available online at: http://www.go-ship.org/HydroMan.html. DOI: http://dx.doi.org/10.25607/OBP-555

Grasshoff, K. 1976. Automated chemical analysis (Chapter 13) in Methods of Seawater Analysis. With contribution by Almgreen T., Dawson R., Ehrhardt M., Fonselius S. H., Josefsson B., Koroleff F., Kremling K. Weinheim, New York: Verlag Chemie.

Grasshoff, K., Kremling K., Ehrhardt, M. et al. 1999. Methods of Seawater Analysis. Third, Completely Revised and Extended Edition. WILEY-VCH Verlag GmbH, D-69469 Weinheim (Federal Republic of Germany).

Hydes, D.J., Aoyama, M., Aminot, A., Bakker, K., Becker, S., Coverly, S., Daniel, A., Dickson, A.G., Grosso, O., Kerouel, R., Ooijen, J. van, Sato, K., Tanhua, T., Woodward, E.M.S., Zhang, J.Z., 2010. Determination of Dissolved Nutrients (N, P, Si) in Seawater with High Precision and Inter-Comparability Using Gas-Segmented Continuous Flow Analysers, In: GO-SHIP Repeat Hydrography Manual: A Collection of Expert Reports and Guidelines. IOCCP Report No. 14, ICPO Publication Series No 134.

Kimura, 2000. Determination of ammonia in seawater using a vaporization membrane permeability method. 7th auto analyzer Study Group, 39-41.

Murphy, J., and Riley, J.P. 1962. Analytica Chimica Acta 27, 31-36.

4.3. Dissolved inorganic carbon

4.3.1. Bottled-water analysis

(1) Personnel

Akihiko Murata (JAMSTEC) – Principal investigator, Not on board
Nagisa Fujiki (Marine Works Japan Ltd.; MWJ) – Operation leader
Yuta Oda (MWJ)

(2) Objective

To clarify vertical distributions of total dissolved inorganic carbon (DIC) in water columns.

(3) Parameter

Total dissolved Inorganic Carbon (DIC)

(4) Instruments and Methods

a. Seawater sampling

Seawater samples were collected by 12 liter Niskin bottles mounted on the CTD/Carousel Water Sampling System and a bucket at 96 stations. Seawater was sampled in a 250 mL glass bottle (SHOTT DURAN) that was previously soaked in 5 % alkaline detergent solution at least 3 hours and was cleaned by fresh water for 5 times and Milli-Q ultrapure water for 3 times. A sampling silicone rubber tube with PFA tip was connected to the outlet of Niskin bottle for water sampling. The glass bottles were filled from its bottom gently, without rinsing, and were overflowed for 20 seconds. They were sealed using the polyethylene inner lids with its diameter of 29 mm with care not to leave any bubbles in the bottle. Immediately after the water sampling on the deck, the glass bottles were carried to the laboratory for the addition of saturated solution of mercury (II) chloride ($HgCl_2$). Small volume (3 mL) of the sample (1 % of the bottle volume) was removed from the bottle and 100 µL of $HgCl_2$ was added. Then the samples were sealed by the polyethylene inner lids with its diameter of 31.9 mm and stored in a refrigerator at approximately 5 °C. About one hour before the analysis, the samples were taken from refrigerator and put in the water bath kept ~20 °C.

b. Seawater analysis

Measurements of DIC were made with total CO_2 measuring system (Nihon ANS Inc.). The system comprises of seawater dispensing unit, a CO_2 extraction unit, and a coulometer (Model 3000, Nihon ANS Inc.) The seawater dispensing unit has an auto-sampler (6 ports), which dispenses the seawater from a glass bottle to a pipette of nominal 15 mL volume. The pipette was kept at 20.00 °C ± 0.05 °C by a water jacket, in which water circulated through a thermostatic water bath. The CO_2 dissolved in a seawater sample is extracted in a stripping chamber of the CO_2 extraction unit by adding

10 % phosphoric acid solution. The stripping chamber is made approx. 25 cm long and has a fine frit at the bottom. First, a constant volume of acid is added to the stripping chamber from its bottom by pressurizing an acid bottle with nitrogen gas (99.9999 %). Second, a seawater sample kept in a pipette is introduced to the stripping chamber by the same method. The seawater and phosphoric acid are stirred by the nitrogen bubbles through a fine frit at the bottom of the stripping chamber. The stripped CO_2 is carried to the coulometer through two electric dehumidifiers (kept at 2 °C) and a chemical desiccant (magnesium perchlorate) by the nitrogen gas (flow rate of 140 mL min^{-1}). Measurements of system blank (phosphoric acid blank), 1.5 % CO_2 standard gas in a nitrogen base, and seawater samples (6 samples) were programmed to repeat. The variation of our own made JAMSTEC DIC reference material was used to correct the signal drift results from chemical alternation of coulometer solutions. The values of DIC were set to a reference value of RM (batch AV, 2043.6 ± 1.0 μmol kg^{-1}) provided by KANOS TECHNOS. The values of DIC are finalized on land by using a value of CRM provided by Prof. Dickson, Scripps Institution of Oceanography, Univ. of California.

(5) Observation log

Seawater samples were collected at 47 stations.

(6) Preliminary results

A few replicate samples were taken at most of the stations and difference between each pair of analyses was plotted on a range control chart (Figure 4.3.1-1). The repeatability was estimated to be provisionally 1.62 ± 1.60 μmol kg^{-1} (n=53), if outliers are excluded.

(7) Data archives

These data obtained in this cruise will be submitted to the Data Management Group (DMG) of JAMSTEC, and will be opened to the public via "Data Research System for Whole Cruise Information in JAMSTEC (DARWIN)" in JAMSTEC web site.
<http://www.godac.jamstec.go.jp/darwin/e>

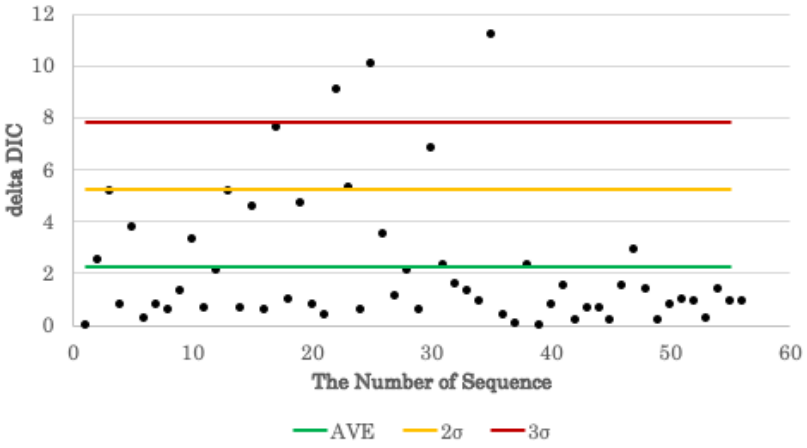

Figure 4.3.1-1: Range control chart of the absolute differences of replicate measurements of DIC carried out during this cruise. The 2σ and 3σ indicate the upper control limits of standard deviation (σ) × 2 and σ × 3, respectively.

4.3.2. Underway DIC

(1) Personnel

Akihiko Murata (JAMSTEC) – Principal investigator, Not on board
Nagisa Fujiki (Marine Works Japan Ltd.; MWJ) – Operation leader
Yuta Oda (MWJ)

(2) Objective

To elucidate spatial variations of total dissolved inorganic carbon (DIC) concentration in sea surface water.

(3) Parameter

Total Dissolved Inorganic Carbon (DIC)

(4) Instruments and Methods

Surface seawater was continuously collected from 4th September to 11th October 2021 (UTC) during this cruise. Surface seawater was taken from an intake placed at the approximately 4.5 m below the sea surface by a pump, and was filled in a 250 mL glass bottle (SCHOTT DURAN) from the bottom, without rinsing, and overflowed for more than 2 times the amount. Before the analysis, the samples were put in the water bath kept about 20°C for one hour. Measurements of DIC were made with total CO_2 measuring system (Nihon ANS Inc.). The system was comprised of seawater dispensing unit, a CO_2 extraction unit, and a coulometer (Model 3000A, Nihon ANS Inc.). The seawater dispensing unit has an auto-sampler (6 ports), which dispenses the seawater from a glass bottle to a pipette of nominal 15 mL volume. The pipette was kept at 20.00 °C ± 0.05 °C by a water jacket, in which water circulated through a thermostatic water bath. The CO_2 dissolved in a seawater sample is extracted in a stripping chamber of the CO_2 extraction unit by adding 10 % phosphoric acid solution. The stripping chamber is made approx. 25 cm long and has a fine frit at the bottom. First, the certain amount of acid is taken to the constant volume tube from an acid bottle and transferred to the stripping chamber from its bottom by nitrogen gas (99.9999 %). Second, a seawater sample kept in a pipette is introduced to the stripping chamber by the same method as that for an acid. The seawater and phosphoric acid are stirred by the nitrogen bubbles through a fine frit at the bottom of the stripping chamber. The stripped CO_2 is carried to the coulometer through two electric dehumidifiers (kept at 2 °C) and a chemical desiccant (Magnesium perchlorate) by the nitrogen gas (flow rate of 140 mL min^{-1}). Measurements of approx.1.5 % CO_2 standard gas in a nitrogen base, system blank (phosphoric acid blank), and seawater samples (6 samples) were programmed to repeat. Both CO_2 standard gas and blank signals were used to correct the signal drift results from chemical alternation of coulometer solutions. The coulometer solutions were renewed every about 2 days, and a reference material (RM, batch AV) provided by KANSO TECHNOS was measured to correct systematic difference between measurements.

(5) Observation log

The cruise track during underway DIC observation is shown in Figure 4.3.2-1.

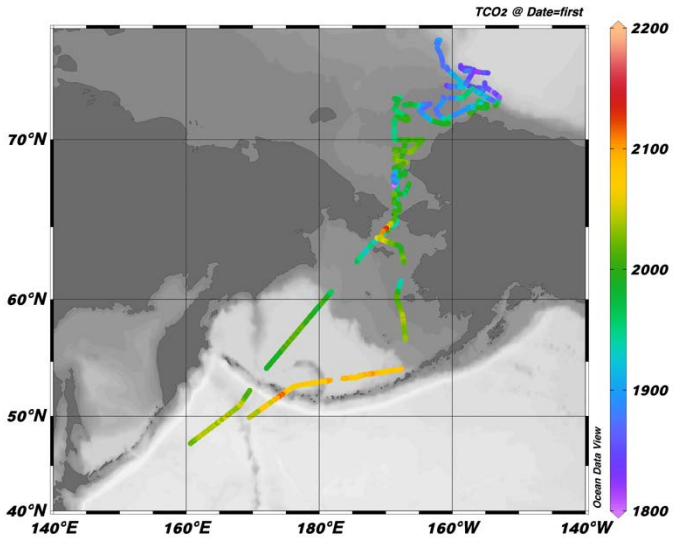

Figure 4.3.2-1: Cruise track where underway DIC was measured during the cruise. Concentrations of DIC were shown in color.

(6) Results

Temporal variations of DIC in surface water are shown in Figure 4.3.2-2, together with those of salinity.

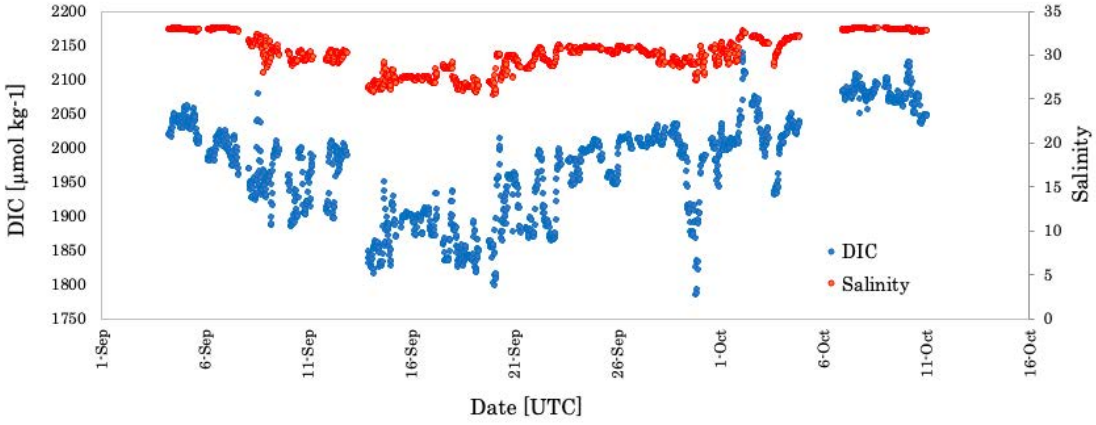

Figure 4.3.2-2: Temporal variations of DIC in surface seawater (blue) and sea surface salinity (red).

(7) Date archives

These data obtained in this cruise will be submitted to the Data Management Group (DMG) of JAMSTEC, and will be opened to the public via “Data Research System for Whole Cruise Information in JAMSTEC (DARWIN)” in JAMSTEC web site.

<http://www.godac.jamstec.go.jp/darwin/e>

4.4. δ^{13}C-DIC

(1) Personnel

Wei-Jun Cai (University of Delaware) – Principal investigator, Not on board
Zhangxian Ouyang (University of Delaware) – Not on board
Akihiko Murata (JAMSTEC) – Not on board
Shigeto Nishino (JAMSTEC) – Not on board
Amane Fujiwara (JAMSTEC)

(2) Objectives

Based on the data collected in previous cruises, we identified the substantial expansion of the subsurface acidified water (Qi et al., 2017). From 1994 to 2010, the aragonite undersaturated water became deeper in the Canada Basin and extended into higher latitude. Our analysis confirms that the atmospheric CO_2 intrusion and sea-ice melt are two dominant drivers for acidification in the stratified and freshened surface waters. Meanwhile, we attributed increased Pacific Winter Water inflow as the main cause for intensified acidification in the subsurface Canada Basin as it has an original low Ω_{ar} and as it is further modified by receiving extra respiratory CO_2 addition in the Chukchi Sea Shelf.

However, it is challenge to separate and quantify the contributions of Pacific corrosive water, terrestrial organic carbon remineralization and local organic matter respiration to ocean acidification. Therefore, our proposed data sampling of δ^{13}C-DIC is designed to collect relevant observations of geochemical tracers and will help to decipher carbon source in different water masses and improve our understanding of mechanisms affecting the western Arctic Ocean acidification.

δ^{13}C-DIC analysis provides us with a useful tool for identifying the carbon source adding into DIC pool. The effects of degradation of organic carbon to DIC, drawdown of DIC by primary production and air-sea CO_2 exchange could be distinguished from one another by analyzing DIC and δ^{13}C-DIC. In the water column, loss of DIC generally leaves isotopically heavy C, whereas addition of DIC by degradation of organic carbon matters adds isotopically light C. As a result, the relative changes in DIC leaves unique carbon isotopic fingerprints in water. Combined with water mixing model, the deviations between observed δ^{13}C-DIC and conservative mixed δ^{13}C-DIC ($\Delta\delta^{13}$C-DIC) associated with the deviation in DIC (ΔDIC) become a useful and powerful tool to quantify the contributions of degradation of terrestrial and local organic carbon at the background of corrosive PWW.

Therefore, we propose to collect δ^{13}C-DIC samples in 2021 JAMSTEC cruise, extending our study scope in carbon isotopic perspective to a more comprehensive area covering from the Chukchi shelf to the Canada Basin. This approach will provide us with a better understanding of Arctic carbon dynamics, in particular, the carbon flows, exports, and degradation from highly productive shelves to oligotrophic basins, and thus a better

ability to predict future changes in the Arctic carbon system, as well as other geophysical and biogeochemical components.

(3) Parameters

δ^{13}C-DIC

(4) Instruments and methods

I. Sampling

δ^{13}C-DIC sampling procedure is basically following the procedure of DIC sampling, described in the book *Guide to Best Practices for Ocean CO_2 Measurements (Dickson et al. 2007).* First, rinse the sample bottle twice with 30–40 ml of sample seawater from Niskin bottle to remove any dust and particles. Second, fill the bottle smoothly from the bottom using a drawing tube which extends from the Niskin drain to the bottom of the glass sample bottle. It is critical to remove any bubbles from the draw tube before filling. Overflow the water by at least a half, and preferably by a full, bottle volume. Insert the stopper and transport the samples from to the lab. Then, a headspace of ~1% of the bottle volume is left to allow for water expansion (i.e., 1 ml for a 125 ml bottle). This can be achieved by pulling out the stopper and using a pipette to remove excess water (1 ml). Mercuric chloride is added to poison the sample using a pipette (to poison a 125 ml sample requires 50 µl of saturated mercuric chloride solution). Next, seal the bottle carefully to ensure that it remains gas-tight. Wipe the excess water from the ground glass in the bottle neck and apply some grease (not too much) around the ground glass stopper, insert the stopper completely, and twist the stopper to squeeze the air out of the grease to make a good seal. Finally, use a rubber band and a clamp to positively reinforce closure and invert the bottle several times to disperse the mercuric chloride solution thoroughly. The samples should be stored in a cool, dark, location.

II. Sample Analysis

Analysis of δ^{13}C-DIC samples are conducted using a DIC- δ^{13}C analyzer (Apollo SciTech, USA). Briefly, a CO_2 extraction device and Cavity Ring-Down Spectrometer (CRDS) isotopic detector (G2131-i, Picarro, USA) were coupled to simultaneously measure DIC and δ^{13}C in a 3–4 mL sample over an ~11 min interval, with average precision of 1.5 ± 0.6 µmol kg^{-1} for DIC and 0.07 ± 0.05‰ for δ^{13}C-DIC. The instrumentation principles and sample analysis procedure are described in detail in Su et al., (2019).

(5) Data archives

These data obtained in this cruise will be submitted to the Data Management Group (DMG) of JAMSTEC, and will be opened to the public via "Data Research System for Whole Cruise Information in JAMSTEC (DARWIN)" in JAMSTEC web site.
<http://www.godac.jamstec.go.jp/darwin/e>

(6) References

Qi, D., Chen, L., Chen, B., Gao, Z., Zhong, W., Feely, R. A., ... & Zhan, L. (2017). Increase in acidifying water in the western Arctic Ocean. *Nature Climate Change*, *7*(3), 195-199.

Dickson, A. G., Sabine, C. L., & Christian, J. R. (2007). *Guide to best practices for ocean CO2 measurements*. North Pacific Marine Science Organization.

Su, J., Cai, W. J., Hussain, N., Brodeur, J., Chen, B., & Huang, K. (2019). Simultaneous determination of dissolved inorganic carbon (DIC) concentration and stable isotope (δ13C-DIC) by Cavity Ring-Down Spectroscopy: Application to study carbonate dynamics in the Chesapeake Bay. *Marine Chemistry*, *215*, 103689.

4.5. Total Alkalinity

(1) Personnel

Akihiko Murata (JAMSTEC) – Principal investigator, Not on board
Nagisa Fujiki (Marine Works Japan Ltd.; MWJ) – Operation leader
Yuta Oda (MWJ)

(2) Objective

To survey influences of sea ice melting water and river input on carbonate system properties.

(3) Parameters

Total alkalinity (TA)

(4) Instruments and Methods

a. Seawater sampling

Seawater samples were collected by 12 L Niskin bottles mounted on the CTD/Carousel Water Sampling System and a bucket at 24 stations. The seawater from the Niskin bottle was filled into the 125 mL borosilicate glass bottles (SHOTT DURAN) using a sampling silicone rubber tube with PFA tip. The water was filled into the bottle from the bottom smoothly, without rinsing, and overflowed for 2 times bottle volume (10 seconds). These bottles were pre-washed in advance by soaking in 5 % alkaline detergent for more than 3 hours, and then rinsed 5 times with tap water and 3 times with Milli-Q deionized water. The samples were stored in a refrigerator at approximately 5 °C before the analysis, and were put in the water bath with its temperature of about 25 °C for one hour before analysis.

b. Seawater analysis

The total alkalinity was measured using a spectrophotometric system (Nihon ANS, Inc.) using a scheme of Yao and Byrne (1998). The calibrated volume of sample seawater (ca. 42 mL) was transferred from a sample bottle into the titration cell with its light path length of 4 cm long via dispensing unit. The TA is calculated by measuring two sets of absorbance at three wavelengths (730, 616 and 444) nm with the spectrometer (TM-UV/VIS C10082CAH, HAMAMATSU). One is the absorbance of seawater sample before injecting an acid with indicator solution (bromocresol green sodium) and another is the one after the injection. To mix the acidified-indicator solution with seawater sufficiently, the mixed solution is circulated in a circulation line by a peristaltic pump for 5 minutes. Nitrogen bubbles were introduced into the titration cell for degassing CO_2 from the mixed solution sufficiently. The TA is calculated based on the following equation:

$$TA = (-[H^+]_T V_{SA} + M_A V_A)/V_S,$$

where M_A is the molarity of the acid titrant added to the seawater sample, $[H^+]_T$ is the total excess hydrogen ion concentration in the seawater, and V_S, V_A and V_{SA} are the initial seawater volume, the added acid titrant volume, and the combined seawater plus acid titrant volume, respectively. $[H^+]_T$ is calculated from the measured absorbances based on the following equation (Yao and Byrne, 1998):

$$pH_T = -\log[H^+]_T = 4.2699 + 0.002578(35 - S) + \log((R - 0.00131)/(2.3148 - 0.1299R)) - \log(1 - 0.001005S),$$

where S is the sample salinity, and R is the absorbance ratio calculated as:

$$R = (A_{616} - A_{730})/(A_{444} - A_{730}),$$

where A_i is the absorbance at wavelength i nm.
Values of TA are corrected and reported based on reference material provided by KANSO TECHNOS (batch AV, 2311.6 ± 1.2 μmol kg^{-1}).

(5) Observation log
Seawater samples for TA were collected at 47 stations.

(6) Preliminary results
The repeatability of this system was provisionally 2.1 ± 1.9 μmol kg^{-1} (n = 55), which was calculated from replicate samples after excluding outliers. A range control chart of TA measurement is illustrated in Figure 4.5-1.

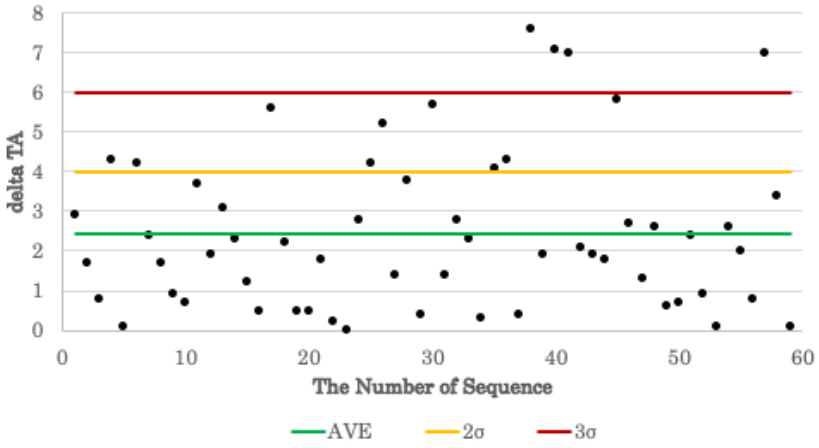

Figure 4.5-1: Range control chart of the absolute differences of replicate measurements of TA. The AVE indicates average. The 2 and 3 sigma indicate the upper control limits of sigma × 2 and that × 3, respectively.

(7) Date archives

These data obtained in this cruise will be submitted to the Data Management Group (DMG) of JAMSTEC, and will be opened to the public via "Data Research System for Whole Cruise Information in JAMSTEC (DARWIN)" in JAMSTEC web site.
<http://www.godac.jamstec.go.jp/darwin/e>

4.6. Chlorophyll *a*

(1) Personnel
Amane Fujiwara (JAMSTEC): Principal Investigator
Erii Irie (Marine Works Japan Ltd.; MWJ): Operation leader
Kohei Sumiya (JAMSTEC)

(2) Objective
Phytoplankton biomass in the ocean can be roughly expressed by photosynthetic pigment, chlorophyll-a concentration. Phytoplankton species are also roughly characterized by the cell size. The objective of this study is to investigate the vertical and horizontal distribution of phytoplankton biomass and size in the Arctic Ocean.

(3) Parameters
Total chlorophyll *a*
Size-fractionated chlorophyll *a*

(4) Instruments and methods
We collected samples for total chlorophyll *a* (chl-*a*) concentration from 7 to 15 depths and size-fractionated chl-*a* from 5 to 7 depths between the surface and 203 m depth including a chl-*a* maximum layer. The chl-*a* maximum layer was determined by a fluorometer (Seapoint Sensors, Inc.) attached to the CTD system. Replicate water samples were taken at chl-*a* maximum depth from the same Niskin bottle in order to assess the precision of chl-*a* measurements.
Seawater samples for total chl-*a* were vacuum-filtrated (< 0.02 MPa) through the 25mm-diameter ADVANTEC GF-75 filter. Seawater samples for size-fractionated chl-*a* were passed through 20 μm pore-size nylon filter (47 mm in diameter), 2μm pore-size polyester membrane filter (47 mm in diameter), and ADVANTEC GF-75 (25 mm in diameter) under gentle vacuum (< 0.02 MPa).
Each filter sample was immediately soaked in 7 ml of N,N-dimethylformamide (DMF, Wako Pure Chemical Industries Ltd.) in a polypropylene tube (Suzuki and Ishimaru, 1990). The tubes were stored at -20 °C under the dark condition to extract chl-*a* at least for 24 hours. Some tubes were kept at –80°C under the dark condition until the extraction.
Chl-*a* concentrations were measured by a fluorometer (10-AU, TURNER DESIGNS) following to the method of Welschmeyer (1994). The 10-AU fluorometer was calibrated against a pure chl-*a* (Sigma-Aldrich Co., LLC) prior to the analysis.

(5) Station list
Samples for total chl-*a* were collected at 46 sites in the Arctic Ocean, and 2 site in the subarctic zone (Figure 4.6-1). Samples for size-fractionated chl-*a* were collected

at 19 casts in the Arctic Ocean (Figure 4.6-2).

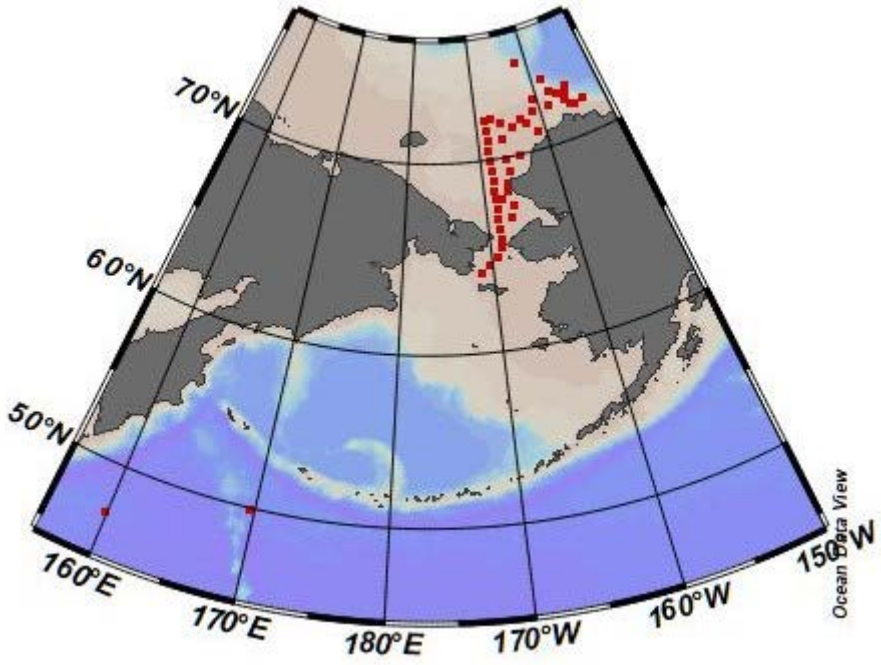

Figure 4.6-1: Sampling positions of total chl-*a*.

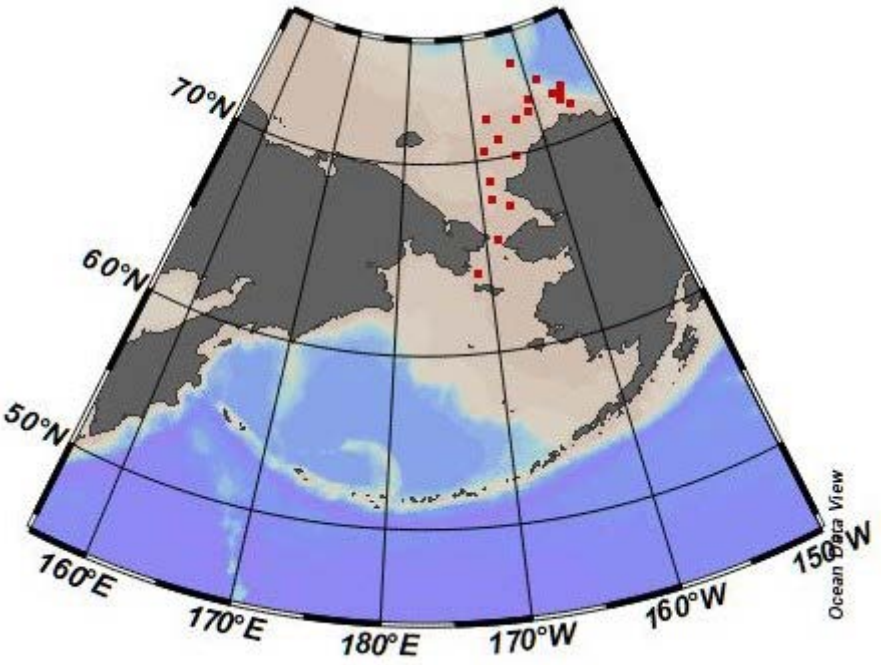

Figure 4.6-2: Sampling positions of size-fractionated chl-*a*.

(6) Preliminary results

Surface distributions of total chl-*a* in the Arctic Ocean are shown in Figure 4.6-3.

Chl-*a* maximum layer distributions of total chl-*a* in the Arctic Ocean are shown in Figure 4.6-4.

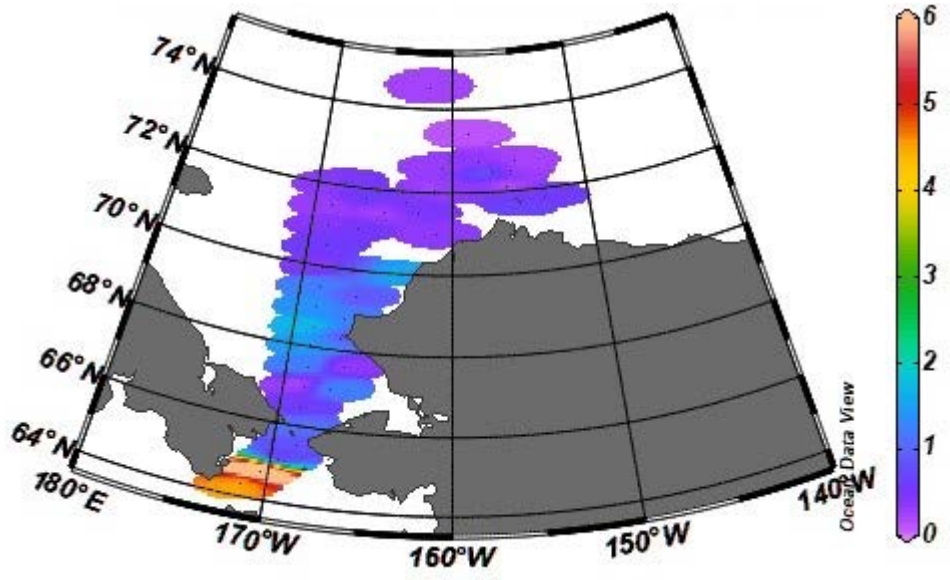

Figure 4.6-3: Surface distributions of total chl-*a* in the Arctic Ocean.

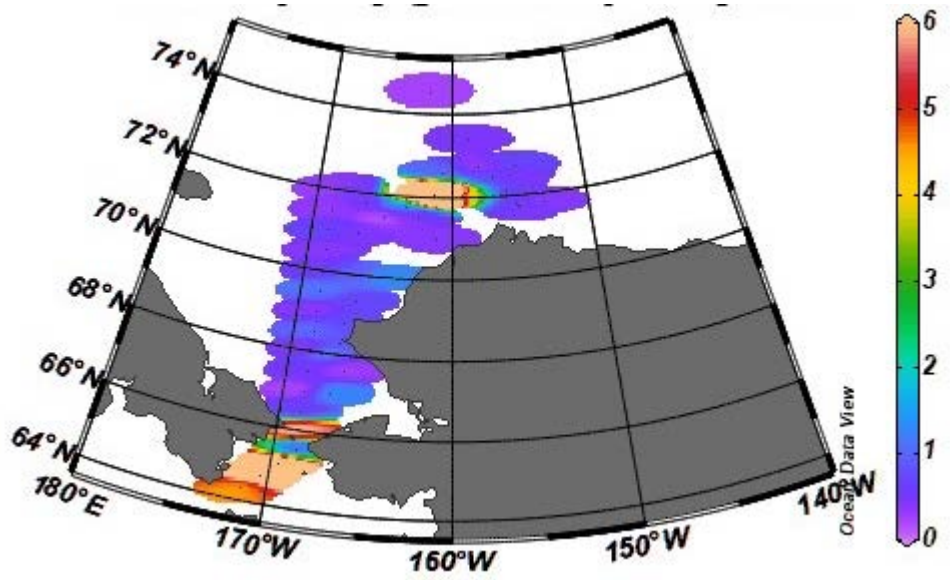

Figure 4.6-4: Chl-*a* maximum layer distributions of total chl-*a* in the Arctic Ocean.

At some station, water samples were taken in replicate for water of chlorophyll *a*

maximum layer. Results of replicate samples were shown in table 4.6-1.

Table 4.6-1: Results of the replicate sample measurements.

Number of replicate sample pairs	Standard deviation (μgL^{-1})	Relative error (%)
46	0.077	4.7

(7) Data archives

These data obtained in this cruise will be submitted to the Data Management Group of JAMSTEC, and will be opened to the public via "Data Research System for Whole Cruise Information in JAMSTEC (DARWIN)" in JAMSTEC web site (http://www.godac.jamstec.go.jp/darwin/e).

4.7. Methane/DMS/DMSP/$\delta^{18}O$

(1) Personnel

Daiki Nomura (Hokkaido University) – Principal investigator
Manami Tozawa (Hokkaido University)
Sohiko Kameyama (Hokkaido University) –Not on board

(2) Objective

In order to understand the greenhouse and climate active gasses in the Arctic Ocean and their exchange process with atmosphere, we have collected water samples from the multiple depths during cruise. The water samples for oxygen isotopic ratio were also collected to understand the freshwater origin in our sampling area in the summer season.

(3) Parameters

・Methane (CH_4)
・DMS
・DMSP (DMSPt, DMSPd)
・Oxygen isotopic ratio ($\delta^{18}O$)

(4) Instruments and methods

Water samples for each station (Table 4.7-1) were collected at multiple depths using 12-L Niskin bottles mounted on a CTD system.

(4-1) Methane

For each sample, an aliquot of 100-mL seawater was transferred from the Niskin bottles to an amber vial (100 mL). The vial was filled smoothly from the bottom with seawater using a drawing tube that extended from the Niskin drain to the bottom of the vial. The seawater was allowed to overflow by an amount of approximately one and a half times the vial volume. After sampling, 0.1-mL saturated mercuric chloride was added to poison the sample. Then, the vial was crimp-sealed with a butyl-rubber stopper and aluminum cap.

The samples were stored at +4°C in the dark onboard the R/V Mirai, and transported chilled to laboratories on land for analysis. The samples will be measured using gas chromatography-flame ionization detector (GC-FID) with equilibrium headspace extraction in Hokkaido University, Japan.

(4-2) DMS

For each sample, an aliquot of 30-mL seawater was transferred from the Niskin bottles to an amber vial (30 mL). The vial was filled smoothly from the bottom with seawater using a tube with GF/F filter that extended from the Niskin drain to the bottom of the

vial. Then, the vial was crimp-sealed with a butyl-rubber stopper and aluminum cap.

The samples were stored at +4°C in the dark onboard by analysis and measured using VOC extraction system and gas chromatography-flame photometric detector (GC-FPD) on board.

(4-3) DMSP

We corrected water samples for total DMSP (DMSPt) and dissolved DMSP (DMSPd). Both samples were transferred from the Niskin bottles to an amber vial (30 mL). The vial was filled smoothly from the bottom with seawater using a drawing tube that extended from the Niskin drain to the bottom of the vial. The seawater was allowed to overflow by an amount of approximately two times the vial volume.

The sample for DMSPt was prepared in 8-ml aliquots and 1 ml of hydrochloric acid was added. The sample for DMSPd was filtered about 4 ml through a GF/F filter and 0.5 ml of hydrochloric acid was added. Then, both vials were crimp-sealed with a butyl-rubber stopper and aluminum cap. Samples were stored at room temperature and brought back to the laboratory for analysis.

(4-4) Oxygen isotopic ratio

Seawater samples for measurement of $\delta^{18}O$ were placed in 15-mL glass screw-cap vials with a minimum volume of air. Samples were stored at +4°C in the dark and brought back to the laboratory for analysis.

Table 4.7-1: Station list

	Date	Latitude	Longitude	CH_4	DMS	DMSP	$\delta^{18}O$
St.3	2021/9/12	71°40.61"N	154°57.61"W	○	○	○	○
St.10	2021/9/14	72°28.49"N	155°35.14"W	–	–	–	○
St.11	2021/9/15	74°31.52"N	161°55.17"W	○	–	–	○
St.14	2021/9/17	72°35.9"N	160°49.95"W	○	○	○	○
St.17	2021/9/18	73°23.87"N	158°42.83"W	○	○	○	○
St.19	2021/9/19	72°43.37"N	155°7.91"W	–	–	–	○
St.22	2021/9/20	72°27.56"N	156°59.39"W	○	○	○	○
St.24	2021/9/21	72°3.26"N	161°22.6"W	–	–	–	○
St.28	2021/9/22	71°45.13"N	163°23.57"W	○	○	○	○
St.31	2021/9/23	72°3.92"N	167°54.2"W	○	○	○	○

St.33	2021/9/24	71°0"N	166°38.73"W	−	○	○	○
St.35	2021/9/25	70°29.97"N	168°44.98"W	○	○	○	○
St.38	2021/9/27	70°0.01"N	164°27.88"W	○	○	○	○
St.42	2021/9/28	69°0.03"N	168°45.17"W	−	○	○	○
St.45	2021/9/29	68°2.01"N	168°49.9"W	○	○	○	○
St.46	2021/9/29	67°30.01"N	168°44.67"W	○	○	○	○
St.49	2021/9/30	68°0.05"N	168°0.17"W	○	○	○	○
St.53	2021/9/30	68°18.11"N	167°3.38"W	○	○	○	○
St.54	2021/9/30	67°36.08"N	166°30.04"W	○			○
St.60	2021/10/2	65°5.68"N	169°31.12"W				○
St.62	2021/10/3	64°18.92"N	171°18.2"W	○	○	○	○

(5) Data archives

These data obtained in this cruise will be submitted to the Data Management Group of JAMSTEC, and will be opened to the public via "Data Research System for Whole Cruise Information in JAMSTEC (DARWIN)" in JAMSTEC web site.

http://www.godac.jamstec.go.jp/darwin/e.

4.8. ^{129}I

(1) Personnel

Yuichiro Kumamoto (JAMSTEC): Principal investigator

(2) Objective

Determination of concentrations of ^{129}I in the Arctic Ocean, Bering Sea, and northern North Pacific Ocean.

(3) Parameters

^{129}I

(4) Instruments and Methods

a. Sampling

Seawater samples for ^{129}I were collected using 12-liter PVC bottles. Surface seawater was collected from continuous pumped-up water at about 4-m depth or using a bucket. The seawater sample was collected into a 1-L plastic bottle after two-time rinsing.

b. Preparation and analysis

Iodine in the seawater samples is extracted by the solvent extraction technique. Extracted iodine is then precipitated as silver iodide by the addition of the silver nitrate. Iodine isotopic ratios ($^{129}I/^{127}I$) of the silver iodide are measured by the Accelerator Mass Spectrometry (AMS). To evaluate the ^{129}I concentration in the seawater samples, iodine concentration (^{127}I) will be measured by the inductively coupled plasma mass spectrometry (ICP-MS) and/or the voltammetry.

(5) Sample list

We collected 60 seawater samples for ^{129}I measurements in the Arctic Ocean, Bering Sea, and northern North Pacific Ocean during this cruise (Table 4.8-1).

(6) Data archives

These data obtained in this cruise will be submitted to the Data Management Group of JAMSTEC, and will be opened to the public via "Data Research System for Whole Cruise Information in JAMSTEC (DARWIN)" in JAMSTEC web site.

http://www.godac.jamstec.go.jp/darwin/e

Table 4.8-1: Seawater samples collected for PAHs measurement.

No.	Station	Depth (m)	Method	Latitude	Longitude	Date (UTC)
1	surface-1	4	pump	50-03.46N	166-03.42E	2021/9/5
2	surface-2	4	pump	53-05.82N	170-14.36E	2021/9/5
3	surface-3	4	pump	57-00.02N	175-56.00E	2021/9/6
4	surface-4	4	pump	60-00.10N	179-11.58W	2021/9/7
5	surface-5	4	pump	62-02.19N	175-38.34W	2021/9/8
6	surface-6	4	pump	64-30.08N	170-31.54W	2021/9/8
7	surface-7	4	pump	66-48.28N	168-22.49W	2021/9/9
8	surface-8	4	pump	69-59.93N	166-59.12W	2021/9/9
9	surface-9	4	pump	72-28.41N	155-29.93W	2021/9/14
10	surface-10	4	pump	74-31.66N	161-57.55W	2021/9/16
11	surface-11	4	pump	71-48.57N	153-15.54W	2021/9/20
12	surface-12	4	pump	72-03.42N	161-23.06W	2021/9/21
13	surface-13	4	pump	72-00.08N	168-41.40W	2021/9/23
14	surface-14	4	pump	60-12.71N	168-23.64W	2021/10/4
15	surface-15	4	pump	57-56.08N	167-18.24W	2021/10/4
16	surface-16	4	pump	54-21.77N	167-31.74W	2021/10/6
17	surface-17	4	pump	53-24.18N	177-43.14W	2021/10/8
18	surface-18	4	pump	45-19.10N	159-24.14E	2021/10/13
19	10	4.6	niskin	72-28.49N	155-35.16W	2021/9/14
20	10	19.5	niskin	72-28.49N	155-35.16W	2021/9/14
21	10	49.4	niskin	72-28.49N	155-35.16W	2021/9/14
22	10	98.8	niskin	72-28.49N	155-35.16W	2021/9/14
23	10	148.2	niskin	72-28.49N	155-35.16W	2021/9/14
24	10	197.5	niskin	72-28.49N	155-35.16W	2021/9/14
25	10	246.9	niskin	72-28.49N	155-35.16W	2021/9/14
26	10	296.2	niskin	72-28.49N	155-35.16W	2021/9/14
27	10	395.6	niskin	72-28.49N	155-35.16W	2021/9/14
28	10	593.3	niskin	72-28.49N	155-35.16W	2021/9/14
29	10	789.9	niskin	72-28.49N	155-35.16W	2021/9/14
30	10	986.0	niskin	72-28.49N	155-35.16W	2021/9/14
31	10	1477.5	niskin	72-28.49N	155-35.16W	2021/9/14
32	10	1820.9	niskin	72-28.49N	155-35.16W	2021/9/14
33	11 (NAP)	4.9	niskin	74-31.52N	161-55.17W	2021/9/15
34	11 (NAP)	19.7	niskin	74-31.52N	161-55.17W	2021/9/15
35	11 (NAP)	49.6	niskin	74-31.52N	161-55.17W	2021/9/15
36	11 (NAP)	98.9	niskin	74-31.52N	161-55.17W	2021/9/15

Table 4.8-1: continued.

No.	Station	Depth (m)	Method	Latitude	Longitude	Date (UTC)
37	11 (NAP)	148.3	niskin	74-31.52N	161-55.17W	2021/9/15
38	11 (NAP)	197.5	niskin	74-31.52N	161-55.17W	2021/9/15
39	11 (NAP)	246.9	niskin	74-31.52N	161-55.17W	2021/9/15
40	11 (NAP)	296.3	niskin	74-31.52N	161-55.17W	2021/9/15
41	11 (NAP)	394.8	niskin	74-31.52N	161-55.17W	2021/9/15
42	11 (NAP)	593.2	niskin	74-31.52N	161-55.17W	2021/9/15
43	11 (NAP)	789.6	niskin	74-31.52N	161-55.17W	2021/9/15
44	11 (NAP)	986.7	niskin	74-31.52N	161-55.17W	2021/9/15

45	11 (NAP)	1480.1	niskin	74-31.52N	161-55.17W	2021/9/15
46	11 (NAP)	1675.5	niskin	74-31.52N	161-55.17W	2021/9/15
47	20	0	bucket	71-48.46N	153-14.95W	2021/9/20
48	20	20.0	niskin	71-48.46N	153-14.95W	2021/9/20
49	20	49.4	niskin	71-48.46N	153-14.95W	2021/9/20
50	20	99.0	niskin	71-48.46N	153-14.95W	2021/9/20
51	20	148.5	niskin	71-48.46N	153-14.95W	2021/9/20
52	20	198	niskin	71-48.46N	153-14.95W	2021/9/20
53	20	216.8	niskin	71-48.46N	153-14.95W	2021/9/20
54	38	5.1	niskin	70-00.00N	164-27.88W	2021/9/27
55	38	19.9	niskin	70-00.00N	164-27.88W	2021/9/27
56	38	30.9	niskin	70-00.00N	164-27.88W	2021/9/27
57	45	5.1	niskin	68-02.01N	168-49.90W	2021/9/29
58	45	10.1	niskin	68-02.01N	168-49.90W	2021/9/29
59	45	29.5	niskin	68-02.01N	168-49.90W	2021/9/29
60	45	49.4	niskin	68-02.01N	168-49.90W	2021/9/29

4.9. Polycyclic Aromatic Hydrocarbons (PAHs)

(1) Personnel
Yuichiro Kumamoto (JAMSTEC): Principal investigator

(2) Objective
Determination of polycyclic aromatic hydrocarbons (PAHs) concentration in surface seawater in the Arctic Ocean, Bering Sea, and northern North Pacific Ocean.

(3) Parameter
Polycyclic Aromatic Hydrocarbons (PAHs)

(4) Instruments and Methods
a. Sampling
Surface seawater samples were collected from continuous pumped-up water from about 4-m depth. The sample volumes for PAHs are 10 L (a 10-L stainless container). Just after the water sampling, 300 ml of methanol was added.

b. Preparation and analysis
Particulate and dissolved phases of 10 L seawater sample are separated by filtration through 0.5 μm glass-fiber filters. Dissolved organic compounds, including PAHs, are concentrated using C18 solid-phase extraction disks. Particulate and dissolved PAHs are respectively extracted from the glass-fiber filters using an ultrasonic method and eluted from the C18 disks with dichloromethane. Dimethyl sulfoxide is added to both extracted solutions, the dichloromethane is evaporated to dryness, and the residue of dimethyl sulfoxide is dissolved in acetonitrile. PAHs in the samples were quantified using the HPLC system with a fluorescence detector.

(5) Sample list
We collected 18 samples for PAHs measurement in the Arctic Ocean, Bering Sea, and northern North Pacific Ocean during this cruise (Table 4.9-1).

(6) Data archives
These data obtained in this cruise will be submitted to the Data Management Group of JAMSTEC, and will be opened to the public via “Data Research System for Whole Cruise Information in JAMSTEC (DARWIN)” in JAMSTEC web site.
http://www.godac.jamstec.go.jp/darwin/e

Table 4.9-1: Seawater samples collected for PAHs measurement.

No.	Station	Depth (m)	Method	Latitude	Longitude	Date (UTC)
1	surface-1	4	pump	50-03.46N	166-03.42E	2021/9/5
2	surface-2	4	pump	53-05.82N	170-14.36E	2021/9/5
3	surface-3	4	pump	57-00.02N	175-56.00E	2021/9/6
4	surface-4	4	pump	60-00.10N	179-11.58W	2021/9/7
5	surface-5	4	pump	62-02.19N	175-38.34W	2021/9/8
6	surface-6	4	pump	64-30.08N	170-31.54W	2021/9/8
7	surface-7	4	pump	66-48.28N	168-22.49W	2021/9/9
8	surface-8	4	pump	69-59.93N	166-59.12W	2021/9/9
9	surface-9	4	pump	72-28.41N	155-29.93W	2021/9/14
10	surface-10	4	pump	74-31.66N	161-57.55W	2021/9/16
11	surface-11	4	pump	71-48.57N	153-15.54W	2021/9/20
12	surface-12	4	pump	72-03.42N	161-23.06W	2021/9/21
13	surface-13	4	pump	72-00.08N	168-41.40W	2021/9/23
14	surface-14	4	pump	60-12.71N	168-23.64W	2021/10/4
15	surface-15	4	pump	57-56.08N	167-18.24W	2021/10/4
16	surface-16	4	pump	54-21.77N	167-31.74W	2021/10/6
17	surface-17	4	pump	53-24.18N	177-43.14W	2021/10/8
18	surface-18	4	pump	45-19.10N	159-24.14E	2021/10/13

4.10. Underway surface water monitoring

4.10.1 Basic biogeochemical analyses

(1) Personnel

Amane Fujiwara (JAMSTEC): Principal Investigator
Misato Kuwahara(MWJ) : Operation leader
Hiroaki Sako (MWJ)
Shintaro Amikura (MWJ)

(2) Objective

Our purpose is to obtain temperature, salinity, dissolved oxygen, fluorescence, turbidity, refractive index density and total dissolved gas pressure data continuously in near-sea surface water.

(3) Parameters

Temperature
Salinity
Dissolved oxygen
Fluorescence
Turbidity
Total dissolved gas pressure
Refractive index density

(4) Instruments and Methods

The Continuous Sea Surface Water Monitoring System (Marine Works Japan Co. Ltd.) has six sensors and automatically measures temperature, salinity, dissolved oxygen, fluorescence, turbidity, total dissolved gas pressure and refractive index density in near-sea surface water every one minute. This system is located in the "sea surface monitoring laboratory" and connected to shipboard LAN-system. Measured data, time, and location of the ship were stored in a data management PC. Sea water was continuously pumped up to the laboratory from an intake placed at the approximately 4.5 m below the sea surface and flowed into the system through a vinyl-chloride pipe. The flow rate of the surface seawater was adjusted to 10 dm^3 min^{-1}.

a. Instruments

Software

Seamoni Ver.1.2.0

Sensors

Specifications of the each sensor in this system are listed below.

Temperature and Conductivity sensor

Model: SBE-45, SEA-BIRD ELECTRONICS, INC.

Serial number: 4563325-0362

Measurement range: Temperature -5 °C - +35 °C

Conductivity 0 S m^{-1} - 7 S m^{-1}

Initial accuracy: Temperature 0.002 °C

Conductivity 0.0003 S m^{-1}

Typical stability (per month): Temperature 0.0002 °C

Conductivity 0.0003 S m^{-1}

Resolution: Temperature 0.0001 °C

Conductivity 0.00001 S m^{-1}

Bottom of ship thermometer

Model: SBE 38, SEA-BIRD ELECTRONICS, INC.

Serial number: 3857820-0540

Measurement range: -5 °C - +35 °C

Initial accuracy: ±0.001 °C

Typical stability (per 6 month): 0.001 °C

Resolution: 0.00025 °C

Dissolved oxygen sensor

Model: RINKO II, JFE ADVANTECH CO. LTD.

Serial number: 0013

Measuring range: 0 mg L^{-1} - 20 mg L^{-1}

Resolution: 0.001 mg L^{-1} - 0.004 mg L^{-1} (25 °C)

Accuracy: Saturation ± 2 % F.S. (non-linear) (1 atm, 25 °C)

Fluorescence & Turbidity sensor

Model: C3, TURNER DESIGNS

Serial number: 2300707

Measuring range: Chlorophyll in vivo 0 µg L^{-1} – 500 µg L^{-1}
Minimum Detection Limit: Chlorophyll in vivo 0.03 µg L^{-1}
Measuring range: Turbidity 0 NTU - 1500 NTU
Minimum Detection Limit: Turbidity 0.05 NTU

Total dissolved gas pressure sensor
Model: HGTD-Pro, PRO OCEANUS
Serial number: 36-296-10
Temperature range: -2 °C - 50 °C
Resolution: 0.0001 %
Accuracy: 0.01 % (Temperature Compensated)
Sensor Drift: 0.02 % per year max (0.001 % typical)

Refractive index density
Model: Prototype 1, JAMSTEC (Uchida et al. 2019)
Serial number: 4D020050 (SI-F80SO [55095])

(5) Observation log

Periods of measurement, maintenance, and problems during this cruise are listed in Table 4.10.1-1.

Table 4.10.1-1: Events list of the Sea surface water monitoring during MR21-05C

System Date [UTC]	System Time [UTC]	Events	Remarks
2021/09/01	00:19	Start data logging	
2021/09/07	00:13-00:18	Filter Cleaning.	-
2021/09/11	18:47-19:12	Filter Cleaning.	-
2021/09/17	14:46-16:09	All the measurements stopped.	Software Maintenance
2021/09/22	06:22-06:32	Filter Cleaning.	-
2021/09/22	06:40-06:47	All the measurements stopped.	Software Maintenance
2021/10/04 2021/10/06	23:01 - 22:06	All the measurements stopped.	Pump stopped
2021/10/18	00:00	End data logging	

We took the surface water samples from this system once a day to compare sensor data with bottle data of salinity, dissolved oxygen, and chlorophyll a. The results are shown in fig. 4.10.1-2. All the salinity samples were analyzed by the Model 8400B "AUTOSAL" manufactured by Guildline Instruments Ltd. (see 3.13), and dissolve oxygen samples were analyzed by Winkler method (see 4.1), chlorophyll *a* were analyzed by 10-AU manufactured by Turner Designs. (see 4.6).

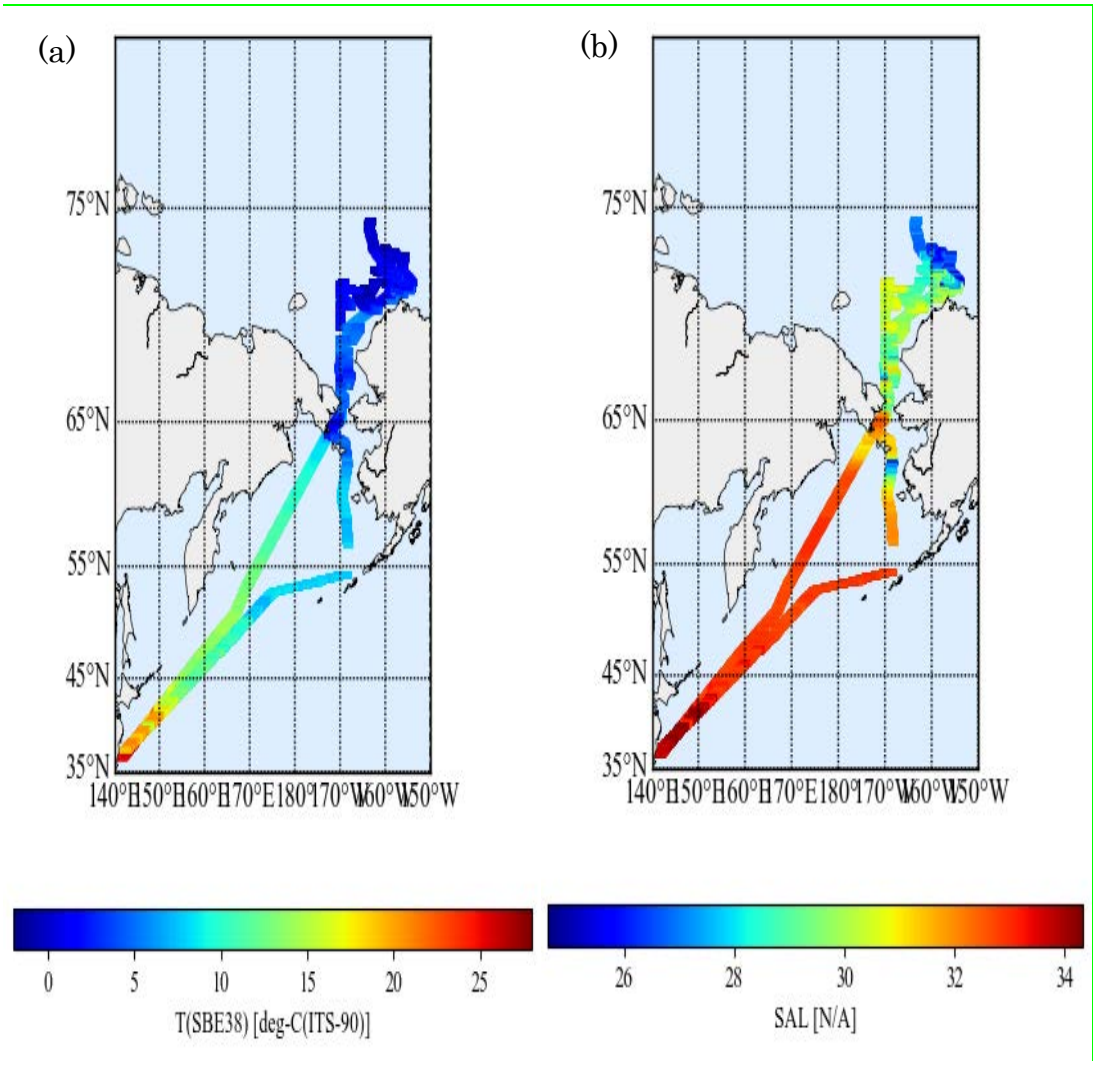

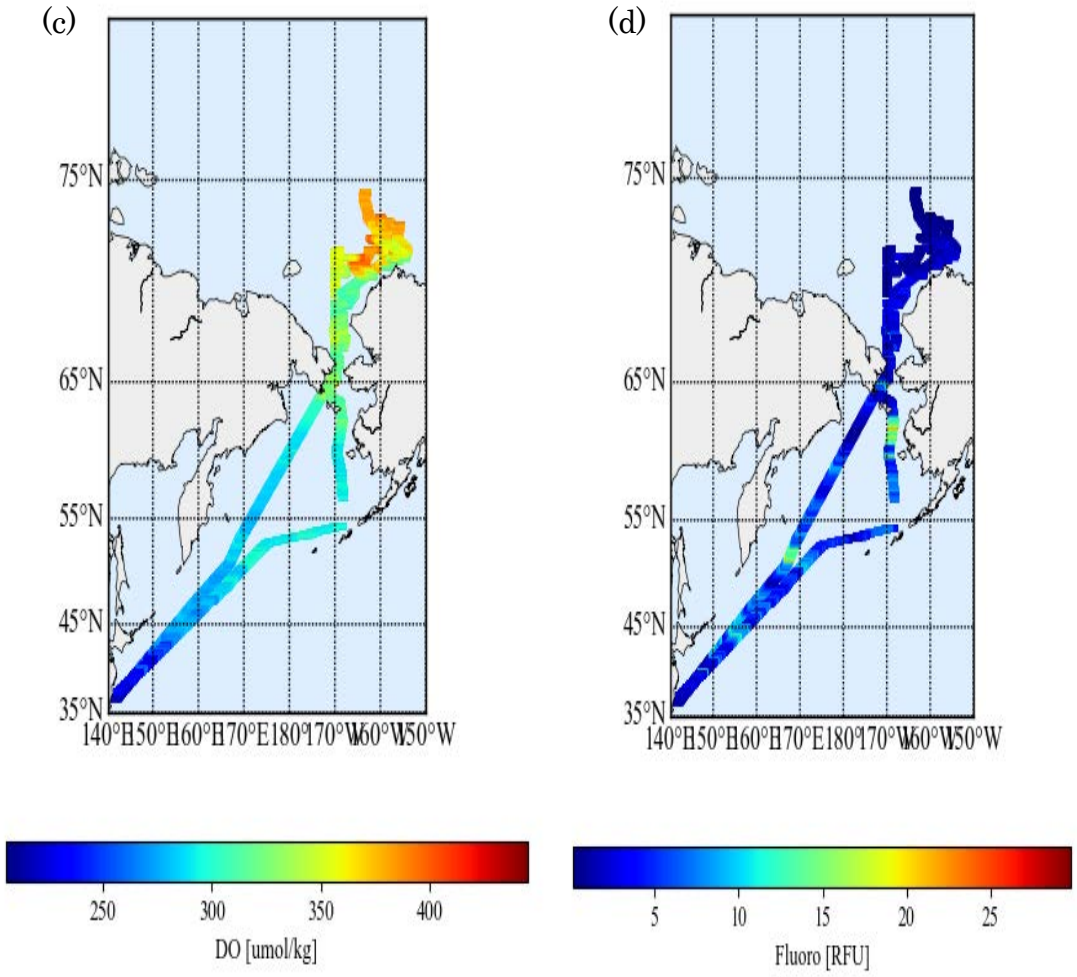

Figure 4.10.1-1: Spatial and temporal distribution of (a) temperature, (b) salinity, (c) dissolved oxygen, and (d) fluorescence in MR21-05C cruise.

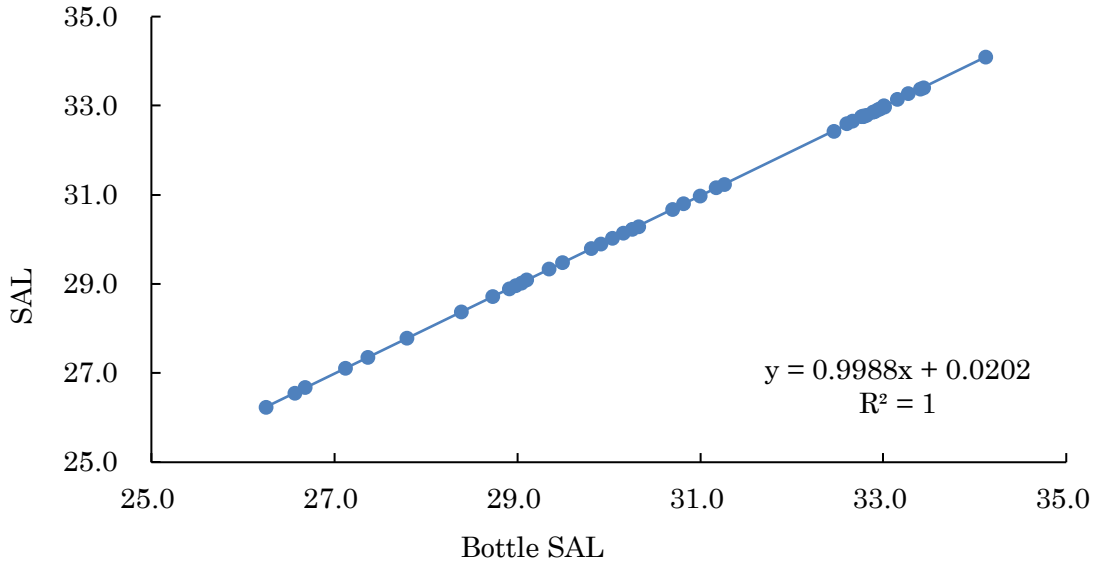

Figure 4.10.1-1: Correlation of salinity between sensor data and bottle data.

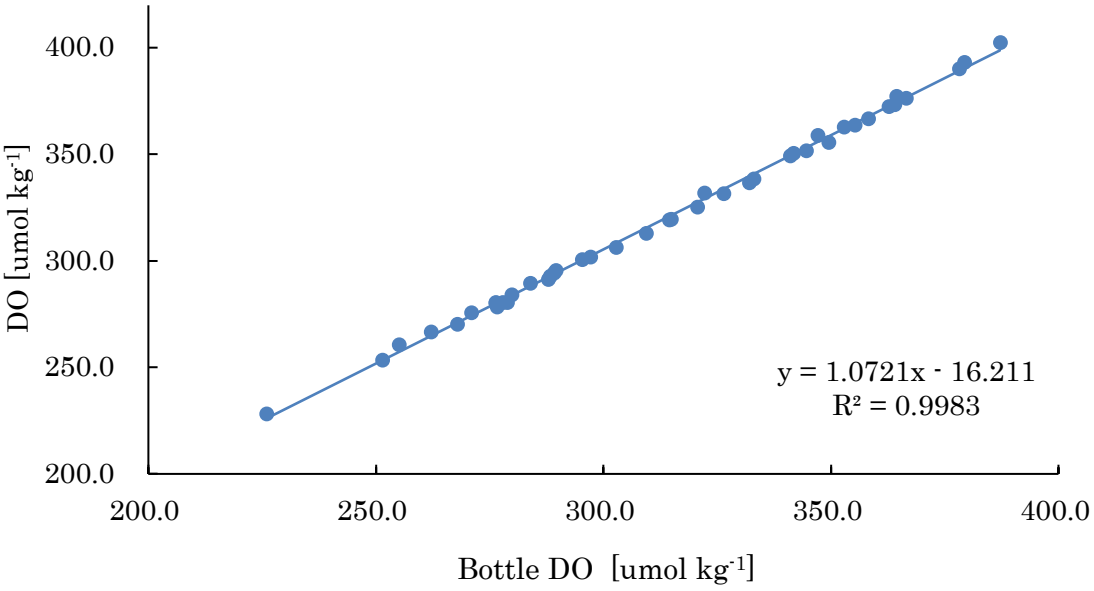

Figure 4.10.1-2: Correlation of dissolved oxygen between sensor data and bottle data.

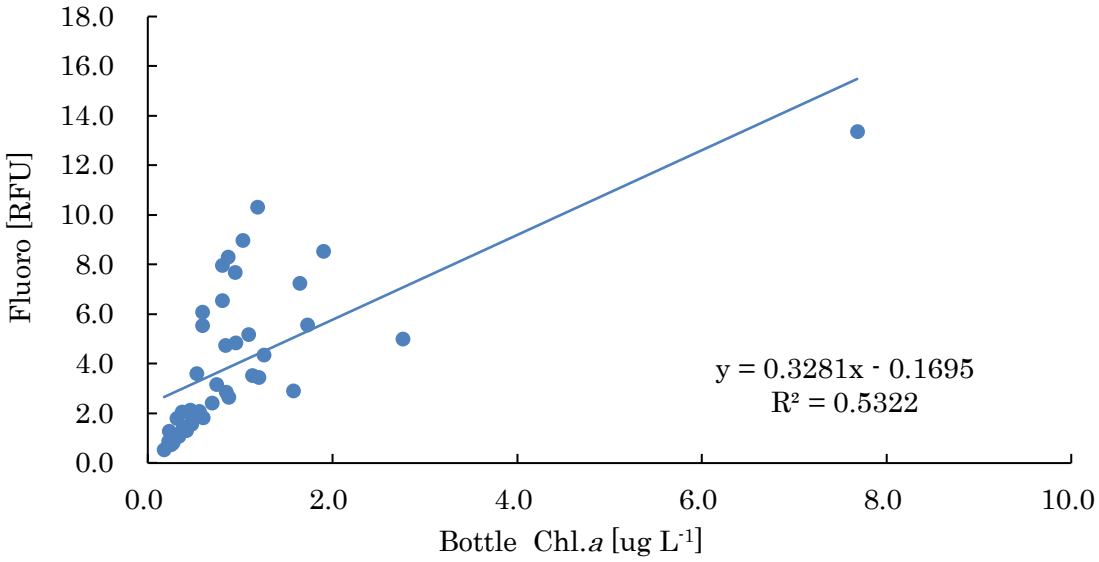

Figure 4.10.1-3: Correlation of fluorescence between sensor data and bottle data.

(6) Data archives

These data obtained in this cruise will be submitted to the Data Management Group (DMG) of JAMSTEC, and will opened to the public via "Data Research System for Whole Cruise Information in JAMSTEC (DARWIN)" in JAMSTEC web site.
<http://www.godac.jamstec.go.jp/darwin/e>

4.10.2. Discrete water samplings

(1) Personnel

Manami Tozawa (Hokkaido University) -Principal investigator
Mariko Hatta (JAMSTEC)
Daiki Nomura (Hokkaido University)
Kohei Matsuno (Hokkaido University)
Wakana Endo (Hokkaido University)
Tatsuya Kawakami (Hokkaido University)
Makoto Ozaki (Hokkaido University)
Amane Fujiwara (JAMSTEC)

(2) Objective

The exchange of biogeochemical components with the atmosphere occurs at the ocean surface. Furthermore, meltwater and river water flow into the ocean surface, which greatly affects the chemical composition and biological activities. By clarifying what proportion of seawater/sea ice melt/glacial meltwater/river water is mixed, we can evaluate how each of them affects the other. For this purpose, we measured the stable oxygen isotopic ratio ($\delta^{18}O$). We also collected samples for nutrients, eDNA, plankton samples, CDOM, and HPLC in conjunction with the timing of these water samples (See each chapter for details).

(3) Parameters

・Methane (CH_4)
・DMS
・DMS/P (DMS/Pt, DMS/Pd)
・Oxygen isotopic ratio ($\delta^{18}O$)
・Nutrients
・CDOM
・HPLC
・eDNA
・Phytoplankton

(4) Instruments and methods

See 4.2, 4.7, 4.15-17

Sampling list

sampling time	Latitude	Longitude	CH_4	DMS/P	$\delta^{18}O$	Nuts	CDOM	HPLC

2021/9/4 6:38	47°1.59"N	160°2.87"E				○		
2021/9/5 4:40	49°55.63"N	165°46.82"E				○		
2021/9/6 2:15	53°44.07"N	171°4.56"E	○		○	○		○
2021/9/7 3:30	58°13.27"N	177°52.69"E	○		○	○		○
2021/9/8 2:30	62°15.82"N	175°13.35"W	○		○	○	○	○
2021/9/8 19:32	65°5.05"N	168°55.61"W			○	○		
2021/9/9 1:30	66°26.31"N	168°22.9"W	○		○	○	○	○
2021/9/9 17:31	70°2.79"N	166°43.29"W			○	○		
2021/9/10 1:45	70°51.73"N	161°55.79"W	○		○	○	○	○
2021/9/10 17:31	71°40.46"N	154°59.51"W			○	○		
2021/9/11 1:30	71°49.68"N	155°29.46"W	○		○	○	○	○
2021/9/11 17:29	71°42.82"N	155°21.66"W			○	○		
2021/9/12 1:30	71°44.86"N	155°36.77"W	○	○	○	○	○	○
2021/9/12 10:23	71°35.66"N	155°45.63"W			○	○		
2021/9/12 16:29	71°35.49"N	154°47.2"W	○		○	○	○	
2021/9/12 22:30	71°42.72"N	154°48.67"W			○	○		
2021/9/13 2:00	71°44.43"N	155°7.36"W	○		○	○	○	○
2021/9/13 8:53	71°49.49"N	155°46.55"W			○	○		
2021/9/13 16:09	72°6.16"N	155°54.68"W			○	○		
2021/9/13 22:31	72°11.66"N	155°49.12"W			○	○		
2021/9/14 6:30	72°25.12"N	155°19.97"W	○	○	○	○	○	○
2021/9/14 9:18	72°24.68"N	155°24.25"W			○	○		
2021/9/14 17:43	72°26.59"N	155°30.92"W			○	○		
2021/9/14 22:48	72°28.31"N	155°30.94"W			○	○		
2021/9/15 1:30	72°31.51"N	156°40.98"W	○		○	○	○	○
2021/9/15 5:10	72°53.3"N	159°11.93"W			○	○		
2021/9/15 8:15	73°23.43"N	160°52.37"W			○	○		
2021/9/15 12:00	74°1.36"N	162°2.48"W			○	○		
2021/9/15 17:32	74°31.12"N	161°54.81"W			○	○		
2021/9/15 21:42	74°31.86"N	161°58.14"W			○	○		
2021/9/16 3:45	74°31.47"N	162°2.63"W	○		○	○	○	○
2021/9/16 10:00	74°31.29"N	162°1.76"W			○	○		

2021/9/16 17:29	74°31.42"N	161°55.67"W			○	○		
2021/9/16 23:15	74°29.14"N	162°2.25"W			○	○		
2021/9/17 1:45	74°1.87"N	161°54.34"W	○	○	○	○	○	○
2021/9/17 4:49	73°26.07"N	161°19.79"W			○	○		
2021/9/17 8:15	73°0.27"N	159°35.5"W		○	○	○	○	
2021/9/17 12:15	72°27.37"N	159°39.94"W		○	○	○		
2021/9/17 15:09	72°32.42"N	160°19.24"W			○	○		
2021/9/17 23:26	72°34.87"N	160°5.44"W			○	○		
2021/9/18 1:30	72°32.33"N	158°44.65"W	○		○	○	○	○
2021/9/18 7:37	72°58.93"N	157°22.29"W			○	○		
2021/9/18 10:01	73°17.82"N	156°48.33"W			○	○		
2021/9/18 16:39	73°25.6"N	158°45.01"W			○	○		
2021/9/19 4:45	73°13.56"N	156°43.7"W	○		○	○	○	○
2021/9/19 8:30	73°9.73"N	154°41.48"W			○	○		
2021/9/19 17:46	72°43.36"N	155°7.98"W			○	○		
2021/9/20 1:45	72°23.36"N	154°20.43"W	○	○	○	○	○	○
2021/9/20 4:48	72°0.74"N	152°59.89"W			○	○		
2021/9/20 8:45	71°44.12"N	153°22.68"W			○	○		
2021/9/20 16:49	72°14.93"N	155°53.79"W			○	○		
2021/9/20 23:10	72°27.17"N	157°2.01"W			○	○		
2021/9/21 1:30	72°17.88"N	157°34.77"W	○		○	○	○	○
2021/9/21 9:00	72°2.15"N	160°20.37"W			○	○		
2021/9/21 18:19	72°3.4"N	161°23.29"W			○	○		
2021/9/22 1:30	71°14.3"N	162°2.41"W	○	○	○	○	○	○
2021/9/22 9:15	70°53.32"N	162°22.59"W			○	○		
2021/9/22 16:50	71°26.4"N	164°57.07"W			○	○		
2021/9/23 1:30	71°44.64"N	164°4.63"W	○		○	○	○	○
2021/9/23 7:30	71°43.02"N	166°51.99"W			○	○		
2021/9/23 18:09	72°0.1"N	168°43.91"W			○	○		
2021/9/24 1:30	71°48.69"N	168°19.53"W	○		○	○	○	○
2021/9/24 9:12	71°6.92"N	166°49.24"W			○	○		
2021/9/24 18:09	71°0.02"N	166°38.73"W			○	○		

2021/9/25 1:45	70°58.39"N	166°43.74"W	○		○	○	○	○
2021/9/25 9:20	71°6.15"N	168°23.96"W			○	○		
2021/9/25 16:10	71°0.17"N	168°43.64"W			○	○		
2021/9/26 1:30	69°59.92"N	168°43.92"W			○	○		
2021/9/26 9:00	69°59.24"N	166°34.92"W			○	○		
2021/9/26 17:00	70°0"N	166°40.08"W			○	○		
2021/9/27 1:30	70°0.15"N	166°17.62"W	○	○	○	○	○	○
2021/9/27 9:15	69°59.96"N	165°0.85"W			○	○		
2021/9/27 19:44	69°53.92"N	164°44.87"W			○	○		
2021/9/28 1:30	69°23.69"N	166°56.41"W			○	○		
2021/9/28 9:30	69°2.7"N	168°30.54"W			○	○		
2021/9/28 17:16	69°0.09"N	168°45.1"W			○	○		
2021/9/28 22:28	68°48.04"N	166°57.28"W			○	○		
2021/9/29 1:32	68°36.33"N	168°7.58"W	○		○	○	○	○
2021/9/29 1:44	68°35.23"N	168°14.07"W	○					
2021/9/29 9:00	68°21.3"N	168°35.24"W			○	○		
2021/9/29 17:12	68°2.06"N	168°49.97"W			○	○		
2021/9/30 0:10	67°45.12"N	168°29.85"W			○	○	○	
2021/9/30 1:16	67°52.54"N	168°14.76"W			○	○	○	
2021/9/30 2:38	68°0.08"N	168°0.27"W			○	○	○	
2021/9/30 4:12	68°6.02"N	167°40.25"W			○	○	○	
2021/9/30 5:30	68°12.12"N	167°20.3"W			○	○	○	
2021/9/30 6:18	68°15.1"N	167°12.5"W			○	○	○	
2021/9/30 10:57	67°39.55"N	166°53.18"W			○	○		
2021/9/30 17:42	67°36.1"N	166°30.01"W			○	○		
2021/10/1 1:30	67°0.22"N	168°24.49"W			○	○	○	○
2021/10/1 10:33	66°16.06"N	168°0.58"W			○	○		
2021/10/1 17:20	65°59.83"N	168°45.11"W			○	○		
2021/10/1 22:08	65°29.81"N	168°45.12"W			○	○		
2021/10/2 1:30	65°5.7"N	169°31.14"W	○		○	○	○	○
2021/10/2 8:55	64°30.82"N	170°52.11"W			○	○		
2021/10/2 18:07	64°18.92"N	171°18.22"W			○	○		

2021/10/2 22:17	64°9.91"N	170°24.96"W			○	○		
2021/10/3 1:30	63°57.45"N	169°4.62"W			○	○		
2021/10/3 5:27	63°34.29"N	167°43.04"W			○	○		
2021/10/3 17:00	63°24.41"N	167°38.51"W			○	○		
2021/10/3 21:36	60°38.04"N	168°11.06"W			○	○		
2021/10/4 1:30	60°4.81"N	168°20.8"W	○	○	○	○	○	○
2021/10/4 7:00	59°12.85"N	167°47.01"W			○	○		
2021/10/4 16:04	57°47.04"N	167°16.27"W			○	○		
2021/10/4 22:00	56°48.86"N	167°3.34"W	○	○	○	○	○	○
2021/10/7 0:30					○	○		○
2021/10/8 1:30					○	○		○
2021/10/9 2:30					○	○		○
2021/10/10 3:30					○	○		○

(5) Data archives

These data obtained in this cruise will be submitted to the Data Management Group of JAMSTEC, and will be opened to the public via "Data Research System for Whole Cruise Information in JAMSTEC (DARWIN)" in JAMSTEC web site. <http://www.godac.jamstec.go.jp/darwin/e>

4.10.3 Continuous silicate determination from the surface water pump system

(1) Personnel

Mariko Hatta JAMSTEC -PI

(2) Objectives

The goals of this study are following:

Establish the shipboard system using programmable flow injection system

Identify the water mass characteristics with Silicate data together with the data set obtained from the surface water monitoring system

(3) Parameters

Conductivity, Temperature, Depth, Turbidity, Chlorophyll, DO from a TSG system

Silicate (SiO_2) data obtained and determined using the programmable flow injection technique

Nutrient data from the discrete samples obtained from the surface pump system

Nutrient data at the station from the regular rosette system

The ranges and accuracies of parameters measured by the TSG are shown in the previous section.

Nutrients data from MWJ were reported in 4.2.

(4) Instruments and methods

(4.1.) Instrumentation

The instrument, miniSIA-2 (Global FIA, Fox Island, WA, USA), comprises two high precision, synchronously refilling milliGAT pumps, two thermostated holding coils, a 6-port LOV (model COV-MANI-6, constructed from polymethyl methacrylate, Perspex®) furnished with a module for an external flow cell (Figure 4.10.3-1). All tubing connections, downstream from the milliGAT pumps including the holding coils (volume 1000 µL), were made with 0.8 mm I.D. polytetrafluoroethylene (PTFE). The holding coils were thermostated at 50 ◦C for all silicate analysis. The tubing between the carrier stream reservoirs and the milliGAT pump was made from 1.6 mm I.D. PTFE tubing to minimize degassing under reduced pressure at higher aspiration flow rates. A spectrophotometer (Flame, Ocean Insight, Orlando, FL, USA) and a light source were connected to the flow cells by using optical fibers with 500-µm silica cores encased in 0.8 mm I.D. green PEEK tubing. The end of each fiber exposed to the liquid was cemented with epoxy, cut square, and polished. An Ocean Optics Tungsten Halogen (HL-2000, Ocean Insight, Orlando, FL, USA) light source was used. All assay steps were computer-controlled using commercially available software (FloZF, GlobalFIA, Fox island, WA, USA). The Linear Light Path (LLP) flow cell was purchased from Global FIA. The outlet of the LLP flow cell, was fitted with a 40-psi flow restrictor (GlobalFIA, Fox Island, WA, USA), which, by elevating the pressure within the flow path, efficiently prevented the formation of

microbubbles from spontaneous outgassing.

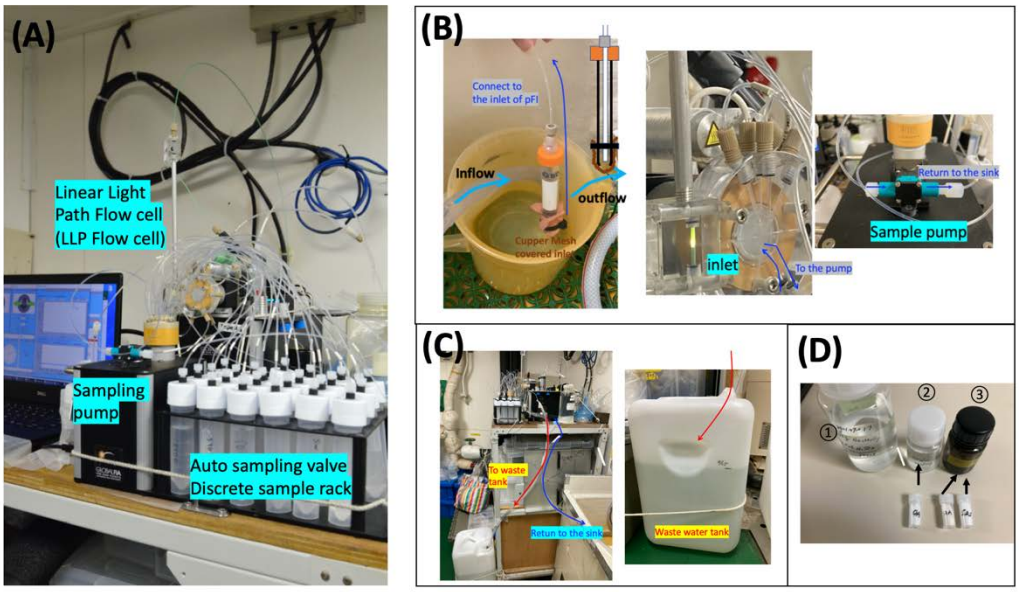

Figure 4.10.3-1: Shipboard analytical system for continuous silicate determination using the programmable flow injection technique. (A) the mini-SIA2 system and the autosampler. (B) Newly established sampling inlet. (C) The waste water drains system (D) Preparation for the reagents for the Silicate analysis during the cruise.

An inlet of the continuous sampling system was built during this MR21-05C cruise (Figure 4.10.3-1 B). The surface water sample were aspirating every 5 mins or 20 mins using the sample pump for 20 seconds and then homogenized the temperature adjust to the room temperature (25C) for 20 seconds. After the sample analysis, the flushed surface samples (not mixed with any reagent) were directly returned to the sink. The waste samples/reagents were drained into the waste tank to be stored until the end of the cruise.

(4.2) Analytical methodology

The detailed the methodology using programmable flow injection technique was published in Hatta et al., 2021. The detailed of each reagent and standards were made as follow:

Carrier solution: MilliQ water. Silicate stock standard containing 3.57 mM Si (10 ppm) was prepared by diluting a commercial 1000 ppm Si standard with 0.5 M HCl. This stock solution was further diluted, to obtain working standards (0 to 28 µM Si) in MilliQ water and sea water (SW). The silica solution had to be neutralized by HCl, because the silica standard is prepared in sodium hydroxide solution (pH12), which must be neutralized to match the pH of MilliQ and SW standard solutions. Using the auto-dilution step, the highest Si standard (28uM) was used and diluted with various aspiration volume to obtain the series of the standard solution while the solution was determined.

The acidified molybdate reagent was prepared by dissolving 6.85 g of sodium molybdate

in 500 mL of acidified MilliQ water (2.5 mL of conc. sulfuric acid was added). This solution was stable for 2 months.
The mixed solution of ascorbic acid and SDS solution was prepared by dissolving 3 g of L (+)-ascorbic acid in 100 mL of MilliQ water, and then 3 g of solid of ultrapure sodium dodecyl sulfate was added into this 3% ascorbic acid solution. Note that it is recommended to prepare this solution 30 min before use, in order to stabilize its reducing strength, as otherwise, the slope of calibration line with freshly prepared reagent will be up to 5% steeper than those obtained later. During the cruise, I prepared this solution one day before and stored in the dark container until it used.
The oxalic acid solution was prepared by dissolving 2 g of oxalic acid in 100 mL of MilliQ water. The solution was prepared one day before and then stored in a container until it used.
All of those reagents were top-upped if they needed.
Hatta et al., 2021. Programmable flow injection in batch mode: Determination of nutrients in sea water by using a single, salinity independent calibration line, obtained with standards prepared in distilled water, Talanta. https://doi.org/10.1016/j.talanta.2021.122354.
(5) Station list or Observation log
The surface samples for the continuous determination were collected every 5 mins or 20 mins during the cruise. The location and Si values were shown in Figure 4.10.3-2. Total 2480 samples were determined over 480 hours during this cruise.

(6) Preliminary results
The obtained Si data were shown in Figure 4.10.3-2. The data was taken every 20 mins or 5 mins. The detection limit of this method was <1uM (0.3uM) during the cruise. The preliminary results of the Si value showed great agreement of the Si value that collected at the station while the ship was stopped, and then determined by the shipboard air-segmented classical flow injection method (Figure 4.10.3-3).

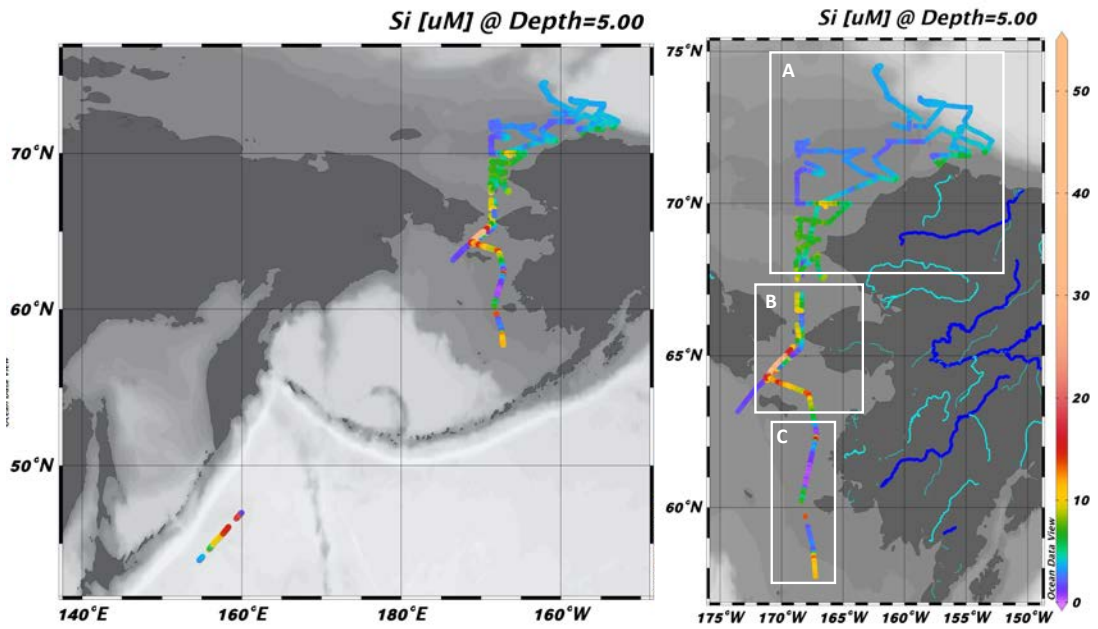

Figure 4.10.3-2: The surface silicate values that determined by pFI method during MR21-05C.

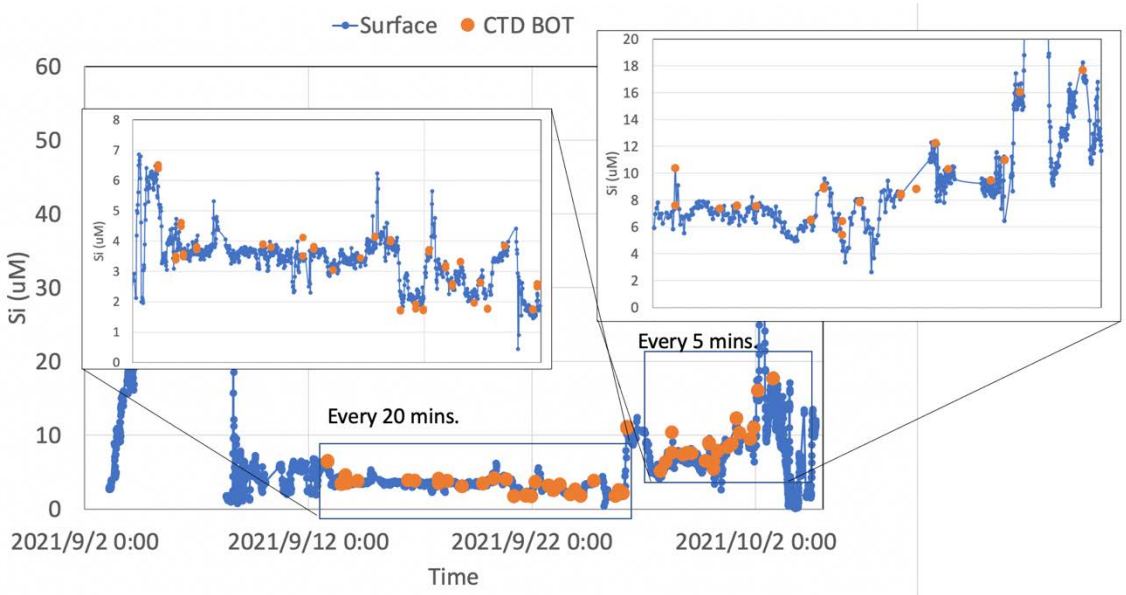

Figure 4.10.3-3: The surface Si values from pFI (blue) and Si value determined by MWJ at surface (bucket) and at 5-meter at the regular rosette sampling stations (orange).

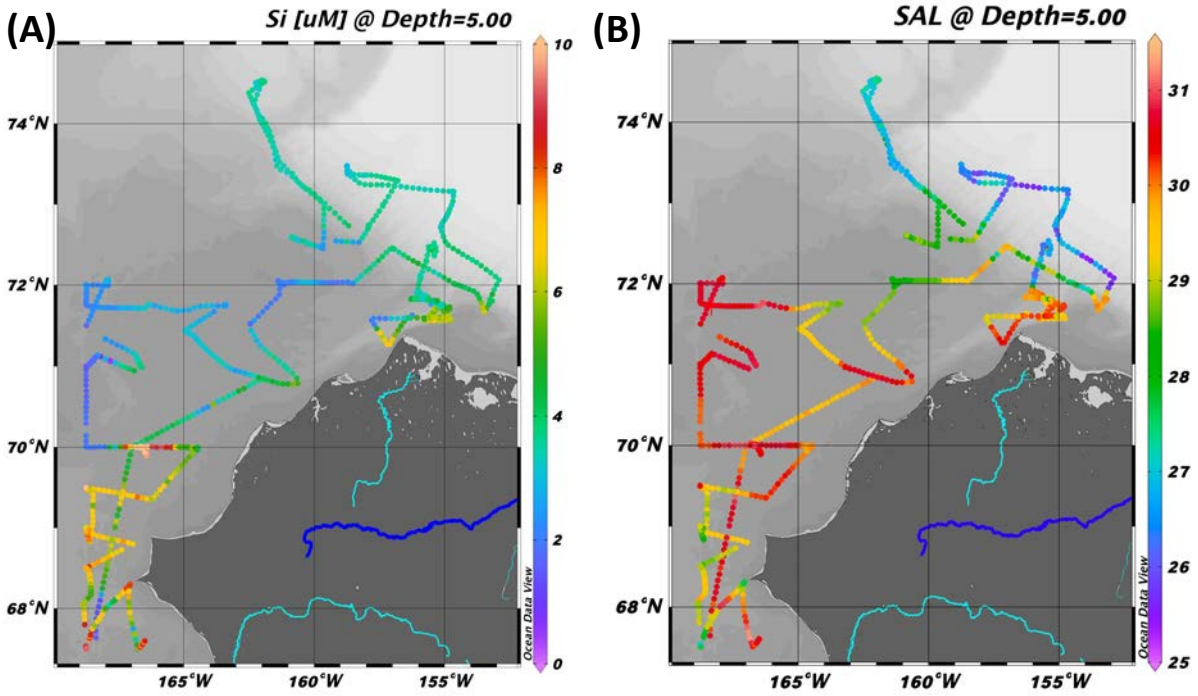

Figure 4.10.3-4: Surface Si values obtained by pFI method (A) and salinity data (B) in the Arctic Ocean during MR21-05C.

The low salinity value indicated that sea-ice melted water have spread in the offshore region (Figure 4.10.3-4). Those offshore surface Si value were ~4uM. The Si values in the sea-ice that we collected during this cruise (Nomura et al.) was 0-4uM, which could be the source or maintained the surface Si value in this region. In contrast, the wide range of the Si on the Chukchi shelf were seen with the significantly low value on the northside of the 168.5W line. Toward to the south of this line, the low salinity water was seen, which contains high Si. To understand the source of the water masses (sea-ice melt, Siberian coastal water, or riverine input?), the detailed discussion and the chemical analysis (e.g. delta-O) needs to be done. Note that this low salinity water wasn't observed on September 9th when RV Mirai came into the Arctic Ocean (Figure 4.10.3-5). There was the significantly high Si water (upto 50uM) were found at the south of the Bering strait, which was strongly influenced by the upwelled Anadyr waters. Those waters were shown with the lower water temperature and higher salinity (Figures 4.10.3-6 & 4.10.3-7). Since the fluorometer values were higher in this water, the upwelled nutrients were probably supported the productivity in this area.

The high Si value (~20uM) was also seen while the ship was passed near the Alaskan continent. The salinity values were dropped to 24psu, suggesting that there was the strong riverine input. Strong fluorometer signal suggests that the riverine input transported nutrients from the continent and probably supported the productivity in this area.

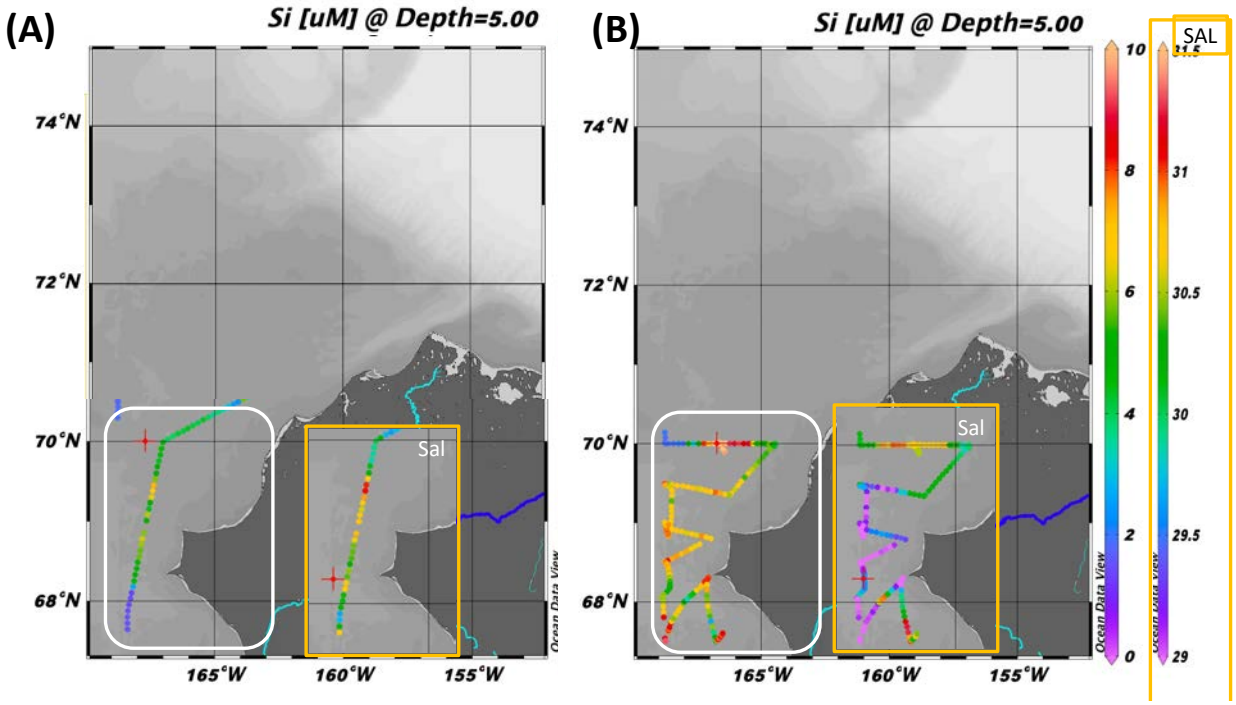

Figure 4.10.3-5: Surface Si and salinity values on (A) Sep 9 and (B) Sep 26-30th.

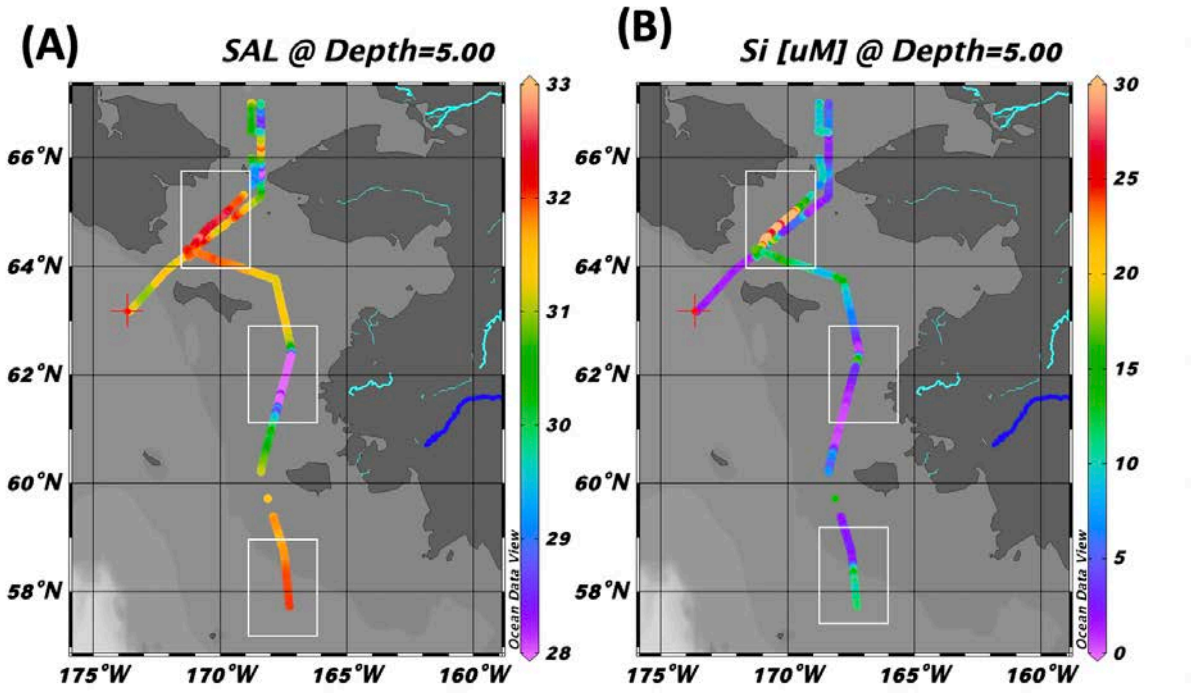

Figure 4.10.3-6: Surface salinity (A) and Si (B) values in the Bering Sea.

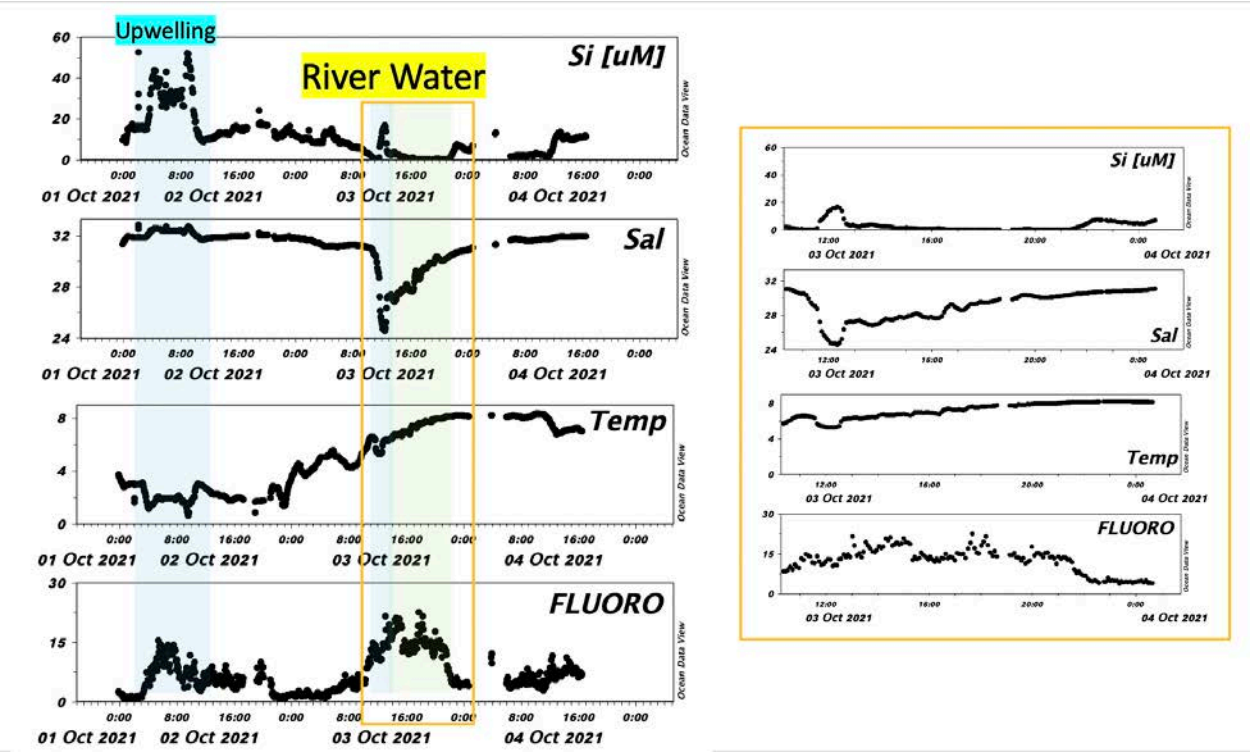

Figure 4.10.3-6: Surface Si, salinity, Temp, and Fluorometer values with time in the Bering Sea.

4.11. Continuous measurement of pCO_2 and pCH_4

(1) Personnel

Akihiko Murata (JAMSTEC) – Principal investigator, Not on board
Nagisa Fujiki (Marine Works Japan Ltd.; MWJ) – Operation leader
Yuta Oda (MWJ)

(2) Objective

To survey spatial distributions of surface seawater pCO_2 in the western Arctic Ocean.

(3) Parameters

Partial pressures of CO_2 (pCO_2) and CH_4 (pCH_4)

(4) Methods, Apparatus and Performance

Atmospheric and surface seawater pCO_2 and pCH_4 were measured with a system having the off-axis integrated-cavity output spectroscopy gas analyzer (Off-Axis ICOS; 911-0011, Los Gatos Research). Standard gases were measured every about 4 hours, and atmospheric air taken from the bow of the ship (approx.13 m above the sea level) were measured every about 3 hours. Seawater was taken from an intake placed at the approximately 4.5 m below the sea surface and introduced into the equilibrator at the flow rate of (4 - 5) L min^{-1} by a pump. The equilibrated air was circulated in a closed loop by a pump at flow rate of (0.6 - 0.7) L min^{-1} through two electric cooling units, a starling cooler, and the Off-Axis ICOS.

(5) Preliminary result

Distributions of atmospheric and surface seawater CO_2 were shown in Figure 4.11-1, along with those of sea surface temperature (SST). Distributions of atmospheric and surface seawater CH_4 were displayed in Figure 4.11-2, along with those SST.

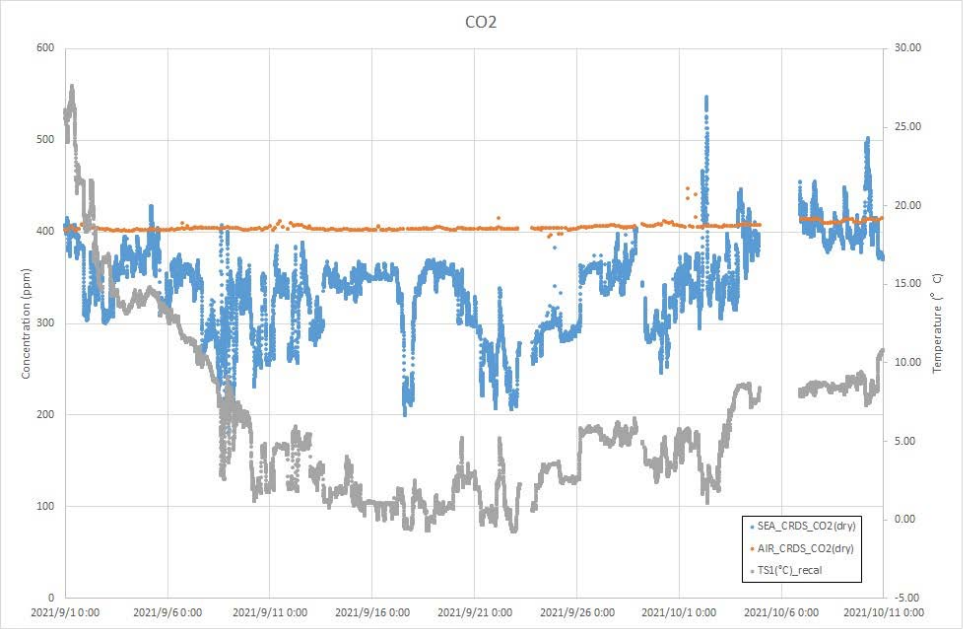

Figure 4.11-1: Distributions of atmospheric (orange) and surface seawater CO_2 (blue), and SST (grey) as a function of observation time.

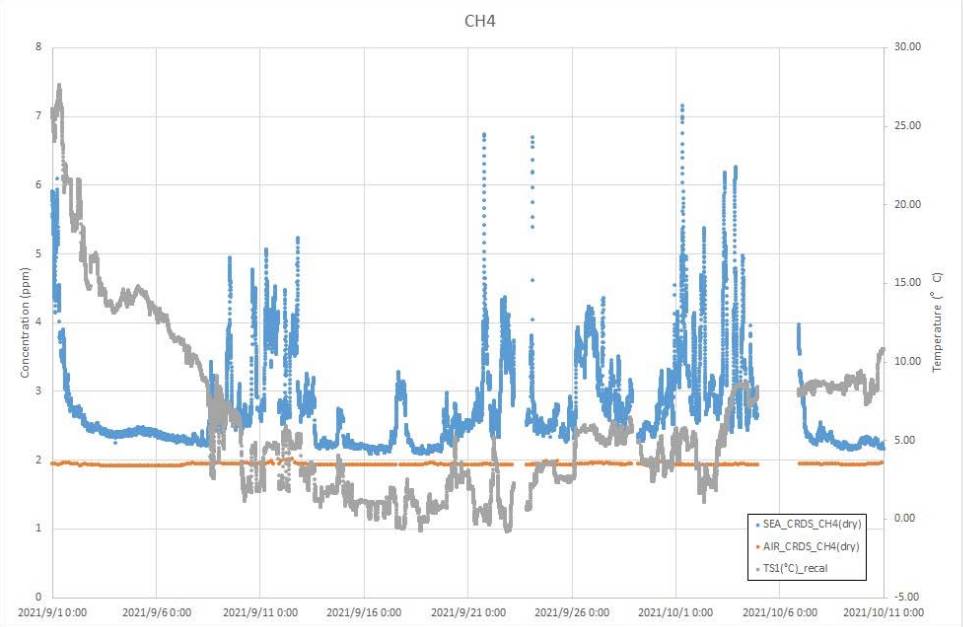

Figure 4.11-2: Distributions of atmospheric (orange) and surface seawater CH_4 (blue), and SST (grey) as a function of observation time.

(6) Date archives

These data obtained in this cruise will be submitted to the Data Management Group (DMG) of JAMSTEC, and will be opened to the public via “Data Research System for Whole Cruise Information in JAMSTEC (DARWIN)” in JAMSTEC web site.

<http://www.godac.jamstec.go.jp/darwin/e>

4.12. Trace metal clean seawater sampling

(1) Personnel

Mariko Hatta JAMSTEC -PI

(2) Objectives

The goals of this study are following:

Improve current trace metal clean sampling technique on the RV Mirai.

Estimate the potential metal contamination from the Niskin bottle attached to the regular CTD system.

Collect seawater samples via Niskin-X bottles attached with a Kevlar cable, and the characterize of the water masses with the trace element concentrations (dissolved iron and Aluminum).

(3) Parameters

Conductivity, Temperature, Depth, Turbidity, Chlorophyll, DO from a portable RINKO-Profiler

Depth from a portable depth sensor

Salinity

Nutrients (NH_4, NO_3, NO_2, PO_4, SiO_2)

Dissolved trace metals (Fe, Al etc.)

Total trace metal (Fe, Al etc.)

The ranges and accuracies of parameters measured by the RINKO-Profiler (ASTD152, S/N:0659) are as follows;

Parameter	Range	Accuracy
Conductivity	0.5 ~ 70 [mS/cm]	+/- 0.01 [mS/cm]
Temperature	-3 ~ 45 [deg-C]	+/- 0.01 [deg-C]
Depth	0 ~ 600 [m]	+/- 0.3 [%] FS
Turbidity	0 ~ 1000 [FTU]	+/- 0.3 [FTU] or +/- 2 [%]
Chlorophyll	0 ~ 400 [ppb]	+/- 1 [%] FS
DO	0 ~ 200 [%]	+/- 2 [%] FS

The calibration data sheet (Date: 2020-07-10):

Parameter.	Actual.	Measured.	Deff.	Accuracy
Temp.[deg-C]	12.655	12.654.	-0.001	+/- 0.008 [deg-C]
Cond. [ms/cm]	40.607	40.607	0.000	+/- 0.008 [mS/cm]
TURB. [FTU]	172.68	172.61	-0.07	+/- 3.11 [FTU]
Chl. [ppb].	75.22.	77.22.	2.00.	+/- 4.00 [ppb]

Depth [MPa].	4.500=447.68m	447.67	-0.01	+/- 2.50 [m]
DO [%].	99.04	98.92.	-0.12.	+/- 1.00 [%]

(4) Instruments and methods

(4.1) Trace metal clean sampling system

The sampling was conducted by each Niskin-X bottle attached to the Kevlar cable directly. The vinyl tape was winded on the Kevlar cable and then each Niskin sampling bottle was attached with a stainless pins fitted to the Kevlar cable. This will minimize any damage to the Kevlar cable while the Niskin bottle is mounted. In the bottom of the cable, the 40kg of the weights (two sets of the 20kg of weights combined by a rope) and a portable RINKO profiler were attached by a shackle. Weights are to provide negative buoyancy for the Kevlar line. In order to avoid the contamination from the equipment, the deepest Niskin bottle were attached at least 10 meters away from the profiler and weights. The shallowest sampling depths were targeted at the mixed layer depth or deeper than the 10 m, which avoid any contamination from the ship. Individual Teflon-coated Niskin bottles hung manually on a Kevlar cable, this is the standard method used successfully for over three decades (Bruland et al., 1979). Individual Niskin bottles were fitted with an internally recording depth sensor (JFA Advantech). The methods and data used in verifying depth should be documented in the metadata for the cruise.

The cable was lowering/rolling up with the speed of less than 0.5 m/sec. Typical sampling depths of the cast were shown as below:

Niskin bottle number	Target depth (Offshore)	Target depth (on Shelf)
29	20m	-
27	50m	-
19	100m	-
18	150m	-
17	250m	15m(or RINKO – 10m)
16	400m (or RINKO – 10m)	-
RINKO/weights	410m (or Bottom – 10m)	Bottom – 10m

(4.2) Niskin-X bottle

In this cruise, Niskin-X, which was Teflon-coated before the cruise started, and then all the O-rings has been replaced with pre-acid washed Viton ones. In the beginning of the MR21-05C, each Niskin bottle was cleaned followed by the GEOTRACES cookbook protocol. No acid contacted the outside of the bottle, the nylon components in particular. Each bottle was filled with 5% detergent for one day.

Rinsed 10x with deionized ultra-high purity water (Milli-Q water) thoroughly until there is no trace of detergent.

Each bottle was filled with 0.1M HCl (analytical grade) for two days, and then empted out through the spigot to rinse these.
Rinsed 5x with deionized ultra-high purity water (Milli-Q water).
Each bottle was filled with ultra-high purity water (Milli-Q water) for two days.
After discarding Milli-Q water from bottles, filled with an open ocean water that were collected during the previous cruise (47N, 173W @1710-2100dbar, collected on August 5th 2021). Those waters were collected and stored in acid-cleaned plastic container in the shipboard refrigerator room over one month before they used. This was because there was very limited time between the first trace metal cast and the acid clean process of those bottles, and we did not have any extra time to do any test cast.
After discarding seawater from the Teflon spigot, the bottles were transferred to the clean van and prepared for sampling.
Each NISKIN bottles, equipped with a depth sensor (JFA Advantech), were set up inside a clean sampling container van. Each bottle was covered with a plastic bag for top and bottom of the bottles. Teflon-coated messenger was set when it needed. Each Niskin bottle were prepared in the clean container, and then transferred to the sampling system, and removed the plastic bags were removed right before it attached to the Kevlar cable.

When the Kevlar cable leached to the target depth, a Teflon coated messenger were released, waited for a 5 mins (or 1 min, depending on the depth) to leach the messenger the last bottle.

After the cast was over, each bottle was transferred to the clean van for the sampling. Each bottle was transferred by a custom built Niskin bottle cart. The sampling nipple were carefully rested on the PVC pipe and transferred to the van. Secondly personnel (a helper) were received the bottle through the large door in the van and transferred and hanged the bottle onto the sampling rack.
(4.3) A clean sampling container van: The clean laboratory "van" is an ISO-sized 20 ft aluminum container built by Silhouette Steel (British Columbia, Canada). This van was originally designed by US group (Cutter and Bruland, 2012) and then it was modified to adjust for the Japanese research (RV Shinsei Maru). The van is divided into two rooms, a small anteroom for storage and sample bottle transfers, and the larger, positive pressure clean room for sampling and sample handling. The inner walls are covered in polypropylene sheeting over the standard aluminum walls, and the floor is Altro rolled vinyl with a total of 5 floor drains. The 5' anteroom contains a closet within which is the heating/cooling system (HVAC; two Cruisair 16,000 BTU marine air conditioner units with seawater heat exchange). The doorway between the anteroom and clean room has top to bottom clear vinyl strips to minimize return airflow (i.e., the clean room is positive pressure and at least 14.2 CMS [cubic meters per second] of HEPA-filtered air exits through the vinyl stripped doorway). The end of the clean lab has a counter with sink (ship's water).

This MR21-05C cruise was the first time to use this clean van on this RV Mirai. This is the research cruise in the Arctic Ocean, which we have to face on several challenges to use this clean van. The van was set up on the port side of the stern on the RV Mirai. This heating/cooling system has been shut down since the seawater and air temperature in the Arctic Ocean was significantly low and often expected to be below the suitable temperature of the use of this heating/cooling system. Thus, external two oil heaters (upto 1500 W) were setup in this container and kept on 24 hours (set at 26 °C) during the cruise. The room temperature was maintained between ~10 °C and 12 °C while the outside temperature was low as -2 °C. In order to maintain the power supply for this heating system (not to interrupt any other operation inside the clean van), two power cords were directly provided from the ship. In order to avoid any frozen pipes and any spill to freeze the deck, all of the floor drains have been closed during the cruise and no fresh water supply were provided. One drain pipe from the water sink was kept connected, which was ~5-meter length from the drain connector to the side of the ship, coated with a heater cable with a tape. This coating was prevented freezing the pipe and clogged with ice.

The clean sampling area was equipped with a stainless streel bottle rack that coated by epoxy paints, holding 6 Niskin-X bottles. This bottle rack was designed and built by Dr. Sugie (JAMSTEC), which has been used for the previous cruises for the clean sampling.

(4.4) Sub-sampling in the clean van:

The following samples were drained from each Niskin bottle:

Parameter	Filtered[y/n]	Analysis on the board[y/n]	Stored samples[y/n]
Salinity	n	y	n
Total metal	n	n	y
Nutrients	y	y	n
Dissolved metal	y	n	y

Salinity and total dissolved samples were drained from the bottle directly to each subsampling bottles. Samples for nutrients and dissolved metal were filtered through 0.2um Acropak filter. Samples for salinity and nutrients were determined on RV Mirai using each shipboard protocol by MWJ (see 3.12 and 4.2).

Total dissolved metal and dissolved metal samples were stored in a pre-cleaned 100mL PFA bottles. Each bottle was cleaned using the GEOTRACES cookbook protocols at the shore-based laboratory.

1. Soaked bottles for one day in an alkaline detergent.
2. Rinsed 10x with ultra-high purity water (MilliQ water) thoroughly until there were no trace of detergent.
3. Soaked in 6 M reagent grade HCl bath for more than one day

5. Rinsed 5x with ultra-high purity water (MilliQ water).
6. Filled with 1M nitric acid (analytical grade) and kept them at 80°C for 5 hours in a heated oven. Each bottle was packed with a plastic bag with milliQ water in case of any spill from each bottle.
7. Rinsed 5x with ultra-high purity water (MilliQ water) inside an ISO Class-5 laminar flow hood.
8. Filled bottles with ultra-high purity water (MilliQ water) and kept them at 80°C for 5 hours in a heated oven. Each bottle was packed with a plastic bag with milliQ water in case of any spill from each bottle.
9. Rinsed 5x with ultra-high purity water (MilliQ water) water inside an ISO Class-5 laminar flow hood. The bottles were packed in 6 within doubled bagged until they used.

(4.4) Data:
A portable CTD (RINKO-Profiler): We observed vertical profiles of sea water temperature, salinity, turbidity, chlorophyll, and DO using a RINKO-Profiler, which was manufactured by JFE Advantech Co., Ltd. The profiler was lowered from the broadside with its lowering speed less than 0.5 m/sec . The sensors were collected every 0.1 second interval. We obtained 26 profiles and the observation log is shown in Table 4.11-1. Additional profiles were obtained at the Sea Ice catching stations (Stations 14, 28, and 31) upper 10-meter water depths. Those operation were conducted by hand. (Figure 4.12-2.).

Salinity: The salinity analysis was carried out on R/V MIRAI during the cruise of MR21-05C using the salinometer. The detailed of the analysis were reported in elsewhere.

Nutrients: The nutrient analysis was carried out on R/V MIRAI during the cruise of MR21-05C using the QuAAtro 5 and 6. The detailed of the analysis were reported in elsewhere.

(5) Station list or Observation log
Trace metal clean sampling were carried out at the following stations, shown in Table 4.11-1. Total 26 casts were carried out, and addition to the two regular CTD cast sampling, we obtained over 76 unique samples.

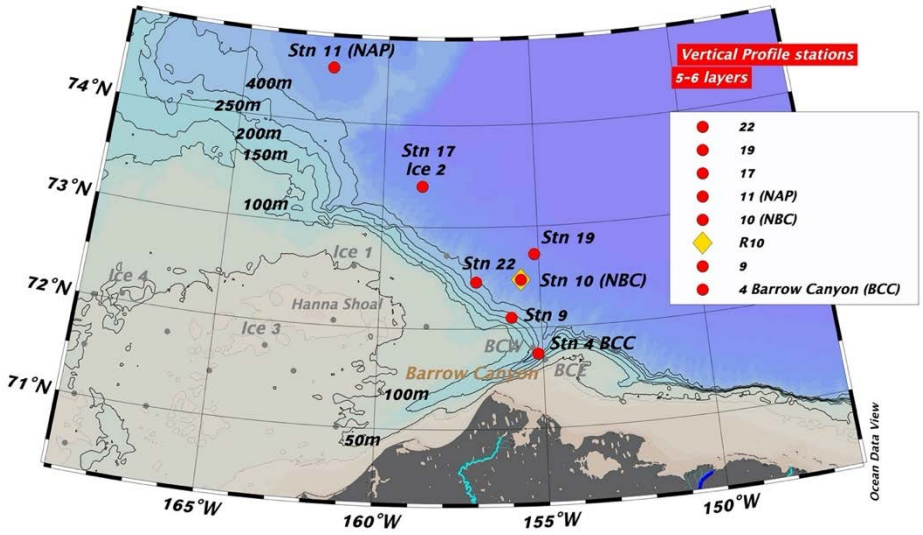

Figure 4.12-1: Trace metal cast at the shelf edge and offshore locations. Trace metal cast were conducted at the red circles. A set of the samples for trace metal back-ground test was drawn from a regular rosette cast at the yellow diamond location. NAP, NBC, are BCC are Northwind Abyssal Plain, North Barrow Canyon, and Barrow Canyon Center, respectively.

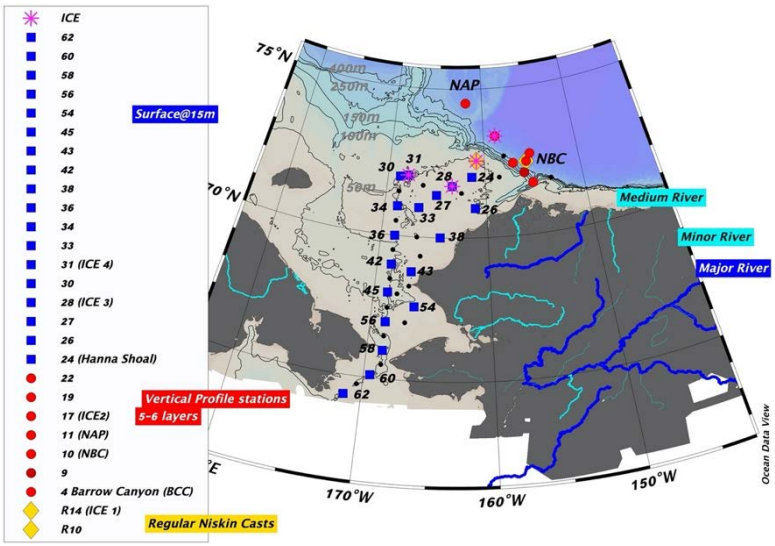

Figure 4.12-2: Trace metal sampling on the Chukchi Shelf region were conducted at the blue squares. Black dots were shown for the sampling location using the regular CTD sampling system. Red circles were shown at the offshore and shelf-edge stations and yellow diamonds were stations conducted by a regular rosette sampling system and then drawn the sampling for the trace metal sample analysis. Pink star symbols were shown the ice sampling stations.

Table 4.12-1: List of the sampling locations for trace metal casts.

	Station	Cast time					Latitude			Longtitude			Note	Sample [y/n]	RINKO (nomal/ice)
1	4	2021	09	13	0:31	UTC	71	44.3940	N	155	8.1480	W	BCC	y	normal
2	9	2021	09	13	19:06	UTC	72	6.1260	N	155	54.7680	W		y	normal
3	10	2021	09	14	2:17	UTC	72	28.4880	N	155	35.1360	W	NBC	y	normal
4	11	2021	09	16	19:40	UTC	74	31.5240	N	161	55.1700	W	NAP	y	normal
5	14	2021	09	17	19:42	UTC	72	35.8980	N	160	49.9500	W	ICE 1	n	ice
6	17	2021	09	19	0:04	UTC	73	23.8680	N	158	42.8340	W	ICE 2	y	normal & ice
7	19	2021	09	19	22:31	UTC	72	43.3740	N	155	7.9140	W		y	normal
8	22	2021	09	20	23:05	UTC	72	27.5640	N	156	59.3880	W		y	normal
9	24	2021	09	21	18:29	UTC	72	3.2580	N	161	22.5960	W	Hanna Shoal	y	normal
10	26	2021	09	22	4:30	UTC	70	59.8740	N	161	6.6000	W		y	normal
11	27	2021	09	22	17:18	UTC	71	26.2920	N	164	57.0000	W		y	normal
12	28	2021	09	22	23:55	UTC	71	45.1320	N	163	23.5740	W	ICE 3	y	normal & ice
13	30	2021	09	23	17:39	UTC	72	0.2520	N	168	45.3000	W		y	normal
14	31	2021	09	23	23:34	UTC	72	3.9240	N	167	54.2040	W	ICE 4	y	normal & ice
15	33	2021	09	24	18:51	UTC	71	0.0000	N	166	38.7300	W		y	normal
16	34	2021	09	25	16:45	UTC	71	0.0060	N	168	44.9580	W		y	normal
17	36	2021	09	26	1:12	UTC	69	59.9160	N	168	43.9200	W		y	normal
18	38	2021	09	27	17:09	UTC	70	0.0120	N	164	27.8760	W		y	normal
19	42	2021	09	28	16:39	UTC	69	0.0300	N	168	45.1680	W		y	normal
20	43	2021	09	28	23:00	UTC	68	48.0420	N	166	57.4200	W		y	normal
21	45	2021	09	29	16:39	UTC	68	2.0100	N	168	49.9020	W		y	normal
22	54	2021	09	30	17:14	UTC	67	36.0780	N	166	30.0360	W		y	normal
23	56	2021	10	01	2:48	UTC	67	0.1740	N	168	46.3800	W		y	normal
24	58	2021	10	01	16:39	UTC	65	59.7720	N	168	44.9940	W		y	normal
25	60	2021	10	02	1:30	UTC	65	5.6760	N	169	31.1160	W		y	normal
26	62	2021	10	02	17:44	UTC	64	18.9240	N	171	18.1980	W		y	normal
1	10R	2021	09	14	3:27	UTC	72	28.4880	N	155	35.1360	W		y	-
2	14R	2021	09	17	19:42	UTC	72	35.8980	N	160	49.9500	W	ICE 1	y	-

(6) Preliminary results

(6.1) The RINKO data compared with CTD sensor.

The preliminary data from RINKO profiler were compared with the rosette CTD senor data at the station. Each cast was conducted within a couple of hours, and the most of the depth data were shown in the good agreement. Typical data were shonw in Figure 4.12-3.

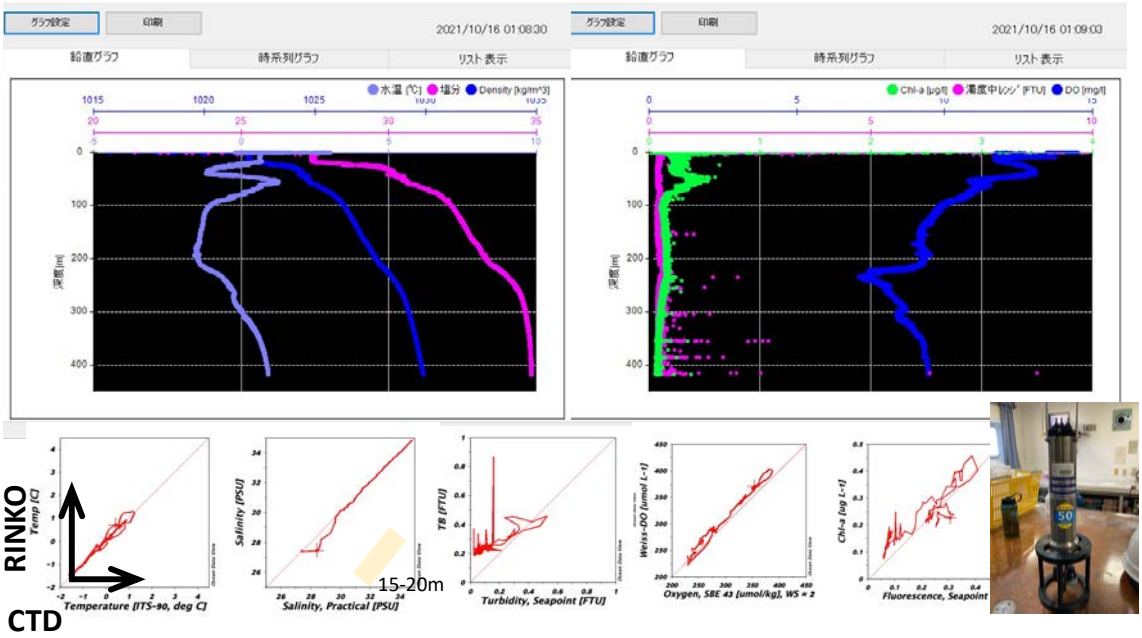

Figure 4.12-3: The vertical profile from RINKO profiler at Station 11 and compared with rosette CTD sensor data.

(6.2) The water structure at the offshore stations based on the preliminary RINKO profiler data set:

To evaluate the overall performance of RINKO profiler data, we compared the raw data between RINKO profiler and the regular CTD cast. Each cast at the same stations were conducted within a couple of hours.

The comparison between temperature values from each sensor (shown in the top left on the Figure 4.12-4) showed the good agreement throughout the water column except for the shallow depth. Some variabilities were seen at stations 9, 10, and 19 (15-18m@Stn 9; 4-26m@Stn 10; 35-60m@ Stn 19). Note that those data were the upper cast of RINKO profiler data and the lower cast of CTD cast from the regular rosette sampling system.

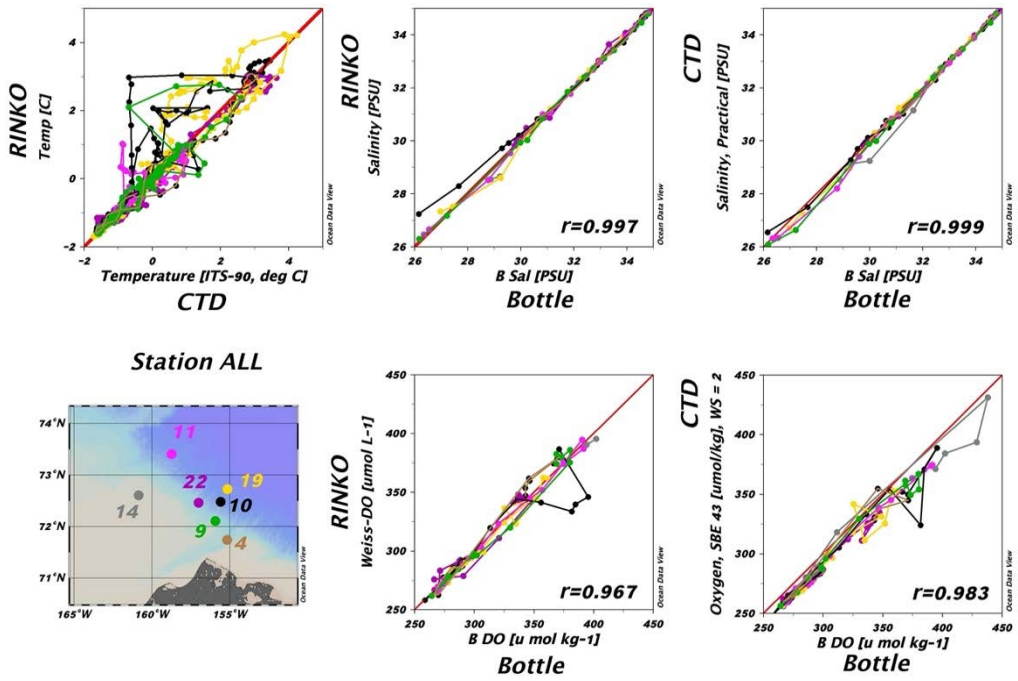

Figure 4.12-4: The comparison between the regular casts with a CTD sensor and the clean casts with a RINKO sensor at offshore stations.

The T-S diagram using the RINKO profiler at the offshore stations were shown in Figure 4.12-5. In this study area, there were three water masses were identified; Atlantic Water (AW), Pacific Winter Water (PWW), and Pacific Summer Water (PSW). Upper 35m water depth, the water characteristics were varied.

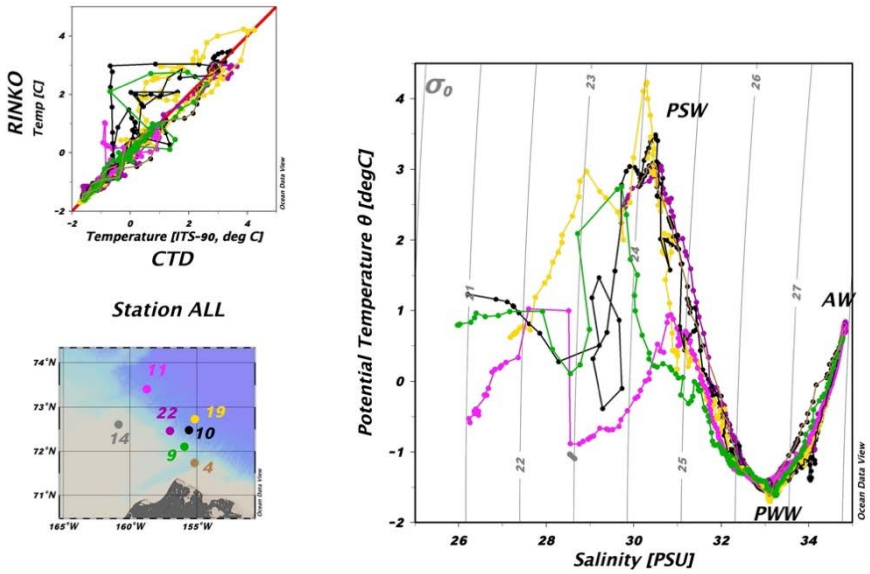

Figure 4.12-5: The water characteristics using T-S diagram. The data were shown in the upper 400m water depth. AW: Atlantic Water; PSW: Pacific Summer Water; PWW: Pacific Winter Water.

(6.3) The comparison of MR21-05C with the GEOTRACES (GN01)

The preliminary data obtained at the offshore stations during MR21-05C were similar characteristics of the water masses compared with GEOTRACES GN01 (2015).

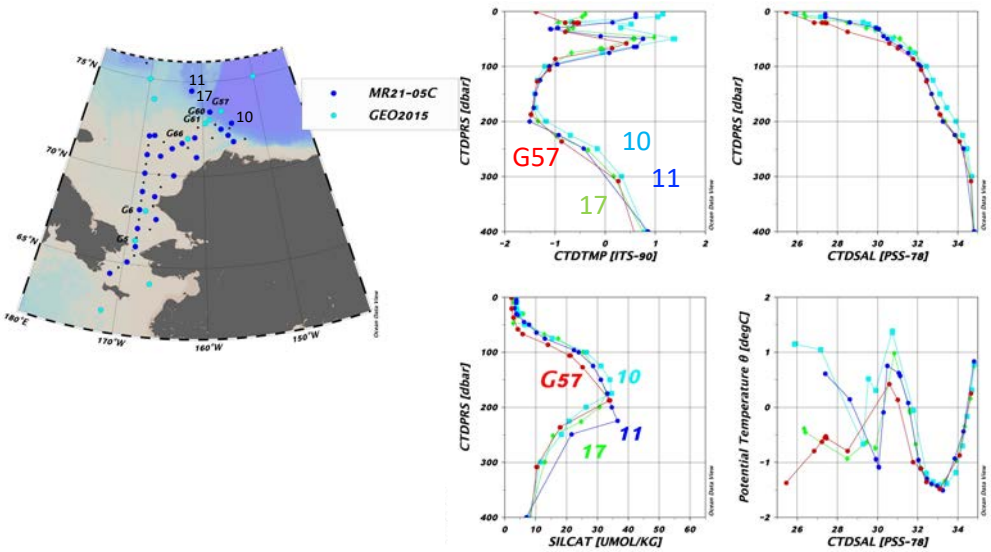

Figure 4.12-6: The comparison of the T-S and Si data at the offshore stations with the historical GEOTRACES station.

(6.4) The sampling on the Chukchi-shelf.

The trace metal sample were collected various stations (Figure 4.12-2). The T-S diagram were shown in the Figure 4.12-7.

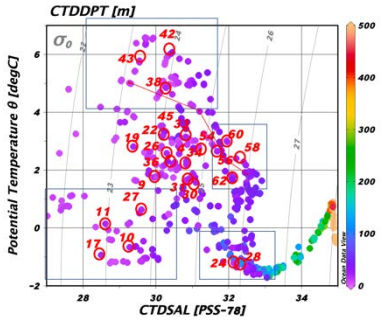

Figure 4.12-7: The water characteristics (T-S diagram) at the sampling stations. The red circle and numbers were the data for the trace metal samples that were collected during MR21-05C.

(6.5) The preliminary RINKO data at the Sea Ice stations

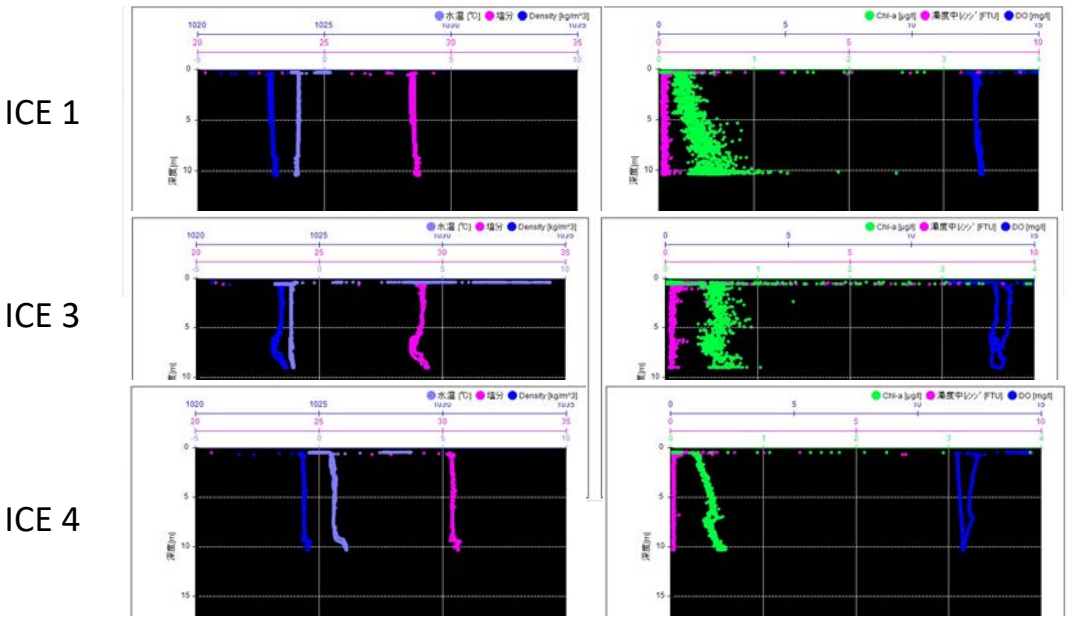

Figure 4.12-8: The vertical profiles of the temperature, salinity, Chl-a, Turbidity and the dissolved oxygen at Sea Ice stations. Data was obtained upper 10-meter water depths at Ice stations. The location were shown in Figure 4.12-2.

(7) Data archives

These data obtained in this cruise will be submitted to the Data Management Group of JAMSTEC, and will be opened to the public via "Data Research System for Whole Cruise Information in JAMSTEC (DARWIN)" in JAMSTEC web site. <http://www.godac.jamstec.go.jp/darwin/e>

4.13. Microbial community structure and production

4.13.1. Microbial community structure in sinking particles

(1) Personnel

Takuhei Shiozaki (Atmosphere and Ocean Research Institute, The University of Tokyo) -PI

(2) Objectives

Sinking particles were collected using Marine Snow Catcher (MSC) to examine the microbial community structure.

(3) Parameters

Size-fractionated DNA (>3 μm and 0.2–3 μm)
Size-fractionated chlorophyll *a* (>3 μm and 0.2–3 μm)
Particulate organic carbon / nitrogen (POC/N)
Bacterial abundance
Salinity

(4) Instruments and methods

Two types of MSC (Normal and Giant) were used in this study. Normal and Giant MSC collects 120 and 370 L water at desired depth, respectively.

The MSC deployment was performed using the ship's A-frame. The speed of wire out is set to be 1.0 m s^{-1}. After reaching the desired depth, the MSC was closed using a messenger. After collecting the water sample, winch wire was wound up at 1.0 m s^{-1}.

Samples were collected from subsurface chlorophyll maximum (SCM) and 1000 m depth (except at St.22 where the sample was collected at 20 m above the seafloor) using Normal and Giant MSC, respectively. The depth of SCM was determined using fluorescence profile taken during CTD cast just before the MSC observation. After the retrieval, the MSC was left undisturbed on the ship's deck for 2 h. Sinking particles were collected from the bottom of the MSC (sinking fraction). Further, suspended particles were collected from the upper column of the MSC (suspended fraction).

Samples for DNA, POC/N, and bacterial abundance were collected from the sinking fraction. From the suspended fraction, samples for size-fractionated DNA and chlorophyll *a*, POC/N, bacterial abundance, and salinity were collected. The DNA in the sinking fraction were filtered onto 3-μm polycarbonate filters. Seawater samples for salinity analysis were collected in 250 ml brown grass bottles, and were immediately measured on board using a salinometer (see 3.13). The details of other sampling method are detailed in Section 4.13.2.

(5) Station list

The stations performed MSC observation are listed in Table 4.13-1.

(6) Data archives
These data obtained in this cruise will be submitted to the Data Management Group of JAMSTEC when ready.

4.13.2. Microbial community structure and production in suspended particles

(1) Personnel
Takuhei Shiozaki (Atmosphere and Ocean Research Institute, The University of Tokyo) -PI
Taichi Yokokawa (JAMSTEC)
Yuki Sato-Takabe (Atmosphere and Ocean Research Institute, The University of Tokyo)

(2) Objectives
Suspended particles were collected using a bucket and Niskin bottles to examine the microbial community structure and production.

(3) Parameters
Size fractionated DNA (>3 μm and 0.2–3 μm)
Total DNA
Size fractionated chlorophyll *a* (>3 μm and 0.2–3 μm)
Total chlorophyll *a*
Particulate organic carbon / nitrogen (POC/N)
Bacterial abundance
Abundance of aerobic anoxygenic phototrophic bacteria (AAnPB)
Nutrients (NO_3, NO_2, NH_4, PO_4, $Si(OH)_4$)
Total dissolved inorganic carbon
Total alkalinity
Primary production
Nitrogen fixation

(4) Instruments and methods
Water samples were collected from depths corresponding to 100, 10, 1, and 0.1% of surface light intensity, and from near bottom in the shelf or from 100 m in the off-shelf with acid-cleaned Niskin-X bottles and a bucket (from surface sample). The depth profiles of light intensity were obtained using a C-OPS (Biospherical Instruments) or CTD-attached PAR sensor just before the sampling.
Samples for size-fractionated DNA (2.3 L) and chlorophyll *a* (0.5 L) were sequentially filtered onto 3- and 0.2-μm filters. Samples for total DNA (2.3 L) and total chlorophyll *a*

(0.3 L) were filtered onto 0.2-μm filters and GF/F filters, respectively. Samples for POC/N (2 L) were filtered onto precombusted (450°C, 6h) GF/F filters. Samples for bacterial abundance were fixed with glutaraldehyde, and were stored at a deep-freezer (-80°C) until onshore analysis. Samples for AAnPB abundance were fixed with glutaraldehyde, stored >3 h at 4°C in the dark, and filtered onto a 0.2-μm black polycarbonate membrane filters under gentle vacuum (≤20 cm Hg). The filters were stored at a freezer (<-20°C) until onshore analysis. Samples for nutrients analysis were collected in 10 mL acrylic tubes and were immediately determined onboard using a QuAAtro system (see 4.2). Samples for total dissolved inorganic carbon and total alkalinity were collected in 250 mL glass bottles and were determined onboard using a CO_2 extraction-coulometric titration system and a spectrophotometric system, respectively (4.3.1 and 4.5). Samples for primary production and nitrogen fixation were collected duplicate 1.2L polycarbonate bottles. Primary production was measured with nitrogen fixation using a dual (^{13}C and ^{15}N) isotopic technique. After addition of the tracers, sample bottles were wrapped with a neutral-density screen or aluminum foil to adjust the light levels and incubated for 24 h in an on-deck incubator filled with flowing surface seawater or in a thermostatic incubator. Incubations were terminated by gentle filtration onto pre-combusted GF/F filters.

(5) Station list
The stations performed MSC observation are listed in Table 4.13-1.

(6) Data archives
These data obtained in this cruise will be submitted to the Data Management Group of JAMSTEC when ready.

4.13.3. Microbial community structure in surface sediments

(1) Personnel
Takuhei Shiozaki (Atmosphere and Ocean Research Institute, The University of Tokyo)
-PI

(2) Objectives
Surface sediments and the waters just above the sediments were collected using a multiple corer system to examine the microbial community structures.

(3) Parameters
DNA

(4) Instruments and methods
Multiple corer system (Ashura) used in this cruise consists of main body (60 kg

weight) and three acryl corer attachments. The core barrel is 60 cm length and 7.4 cm inner diameter.

At the begging of multiple corer system going down, the speed of wire out was set to be 0.5 m s^{-1}. Wire out was stopped at a depth about 10 m above the seafloor and the corer system was left stand for 1 minute to reduce any pendulum motion of the system. After the multiple corer system was stabilized, the wire was stored out at a speed of 0.5 m s^{-1} with carefully watching a tension meter. After confirmation of the multiple corer system touching the bottom, the wire continued out till bowing. The rewinding of the wire was started at a dead slow speed (0.3 m s^{-1}), and then winch wire was wound up at 0.5 m s^{-1}.

Samples for DNA analysis were collected from the surface sediment and seawater just above the sediment core. The seawater was filtered onto 3-μm polycarbonate filters. The sediment and filter were stored at a freezer (<-20°C) until onshore analysis.

(5) Station list

The stations performed MSC observation are listed in Table 4.13-1.

(6) Data archives

These data obtained in this cruise will be submitted to the Data Management Group of JAMSTEC when ready.

Table 4.13-1: Station list for sample collections

Station	3	9	11	14	17	19	22	24	28
MSCN		○[a]	○	○	○	○	○	○	○
MSCG			○		○	○	○		
Niskin	○	○	○	○	○	○	○	○	○
Ashura		○		○				○	○

31	33	35	38	39	42	45	54	58	62
○	○	○	○		○	○	○	○	○
○	○	○	○	○[b]	○	○	○	○	○
○	○	○	○		○	○	○	○	○[c]

[a] samples collected at the 0.1% light depth.

[b] samples were collected only at 5, SCM, 20, and B-5 m.

[c] sediment sample could not be collected.

4.13.4. Incubation experiments

(1) Personnel

Takuhei Shiozaki (Atmosphere and Ocean Research Institute, The University of Tokyo) -PI

Amane Fujiwara (JAMSTEC)

(2) Objectives

Arctic nitrification is primarily regulated by the light environment and may have experienced a decreasing trend over the last two decades (Shiozaki et al., 2019). The suppression of nitrification may alter the composition of inorganic N nutrient. Here we examined how microbial ecosystem change with different inorganic N nutrient composition by microcosm experiments.

(3) Parameters

Chlorophyll *a*

Nutrients (NO_3, NO_2, NH_4, PO_4, $Si(OH)_4$)

DNA

Phytoplankton pigments

(4) Instruments and methods

The experiments were performed using seawater collected from 5 m and 35 m at St. 3 and from 5 m at Sta. 42. The seawater was sieved by 112.5 μm-mesh to reduce grazing pressure and dispensed into nine 10 L polyethylene bags at each depth and station. Three different triplicate treatments were set up for the samples collected from 5 m: control without any nutrient addition, nitrate and ammonium addition treatment (final concentration: ~2.5 μM each), and ammonium addition treatment (final concentration: ~5 μM). For samples collected at 35 m, the treatment were as follows: control without any nutrient addition, nitrate addition treatment (final concentration: ~5 μM), and ammonium addition treatment (final concentration: ~5 μM). The bags from 5 m and 35 m were treated under high (350 μmol photon s^{-1} m^{-2}) and dim light condition (75 μmol photon s^{-1} m^{-2}) representing 1% light levels relative to the surface, respectively, with a 12:12 light:dark cycle in a thermostatic room (4 °C). Experiments were lasted for 10, 25, and 20 days for samples collected 5 m and 35 m at St. 3 and 4 m at St. 42, respectively. Sampling frequencies of each parameter are listed as follows (Table 4.13-2, 4.13-3, and 4.13-4).

Table 4.13-2: Sampling frequency of each parameter for samples collected 5 m at St. 3

Day	0	2	4	6	8	9	10
Chla	○	○	○	○	○	○	○
Nutrients	○	○	○	○	○	○	○
Pigments	○					○	
DNA	○					○	

Table 4.13-3: Sampling frequency of each parameter for samples collected 35 m at St. 3

Day	0	3	5	7	9	11	13	15	17
Chla	○	○	○	○	○	○	○	○	○
Nutrients	○	○	○	○	○	○	○	○	○

Pigments	○						○		
DNA	○						○		

19	21	23	25
○	○	○	○
○	○	○	○
			○
			○

Table 4.13-4: Sampling frequency of each parameter for samples collected 5 m at St. 42

Day	0	2	4	6	8	10	12	14	16
Chla	○	○	○	○	○	○	○	○	○
Nutrients	○	○	○	○	○	○	○	○	○
Pigments	○					○			○
DNA	○					○			○

18	20
○	○
○	○
	○
	○

(5) Data archives

These data obtained in this cruise will be submitted to the Data Management Group of JAMSTEC when ready.

4.14. Zooplankton

(1) Personnel
Kohei Matsuno (Hokkaido University) - Principal Investigator
Atsushi Yamaguchi (Hokkaido University) , Not on board
Koki Tokuhiro (Hokkaido University), Not on board
Kohei Sumiya (Hokkaido University)
Wakana Endo (Hokkaido University)

(2) Objectives
The goals of this study are following:
Clarify the spatial changes of mesozooplankton community
Evaluate physical conditions (gut pigments, stable isotope and fatty acid) of the Pacific and Arctic zooplankton
Clarify the population structure, size frequency and haplotype of the copepod *Calanus glacialis* in the pacific sector of Arctic Ocean
Clarify the species distribution and size of jellyfish in the western Arctic Ocean

(3) Parameters
Mesozooplankton abundance
Gut pigments
Stable isotope
Fatty acid
Prosome length of *Calanus glacialis*
Photograph of jelly fish

(4) Sampling and treatment
(4-1) Plankton net sampling
Zooplankton samples were collected by vertical haul of Quad-NORPAC nets at 46 stations in the pacific sector of Arctic Ocean. Quad-NORPAC net (mesh sizes: 335, 150 and two 63 μm with large cod-end, mouth diameter: 45 cm) was towed between surface and 150 m depth or bottom -7 m (stations where the bottom shallower than 150 m) at all stations (Fig. 4.14-1 and Table 4.14-1). Zooplankton samples collected by the NORPAC net with 335 and 150 μm mesh were immediately fixed with 5% buffered formalin for zooplankton community structure analysis. Samples collected with 63 μm mesh were used for picking up alive pterapods (for NHK) and evaluation of the zooplankton physiological parameters (i.e., gut pigments, stable isotope and lipid composition). After the sorting, the remaining sub-samples were fixed with 99.5% ethanol as backup samples for haplotype analysis of *Calanus glacialis*. The volume of water filtered through the net was estimated from the reading of a flow-meter mounted in the mouth ring.
80 cm ring net (mesh: 335 μm, mouth diameter: 80 cm) was towed between surface and

300-500 m or bottom -7 m at 46 stations (Fig. 4.14-1 and Table 4.14-2). Fresh samples were used for picking up alive pterapods (for NHK) and evaluation of the zooplankton physiological parameters (i.e., gut pigments, stable isotope and lipid composition). After the sorting, the remaining sub-samples were fixed with 99.5% ethanol for DNA analysis of jellyfish (investigator: Dr. Gerlien Verhaegen in JAMSTEC).

(4-2) On-board treatment

After net sampling, *Limacina helicina* was picked up immediately from the fresh zooplankton samples collected with Bucket net and/or ring net. If the species was not collected, we added with 10% soda water (CO_2 water) immediately used for gut pigment, stable isotope, lipid composition and DNA haplotype analyses. If over five minutes after sampling took for picking up *L. helicina*, we did not use the sample for measuring the gut pigment.

We sorted with all zooplankton at species level as many as possible for copepods, euphausiids, chaetognaths, appendicularians, amphipods, ostracods. Firstly, major fell fishes were transported into a glass petri dish for taking a photo to measure original size before ethanol preservation (by Dr. Gerlien Verhaegen in JAMSTEC). For measuring gut pigment, the sorted specimens were transferred into a cuvette tube immersed with 6 ml dimethylformamide, stored and extracted for >24 hours. After extract the pigment, these samples were measured fluorescence with a Trilogy Model 7200-000 with the Chl *a* acidification fluorescent module 7200-040. Some specimens were transferred into a small plastic case (3 mL) or a bial tube (6 mL), and stored in –80°C for fatty acid composition analysis (by Dr. Yasuhiro Ando and Dr. Fumiaki Beppu in Hokkaido University). To same species in the lipid analysis, we also transferred the specimens into a bial tube, and dried at 60ºC in an oven for measuring stable isotope (by Dr. Maki Noguchi in JAMSTEC). For the *C. glacialis*, the prosome length of up to twenty specimens were measured with an eye-piece micrometer under a stereo microscope, and each specimen was preserved in a 1.5 mL tube filled with 99% ethanol for haplotype (16s rRNA) analysis (by Dr. Junya Hirai in The University of Tokyo).

(5) Station list

Table 4.14-1: Data on plankton samples collected by vertical hauls with Quad-NORPAC net.

Station	Position		S.M.T.		Length of	Angle of	Depth estimated	Mesh	Flowmeter		Estimated volume of	
no.	Lat. (N)	Lon.	Date	Hour	wire (m)	wire (°)	by wire angle (m)	size (μm)	No.	Reading	water filtered (m^3)	Remark
3	71 41.04	154 55.59 W	12 Sep.	12:06 - 12:12	93	2	93	335	3690	925	13.16	
								150	3996	885	12.50	
								63				1)
								63				2)
4	71 44.17	155 10.81 W	12 Sep.	15:48 - 15:54	150	1	150	335	3690	1380	19.64	
								150	3996	1265	17.87	
								63				1)
								63				2)
9	72 6.12	155 54.69 W	12 Sep.	15:48 - 15:54	150	1	150	335	3690	1411	20.08	
								150	3996	1422	20.09	
								63				1)
								63				2)
10	72 28.18	155 31.48 W	12 Sep.	15:48 - 15:54	150	1	150	335	3690	1419	20.19	
								150	3996	1348	19.05	
								63				1)
								63				2)
11	74 31.28	161 57.21 W	16 Sep.	10:56 - 11:03	150	3	150	335	3690	1369	19.48	
								150	3996	1360	19.22	
								63				1)
								63				2)
12	73 0.86	159 37.46 W	17 Sep.	0:09 - 0:14	151	6	150	335	3690	1410	20.07	
								150	3996	1411	19.94	
								63				1)
								63				2)
14	72 35.44	160 50 W	17 Sep.	12:15 - 12:17	42	1	42	335	3690	379	5.39	
								150	3996	318	4.49	
								63				1)
								63				2)
15	72 43.25	157 54.47 W	17 Sep.	18:25 - 18:33	153	11	150	335	3690	1460	20.78	
								150	3996	1416	20.01	
								63				1)
								63				2)
17	73 23.25	158 43.96 W	18 Sep.	15:19 - 15:25	151	6	150	335	3690	1411	20.08	
								150	3996	1392	19.67	
								63				1)
								63				2)
18	73 9.73	154 41.47 W	18 Sep.	23:29 - 23:36	153	11	150	335	3690	1572	22.37	
								150	3996	1519	21.46	
								63				1)
								63				2)
19	72 43.13	155 8.62 W	19 Sep.	13:46 - 13:56	151	6	150	335	3690	1570	22.34	
								150	3996	1555	21.97	
								63				1)
								63				2)
20	71 48.65	153 16.62 W	19 Sep.	21:03 - 21:10	155	14	150	335	3690	1613	22.95	
								150	3996	1485	20.98	
								63				1)
								63				2)
22	72 27.08	157 2.2 W	20 Sep.	14:21 - 14:29	150	2	150	335	3690	1385	19.71	
								150	3996	1397	19.74	
								63				1)
								63				2)
23	72 1.38	158 31.09 W	20 Sep.	18:33 - 18:37	49	2	49	335	3690	662	9.42	
								150	3996	537	7.59	
								63				2)
								63				2)
24	72 3.42	161 23.27 W	21 Sep.	9:38 - 9:41	23	1	23	335	3690	239	3.40	
								150	3996	191	2.70	
								63				2)
								63				2)
25	71 31.32	162 27.42 W	21 Sep.	13:47 - 13:49	36	9	36	335	3690	371	5.28	
								150	3996	305	4.31	
								63				1)
								63				2)

S.M.T. is UTC-9h

1) Experiment, remaining was preserved in ethanol

2) Samples was used for experiments on board

Table 4.14-1: (Continued).

Station no.	Position				S.M.T.			Length of wire (m)	Angle of wire (°)	Depth estimated by wire angle (m)	Mesh size (μm)	Flowmeter		Estimated volume of water filtered (m^3)	Remark
	Lat. (N)		Lon.		Date	Hour						No.	Reading		
26	70	59.98	161	6.89 W	21 Sep.	19:00	19:03	39	9	39	335	3690	473	6.73	
											150	3996	450	6.36	
											63				1)
											63				2)
27	71	26.43	164	57.07 W	22 Sep.	7:34	7:37	35	6	35	335	3690	320	4.55	
											150	3996	250	3.53	
											63				1)
											63				2)
28	71	44.41	163	24.25 W	22 Sep.	14:59	15:01	33	3	33	335	3690	281	4.00	
											150	3996	218	3.08	
											63				1)
											63				2)
29	71	45.8	166	21.59 W	22 Sep.	20:06	20:09	38	3	38	335	3690	359	5.11	
											150	3996	305	4.31	
											63				1)
											63				2)
30	72	0.22	168	45.42 W	23 Sep.	8:44	8:47	44	4	44	335	3690	356	5.07	
											150	3996	308	4.35	
											63				1)
											63				2)
31	72	3.84	167	57.78 W	23 Sep.	14:38	14:40	42	11	41	335	3690	330	4.70	
											150	3996	270	3.82	
											63				1)
											63				2)
32	71	30	168	44 W	23 Sep.	18:23	18:25	41	2	41	335	3690	418	5.95	
											150	3996	355	5.02	
											63				1)
											63				2)
33	71	0.04	166	38.38 W	24 Sep.	9:54	9:57	37	1	37	335	3690	392	5.58	
											150	3996	369	5.21	
											63				1)
											63				2)
34	71	0	168	44.98 W	25 Sep.	7:50	7:52	37	9	37	335	3690	352	5.01	
											150	3996	281	3.97	
											63				1)
											63				2)
35	70	29.92	168	44.84 W	25 Sep.	12:46	12:49	31	8	31	335	3690	299	4.26	
											150	3996	280	3.96	
											63				1)
											63				2)
36	70	0	168	44.88 W	25 Sep.	15:50	15:52	33	2	33	335	3690	343	4.88	
											150	3996	320	4.52	
											63				1)
											63				2)
37	70	0.27	166	39.12 W	25 Sep.	21:24	21:26	40	5	40	335	3690	390	5.55	
											150	3996	390	5.51	
											63				1)
											63				2)
38	70	6.02	164	27.92 W	27 Sep.	8:14	8:16	28	2	28	335	3690	289	4.11	
											150	3996	289	4.08	
											63				1)
											63				2)
39	69	21.03	166	14.27 W	27 Sep.	14:57	15:00	30	1	30	335	3690	280	3.98	
											150	3996	259	3.66	
											63				1)
											63				2)
41	69	29.97	168	45.16 W	27 Sep.	21:30	21:33	44	1	44	335	3690	390	5.55	
											150	3996	385	5.44	
											63				1)
											63				2)
42	69	0.07	168	45.09 W	27 Sep.	7:43	7:46	45	7	45	335	3690	428	6.09	
											150	3996	426	6.02	
											63				1)
											63				2)

S.M.T. is UTC-9h

1) Experiment, remaining was preserved in ethanol

2) Samples was used for experiments on board

Table 4.14-1. (Continued).

Station no.	Position				S.M.T.			Length of wire (m)	Angle of wire (°)	Depth estimated by wire angle (m)	Mesh size (μm)	Flowmeter		Estimated volume of water filtered (m^3)	Remark
	Lat. (N)		Lon.		Date	Hour						No.	Reading		
43	68	48.12	166	57.04 W	28 Sep.	14:05	14:07	34	4	34	335	3690	340	4.84	
											150	3996	332	4.69	
											63				1)
											63				2)
44	68	30.04	168	44.88 W	28 Sep.	17:50	17:52	46	3	46	335	3690	458	6.52	
											150	3996	435	6.15	
											63				1)
											63				2)
45	68	1.99	168	49.96 W	29 Sep.	7:43	7:45	51	20	48	335	3690	511	7.27	
											150	3996	442	6.25	
											63				1)
											63				2)
46	67	30.01	168	44.63 W	29 Sep.	12:55	12:58	42	5	42	335	3690	432	6.15	
											150	3996	420	5.93	
											63				1)
											63				2)
49	68	0.1	168	0.43 W	29 Sep.	17:50	17:53	47	4	47	335	3690	402.0	5.72	
											150	3996	358.0	5.06	
											63				1)
											63				2)
54	67	36.07	166	29.94 W	30 Sep.	8:20	8:23	40	12	39	335	3690	398.0	5.66	
											150	3996	355.0	5.02	
											63				1)
											63				2)
55	67	1.73	167	9.7 W	30 Sep.	13:41	13:44	34	4	34	335	3690	482.0	6.86	
											150	3996	419.0	5.92	
											63				1)
											63				2)
56	67	0	168	45 W	30 Sep.	17:53	17:56	36	4	36	335	3690	630.0	8.97	
											150	3996	490.0	6.92	
											63				1)
											63				2)
57	66	29.76	168	46.33 W	30 Sep.	22:14	22:17	42	11	41	335	3690	571.00	8.13	
											150	3996	481	6.80	
											63				1)
											63				2)
58	65	59.73	168	45.16 W	1 Oct.	7:44	7:46	43	11	42	335	3690	516	7.34	
											150	3996	442	6.25	
											63				1)
											63				2)
59	65	29.9	168	45.12 W	1 Oct.	13:20	13:23	44	7	44	335	3690	608	8.65	
											150	3996	480	6.78	
											63				1)
											63				2)
60	65	5.69	169	31.13 W	1 Oct.	16:35	16:38	41	1	41	335	3690	312	4.44	
											150	3996	288	4.07	
											63				1)
											63				2)
61	64	43.52	170	25.55 W	1 Oct.	21:28	21:30	40	6	40	335	3690	590	8.40	
											150	3996	582	8.22	
											63				1)
											63				2)
62	64	18.93	171	18.24 W	2 Oct.	8:51	8:54	38	1	38	335	3690	539	7.67	
											150	3996	524	7.40	
											63				1)
											63				2)

S.M.T. is UTC-9h

1) Experiment, remaining was preserved in ethanol

2) Samples was used for experiments on board

Table 4.14-2. Data on plankton samples collected by vertical hauls with ring net. GG54: 0.335 mm mesh size.

Station no.	Position			S.M.T.		Length of wire (m)	Angle of wire (°)	Depth estimated by wire angle (m)	Kind of cloth	Remark
	Lat. (N)	Lon.		Date	Hour					
3	71-41.04	154-55.59	W	12 Sep.	12:06	93	2	93	GG54	Experiment, remaining to ethanol
4	71-44.17	155-10.81	W	12 Sep.	15:48	150	1	150	GG54	Experiment, remaining to ethanol
9	72-6.12	155-54.69	W	13 Sep.	8:58	150	3	150	GG54	Experiment, remaining to ethanol
10	72-28.18	155-31.48	W	13 Sep.	15:44	400	2	400	GG54	Experiment, remaining to ethanol
11	74-31.28	161-57.21	W	16 Sep.	11:10	500	2	500	GG54	Experiment, remaining to ethanol
12	73-0.86	159-37.46	W	17 Sep.	0:14	150	1	150	GG54	Experiment, remaining to ethanol
14	72-35.43	160-49.49	W	17 Sep.	12:22	41	2	41	GG54	Experiment, remaining to ethanol
15	72-43.33	157-54.73	W	17 Sep.	18:39	300	8	297	GG54	Experiment, remaining to ethanol
17	73-23.25	158-43.96	W	18 Sep.	15:29	500	1	500	GG54	Experiment, remaining to ethanol
18	73-9.73	154-41.47	W	18 Sep.	23:40	500	7	496	GG54	Experiment, remaining to ethanol
19	72-43.13	155-8.62	W	19 Sep.	13:46	500	10	492	GG54	Experiment, remaining to ethanol
20	71-48.65	153-16.62	W	19 Sep.	21:15	150	12	147	GG54	Experiment, remaining to ethanol
22	72-27.08	157-2.2	W	20 Sep.	14:34	300	5	299	GG54	Experiment, remaining to ethanol
23	72-1.38	158-31.09	W	20 Sep.	18:41	49	1	49	GG54	Experiment
24	72-3.42	161-23.27	W	21 Sep.	9:38	23	1	23	GG54	Experiment
25	71-31.32	162-27.42	W	21 Sep.	13:47	36	3	36	GG54	Experiment, remaining to ethanol
26	70-59.98	161-6.89	W	21 Sep.	19:00	39	8	39	GG54	Experiment, remaining to ethanol
27	71-26.43	164-57.07	W	22 Sep.	7:42	35	4	35	GG54	Experiment, remaining to ethanol
28	71-44.41	163-24.25	W	22 Sep.	15:05	33	5	33	GG54	Experiment, remaining to ethanol
29	71-45.8	166-21.59	W	22 Sep.	20:14	38	1	38	GG54	Experiment, remaining to ethanol
30	72-0.22	168-45.42	W	23 Sep.	8:52	44	8	44	GG54	Experiment, remaining to ethanol
31	72-3.84	167-57.78	W	23 Sep.	14:44	43	3	43	GG54	Experiment, remaining to ethanol
32	71-30	168-44	W	23 Sep.	18:31	41	9	40	GG54	Experiment, remaining to ethanol
33	71-00	166-38	W	24 Sep.	10:01	37	2	37	GG54	Experiment, remaining to ethanol
34	71-00	168-45	W	25 Sep.	7:53	37	4	37	GG54	Experiment, remaining to ethanol
35	70-30	168-45	W	25 Sep.	12:54	31	1	31	GG54	Experiment, remaining to ethanol
36	70-00	168-44.88	W	25 Sep.	15:56	33	7	33	GG54	Experiment, remaining to ethanol
37	70-00	166-39.12	W	25 Sep.	21:24	40	4	40	GG54	Experiment, remaining to ethanol
38	70-06	164-27.92	W	27 Sep.	8:21	30	1	30	GG54	Experiment, remaining to ethanol
39	69-21	166-14.27	W	27 Sep.	15:04	30	2	30	GG54	Experiment, remaining to ethanol
41	69-30	168-45.16	W	27 Sep.	21:38	44	0	44	GG54	Experiment, remaining to ethanol
42	69-00	168-45	W	28 Sep.	7:51	45	2	45	GG54	Experiment, remaining to ethanol
43	68-48.12	166-57.04	W	28 Sep.	14:11	46	3	46	GG54	Experiment, remaining to ethanol
44	68-30	168-44.88	W	28 Sep.	17:57	46	7	46	GG54	Experiment, remaining to ethanol
45	68-02	168-50	W	29 Sep.	7:51	51	4	51	GG54	Experiment, remaining to ethanol
46	67-30	168-44.63	W	29 Sep.	13:01	42	6	42	GG54	Experiment, remaining to ethanol
49	68-00	168-00	W	29 Sep.	17:57	47	3	47	GG54	Experiment, remaining to ethanol
54	67-36.07	166-29.94	W	30 Sep.	8:29	40	12	39	GG54	Experiment, remaining to ethanol
55	67-01.73	167-9.70	W	30 Sep.	13:48	33	6	33	GG54	Experiment, remaining to ethanol
56	67-00	168-45	W	30 Sep.	18:00	37	5	37	GG54	Experiment, remaining to ethanol
57	66-29.76	168-46.33	W	30 Sep.	22:23	42	6	42	GG54	Experiment, remaining to ethanol
58	65-59.73	168-45.16	W	1. Oct	7:51	43	10	42	GG54	Experiment, remaining to ethanol
59	65-29.96	168-45.12	W	1. Oct	13:26	44	5	44	GG54	Experiment, remaining to ethanol
60	65-5.69	169-31.13	W	1. Oct	16:41	41	4	41	GG54	Experiment, remaining to ethanol
61	64-43.52	170-25.55	W	1. Oct	21:37	40	0	40	GG54	Experiment, remaining to ethanol
62	64-18.93	171-18.24	W	2. Oct	9:00	38	5	38	GG54	Experiment, remaining to ethanol

S.M.T. is UTC-9h

(6) Preliminary results

As a preliminary results, we present following items.

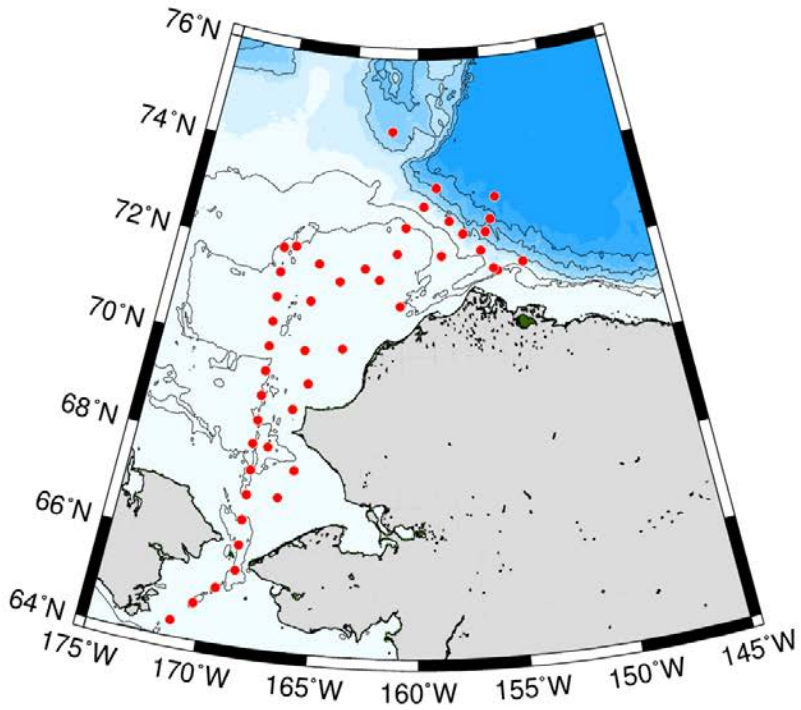

Fig. 4.14-1: Location of the zooplankton sampling stations in the Pacific sector of Arctic Ocean from 12 September to 2 October in 2021. Vertical hauls by both Quad-NORPAC net and ring net were made at all stations.

(7) Data archives

These data obtained in this cruise will be submitted to the Data Management Group of JAMSTEC, and will be opened to the public via "Data Research System for Whole Cruise Information in JAMSTEC (DARWIN)" in JAMSTEC web site.
<http://www.godac.jamstec.go.jp/darwin/e>

4.15. Phytoplankton

(1) Personnel
Kohei Matsuno (Hokkaido University) - Principal Investigator
Atsushi Yamaguchi (Hokkaido University), Not on board
Koki Tokuhiro (Hokkaido University), Not on board
Kohei Sumiya (Hokkaido University)
Wakana Endo (Hokkaido University)

(2) Objective
The goals of this study are following:
Clarifying the spatial distribution of phytoplankton and microprotist assemblages by multispectral excitation–emission fluorometer (MFL) and microscopy
Evaluating photosynthetic activity and cell viability by pulse-amplitude modulated fluorometer and double staining method.
Clarifying the spatial distribution of diatom resting stage cells in sediment

(3) Parameters
Phytoplankton community in cell number
Fluorescence by phytoplankton taxa
maximum photochemical efficiency (Fv/Fm)
alpha
maximum electron transport rate (ETRm)
IK
Living cell ratio

(4) Sampling and treatment
(4-1) Surface monitoring
A multi-spectral excitation/emission fluorometer (MFL, JFE-Advantech Co. Ltd.) was set in a black bucket. The surface water from a branch line of underway monitoring system was continuously flowing into the bucket from 3 September to 11 October. We took the surface water samples from underway system once a day for microscopic analysis, photosynthetic activity and cell viability. The water sample was fixed by glutaraldehyde (1% final concentration). The maximum photochemical efficiency (Fv/Fm) was measured using a pulse-amplitude modulated fluorometer (Water-PAM; Walz, Effeltrich, Germany) in sediment preservation room (3-5ºC). Samples (4 mL) for this analysis were placed in a quartz cuvette, and were acclimated in dark over 15 minutes. After the light-acclimation, the Fv/Fm of each sample was determined by red LED with a peak illumination at 650 nm. The measurements of the Fv/Fm were repeated twice for each sample. Then, the samples in the measuring cuvette were light-acclimated for several minutes using the internal actinic light source of the PAM fluorometer. After 30 s of

darkness, rapid light curves were obtained by illuminating the samples for 10 s before each ΔF/Fm' measurement at each of a series of eight irradiances that increased in steps from 92 to 1352 lmol photons m^{-2} s^{-1}. After measuring photosynthetic activity by PAM, the sample was vacuum-filtrated (< 0.013 MPa) on a black Nuclepore filter with Bac-light viability Kit (Molecular Probes Invitrogen), placed in slides and maintained frozen at -20 ºC for measuring living cell ratio.

(4-2) Spatial distribution by Niskin sampler and bucket

Sea water samples (1 L) were collected from 0, chlorophyll *a* maximum layer (SCM) and bottom -5 m or 200 m by bucket and Niskin water sampler at 45 stations (Fig. 4.15-1, Table 4.15-1). The water samples were fixed by glutaraldehyde (1% final concentration) for microscopic analysis. In the land laboratory, the samples will be concentrated to 20 mL with a syphon, and microprotists will be enumerated and identified under an inverted microscopy. Additionally, seawater samples (20 mL) for measuring photosynthetic activity and cell viability (see detail method in above section). A MFL was attached on the CTD frame to measure the vertical profile of phytoplankton taxonomic composition.

(4-3) Sediment sampling

Sea bottom sediments were collected by a multiple corer system (Ashura) at 12 stations in the Pacific sector of Arctic Ocean (Fig. 4.15-1, Table 4.15-2). Detail operation of the Ashura was referred in 4.13.3. After sampling, water above the sediment was collected by a syphon for microscopic observation, photosynthetic activity and cell viability as same as water samples by Niskin water sampler. Surface sediment (0-1 cm) were cut and preserved in dark and cool (~4ºC) condition for diatom resting stage cells and dinoflagellates (by Dr. Satoshi Nagai in Japan Fisheries Research and Education Agency and Dr. So-Young Kim in KOPRI). An aliquot from the surface was frozen for chlorophyll a measurement. The other aliquot from surface (0-1 cm) and bottom layer (4-32 cm depending on core length) in each core were frozen for bacteria analysis (by Dr. Satoshi Nagai in Japan Fisheries Research and Education Agency).

(5) Station list

Table 4.15-1: Data on water samples collected by Niskin water sampler and bucket. Circles indicate MFL was attached on the CTD frame.

St.	Date	Latitude (°N)		Longitude (°W)		Sampling depth (m)	MFL
3	12 Sep.	71	41.04	154	55.59	0, 15.8, 95.5	○
4	12 Sep.	71	44.17	155	10.81	0, 15.6, 282.6	○
9	12 Sep.	72	6.12	155	54.69	0, 21.6, 99.1	○
10	12 Sep.	72	28.18	155	31.48	0, 23, 1820.9	
11	16 Sep.	74	31.28	161	57.21	0, 44.6, 200	○
14	17 Sep.	72	35.44	160	50	0, 17.8, 43.1	○
15	17 Sep.	72	43.25	157	54.47	0, 20.9, 200	○
17	18 Sep.	73	23.25	158	43.96	0, 46.7, 200	
19	19 Sep.	72	43.13	155	8.62	0, 30.4, 200	
20	19 Sep.	71	48.65	153	16.62	0, 15.6, 200	○
22	20 Sep.	72	27.08	157	2.2	0, 13.9, 200	
23	20 Sep.	72	1.38	158	31.09	0, 31.2, 50.3	○
24	21 Sep.	72	3.42	161	23.27	0, 20.2, 25.3	○
25	21 Sep.	71	31.32	162	27.42	0, 15.2, 37	○
26	21 Sep.	70	59.98	161	6.89	0, 18.1, 40.6	○
27	22 Sep.	71	26.43	164	57.07	0, 18.6, 36.4	○
28	22 Sep.	71	44.41	163	24.25	0, 15.7, 35.5	○
29	22 Sep.	71	45.8	166	21.59	0, 14.9, 39.4	○
30	23 Sep.	72	0.22	168	45.42	0, 15, 45.1	○
31	23 Sep.	72	3.84	167	57.78	0, 15.9, 44	○
32	23 Sep.	71	30	168	44	0, 17.7, 42.6	○
33	24 Sep.	71	0.04	166	38.38	0, 12.8, 39	○
34	25 Sep.	71	0	168	44.98	0, 12.8, 38.7	○
35	25 Sep.	70	29.92	168	44.84	0, 14.8, 32.8	○
36	25 Sep.	70	0	168	44.88	0, 14.9, 35.3	
37	25 Sep.	70	0.27	166	39.12	0, 17.9, 38	○
38	27 Sep.	70	6.02	164	27.92	0, 12.2, 30.9	○
39	27 Sep.	69	21.03	166	14.27	0, 7, 31.1	○
41	27 Sep.	69	29.97	168	45.16	0, 11.8, 45.8	○
42	27 Sep.	69	0.07	168	45.09	0, 14, 46.9	○
43	28 Sep.	68	48.12	166	57.04	0, 14.8, 35.3	○
44	28 Sep.	68	30.04	168	44.88	0, 6.9, 47.7	○
45	29 Sep.	68	1.99	168	49.96	0, 14.9, 51.9	○
46	29 Sep.	67	30.01	168	44.63	0, 21.3, 43.9	○
49	29 Sep.	68	0.1	168	0.43	0, 6.6, 48.7	○
53	29 Sep.	68	18.11	167	3.38	0, 11.8, 33.7	
54	30 Sep.	67	36.07	166	29.94	0, 12, 40.5	○
55	30 Sep.	67	1.73	167	9.7	0, 10, 34.1	○
56	30 Sep.	67	0	168	45	0, 10.1, 39.8	○
57	30 Sep.	66	29.76	168	46.33	0, 7.5, 47.8	○
58	1 Oct.	65	59.73	168	45.16	0, 21.6, 46.8	○
59	1 Oct.	65	29.9	168	45.12	0, 8.5, 48.6	○
60	1 Oct.	65	5.69	169	31.13	0, 28.5, 44.5	○
61	1 Oct.	64	43.52	170	25.55	0, 17, 44.1	○
62	2 Oct.	64	18.93	171	18.24	0, 14.9, 40.5	○

Table 4.15-2: Station list of sediments samples collected with Multiple corer system (Ashura) at 12 stations in the Pacific sector of Arctic Ocean from September to October 2021.

St.	Date	Latitude (°N)	Longitude (°W)	Bottom depth (m)	Sampling depth (cm)
9	13 Sep.	72-6.12	155-54.69	209	0-1, 25-26
14	17 Sep.	72-35.43	160-49.49	49	0-1, 31-32
24	21 Sep.	72-3.42	161-23.27	31	0-1, 4-5
28	22 Sep.	71-44.41	163-24.25	41	0-1, 17-18
31	23 Sep.	72-3.84	167-57.78	50	0-1, 25-26
33	24 Sep.	71-00	166-38	45	0-1, 17-18
35	25 Sep.	70-30	168-45	39	0-1, 16-17
38	27 Sep.	70-06	164-27.92	36	0-1, 11-12
42	28 Sep.	69-00	168-45	53	0-1, 25-26
45	29 Sep.	68-02	168-50	59	0-1, 27-28
54	30 Sep.	67-36.07	166-29.94	47	0-1, 28-29
58	1. Oct	65-59.73	168-45.16	53	0-1, 6-7

(6) Preliminary results

As a preliminary results, we present following items.

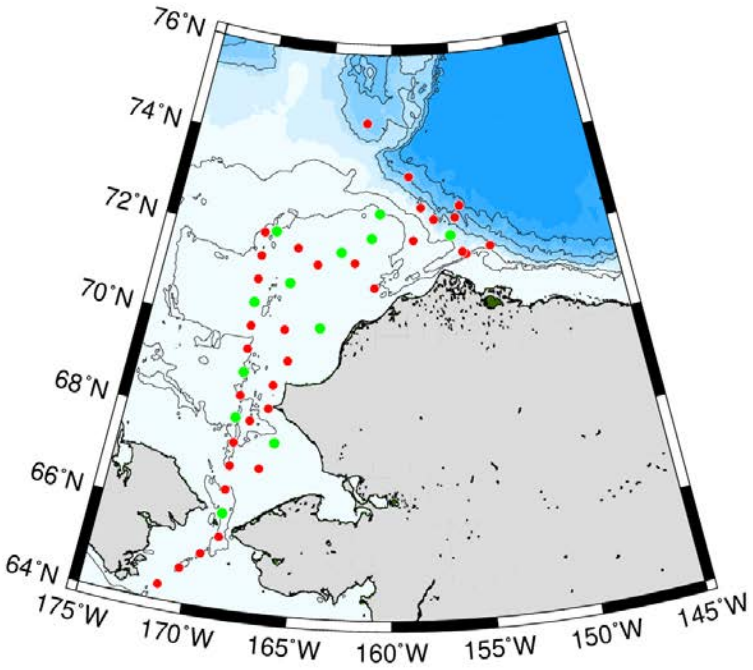

Fig. 4.15-1: Location of the water, MFL and sediment sampling stations in the Pacific sector of Arctic Ocean (red circles: CTD+bucket, green circles: CTD+bucket+sediment).

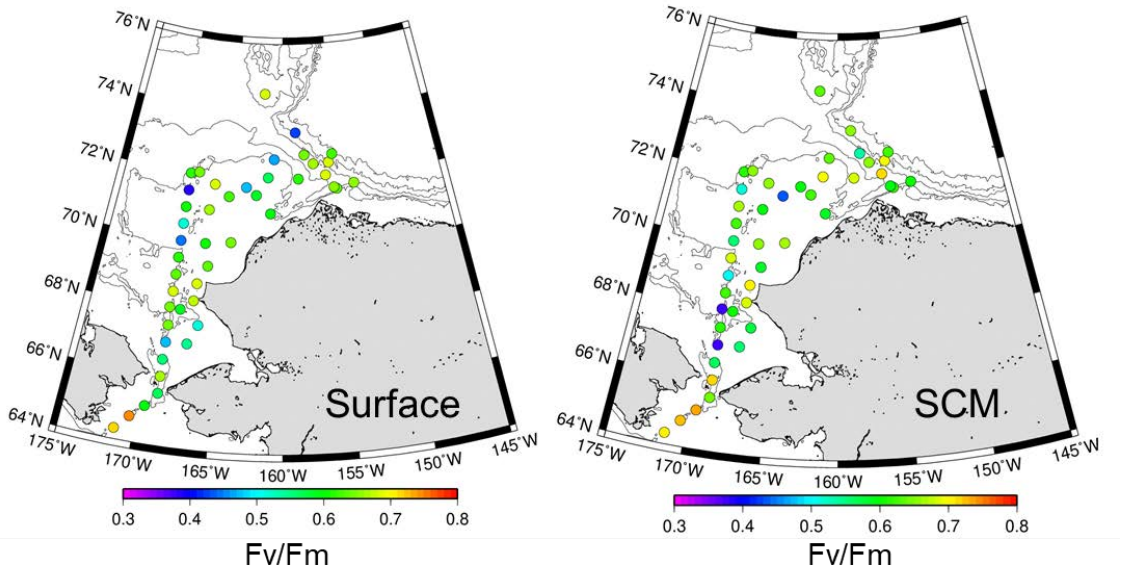

Fig. 4.15-2: Spatial distribution of the maximum photochemical efficiency (Fv/Fm) at the surface and the sub-surface chlorophyll-*a* maximum layer (SCM).

(7) Data archives

These data obtained in this cruise will be submitted to the Data Management Group of JAMSTEC, and will be opened to the public via "Data Research System for Whole Cruise Information in JAMSTEC (DARWIN)" in JAMSTEC web site.
<http://www.godac.jamstec.go.jp/darwin/e>

4.16. Bio-optical observations

(1) Personnel

Amane Fujiwara (JAMSTEC) -Principal Investigator

(2) Objectives

The objective of these observations is to develop and evaluate ocean color algorithms to estimate phytoplankton community composition and algal size using optical properties of seawater as well as investigating in-situ phytoplankton community structure and in-water optical properties. Results from these investigations will be applied to satellite remote sensing and used to clarify the responses of phytoplankton to the recent climate change in the western Arctic Ocean.

(3) Parameters

Surface and underwater spectral radiance and irradiance

Phytoplankton pigments and absorption coefficient

Underway measurement of Multi-spectral excitation/emission fluorescence

(4) Instruments and methods

Surface and underwater spectral radiance and irradiance

Underwater spectral downwelling planar irradiance, $E_d(\lambda, z)$ [μW cm^{-2} nm^{-1}], and upwelling radiance, $L_u(\lambda, z)$ [μW cm^{-2} nm^{-1} str^{-1}], at 17 wavelengths over the spectral range 380 – 765 nm were measured using a C-OPS spectroradiometer (Biospherical Instrument Inc.). The C-OPS was deployed in free-fall mode up to ~100 m deep at a distance from the stern of ship to avoid ship shadows. Downwelling irradiance incident upon the sea surface $E_d(\lambda, z = 0+)$ was also monitored by a reference sensor with the same specifications as the underwater sensor. Before each deployment of the instrument, 30 seconds of averaged dark values were recorded. Underwater photosynthetically available radiation (PAR) was also calculated by converting the $E_d(\lambda, z)$ to quantum units, $E_{d,q}(\lambda, z)$ [μmol photons m^{-2} s^{-1}], and integrating the $E_{d,q}(\lambda, z)$ from 395 to 710 nm.

B) Seawater samples for phytoplankton pigments were collected from the sea surface and other depths using Niskin-X bottles on the CTD/R. 1 – 4 L of water sample were filtered onto a glass fiber filter (GF/F, 47 mm) and stored in liquid nitrogen. Pigment concentrations will be analyzed on land using high performance liquid chromatography (HPLC) (Agilent Technologies 1300 series) following to the method of van Heukelem and Thomas (2001) after the cruise.

Seawater samples for absorption coefficients measurement were collected from the sea surface. For measurements of spectral absorption coefficient of particles, particles in 1-4 liter(s) of water sample were concentrated on a glass fiber filter (Whatman GF/F, 25 mm). Filter samples were stored in liquid nitrogen. Optical density (OD) of particles on

the filter pad will be measured on land with a spectrophotometer following to the method of Stramski et al. (2015), and then, absorption coefficient of particles ($a_p(\lambda)$), detritus ($a_d(\lambda)$), and phytoplankton ($a_{ph}(\lambda)$) we be determined. For measurements of spectral absorption coefficient of CDOM ($a_{CDOM}(\lambda)$), ~300 ml of water sample was filtrated through a 0.2 µm Nuclepore filter (Whatman, 47 mm). Filtered water samples were stored in a refrigerator until analysis on land. $a_{CDOM}(\lambda)$ will also be measured using a spectrophotometer.

C) Horizontal distribution of multi-spectral excitation/emission fluorescence was measured using a *Multi-Exciter* instrument (JFE-Advantech Inc.). *Multi-Exciter* detects fluorescence signals from 630 to 1000 nm which excited at 9 bands (375, 400, 420, 435, 470, 505, 525, 570, and 590 nm). The *Multi-Exciter* was attached to the continuous surface water monitoring system and measured the spectral fluorescence of surface water for every 15 minutes along the cruise track. 28 HPLC samples were also taken from continuous surface water monitoring system to compare the fluorometric signals and phytoplankton pigment composition.

(5) Station list and sampling location

Table 4.16-1. Number of instrument deployments or discrete water samples collected for each parameter on the cruise.

Instrument	*Number of stations*
C-OPS	7
Parameter	*Number of samples*
$a_p(\lambda)$, $a_d(\lambda)$, $a_{ph}(\lambda)$,	17
$a_{CDOM}(\lambda)$	17
Phytoplankton pigments (HPLC)	95 (67 for vertical, 28 for surface)

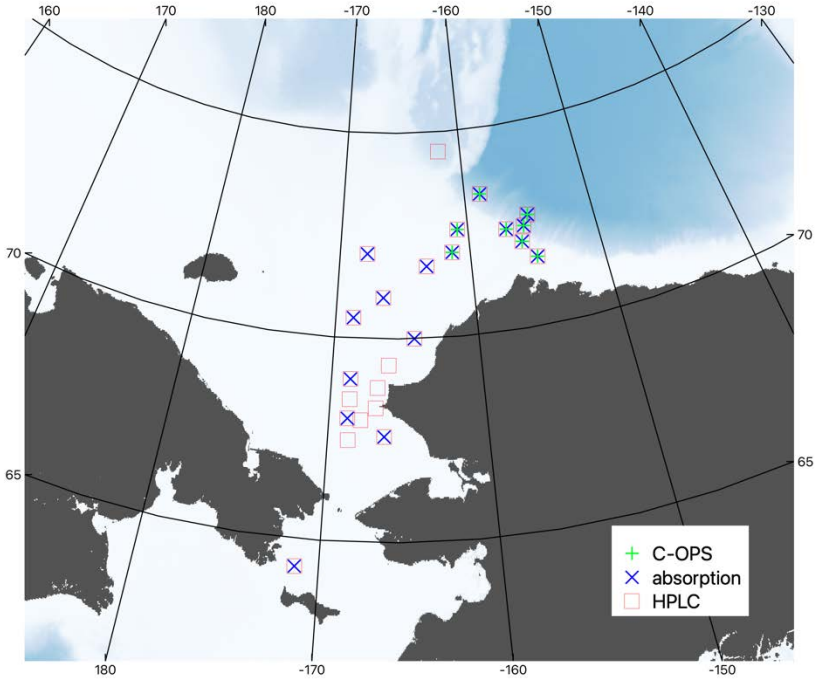

Figure 4.16-1: Sampling locations of bio-optical observations. Red squares, blue crosses and green pluses indicate the sites where samples/data for HPLC, absorption coefficient and in-water radiance/irradiance were collected, respectively.

(6) Data archives

These data obtained in this cruise will be submitted to the Data Management Group of JAMSTEC, and will be opened to the public via "Data Research System for Whole Cruise Information in JAMSTEC (DARWIN)" in JAMSTEC web site.
<http://www.godac.jamstec.go.jp/darwin/e>

(7) References cited

Stramski, D., R. A. Reynolds, S. Kaczmarek, J. Uitz and G. Zheng. 2015. Correction of pathlength amplification in the filter-pad technique for measurements of particulate absorption coefficient in the visible spectral region. *Appl. Opt.*, 54, 6763-6782. doi: 10.1364/AO.54.006763.

Van Heukelem, L, Thomas C. S. 2001. Computer-assisted high-performance liquid chromatography method development with applications to the isolation and analysis of phytoplankton pigments. *J Chromatogr A*, 910, 31–49.

4.17. Environmental DNA

(1) Personnel

Tatsuya Kawakami	Hokkaido University	- Principal Investigator
Makoto Ozaki	Hokkaido University	
Akihide Kasai	Hokkaido University	- not on board

(2) Objectives

Analyzing environmental DNA (eDNA) of macro-organisms is a promising approach to reveal the response of the Arctic ecosystem to recent global climate change. In the last cruise, we successfully detected fish eDNA from surface seawater collected in the Arctic Ocean and demonstrated the usefulness of eDNA for understanding the hidden link between fish community structure and oceanographic environments. On the other hand, experimental comparison among replicate samples indicated that optimization of sampling effort is required to improve the detection probability of fish eDNA. Furthermore, various environments such as floating sea ice possibly contain macro-organism's DNA, but it has not been testified.

Therefore, we collected eDNA samples through this cruise to accomplish the aims listed below.

To obtain a comprehensive view of fish community structure in the basin scale.

To clarify the spatial distribution of common fish species in the Arctic region corresponding to the oceanographic environment.

To optimize the sampling effort for the detection of fish eDNA.

To testify the filtration of the mass volume of seawater for improving the efficacy of eDNA collection.

To evaluate the potential of untested environments (sea ice and seawater just above the seafloor) as a source of macro-organism's eDNA.

(3) Parameters

Environmental DNA

(4) Instruments and methods

(4.1) eDNA collection from seawater

Surface seawater continuously pumped up from about 5 m depth for the underway sea-surface monitoring was routinely collected through the cruise. The collection was performed twice a day, around sunrise and sunset. Seawater was also collected using 12 L Niskin bottles mounted on the CTD/Carousel Water Sampling System at 30 stations from several depths, including the bottom layer. When the CTD observation was conducted, pumped seawater was concurrently collected.

Twenty liters of water samples were collected in 5 L plastic tanks or 10 L foldable plastic

bags at each water collection. The 5 L of each water sample was filtered through 0.45 μm pore size cartridge filters (Sterivex™ HV, Millipore, Billerica, MA, USA) in four replicates using a peristaltic tubing pump (Masterflex 07528-10, Cole-Parmer, IL, USA) at a flow rate of 100 ml/min. After filtration, the filters were filled with 2.0 ml of RNA later and then stored at −20 °C. Accordingly, eDNA samples were obtained from 77 sites (Table 4.17-1).
All sampling equipment and working space were decontaminated using bleach solution before use, and new nitrile gloves were worn at each water sampling to minimize cross-contamination. Further, 500 mL of Milli-Q water was also filtered as a negative control for every 3–5 sites to check for cross-contamination during the filtration process.

(4.2) Replicate sampling and size fraction
Additional water collection was performed at four sites (Table 4.17-2: St. 32, St. 35 and St. 45 in the Arctic Ocean, St. 62 in the Bering Sea) to collect eDNA samples as complements to the replicate sampling conducted in the last cruise (MR20-05C) that aimed to determine the optimal sampling effort and evaluate the efficacy of replicate sampling to improve detection probability of fish eDNA. Seawater was collected from pumped surface seawater and the Niskin sampler. Eight filtering replicates of the 0.45 μm filter were collected at each site, except St. 35 where seawater was filtered in four replicates. Furthermore, to compare eDNA capture efficiency between two filters having different pore sizes, replicate sampling using 0.22 μm pore size cartridge filters (Sterivex™ GV, Millipore, Billerica, MA, USA) was also conducted in St. 62. Subsequently, size fractioned eDNA was also collected in St. 35 and St. 45 by sequential filtration using the 0.22 μm pore size filter following filtration using the 0.45 μm pore size filter. Water collection, filtration, and preservation were conducted in the same manner as 4.1.

(4.3) Mass filtration
Mass filtration experiments up to 100 L were performed at nine sites (Table 4.17-2). The pumped-up surface seawater was filtered onto a high-capacity capsule filter (AS-ONE CF-45PT, 0.45 μm pore size) using a peristaltic tubing pump. Filtration speed was measured using an instantaneous/accumulated flow sensor (NW05-NTN, Aichi tokei, Japan), approximately 1 L/min. Filters were stored at −80 °C without any preservation buffer after filtration.

(4.4) eDNA collection from sea ice
Floating sea ice was collected at ICE1, ICE3, and ICE4 (Table 4.17-2). The ice mass was dissected into several blocks and gently melted at 4℃ in a clean plastic bag individually. The meltwater was measured for salinity and subsampled for nutrients and chlorophyll-a concentration measurement. Subsequently, the meltwater was filtered and preserved following the method described in 4.1. To compare eDNA capture efficiency from the

meltwater, two filters having different pore sizes (0.22 μm and 0.45 μm) were used for filtration.

(4.5) eDNA collection from seawater just above the bottom sediments

Seawater just above the bottom sediments was collected at St. 45 and St. 54 from the sediment core sample obtained using a multiple corer system (Ashura) (Table 4.17-2). The detailed operation was described in 4.13.3. The water was sequentially filtered using nylon net filters (20 and 10 μm mesh size), an MCE filter (3 μm pore size) and a Sterivex-GV filter (0.22 μm) using a peristaltic tubing pump at a flow rate of 100 mL/min.

(5) Station list

Table 4.17-1: List of sampling sites for eDNA collection from pumped-up surface seawater and seawater collected using Niskin samplers attached to a CTD.

Site (CTD Station)	Date (UTC)	Latitude (N)	Longitude (E)	Bottom depth (m)	Sampling depth (m)
NP01	1-Sep	36.56	142.95	6540	5
NP02	1-Sep	38.04	145.19	5361	5
NP03	1-Sep	39.70	147.79	5337	5
NP04	2-Sep	41.67	150.95	5298	5
NP05	2-Sep	43.53	154.01	5409	5
NP06	3-Sep	44.79	156.15	5071	5
NP07 (St.01)	4-Sep	46.88	159.79	5090	5, 21
NP08	4-Sep	49.13	164.17	5590	5
NP09	5-Sep	50.66	167.31	2509	5
NP10	5-Sep	52.33	169.41	5088	5
BS01	6-Sep	53.42	170.62	948	5
BS02	6-Sep	54.69	172.45	2886	5
BS03	6-Sep	56.56	176.25	3835	5
BS04	7-Sep	58.27	177.96	3770	5
BS05	7-Sep	60.58	181.80	161.1	5
BS06	7-Sep	61.75	183.85	99.1	5
BS07	8-Sep	64.60	189.74	47.2	5
BS08	8-Sep	65.72	191.62	54.9	5
AO01	9-Sep	69.77	192.85	46.7	5
AO02	10-Sep	70.88	198.18	43.3	5
AO03	10-Sep	71.67	204.99	107	5
AO04	11-Sep	71.84	204.43	138	5
AO05	12-Sep	71.70	204.15	117.7	5
AO06 (St.02)	12-Sep	71.59	205.19	39.3	5

Table 4.17-1: Continued.

Site (CTD Station)	Date (UTC)	Latitude (N)	Longitude (E)	Bottom depth (m)	Sampling depth (m)
AO07 (St.03)	12-Sep	71.68	205.08	96.4	5, 30, 95
AO08 (St.04)	12-Sep	71.74	204.80	305.6	5, 30, 283
AO09 (St.05)	13-Sep	71.80	204.71	194.8	5, 30, 190
AO10 (St.09)	13-Sep	72.10	204.09	209	5, 30
AO11 (St.10)	14-Sep	72.48	204.42	1831	5, 50, 200, 400, 1000, 1820
AO12	15-Sep	72.54	202.98	682	5
AO13 (St.11)	15-Sep	74.53	198.08	1689	5, 50, 200, 400, 1000, 1675
AO14	17-Sep	73.97	198.18	333	5
AO15 (St.14)	17-Sep	72.60	199.17	49.2	5, 30, 43
AO16 (St.15)	18-Sep	72.72	202.09	379.6	5
AO17 (St.17)	18-Sep	73.40	201.29	2212	5, 50
AO18 (St.19)	19-Sep	72.72	204.87	2970	5, 50
AO19 (St.20)	20-Sep	71.81	206.73	238	5, 30
AO20 (St.22)	20-Sep	72.46	203.01	468	5, 30, 450
AO21 (St.23)	21-Sep	72.02	201.47	56.2	5, 50
AO22 (St.24)	21-Sep	72.06	198.62	31.1	5, 25
AO23 (St.26)	22-Sep	71.00	198.89	46.6	5, 40
AO24 (St.27)	22-Sep	71.44	195.05	42.3	5, 36
AO25 (St.28)	22-Sep	71.74	196.60	40.2	5, 35
AO26 (St.29)	23-Sep	71.76	193.64	44.8	5, 39
AO27 (St.31)	23-Sep	72.06	192.04	50.2	5, 44
AO28 (St.33)	24-Sep	71.00	193.36	44.9	5, 39
AO29 (St.34)	25-Sep	71.00	191.25	44.5	5, 39
AO30 (St.36)	26-Sep	70.00	191.29	40.9	5, 35
AO31 (St.37)	26-Sep	70.00	193.33	47	5, 38
AO32 (St.38)	27-Sep	70.00	195.54	35.6	5, 31
AO33 (St.39)	27-Sep	69.35	193.76	37.4	5, 31
AO34 (St.42)	28-Sep	69.00	191.25	53	5, 47
AO35 (St.53)	30-Sep	68.30	192.94	39.4	5, 34
AO36 (St.54)	30-Sep	67.60	193.52	46.5	5, 40
AO37 (St.56)	1-Oct	67.00	191.23	46.1	5, 40
AO38 (St.58)	1-Oct	65.96	191.24	52.8	5, 47
BS09 (St.60)	2-Oct	65.09	190.48	50.7	5, 45
BS10	3-Oct	63.61	192.26	30.4	5
BS11	3-Oct	60.60	191.80	31.1	5
BS12	4-Oct	59.74	191.87	37.8	5
BS13	4-Oct	57.77	192.73	67.2	5
BS14	6-Oct	54.36	192.54	766	5
BS15	6-Oct	53.88	187.19	3442	5
BS16	8-Oct	53.70	185.81	3645	5
BS17	8-Oct	53.50	183.33	3758	5
BS18	9-Oct	53.25	180.54	1566	5

Table 4.17-1: Continued.

Site (CTD Station)	Date (UTC)	Latitude (N)	Longitude (E)	Bottom depth (m)	Sampling depth (m)
BS19	9-Oct	52.88	176.61	3928	5
NP11	10-Oct	51.72	173.58	4442	5
NP12	10-Oct	50.28	170.31	4835	5
NP13	11-Oct	49.56	168.72	4511	5
NP14	11-Oct	48.90	167.40	5591	5
NP15	12-Oct	48.31	166.02	5880	5
NP16	12-Oct	47.41	164.13	5776	5
NP17	13-Oct	45.39	159.53	5206	5
NP18	14-Oct	42.97	154.55	5440	5
NP19	15-Oct	40.60	149.81	5439	5
NP20	16-Oct	38.98	146.67	5218	5

Table 4.17-2 List of stations where replicate sampling, size fraction experiment, mass filtration experiment, and water collection from floating sea ice and Ashura samples for eDNA collection was performed.

Purpose	Site	Date (UTC)	Latitude (N)	Longitude (E)	Bottom depth (m)
Replicate sampling and size fraction	St.35	25-Sep	70.50	191.25	38.8
	St.45	29-Sep	68.03	191.17	59
Replicate sampling	St.32	23-Sep	71.50	191.25	48.4
	St.62	2-Oct	64.32	188.70	46
Mass filtration	NP04	2-Sep	41.67	150.95	5298
	BS03	6-Sep	56.81	175.64	3023
	BS06	8-Sep	62.32	184.90	76.7
	St.10	14-Sep	72.47	204.48	1913
	St.11	15-Sep	74.52	198.08	1686
	St.37	26-Sep	70.00	193.34	47.3
	St.58	1-Oct	65.61	191.39	50.2
	BS12	4-Oct	59.38	192.11	39.7
	NP21	18-Oct	37.42	143.74	7806
eDNA collection from sea ice	ICE1	17-Sep	72.59	199.15	46
	ICE3	22-Sep	71.76	196.61	40.2
	ICE4	23-Sep	72.07	192.10	50.2
eDNA collection from seawater just above the bottom sediments	St.45	29-Sep	68.03	191.17	59
	St.54	30-Sep	67.60	193.52	47

(6) Preliminary results

During the cruise, eDNA samples from surface water were obtained from 77 sites across the North Pacific Ocean (20 sites), the Bering Sea (19 sites), and the Arctic Ocean (38

sites) (Fig. 4.17-1). eDNA samples from the bottom layer or water column were also collected at 31 sites using Niskin samplers (Fig. 4.17-1). These samples will be the subject of metabarcoding analysis to clarify the species composition of fishes and their regional differences. Quantitative PCR (qPCR) will also be used for species-specific detection of eDNA of common Arctic fishes (e.g., salmons, cods, flatfishes) to track their distribution and to estimate their abundance. Replicate sampling, size fraction, and mass filtration (Fig. 4.17-2) will provide valuable information to standardize the eDNA sampling method in the Arctic region. eDNA from sea ice and water just above the bottom sediments will also be analyzed to find their potential as an eDNA source. Integrating the results and oceanographic conditions observed in this cruise will contribute to clarifying how the environmental change influences the Arctic ecosystem.

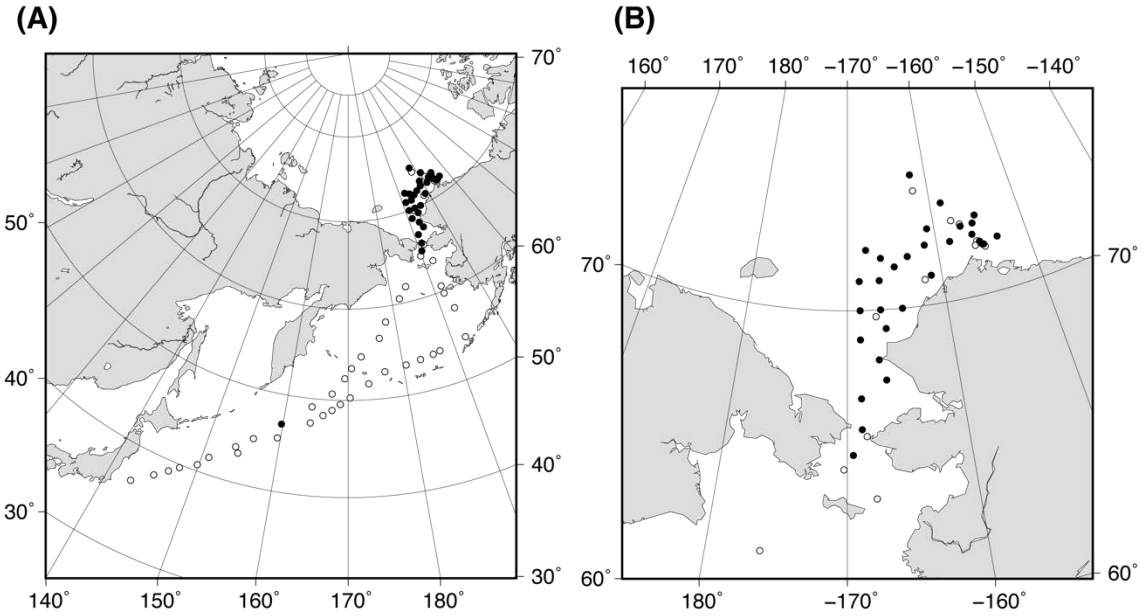

Fig. 4.17-1: Map showing the sites where eDNA samples were collected from pumped-up surface water (white circles) and both pumped-up surface water and seawater collected using Niskin samplers (black circles). (A) Locations of the sampling sites during the whole cruise. (B) Locations of the sampling sites in the Arctic region.

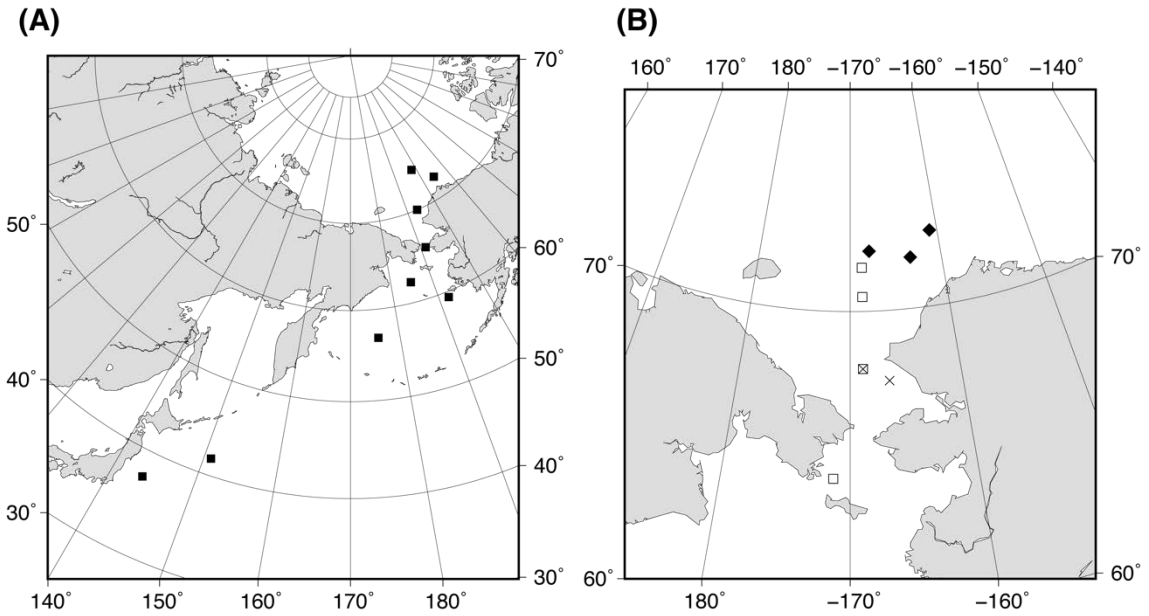

Fig. 4.17-2: Map showing the sites where additional experimental filtrations were conducted. (A) Locations of the sites where the mass filtration experiment was performed (black squares). (B) Locations of the sites where the replicate sampling with size fractioning was performed (white squares), and floating sea ice (black diamonds) and seawater just above the bottom sediments (crosses) were collected for eDNA sampling.

(7) Data archives

These data obtained in this cruise will be submitted to the Data Management Group of JAMSTEC, and will be opened to the public via "Data Research System for Whole Cruise Information in JAMSTEC (DARWIN)" in JAMSTEC web site.
<http://www.godac.jamstec.go.jp/darwin/e>

4.18. Microplastic samplings

(1) Personnel

Ryota Nakajima (JAMSTEC): Principal investigator (not onboard)
Amane Fujiwara (JAMSTEC)
Motoyo Itoh (JAMSTEC)
Jonaotaro Onodera (JAMSTEC)

(2) Objective

The distribution of microplastic in the open ocean of the Arctic Ocean is largely undocumented. Substantial numbers of studies on microplastics have been reported in the Pacific and Atlantic Oceans, yet very few data are available in the polar oceans. In the present study, we conducted microplastic surveys along the cruise track to fill gaps in the Arctic Ocean.

(3) Method

(3-1) *Neuston net sampling for surface microplastic analysis*

Floating microplastic samples were collected using a neuston net with a square mouth opening of 75 cm height and 75 cm width, equipped a 333 μm mesh opening net with a collecting bottle at the cod end. At each station, the net was towed once for 20 min each along the surface of the starboard side. The trawl speed ranged between 1 and 2 knots. A flow meter was installed at the net mouth to estimate the volume of water filtered during each tow. The collected samples were fixed with 5% formalin and stored at room temperature until analysis.

(3-2) *Sea floor sediment sampling for microplastic analysis*

An Ashura corer was used to collect microplastics in the sea floor sediment (see 4.13.3 for the detailed sediment sampling method). Nepheloid layer (suspended sediment layer) and surface sediment (top ca. 5 cm of sediment core) were taken from the sediment core samples and stored in a freezer until analysis.

(3-3) *Sea ice sampling for microplastic analysis*

A wire mesh pallet cage (1.2 x 1.0 x 0.9 m) connected to the ship's crane was used to collect microplastics in the sea ice (see 4.19 for the sea ice sampling method). Sea ice was broken into ca. 500 g weight size and stored in a freezer until analysis.

Microplastic samples will be subjected to enumeration and identification of plastic types using a microscope and FT-IR. The microplastics will also be weighed for mass calculation. The distribution, density and concentration of microplastic in this study will be compared with the previous reports in the Arctic Ocean.

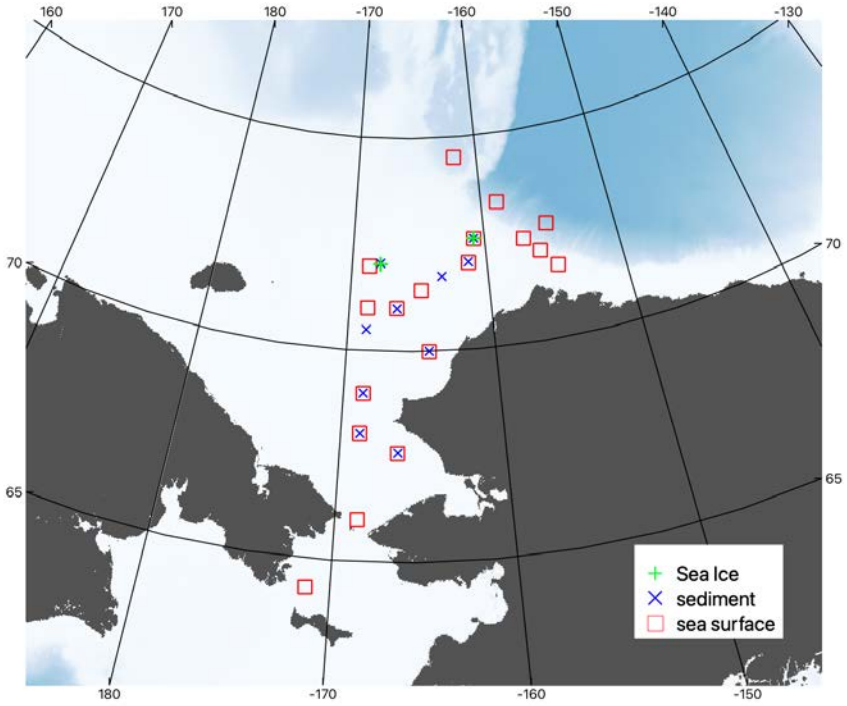

Figure 4.18-1: Position of the microplastic samplings. Green pluses, blue crosses, red squares indicate the sites where microplastic samplings from sea ice, sea floor, and sea surface were conducted, respectively.

(4) Data archives

These data obtained in this cruise will be submitted to the Data Management Group of JAMSTEC, and will be opened to the public via "Data Research System for Whole Cruise Information in JAMSTEC (DARWIN)" in JAMSTEC web site.
<http://www.godac.jamstec.go.jp/darwin/e>

4.19. Sea Ice Biogeochemistry

4.19.1. Sea ice sampling

(1) Personnel

Daiki Nomura (Hokkaido University) – Principal investigator
Manami Tozawa (Hokkaido University)
Mariko Hatta (JAMSTEC)
Tatsuya Kawakami (Hokkaido University)
Kohei Matsuno (Hokkaido University)
Wakana Endo (Hokkaido University)
Takuhei Shiozaki (The University of Tokyo)
Amane Fujiwara (JAMSTEC)
Takeshi Kinase (JAMSTEC)
Masato Ito (National Institute of Polar Research), not onboard
Sohiko Kameyama (Hokkaido University), not onboard

(2) Objective

Arctic sea ice is changing dramatically, with rapid declines in summer sea ice extent and a shift towards younger and thinner first-year ice rather than thick multi-year ice. Although the effects of sea ice formation and melting on biogeochemical cycles in the ocean have previously been discussed, the effects of sea ice melt processes on biogeochemistry for the surface ocean of the Arctic Ocean is still largely unknown. Therefore, in this study, we have collected sea ice and snow samples.

(3) Parameters

Ice temperature
Ice salinity
carbonate chemistry (DIC and TA)
Methane (CH_4)
DMS
DMSP (DMSPt, DMSPd)
Oxygen isotopic ratio
Nutrients
Dissolved oxygen
Turbidity
Chl.a
eDNA
Particle amount
Ice algae composition
Bacterial DNA
POC/PON

CDOM
Flow cytometry
Mineral composition
Thin section analysis

(4) Instruments and methods

Sea ice samples (less than 1 m^3) were collected at three sites (Table 4.19-1) using a wire mesh pallet cage (1.2 x 1.0 x 0.9 m) connected to the ship's crane. Temperature of ice (outside and inside) samples were measured by a needle-type temperature sensor (Testo 110 NTC, Brandt Instruments, Inc., USA) immediately after the sea ice sampling. Snow samples on deck were collected when it snowed for salinity and $\delta^{18}O$. By using Rinko profiler (model ASTD152, JFE Advantech, Japan), surface water (<10 m) temperature, salinity, dissolved oxygen concentration, turbidity, and chl.a concentration were measured for each site.

Sea ice were cut into small size (0.15 x 0.15 x 0.15 m) and melted in the gas-tight bags (AAK10, GL Science, Japan) in the dark and cool condition. Snow samples were melted in the ziploc type bags in the dark and cool condition. For each sample, sample ID was assigned (Table 4.19-2).

The salinity of melted sea ice and snow were measured with a conductivity sensor (Cond 315i, WTW, Germany). By using Rinko profiler (model ASTD152, JFE Advantec, Japan), dissolved oxygen concentration, turbidity, and chl.a concentration were measured for ice meltwater. Meltwater were subsampled into (1) a 250-mL glass vial (Duran Co., Ltd., Germany) for measurement of carbonate chemistry (DIC and TA), (2) a 120-mL glass vial (Maruemu Co., Ltd., Japan) for measurement of CH_4, (3) a 30-mL glass vial (Maruemu Co., Ltd., Japan) for measurement of DMS and DMSP, (4) a 15-mL glass screw-cap vial (Nichiden-Rika Glass Co. Ltd, Japan) for measurement of $\delta^{18}O$, (5) a 10-mL polyethylene screw-cap vial (Eiken Chemical Co. Ltd, Japan) for nutrient and mineral composition, (6) a 200-mL Nalgene polycarbonate bottle (Thermo Fisher Scientific Inc., USA) for particle amount, (7) a 500-mL Nalgene polycarbonate bottle (Thermo Fisher Scientific Inc., USA) for ice algae composition, (8) a 120-mL glass vial (Maruemu Co., Ltd., Japan) for measurement of CDOM, and (9) a small cryovial for Flow cytometry. Samples for chl.a, bacterial DNA, eDNA, and POC/PON were filtered. Each sample (water and filter) was stored followed by the protocol for each parameter until analysis. Analytical method for each parameter was shown in the previous sections.

For thin section analysis, ice sample was sliced (1 cm) by an electric band saw in the low temperature room. Ice sections were attached to a glass plate and cut to a thickness of 0.1 cm with a knife. Ice crystallographic structures were photographed by illuminating

the thin sections under polarized light.

Sampling site list (Table 4.19.1-1)

Station	Date	Latitude	Longitude
ICE_1	2021/9/17	72˚20.98"N	160˚29.40"W
ICE_3	2021/9/22	72˚27.00"N	163˚13.18"W
ICE_4	2021/9/23	72˚01.80"N	167˚38.38"W
SNOW_1	2021/9/17	72˚34.15"N	160˚41.38"W
SNOW_2	2021/9/18	73˚28.79"N	158˚45.02"W
SNOW_3	2021/9/19	72˚43.37"N	155˚08.00"W
SNOW_4	2021/9/20	72˚27.57"N	156˚59.39"W
SNOW_5	2021/9/25	71˚00.01"N	168˚44.94"W

Sample list (Table 4.19.1-2)

Sample ID	Station No.	Cast No.	Sample name
1	ICE_1	1	top
2	ICE_1	1	middle
3	ICE_1	1	bottom
4	ICE_1	1	N_1
5	ICE_1	1	N_2
6	ICE_1	1	N_3
7	ICE_1	1	N_4
8	ICE_1	1	N_5
9	ICE_1	1	N_6
10	ICE_1	1	N_7
11	ICE_1	2	N_1
12	ICE_1	2	N_2
13	ICE_1	2	N_3
14	ICE_1	2	N_4
15	ICE_1	2	N_5
16	ICE_1	2	N_6
17	ICE_1	2	N_7
18	ICE_1	2	N_8
19	ICE_1	3	N_A-1
20	ICE_1	3	N_A-2
21	ICE_1	3	N_B-1
22	ICE_1	3	N_B-2
23	ICE_1	3	N_C-1
24	ICE_1	3	N_C-2
25	ICE_1	3	N_C-3
26	ICE_3	-	N_1
27	ICE_3	-	N_2
28	ICE_3	-	N_3

29	ICE_3	-	N_4
30	ICE_3	-	N_5
31	ICE_3	-	N_6
32	ICE_3	-	N_7
33	ICE_3	-	N_8
34	ICE_3	-	N_9
35	ICE_3	-	N_10
46	ICE_4	1	N_1
47	ICE_4	1	N_2
48	ICE_4	1	N_3
49	ICE_4	1	N_4
50	ICE_4	1	N_5
51	ICE_4	1	N_6
52	ICE_4	2	Top-1
53	ICE_4	2	Top-2
54	ICE_4	2	Bottom-1
55	ICE_4	2	Bottom-2
56	ICE_4	2	Bottom-3
57	ICE_4	2	Top-3
58	ICE_4	2	Top-4
59	ICE_4	2	Bottom-4
60	ICE_4	2	Bottom-5
61	ICE_4	2	Mix-1
62	ICE_4	2	Mix-2
63	ICE_1	1	N_8
64	ICE_1	1	N_9
65	ICE_1	2	N_9
66	ICE_1	2	N_10
67	ICE_1	3	N_C-4
68	ICE_1	3	N_B-3
69	ICE_1	3	N_A-3
70	ICE_1	3	N_A-4
71	ICE_3	-	N_11
72	ICE_3	-	N_12
73	ICE_3	-	N_13
74	ICE_3	-	N_14
75	ICE_3	-	N_15
76	ICE_4	1	N_7
77	ICE_4	2	Top-5
78	ICE_4	2	Bottom-6

79	ICE_4	2	Bottom-7
80	ICE_4	2	Mix-3
81	ICE_4	2	Mix-4
82	ICE_1	-	K_1
83	ICE_3	-	K_1
84	SNOW_1	-	1
85	SNOW_1	-	2
86	SNOW_1	-	3
87	SNOW_1	-	4
88	SNOW_1	-	5
89	SNOW_1	-	6
90	SNOW_2	-	1
91	SNOW_2	-	2
92	SNOW_2	-	3
93	SNOW_3	-	1
94	SNOW_3	-	2
95	SNOW_3	-	3
96	SNOW_3	-	4
97	SNOW_3	-	5
98	SNOW_4	-	1
99	SNOW_4	-	2
100	SNOW_4	-	3
101	SNOW_4	-	4
102	SNOW_4	-	5
103	SNOW_5	-	1
104	SNOW_5	-	2
105	SNOW_5	-	3
106	SNOW_5	-	4
107	SNOW_5	-	5
108	SNOW_5	-	6
109	SNOW_5	-	7
110	SNOW_5	-	8
111	SNOW_5	-	9
112	SNOW_5	-	10

(5) Data archives

These data obtained in this cruise will be submitted to the Data Management Group of JAMSTEC, and will be opened to the public via "Data Research System for Whole Cruise Information in JAMSTEC (DARWIN)" in JAMSTEC web site http://www.godac.jamstec.go.jp/darwin/e.

4.19.2. Sea Ice Incubation

(1) Personnel
Amane Fujiwara (JAMSTEC) – PI
Takuhei Shiozaki (The University of Tokyo)
Kohei Matsuno (Hokkaido University)
Mariko Hatta (JAMSTEC)
Daiki Nomura (Hokkaido University)
Koji Sugie (JAMSTEC) (not on board)

(2) Objective
To assess the potential of the Arctic sea ice as a career for the phytoplankton seed, which can be a source of the spring phytoplankton bloom, we conducted a mesocosm incubation experiment simulating sea ice melting during spring.

(3) Parameters
Chlorophyll-a concentration
Phytoplankton pigment concentration
Nutrients
DNA
Flowcytometry
Phytoplankton cell count (Microscopy)

(4) Method
The experiment was performed using sea ice sampled at the ice-edge observation sites (see 4.19.2) and sea water collected from 175 m depth of St. 20 (Pacific Winter Water (PWW) layer), respectively. Sampled PWW was filtered using 0.2-µm-pore-sized nucleopore filter to remove all suspended particle (e.g. phytoplankton cell and detritus) and dispensed into 9 sets of acid rinsed 9-L polycarbonate bottles. The 9 different pieces of sea ice were melted under 1°C controlled water bath, and 800-mL of each melt water was added to 8 L of filtered PWW. The incubation bottles were treated under 1°C and 330 µmol photons^{-1} m^{-2} for 24 h representing the typical early July temperature and light condition in the Chukchi Sea (70°N). Thus, we set up 9 mesocosm incubation systems (photo 4.19.2). The experiment was lasted for 17 days, and we monitored the parameters listed above every 2–3 days.

Photo 4.19.2: Temperature and light controlled incubation experiment system

Table 4.19.2-1: Sampling frequency of each parameter

Day	0	2	4	6	8	11	14	17
Chla	○	○	○	○	○	○	○	○
Nutrients	○	○	○	○	○	○	○	○
Pigments	○		○			○		○
DNA	○							○
Microscopy								○
Flowcytometry								○

(5) Data archives

These data obtained in this cruise will be submitted to the Data Management Group of JAMSTEC, and will be opened to the public via "Data Research System for Whole Cruise Information in JAMSTEC (DARWIN)" in JAMSTEC web site http://www.godac.jamstec.go.jp/darwin/e.

5. Under-the-Ice Drone Trials

(1) Personnel

Shojiro Ishibashi (JAMSTEC) – System Integrator (Not on board)
Kiyotaka Tanaka (JAMSTEC) – Operation Leader
Yosaku Maeda (JAMSTEC) – Not on board
Hiroshi Matsumoto (JAMSTEC) – Not on board
Makoto Sugesawa (JAMSTEC)
Ryo Kimura (Nippon Marine Enterprises, Ltd.; NME)
Ryo Oyama (NME)
Hiroshi Yoshida (JAMSTEC)

(2) Objective

The under-the-ice drone named COMAI (Fig. 5.1) is a middle size autonomous underwater vehicle (AUV) for observations under the ice in the Arctic. In this trial we concentrate on the evaluations of items effected by the Arctic location because of the first trial in the polar region. The test items are:

1) system performance check in low temperature environment,
2) error evaluation of the navigation system in high longitude area,
3) acoustic homer performance (Acoustic propagation measurement),
4) operation test with acoustic remote control mode, and
5) autonomous cruising demonstration with a safety tether.

The test results (which may include system bugs) will show us action items to fix problems and to improve the drone performance. We intend to carry out under ice surveys with the drone fixed bugs in FY2022.

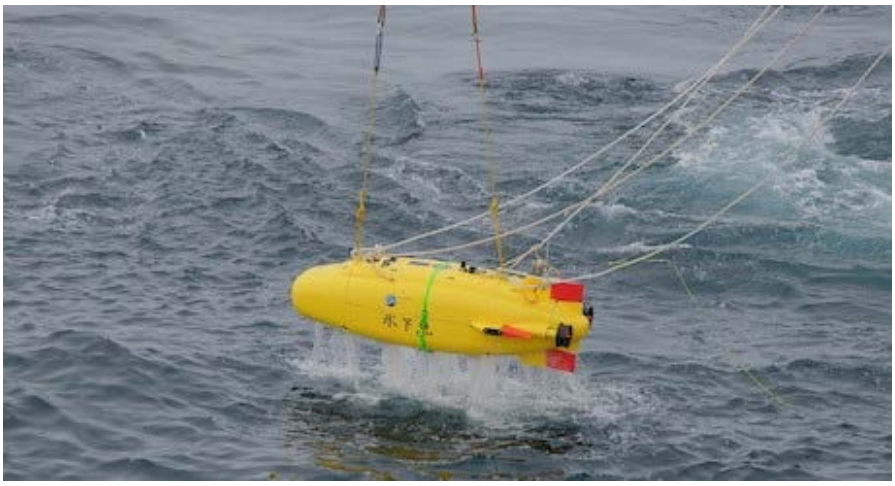

Figure 5-1: A recovery scene of COMAI. (photographed by Joh)

(3) Parameters

None

(4) Instruments and Methods

The drone is a platform of observation sensors for under the ice area. It autonomously cruises and surveys under the ice without a tether cable. The maximum cruising range is about 30 km or endurance is about 16 hours (at cruising speed of 1 kt) as shown in Table 5.1. The drone has four operation modes: 1) an untethered remotely operated vehicle mode (UROV) , 2) an acoustical ROV mode (AROV), 3) a radio wave ROV mode (RROV), and 4) an autonomous underwater vehicle (AUV) mode. In the AUV mode, three cruising patterns (heading-depth control, way-point control, and way-line control) are selectable. It has a special "return control" in addition to them. The return control is an automatic vehicle control to escape from ice covered area to open sea area. The control is used in avoiding the ice in a mission completion or escaping the ice when somewhat system failures emerge. In the control, the drone heads to a position preprogramed with the navigation system when all navigation devices are healthy. If some navigation devices are down, the drone uses a heading control with an acoustical super short baseline navigation toward an acoustic light house pre-deployed as shown in Fig. 5.2. The drone utilizes a hybrid Inertial navigation system (INS) applied a magnetic compass. The navigation system block diagram is shown in Fig. 5.3.

The drone system consists of major three parts: a vehicle body, a ship-side console, and an acoustic system. Its body is made from aluminum and covered with an FRP fairing cover. The ship-side console provides a graphical user interface of the drone system for operation and maintenance. The acoustic system consists of an acoustical communication modem/ locator and an acoustic pinger for the acoustical lighthouse.

Table 5-1: Specifications of COMAI.

Items	Specifications	Remarks
Size	2.3 x 0.6 x 0.7 m	
Weight	330 kg	in air
Depth rating	300 m	
Cruising speed	2 kt	3 kt max.
Cruising range	30 km	
Power	Li-ion battery (5.7 kWh)	
Actuators	Horizontal thrusters (100 W) x 2 Vertical thruster (100 W) x 1 Rudders	
Scientific payloads	CTD (conductivity, Temperature, depth) sensor Turbidity and chlorophyll meter Snap shot camera Multi beam sonar	 installed on top side installed on top side

COMAI is equipped with scientifical sensors: a CTD sensor (miniCTD, Valeport), a turbidity and chlorophyll meter (ECO FLUNTU, WET Labs), a snap shot camera (2592 x 1944 pixels, F2.2) with LED strobe lights, and a 260 kHz multi beam sonar (837B Delta T, IMAGENEX). The camera and the multi beam sonar are mounted on the top side of the body because of ice bottom observations. All data obtained are automatically logged in the drone internal memory and a hard disk of the personal computer of the ship-side console (if ROV mode).

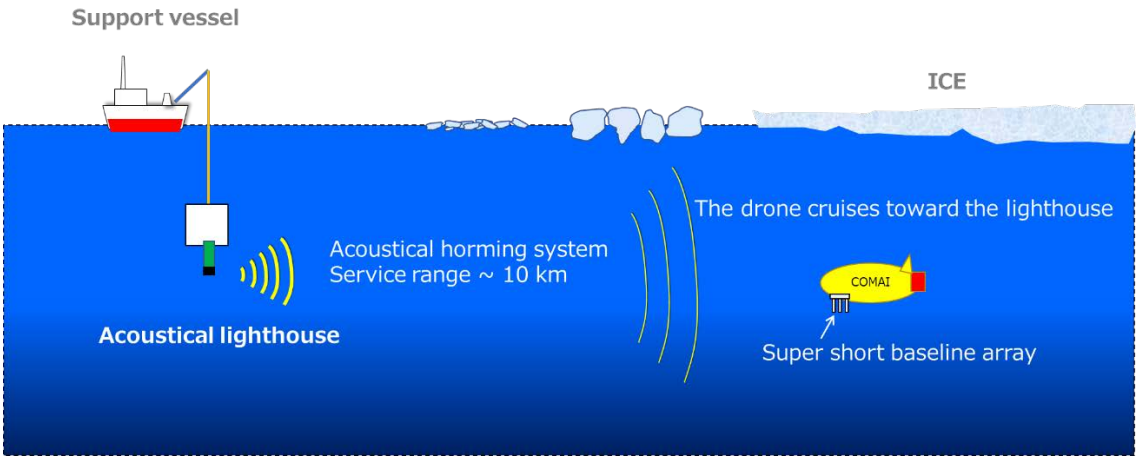

Figure 5-2: A working image of the heading control with the acoustical super short baseline navigation of the return control.

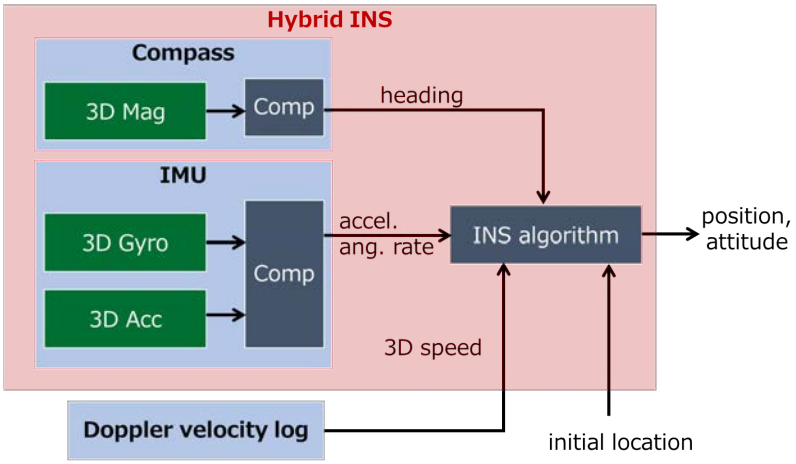

Figure 5-3: Block diagram of the hybrid navigation system.

(5) Test log

Station No.	Position		Date	Time (Local)		Water depth	Test No.	Test item	Descriptions
	Lat.	Lon.		Start	End				
BCW	71-34.27943N	154-45.38854W	11-Sep-21	15:30	15:49	34 m	Pre-1	pre-test	Low temperature wotking test and buoyancy adjustment
10	72-28.55598N	155-35.36866W	14-Sep-21	13:45	14:53	1827 m	Test-1	Test#1	INS performance test
11	73-09.93684N	160-07.59861W	15-Sep-21	15:30	16:30	322 m	Pre-2	pre-test	Life like Buoy test
33	71-27.31783N	168-31.16588W	24-Sep-21	14:00	15:22	48 m	Test-3-dive1	Test#3	Acoustical remote control test with AUV mode
37	69-59.96744N	168-44.56440W	26-Sep-21	10:00	11:29	41 m	Test-3-dive2	Test#3	Acoustical remote control test with AUV mode
37	70-00.13638N	167-10.87360W	26-Sep-21	13:30	14:14	47 m	Test-3-dive3	Test#3	Acoustical remote control test with AUV mode
37	70-00.10655N	166-39.60060W	26-Sep-21	15:05	15:29	47 m	Test-3-dive4	Test#3	Acoustical remote control test with AUV mode
none	45-18.71716N	159-24.75113E	14-Oct-21	9:40	12:11	5337 m	Test-2	Test#2	Acoustic homer performance test

The test #4 was not done because of the system bugs which were recognized in the test.

(6) Preliminary results

The drone normally worked below zero degree in the Arctic environment. We recognized major two problems through the tests. One is a software bug which results in huge navigation error. The other is a system problem. Fig. 5.4 shows tracks of the drone measured with the GPS (dotted line) and the hybrid inertial navigation system (solid line) installed in the drone in the test #1. The real track measured with the GPS completely differs from the track measured with the INS which almost stays at a position. We recognize that this is caused by a software bug of a communication interface module of the doppler velocity log. This bug might be made at the latest software revising right before this cruising and we missed it. (It is matter for deep regret…)

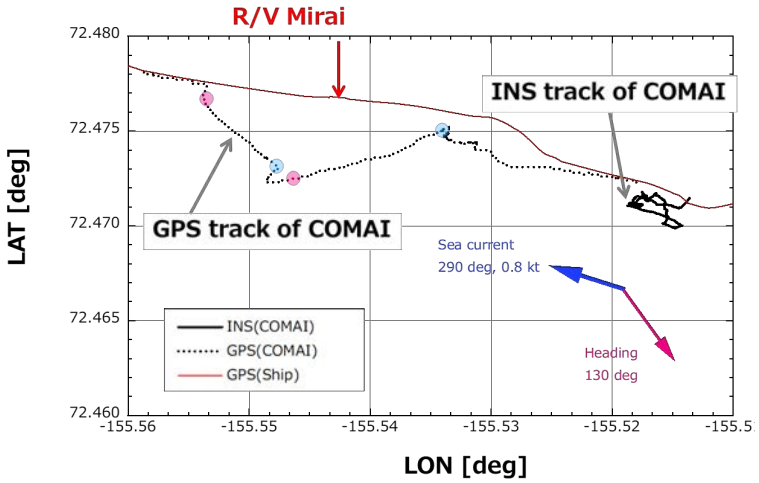

Figure 5-4: The drone tracks measured by the GPS and INS in the test #1.

The system problem occurred with multiple factors. A major factor is strange underwater magnetic field around the research ship Mirai. We carried out a test to measure time variation of heading of the drone in seawater in the test #3 – dive 3. The drone was towed by a small boat to increase distance from the ship up to 50 m and then the drone was hauling with the tether rope from the ship. Fig. 5.5 shows the drone heading and depth during towing. Heading measured was oscillated near the ship. This means that underwater magnetic field is inordinate. To avoid this field effect, the drone launching place should be apart from the ship over 20 meters. Other factors of the system problem are magnetic field deformation on the deck and weakening of horizontal components of

Earth magnetic field in high altitude region. These three things made failure of heading measurement with the hybrid INS and thus we resigned the test #4, autonomous cruising test which must uses heading and absolute positions for the control.

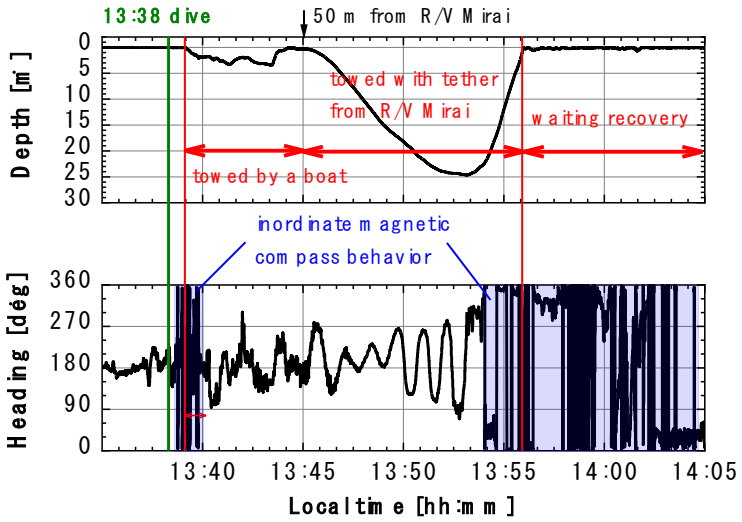

Figure 5-5: Depth and heading around the R/V Mirai measured by the drone sensors.

We measured magnetic field on the open deck of the R/V Mirai. To measure the field, a 3-axis magnetic compass (VMU931) and a logger (Rapsberry Pi 3B+) was prepared. Fig. 5.6 is illustrated measuring points. The compass was set at height of about 1 m. The measurement was done in latitude of about 70 degree where ratio of horizontal and vertical magnetic field components is about 1:10. Each magnetic field components obtained is shown in Fig. 5.7. Form the result, we recognize that there are no natural magnetic fields on the deck of Mirai. We should not perform compass calibrations on the deck.

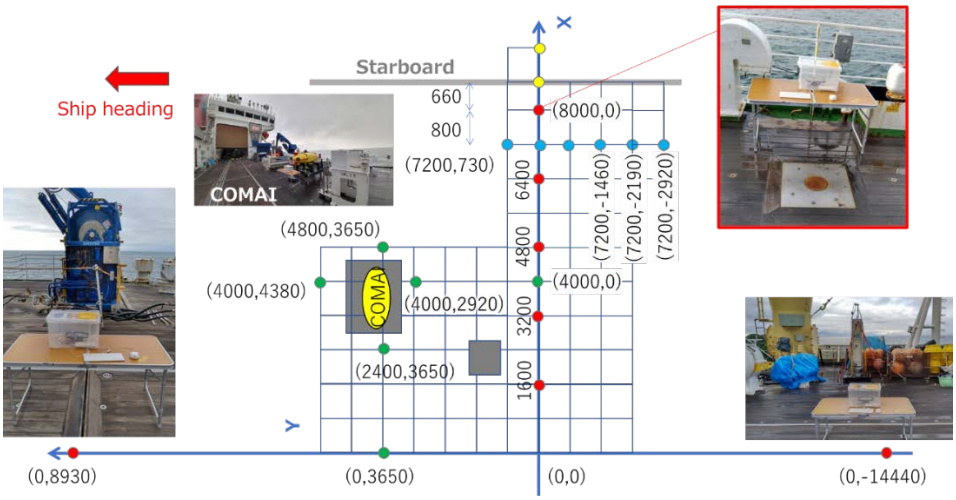

Figure 5-6: Magnetic field measurement map on the deck.

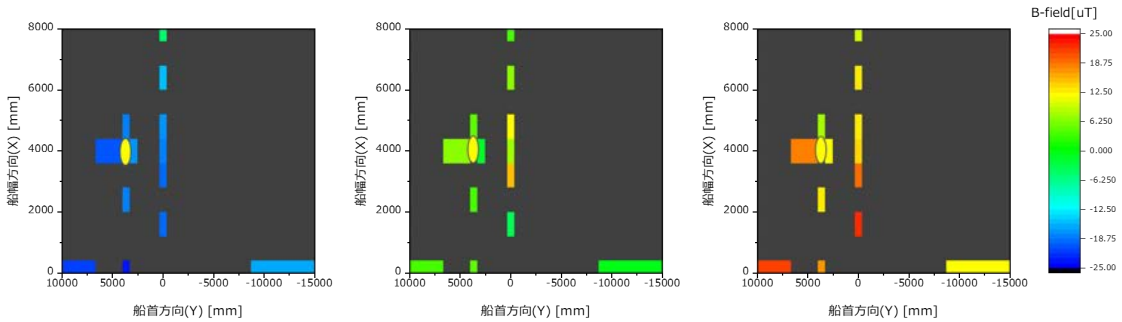

Figure 5-7: Magnetic field components measured on the deck. Left: Bx, middle: By, and right: Bz components. Yellow ellipse means the place of the drone.

(7) Data archives

These data obtained in this cruise will be submitted to the Data Management Group (DMG) of JAMSTEC, and will be opened to the public via "Data Research System for Whole Cruise Information in JAMSTEC (DARWIN)" in JAMSTEC web site. <http://www.godac.jamstec.go.jp/darwin/e>

6. Geology

6.1. Sea bottom topography measurements

(1) Personnel

Amane Fujiwara JAMSTEC -PI
Ryo Oyama NME (Nippon Marine Enterprises, Ltd.)
Kazuho Yoshida NME
Satomi Ogawa NME
Ryo Kimura NME
Yoichi Inoue MIRAI Crew

(2) Objectives

R/V MIRAI is equipped with the Multi Beam Echo Sounding system (MBES; SEABEAM 3012 (L3 Communications ELAC Nautik, Germany)). The objective of MBES is collecting continuous bathymetric data along ship track to make a contribution to geological and geophysical studies.

(3) Parameters

Depth [m]

(4) Instruments and Methods

The "SEABEAM 3012" on R/V MIRAI was used for bathymetry mapping during this cruise.
To get accurate sound velocity of water column for ray-path correction of acoustic beams, we determined sound velocities at the depth of 6.62m, the bottom of the ship, by a surface sound velocimeter. We made sound velocity profiles based on the observations of CTD, XCTD and Argo float conducted in this cruise by the equation in Del Grosso (1974).
The system configuration and performance are shown in Table 6.1-1.

Table 6.1-1: SEABEAM 3012 System configuration and performance

---

Frequency: 12 kHz
Transmit beam width: 2.0 degree
Transmit power: 4 kW
Transmit pulse length: 2 to 20 msec.
Receive beam width: 1.6 degree
Depth range: 50 to 11,000 m
Number of beams: 301 beams (Spacing mode: Equi-angle)
Beam spacing: 1.5 % of water depth (Spacing mode: Equi-distance)
Swath width: 60 to 150 degrees

Depth accuracy: < 1 % of water depth (average across the swath)

(5) Observation log
31 Aug. 2021 - 18 Oct. 2021 (UTC)

(6) Preliminary Results
The results will be published after the primary processing.

(7) Data archives
These data obtained in this cruise will be submitted to the Data Management Group of JAMSTEC, and will be opened to the public via "Data Research System for Whole Cruise Information in JAMSTEC (DARWIN)" in JAMSTEC web site.
<http://www.godac.jamstec.go.jp/darwin/e>

(8) Remarks
i). The following periods, data acquisition was suspended due to sending acoustic commands of ANS system.
00:20UTC 04 Sep. 2021 - 01:59UTC 04 Sep. 2021
17:03UTC 10 Sep. 2021 - 17:07UTC 10 Sep. 2021
20:49UTC 10 Sep. 2021 - 20:53UTC 10 Sep. 2021
21:59UTC 10 Sep. 2021 - 22:02UTC 10 Sep. 2021
18:35UTC 11 Sep. 2021 - 19:19UTC 11 Sep. 2021
20:15UTC 11 Sep. 2021 - 20:51UTC 11 Sep. 2021
22:45UTC 11 Sep. 2021 - 23:16UTC 11 Sep. 2021
19:12UTC 14 Sep. 2021 - 19:53UTC 14 Sep. 2021
16:50UTC 15 Sep. 2021 - 17:30UTC 15 Sep. 2021
17:36UTC 15 Sep. 2021 - 18:14UTC 15 Sep. 2021

ii). The following periods, data acquisition was suspended due to TurboMAP(Turbulence Ocean Microstructure Acquisition Profiler) observations.
03:55UTC 04 Sep. 2021 - 06:10UTC 04 Sep. 2021
20:45UTC 13 Sep. 2021 - 20:53UTC 13 Sep. 2021
21:01UTC 13 Sep. 2021 - 21:30UTC 13 Sep. 2021
23:06UTC 13 Sep. 2021 - 23:33UTC 13 Sep. 2021
04:54UTC 14 Sep. 2021 - 05:16UTC 14 Sep. 2021
18:11UTC 16 Sep. 2021 - 18:40UTC 16 Sep. 2021
08:22UTC 17 Sep. 2021 - 08:59UTC 17 Sep. 2021
05:10UTC 18 Sep. 2021 - 05:57UTC 18 Sep. 2021
07:33UTC 18 Sep. 2021 - 08:01UTC 18 Sep. 2021
21:08UTC 18 Sep. 2021 - 21:30UTC 18 Sep. 2021
07:51UTC 19 Sep. 2021 - 08:18UTC 19 Sep. 2021

16:01UTC 19 Sep. 2021 - 16:26UTC 19 Sep. 2021
07:30UTC 20 Sep. 2021 - 08:19UTC 20 Sep. 2021
13:57UTC 20 Sep. 2021 - 14:22UTC 20 Sep. 2021
20:24UTC 20 Sep. 2021 - 20:47UTC 20 Sep. 2021

iii). The following periods, data acquisition was suspended due to the shallow sea area.
13:43UTC 07 Sep. 2021 - 15:58UTC 10 Sep. 2021
06:11UTC 11 Sep. 2021 - 08:06UTC 11 Sep. 2021
04:32UTC 12 Sep. 2021 - 15:57UTC 13 Sep. 2021
11:00UTC 17 Sep. 2021 - 02:20UTC 18 Sep. 2021
01:45UTC 21 Sep. 2021 - 21:12UTC 06 Oct. 2021 (include the period of calling at Dutch Harbor)

iv). The following period, data acquisition was stopped due to the system trouble.
22:24UTC 06 Oct. 2021 - 22:39UTC 06 Oct.2021

6.2. Sea surface gravity measurements

(1) Personnel

Amane Fujiwara	JAMSTEC	-PI
Ryo Oyama	NME (Nippon Marine Enterprises, Ltd.)	
Kazuho Yoshida	NME	
Satomi Ogawa	NME	
Ryo Kimura	NME	
Yoichi Inoue	MIRAI Crew	

(2) Objective

The local gravity is an important parameter in geophysics and geodesy. The gravity data were collected during this cruise.

(3) Parameters

Relative Gravity [CU: Counter Unit]

[mGal] = (coefl: 0.9946) * [CU]

(4) Instruments and Methods

The relative gravity using LaCoste and Romberg air-sea gravity meter S-116 (Micro-g LaCoste, LLC) was measured during the cruise. To convert the relative gravity to absolute one, we measured gravity, using portable gravity meter (Scintrex gravity meter CG-5), at Shimizu port as the reference points.

(5) Observation log

31 Aug. 2021 - 21 Oct. 2021 (UTC)

(6) Preliminary Results

Absolute gravity table is shown in Table 6.2-1

Table 6.2-1: Absolute gravity table of the MR21-05C cruise

No.	Date	UTC	Port	Absolute Gravity [mGal]	Sea Level [cm]	Ship Draft [cm]	Gravity at Sensor * [mGal]	S-116 Gravity [mGal]
#1	31-Aug.	05:48	Shimizu	979,728.87	153	670	979,729.65	12006.15
#2	21-Oct.	22:58	Shimizu	979,728.87	124	615	979,729.44	12004.13

*: Gravity at Sensor = Absolute Gravity + Sea Level*0.3086/100 + (Draft-530)/100*0.2222

(7) Data archives

These data obtained in this cruise will be submitted to the Data Management Group of JAMSTEC, and will be opened to the public via "Data Research System for Whole Cruise Information in JAMSTEC (DARWIN)" in JAMSTEC web site.

<http://www.godac.jamstec.go.jp/darwin/e>

6.3. Surface magnetic field measurement

(1) Personnel

Amane Fujiwara	JAMSTEC	-PI
Ryo Oyama	NME (Nippon Marine Enterprises, Ltd.)	
Kazuho Yoshida	NME	
Satomi Ogawa	NME	
Ryo Kimura	NME	
Yoichi Inoue	MIRAI Crew	

(2) Objective

Measurement of magnetic force on the sea is required for the geophysical investigations of marine magnetic anomaly caused by magnetization in upper crustal structure. We measured geomagnetic field using a three-component magnetometer during this cruise.

(3) Parameters

Three components of a magnetic field vector observed on-board, Hx, Hy, Hz [nT]

Hx : a magnetic field component in the bow/stern direction on the vessel horizontal plane. "To bow" is positive.

Hy : a magnetic field component in the port/starboard direction on the vessel horizontal plane. "To starboard" is positive.

Hz : a perpendicular magnetic field component to the vessel horizontal plane. "upward" is positive.

(4) Instruments and Methods

A shipboard three-components magnetometer system (SFG2018, Tierra Tecnica) is equipped on-board R/V MIRAI. Three-axes flux-gate sensors with ring-cored coils are fixed on the fore mast. Outputs from the sensors are digitized by a 20-bit A/D converter (1 nT/LSB) and sampled at 8 times per second. Yaw (heading), Pitch and Roll are measured by the Inertial Navigation Unit (INU) for controlling attitude of a Doppler radar. Ship's position, speed over ground (Differential GNSS) and gyro data are taken from LAN every second.

The relation between a magnetic-field vector observed on-board, $\mathbf{H}_{\mathrm{ob}}$, (in the ship's fixed coordinate system) and the geomagnetic field vector, $\mathbf{F}$, (in the Earth's fixed coordinate system) is expressed as:

$$\mathbf{H}_{\mathrm{ob}} = \widetilde{\mathbf{A}}\ \widetilde{\mathbf{R}}\ \widetilde{\mathbf{P}}\ \widetilde{\mathbf{Y}}\ \mathbf{F} + \mathbf{H}_{\mathrm{p}} \qquad \text{(a)}$$

where $\widetilde{\mathbf{R}}$, $\widetilde{\mathbf{P}}$ and $\widetilde{\mathbf{Y}}$ are the matrices of rotation due to roll, pitch and heading of a ship, respectively. $\widetilde{\mathbf{A}}$ is a 3 x 3 matrix which represents magnetic susceptibility of the ship, and $\mathbf{H}_{\mathrm{p}}$ is a magnetic field vector produced by a permanent magnetic moment of the ship's body. Rearrangement of Eq. (a) makes

$$\widetilde{\mathbf{B}}\,\mathbf{H}_{\mathrm{ob}} + \mathbf{H}_{bp} = \widetilde{\mathbf{R}}\ \widetilde{\mathbf{P}}\ \widetilde{\mathbf{Y}}\ \mathbf{F} \quad \text{(b)}$$

where $\widetilde{\mathbf{B}} = \widetilde{\mathbf{A}}^{-1}$, and $\mathbf{H}_{bp} = -\widetilde{\mathbf{B}}\,\mathbf{H}_{\mathrm{p}}$. The magnetic field, $\mathbf{F}$, can be obtained by measuring, $\widetilde{\mathbf{R}}$, $\widetilde{\mathbf{P}}$, $\widetilde{\mathbf{Y}}$ and $\mathbf{H}_{\mathbf{ob}}$, if $\widetilde{\mathbf{B}}$ and $\mathbf{H}_{bp}$ are known. Twelve constants in $\widetilde{\mathbf{B}}$ and $\mathbf{H}_{\mathbf{bp}}$ can be determined by measuring variation of $\mathbf{H}_{\mathbf{ob}}$ with, $\widetilde{\mathbf{R}}$, $\widetilde{\mathbf{P}}$, and, $\widetilde{\mathbf{Y}}$ at a place where the geomagnetic field, $\mathbf{F}$, is known.

(5) Observation log
31 Aug. 2021 - 21 Oct. 2021 (UTC)

(6) Preliminary Results
The results will be published after the primary processing.

(7) Data archives
These data obtained in this cruise will be submitted to the Data Management Group of JAMSTEC, and will be opened to the public via "Data Research System for Whole Cruise Information in JAMSTEC (DARWIN)" in JAMSTEC web site.
<http://www.godac.jamstec.go.jp/darwin/e>

(8) Remarks
For calibration of the ship's magnetic effect, "figure-eight" turns (a pair of clockwise and anti-clockwise rotation) were held at the following periods and positions.
03:00UTC 11 Sep. 2021 - 03:21UTC 11 Sep. 2021, around 71-54N, 156-04W
03:00UTC 25 Sep. 2021 - 03:22UTC 25 Sep. 2021, around 70-57N, 166-52W
01:32UTC 14 Oct. 2021 - 01:56UTC 14 Oct. 2021, around 45-19N, 159-26E

7. Notice on using

This cruise report is preliminary, but it represents final documentation as of the end of the cruise. This report might not be corrected even if changes regarding its content (e.g., taxonomic classifications) are found after its publication. Moreover, this report might also be changed without notice. Data in this cruise report might be raw or unprocessed. If you intend to use or to refer to the data presented in this report, please ask the Chief Scientist for the latest information.
Users of information on this report are requested to submit Publication Report to JAMSTEC.
http://www.godac.jamstec.go.jp/darwin/explain/1/e#report
E-mail: submit-rv-cruise@jamstec.go.jp